THE DESIGN AND ANALYSIS OF INFLATABLE DAMS

BY

Andrea M. Stodulka

This thesis is submitted in accordance with
the requirement of the By Laws of The
University of Sydney for the Degree of
Master of Engineering Science

September, 1973

ACKNOWLEDGMENTS

The author wishes to thank The Director of Works (Canberra Branch) for his generous approval of leave to undertake this present study, and the Department of Education for the Funds which made the research possible.

The research was carried out in the School of Civil Engineering of the University of Sydney; The Head of the School is Professor J.W. Roderick whose support in this work is gratefully acknowledged.

The author especially wishes to thank Dr. R.D. Watkins for his encouragement and assistance, and acknowledge the help from the Hydraulics Laboratory staff.

Synopsis

A number of models were constructed to study the static and dynamic behaviour of hydraulic inflatable dams. Points of particular interest included fabric tension and profile shape in an 'infinitely' long dam. Qualitative assessments were also made of anchorage design and end conditions.

The experimental shapes and forces were compared with values obtained by mathematical methods of solution, in particular those of Anwar and Binnie, and that of Harrison. Harrison's method was modified using the Simplex iterative method, with satisfactory results. Another method of analysis by cord analogue was devised and worked very satisfactorily. A number of Graphs were drawn from the results to aid the prospective designer in the optimization of materials and minimisation of stress.

In addition, a novel form of inflatable dam consisting of a set of motor vehicle tyre tubes was evaluated and its performance indicated that it could provide a cheap and serviceable temporary channel control structure.

Notation

Due to non-uniformity in the use of symbols among various investigators the symbols used are adequately defined in each section as they are used.

CONTENTS

		PAGE
CHAPTER 1 -	APPLICATION AND USES OF INFLATABLE DAMS	
1.1	Description of Inflatable Dams	1
1.2	Operation Aspects of, and Design Bases for Inflatable Dams	4
CHAPTER 2 -	DEVELOPMENT AND DESIGN OF INFLATABLE DAMS	
2.1	Introduction	7
2.2	Imbertson or Fabridam Type	7
2.3	The Buijze or Steel Panel Type	7
2.4	The Mesnager-Schofield or Parachute Type	12
2.5	B.N.R.D.C. Type	15
CHAPTER 3 -	THE FABRIDAM TYPE INFLATABLE DAM	
3.1	Historical note	16
3.2	Design and Construction of Fabridam	19
3.3	Fabridams in Australia	31
3.4	Fabridam of Special Interest	31
3.5	Failures	36
CHAPTER 4 -	MATHEMATICAL AND MODEL STUDIES OF INFLATABLE DAMS	
4.1	Previous Investigations	37
4.2	Analysis of Infaltable Dams	41
4.3	Anwar's mathematical method	42
4.4	Binnie's mathematical method	50
4.5	Comparisons between Anwar's and Binnie's Analysis and Experimental Results	53
4.6	Harrison-Newton method	59
4.7	Conclusion of Analysis	63
4.8	Summary of Previous Model Tests of Inflatable Dams	64
4.9	Findings of Koombooloomba Model Study	67
4.10	Mangla Bag Dam Model	69
4.11	Anwar's Model	72
4.12	Stodulka-Marr Model	73
4.13	Discussion of End Effects	81

		PAGE
CHAPTER 5 - MODEL ANALYSIS		
5.1	Introduction	82
5.2	Design of Tank	82
5.3	Construction of the Models	84
5.4	Instrumentation	90
5.5	Construction - Instrumentation of the Small Model	92
5.6	Behaviour of Model and Results	95
5.7	Model Deficiencies and Approach to Further Tests	104
CHAPTER 6 - THE CORD ANALOGUE METHOD OF ANALYSIS		
6.1	Description	105
6.2	Procedure and Apparatus	105
6.3	Possible Errors	112
6.4	Shape Verification Starting with known shape	122
6.5	Prediction of Shape	130
6.6	Possible Improvements and Potential Uses of Analogue Method	137
CHAPTER 7 - HARRISON SIMPLEX METHOD		
7.1	Introduction	138
7.2	Problems Associated with the Harrison Analysis and their Attempted Solution and Other Alterations	138
7.3	Change from Newton to Simplex Iterative Method	143
7.4	Results	148
7.5	Summary and Implications	158
CHAPTER 8 - COMPARISONS OF METHODS OF ANALYSIS		
8.1	Comparison of Methods	159

PAGE

CHAPTER 9 - TYRE TUBE MODEL OF A MULTI-TOROID DAM

9.1 Introduction 161
9.2 Experimental Procedure 163
9.3 Tube Behaviour 165
9.4 Behaviour of Air-Inflated Tubes 167
9.5 Behaviour of Water-Inflated Tubes 168
9.6 Behaviour of Air-Water Inflated Tubes 170
9.7 Conclusion and Suggested Improvements 171

CHAPTER 10 - DESIGN GRAPHS

10.1 Introduction 172
10.2 Limitations of Design Graphs 173
10.3 Description of Graphs 183
10.4 Worked examples Using Design Graphs 184

CHAPTER 11 - FINAL DISCUSSION AND CONCLUDING REMARKS ON THE INFLATABLE DAMS

11.1 Discussion of Results Pertaining to the Fabridam Type Inflatable Dams 185
11.2 Types of Inflatable Dam other than Fabridam Type 188
11.3 Conclusion 189

REFERENCES

APPENDIX 1 HARRISON - SIMPLEX COMPUTER PROGRAM(CHAPTER 7) (i)

APPENDIX II CORRECT LOAD POSITIONS FOR AN LOGUEMETHOD (CHAPTER 6) (ix)

TABLES

		Reproduced from Ref.	Page
CHAPTER 2			
2.1	Critical Parameters of Buijze Type Dam	(8)	11
CHAPTER 3			
3.1	Properties of Fabridam Fabric	(3a)	25
3.2	Features of Seven Australian Fabridams		33
CHAPTER 4			
4.1	Summary of Conditions Analysed and Assumptions		40
4.2	Effect of Elastic Modulus on Tension and Shape	(12)	42
4.3	Decrease in Tension for Increased U/S water level	(12)	43
4.4	Comparison of Radii of U/S Profiles by Anwar & Binnie Methods		53
4.5	Comparison of Tension		56
4.6	Sample Table of Graphical Tension Calculations		58
4.7	Previous Model Comparisons		65
4.8	Summary of Model Function and Aspects Considered		66
4.9	Vibration of Koombooloomba Model		68
CHAPTER 6			
6.1	Summary of Tension Data for Air-Water Inflated Case		113
6.2	Comparison of Ave. Tension Values		113
6.3	Comparison of Tension using 5 and 12 Nodes		119
6.4	Load Calculation for Profile Verification (Air-Water Inflated Case)		124
6.5	Comparison of Tension of Air-Water Inflated Case		125
6.6	Comparison of Tension with Varying Base Widths		127
6.7	Load Calculation from 1st Guess		131
6.8	Load Calculation from 1st Iteration.		131
6.9	Comparison of Tension for Water-Inflated Case		132
6.10	Comparison of Tension for Air-Inflated Case		135
6.11	Comparison of Tension for Air-Inflated Case		136
CHAPTER 8			
8.1	Summary of Properties of Methods in Shape and Tension Analysis		160
CHAPTER 10			
10.1	Relation of Perimeter to Inflation Head for 5ft. High Water-Inflated Fabridam	(4a)	172

DIAGRAMS*

			Reproduced from Ref.	Page
CHAPTER 1				
1.1	General Aspects of Inflatable Dams - Alumy Ck	P	(3a)	2
1.2	- Koombooloomba	P		2
1.3	- March Run	P		2
1.4	- Bay City	P		2
CHAPTER 2				
2.1	Buijze - Steel Panel Type	P	(9)	8
2.2	General Arrangement		(8)	8
2.3	Sectional Views		(8)	10
2.4	Sketch of Parachute Dam		(22)	13
2.5	Operation of Parachute Dam		(22)	13
2.6	Conditions of Vibrations		(22)	15
CHAPTER 3				
3.1 - 3.4	Fabridams under Various Conditions	P	(3a)	17
3.5	Fabridam Plan		(3a)	18
3.6-3.11	Construction Sequence Alumy Ck.	P (Grafton Council)		21,22
3.12-3.14	Operation of Alumy Ck.	P		23
3.15-3.16	Anchorage Systems			26
3.17	Clamping Detail		(12)	27
3.18	Skew Splicing of Fabric			28
3.19	Operation Sequences of Water-Inflated Fabridam	P	(3a)	30
3.20,3.22	Kinchela Ck. Partially deflated	P	(12)	32
3.21	Kinchela Ck. Deflated	P		32
3.23,3.24	Koombooloomba Fabridam	P	(3a)	32
3.25-3.32	Belmore Fabridam Failure (1969)	P	(12)	34,35
3.33,3.34	Belmore Fabridam Failure (1973)	P	(12)	35

* P denotes Photograph

G denotes Graph

			Reproduced from Ref.	Page
CHAPTER 4				
4.1	Equilibrium Diagram			41
4.2	Loading on Air-Inflated Case			44
4.3	Loading on Water Inflated Case			46
4.4	Profile of Water-Inflated Case		(15)	48
4.5	Air-Inflated Overflow Case			49
4.6	Loading on Water-Inflated Case			51
4.7	Comparison of Profiles of Water-Inflated Case ($^{H}/_{h}$ = 1.38)			54
4.8	Comparison of Profiles of Water-Inflated Case ($^{H}/_{h}$ = 1.60)			55
4.9	Forces acting on a membrane dam		(12)	59
4.10	Finite element analysis element and node forces		(12)	60
4.11	Extension of Element			60
4.12	Solution Process - initial variables		(12)	61
4.13	Solution Process - calculated miscloses		(12)	61
4.14-4.16	Stodulka-Marr Model Study	P	(17)	74
4.17	Discharge Coeff. vs. Ht. of water above crest	G	(17)	77
4.18	Tension Range vs. Overflow	G	(17)	78
4.19	Clamp Detail			80
CHAPTER 5				
5.1-5.4	Large Experimental Model Analysis			83
5.5	Experimental Tank			84
5.6	Clamping Systems			85
5.7	Downstream Clamp Regions			86
5.8	Bag Construction			87
5.9	Valve Design			88
5.10	U/S Clamp Fabric Detail			88
5.11	End conditions			89
5.12-5.16	Vee Notch Effect in Small Model	P		93
5.17-5.21	Vee Notch Effect in Large Model	P		94
5.22-5.25	Overflow of Large Model	P		96
5.26	Relation between $^{H}/_{h}$ for Vee Notch	G		98
5.27-5.30	Overflow of Small Model Water-Inflated	P		101
5.31-5.35	U-V Recordings of Strain fluctuations under overflow Conditions			103

CHAPTER 6

		Page
6.1-6.5	Cord Analogue Method - Typical Cases P	106
6.6	Forces Acting on Cord Analogue	107
6.7	Pressure Distribution	107
6.8	Force on an Element	108
6.9	Load on a Node	108
6.10	Relation between Load, Tension and Bisected Angles	110
6.11	Friction between Load Hook and Perimeter Cord	115
6.12	Typical Example of unequal Tension in Membrane due to Friction in Pulley	117
6.13	Comparison between 5 and 12 nodes	120
6.14	Experimental air-water profile	122
6.15	Load distribution around Perimeter	124
6.16	Comparison between Analogue and Experimental Profilesfor Air-Water Case	126
6.17	Comparison between Analogue and Harrison Profiles for 3.0 ft. Base	128
6.18	Comparison between Analogue and Harrison for 2.3 ft Base	128
6.19	Definition of Various Base Widths	129
6.20	Guessed Profile for unknown Water-Inflated Profile	130
6.21	Results of Guess and 1st Iteration for water-inflated case	133
6.22	Comparison of 2nd Analogue Iteration, Experimental and Harrison Profiles	133
6.23	Iterations for Air-Inflated Case	135
6.24	Determination of shape for air-inflated case	136
6.25	Comparison of Air-Inflated Profiles for low H/h.	137

CHAPTER 7

7.1	Analysis with U/S water level higher than crest level	140
7.2	Examples of Instability	141
7.3	Effect of Misclose	143
7.4	Simplex Method	144
7.5	Simplex Process	145
7.6	Simplex Flowchart	146
7.7	Examples of instability and comparison of water-inflated profiles between computer and experiment.	149
7.8	Comparison between 20 and 60 nodes and experimental profiles.	150
7.9	Comparison between profiles for 20, 60, and 120 nodes	151

cont/...

			Page
CHAPTER 7 cont.			
	7.10 Comparison between 120 node profile and experimental profile (water-inflated)		152
	7.11 Comparison of profiles between 20, 60, and 120 nodes (air-inflated)		154
	7.12 Comparison between 120 node profile and experimental profile		155
	7.13 Instability and comparison between vee notch experimental case		156
CHAPTER 9			
	9.1-9.4 Tyre Tube Dam Model under varying conditions (air-inflated)	P	162
	9.5 Air-water inflated	P	162
	9.6 General Arrangement		163
	9.7 Cusp Leakage		166
	9.8 Low pressure water inflated tubes		168
	9.9-9.13 Water-inflated tube dam under varying conditions of U/S Head	P	169
	9.14 Modified system of anchorage and scaling tube dam		171
CHAPTER 10			
	10.1 Perimeter/Base U.S. $^{H}/_{h}$ (water)	G	174
	10.2 Tension $/_{h^2}$ vs. H/h (water)	G	175
	10.3 h/Total Perimeter vs. H/h (water)	G	176
	10.4 Water inflated profiles (water)		177
	10.5 Perimeter/Base vs. H/h (air-water)	G	178
	10.6 T/h^2 vs. H/h (air-water)	G	179
	10.7 h/Total Perimeter vs. H/h (air-water)	G	180
	10.8 Upstream Angle vs. H/h (water)	G	181
	10.9 Upstream angle vs. H/h (air)	G	182
CHAPTER 11			
	11.1 Strapped Bag		185
	11.2 Modified Mesnager-Parachute Type		188

CHAPTER I - APPLICATION AND USES OF INFLATABLE DAMS

1.1 DESCRIPTION OF INFLATABLE DAMS

1.1.1 Background of Inflatable Dams

The simplest and most common type of inflatable dam consists of a single sheet of rubberised fabric folded into a tubular shaped bag, which is then sealed in place during installation. The bag is attached by structural steel members and anchor bolts to a reinforced concrete slab base and sides of a channel or weir. The upstream water level is controlled by inflating or deflating the bag with air, water or a combination of both. (For a general view see Diags. 1.1 to 1.4).

This type of bag dam has been given the trade name 'Fabridam' and was originally developed as an adjustable gate to control the water level in rivers and reservoirs. It can be more economical and practical than either the conventional steel gate system which requires large concrete abutments and foundations, or the wooden flash board system which needs continual replacement.

1.1.2 Uses of Inflatable Dams

The importance and widespread application of inflatable dams can be seen from a brief summary of their uses:

(a) Flood Control

Installed across rivers, or as levee banks in flood plains, the inflatable dam provides ready control in cases of flood, by allowing the inflow of flood waters into diversion basins before the river reaches levee height. (See Diagram 3.22).

GENERAL ASPECTS OF INFLATABLE DAMS

DIAGRAM 1.1 - A WATER INFLATED DAM USED AS A SALINITY BARRIER (ALUMY CK. NSW) TIDAL SALT WATER IS ON THE LEFT.

DIAGRAM 1.2 - INCREASING THE HEIGHT OF KOOMBOOLOOMBA DAM (TULLY FALLS, QUEENSLAND), FOR HYDROELECTRIC PURPOSES, BY THE INSTALLATION OF A 5' WATER INFLATED DAM. THIS DAM IS LOCATED ON TOP OF AN OGEE SPILLWAY.

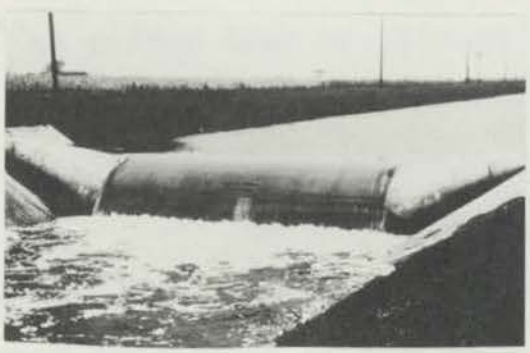

DIAGRAM 1.3 - WATER INFLATED DAM USED FOR IRRIGATION, MARCH-RUN (N.Y. USA)

DIAGRAM 1.4 - A WATER INFLATED DAM ON LOWER COLORADO RIVER, BAY CITY, USA. (13FT. HIGH BY 227 FT. LONG)

Subsequently, when it is deflated and is lying flat, the dam provides minimum resistance to flood waters and debris.

(b) Tidal Control and Salinity Barriers

In streams near sea coasts the inflatable dam may be an economical and effective barrier to tidal salt water - making possible reclamation of land for agriculture and greatly increased fresh water supplies for water short communities (see Diag. 1.1).

(c) Increasing Heights of Existing Dams

Installed on top of a permanent dam crest or spillway, the inflatable dam provides the reservoir with controllable extra storage. The major advantages are: it costs less to maintain than flash boards; conserves water by not leaking; and is quickly inflated after the passage of flood peaks to maintain desired water levels (see Diag. 1.2).

(d) Further Possible Applications

(i) The use of large doughnut shaped inflatable dams as coffer dams or service reservoirs.

(ii) As groynes or barriers to prevent beach erosion.

(iii) As wave attenuators and breakwaters.

However, in the case of (ii) and (iii), it would seem desirable to test out by model study any proposal where dynamic forces act on the dam, since most applications to date have been in situations where dynamic loading has been assumed relatively small.

1.1.3 Advantages and Disadvantages

The following advantages and disadvantages of inflatable dams are considered obvious and are recorded here without comment. Further details however are given in Ref.3b.

Advantages include:-

(a) Low initial cost;

(b) Little maintenance;

(c) Negligible resistance to flood waters and debris;

(d) Easy water level control and two-way flow;

(e) Impossibility of jamming as in the case of a steel gate.

Disadvantages:-

(a) Life expectancy of 20 years;

(b) Vulnerability to vandalism;

(c) Uncertainty of behaviour under dynamic conditions, such as overflow, wind waves, and/or reinflation cycles;

(d) Uncertainty of fabric behaviour with age and effects of creases;

(e) Possibility of clogging of outlet pipe by weeds.

1.2 OPERATION ASPECTS OF, and PRESENT DESIGN BASES FOR INFLATABLE DAMS

Several interdependent factors affect the operational behaviour of inflatable dams. The two most important are:-

(a) The permissable fabric tension.

(b) The curved perimeter of the dam.

The amount of inflation and thereby the maximum height is largely determined by allowable fabric tension. The maximum height is also dependent on the curved perimeter and the base width of the dam. As in all inflatable structures, the inflatable dam is held in shape by fabric tensions and the disposition of

fluid pressure loading around its surfaces.

Of particular significance are the pressures acting on the bag interior, which are exerted by filling fluids, the quantity and pressure of which may be varied according to operational requirements.

Most inflatable dams seem to have been designed on a semi-empirical basis, as the earliest published mathematical analysis of this type of structure appears to be that of Anwar in 1966 (Ref.15) whereas these structures have been successfully used since 1957. The only other known mathematical treatments are by Harrison 1969 (Ref.12) and Ogiwarra 1970 (Ref.16) which were extended by Binnie 1973 (Ref.23). Unfortunately, none of these methods lend themselves to design using a slide rule or desk calculator and none deals in any detail with optimisation of materials in a form which may be useful to the potential designer. Also, recent failures of this type of dam, for example, Belmore Fabridam (described later in Chapter 3) in N.S.W., Australia, which failed in 1969 and then again in 1973 under a test operation load, indicate the desirability of further study of the stresses and strains in the membrane, especially in an area around the anchoring clamps.

Analysis of dynamic loading and determination of stresses and strains on the opposite side to creases, would seem to necessitate further model studies, and a three dimensional finite element approach perhaps would be the next step.

Although a wide range of inflatable structures (mainly air-filled) have been fully analysed, such as those described in Ref.1 , there is no general method of analysis which can be conveniently applied to different types of inflatable structures.

1.3 PRESENT AIMS

The aim of this thesis was to report on the design and analysis of inflatable dams. The following topics were investigated and broadly divided into the areas of study outlined below:-

(i) A review of the operation, behaviour and construction methods, of existing inflatable dams in Australia and overseas (Chapter 2 and 3).

(ii) Evaluation of existing analytical methods for the static behaviour of inflatable dams, and comparisons of the analysed shape and stresses in the fabric, with those deduced from experimental results obtained from model studies (Chapter 4 and 5).

(iii) Development of existing methods of analysis in static cases, and investigation of new, less complex methods (Chapter 6 and 7).

(iv) Assessment of possible stressing under dynamic conditions from observations in experimental model studies (Chapter 5).

(v) Presentation of relevant data in a form useful to prospective designers (Chapter 10).

(vi) Investigation into other possible forms of inflatable dam and dam fittings, such as inflated tyre tubes (Chapter 9).

CHAPTER 2 - DEVELOPMENT AND DESIGN OF INFLATABLE DAMS

2.1 INTRODUCTION

Four distinct types of inflatable dams exist. The most common type is the Fabridam. The other less well-known types are: - The Buijze - Steel panel type; the Mesnager-Schofield-Parachute type; and the N.B.R.D.C. type. At present all these seem to be in various stages of development.

2.2 IMBERTSON OR FABRIDAM TYPE

This is one of the earliest types of inflatable dam and was invented in the U.S.A. in 1956 by N.M. Imbertson. It was patented in 1960 and has the commercial name of "Fabridam". The construction and operation of the Fabridam already referred to in Section 1.1 will be discussed further in Chapter 3.

2.3 THE BUIJZE OR STEEL PANEL TYPE

This type of dam was designed by J.C. Buijze, in the Netherlands during the sixties. Its design differs from the Fabridam in that a pair of rigid hollow hinged steel flaps or panels are connected between the fabric and the base by means of watertight hinges on the upstream and downstream side, (Diags. 2.1 and 2.2). The operation of this type will be discussed below.

The dam is designed to operate (Refs. 7,8,9) as a temporary, emergency cut off gate in case of a dyke burst with no provision for continuous overflow. Normally the dam would be in a deflated submerged condition. Nevertheless there is no obvious reason why it should not be used in the same way as the Fabridams.

Two dams of this type have been constructed and a further two are under construction. The dimensions of the

DIAGRAM 2.1 - BUIJZE -STEEL PANEL TYPE WATER INFLATED DAM, SHOWN HERE SUPPORTING LIGHT TRAFFIC. THE UPSTREAM AND DOWNSTREAM HEADS APPEAR ALMOST EQUAL.

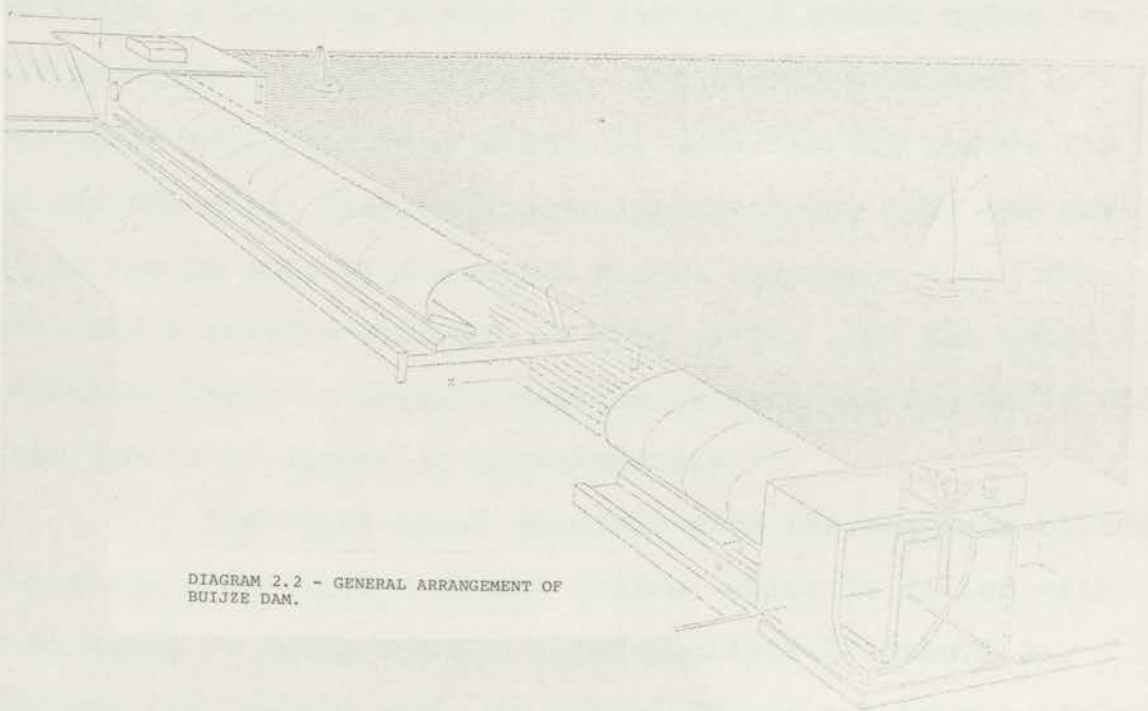

DIAGRAM 2.2 - GENERAL ARRANGEMENT OF BUIJZE DAM.

constructed dams are 40 feet and 95 feet long respectively, and 7 feet and 10 feet high respectively - both being water inflated.

2.3.2 Description of Construction and Operation

The concrete sill, under which a sheet pile wall is initially driven if considered necessary to prevent seepage and scour, is constructed with two vertical abutments. Next, a self-contained steel chest, independent of the foundations and heavy enough to resist overturning moment under operating conditions, and containing the inflatable part of the weir, is positioned on the sill and the inlet/outlet valves connected to the inflation/deflation pumps. Hollow air filled steel flaps C, 1½ feet by 6 feet wide, (see Diag. 2.3(a)) are affixed by watertight hinges B to the steel chest A. Between the edges D of the flaps, a membrane bladder of laminated rubber nylon material E provides a waterproof seal. The curved perimeter is approximately twice the base width, in order to fit inside the casing and the steel flaps are each approximately half the base width, as can be seen from Diagram 2.3(c) and Table 2.1. The material has a tensile strength of 2000 lb/in; for the small dam, a design value of working tension is taken as 280 lb/in width, i.e. the factor of safety is approximately 7.

The steel chest together with the membrane bladder and the flaps constitute a closed casing, which is filled with water by means of pumps through inlets/outlets G (Diag.2.2). For the smaller dam the water is pumped in and out by two electrically operated vertical screw pumps, each with a capacity of 12.5M^3/minute.

The steel flaps have a slight buoyancy and remain

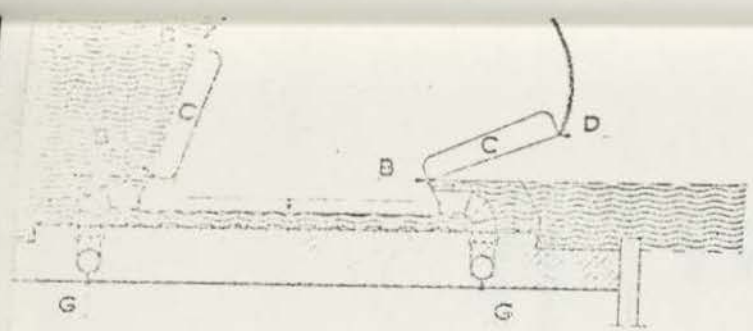

(a)

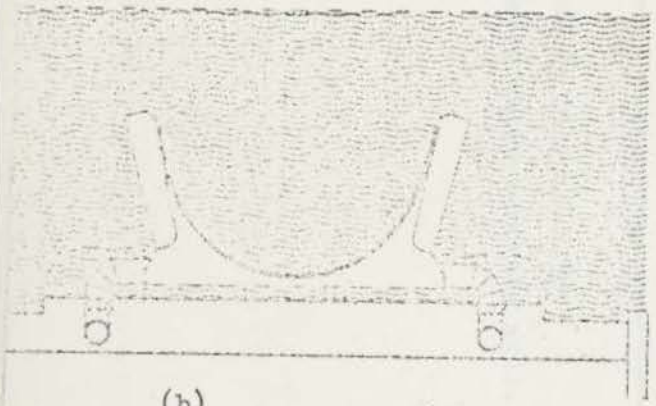

(b)

(c)

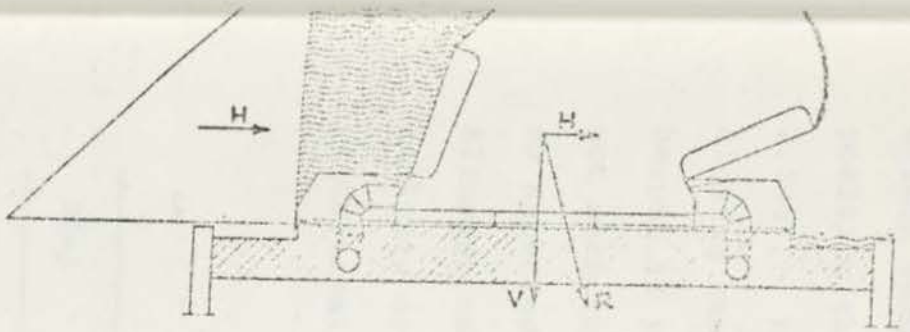

(d)

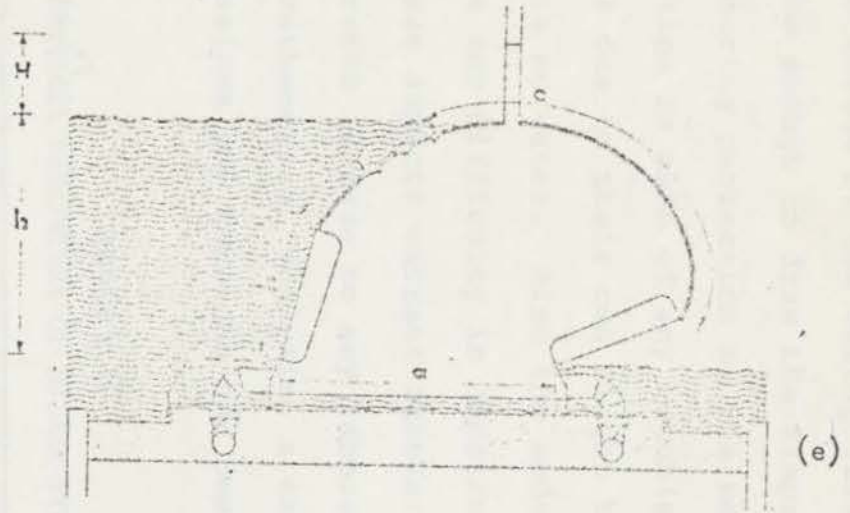

(e)

DIAGRAM 2.3 SECTIONAL VIEWS SHOWING OPERATION SEQUENCE

upright until the membrane is sucked down and stretched tightly along the inside of the casing (Diag. 2.3(b))). This effect seems to be enough to draw the flaps into a closed locked position thus ensuring protection of the membrane bladder (Diag. 2.3(c)). No mention is made of any trouble experienced in closing the flaps due to their own slight buoyancy or what may happen if there is no water. Also the ends of the membrane do not seem to cause any difficulty in construction or operation, as expected. These aspects warrant further investigation. Although no reference is made to any laboratory conducted model analysis or any mathematical analysis, a table of scaled values of critical dimensions and tensions has been included in Table 2.1.

TABLE 2.1+

CRITICAL PARAMETERS OF BUIJZE TYPE DAM

h(m)	a(m)	b(m)	c(m)	H(m)	T(tf/m)	G *
1,00	1,00	0,48	1,92	1,25	0,875	1100 kg
2,00	2,00	0,97	3,88	2,30	3,30	1300 kg
3,00	3,20	1,57	6,28	2,40	5,86	1600 kg
4,00	4.40	2.16	8,64	2,70	9,40	2000 kg
5,00	5,70	2,80	11,20	3,00	12,75	2500 kg
6,00	7,00	3.45	13,80	3,10	18,25	3100 kg

+ Symbols are defined in Diagram 2.3e

* Weight of steel/metre above concrete sill.

2.3.3 Advantages and Disadvantages

(i) Advantages

The steel flaps supply protection, where river traffic such as barges, ships etc. could cause damage to a submerged-deflated dam, which may wave about on the river bed. Under wind and wave attack, the steel flaps would appear to make the dam stiff enough to resist flutter and rolling or snaking action.

(ii) Disadvantages

Disadvantages include the problems of maintenance, hinge lubrication, and problems arising in clamping the membrane to the steel flaps. As already mentioned, occasions could arise where there may be insufficient water to keep the flaps upright when stowing the dam and membrane.

2.4 THE MESNAGER-SCHOFIELD OR PARACHUTE TYPE

A parachute or sheet barrier type of dam as shown in Diagram 2.4 was being investigated by Schofield at the Manchester Institute of Science and Technology, England, for particular use on the Thames for prevention of flooding due to high tides.

This type of dam was actually patented by Mesnager in 1952 (U.S.A. Patent No. 2609666). The advantage of this type of dam is that a single membrane only is used and thus greater economy can be obtained in deep water where there is only a relatively small head differential.

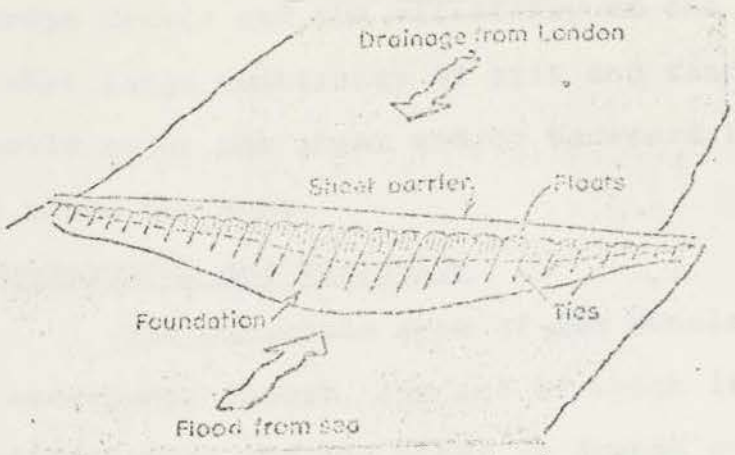

DIAGRAM 2.4 SKETCH OF PARACHUTE DAM

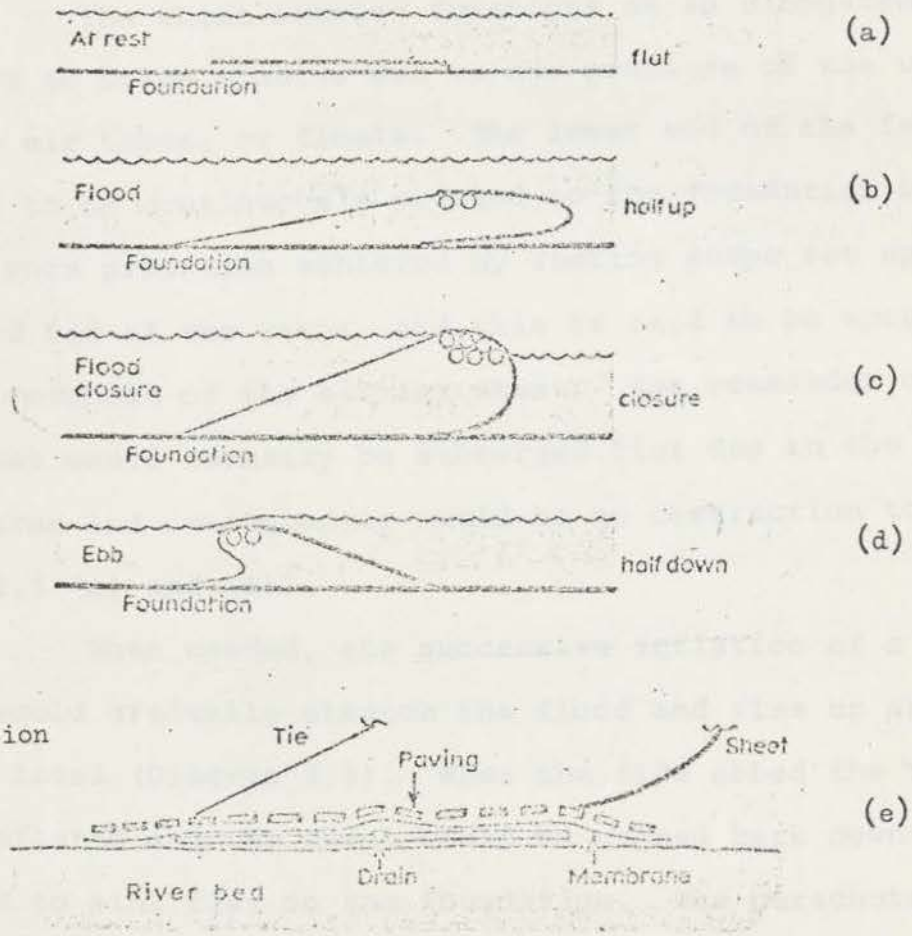

DIAGRAM 2.5 OPERATION OF DAM

The major disadvantages of the system seem to be the anchorage device and the efficiency of the seal, as it is probable that large quantities of silt and sand shifted during a storm could cover the sheet and/or decrease the efficiency of the pumps along the base.

2.4.2 Construction and Operation

The parachute type of dam consists of a single sheet of waterproof fabric, one end of which is attached to the floor of the channel and the other is draped over a series of inflated tubes and attached to tie or anchor lines which are in turn attached to the floor of the channel (see Diagram 2.5).

The sheet barrier functions as an elongated parachute forced to bulge upwards due to the pressure of the upstream head on the air tubes, or floats. The lower end of the fabric sheet seems to be continuously pressed to the foundation by means of reduced pore pressures achieved by suction pumps set up along the base and bed of the river, and this is said to be enough to resist any movement of the barrier sheet. The remainder of the barrier sheet would normally be submerged flat due to the negative pore pressures and consequently would be no obstruction to shipping (Diagrams 2.5 (a) and (e)).

When needed, the successive inflation of a series of floats would gradually staunch the flood and rise up above flood tide level (Diagram 2.5). When the tide ebbed the tubes would be deflated and the sheet would be washed back down-stream and allowed to sink flat on the foundation. The parachute would be designed such that if, while in operation, a vessel collided with the dam, only a panel would be ripped and the rest of the dam would continue to function.

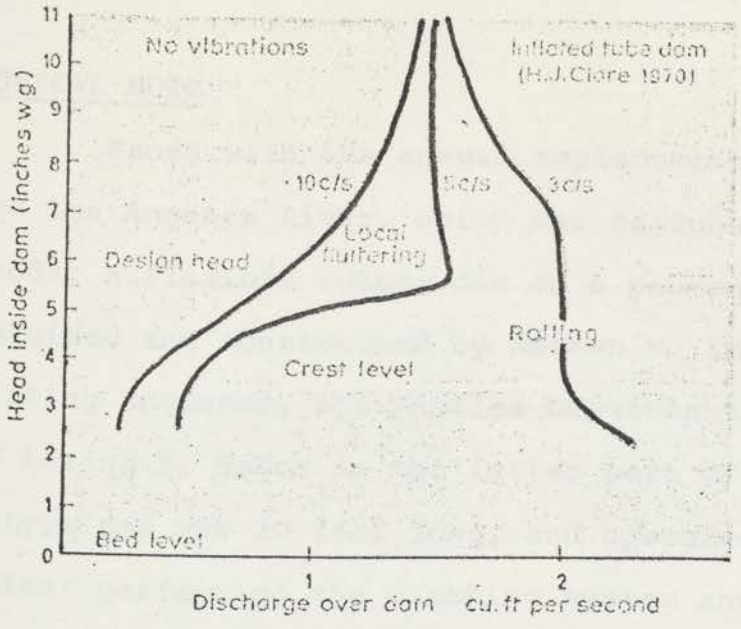

DIAGRAM 2. 6 CONDITIONS OF VIBRATIONS

Model tests have shown that these types of dams can be designed to be stable under water waves and to function without rolling or fluttering under overflows at certain pressure heads (Diagram 2.6).

2.5 B.N.R.D.C. TYPE

A fourth type of inflatable dam is in the process of development by The British National Research Development Corporation (B.N.R.D.C.) and consists of a "series of fabric bags, wedge shaped, with the apex at the bottom and filled with water" (Ref.7). No further information of this type seems to be available, and will not be discussed.

CHAPTER 3 - THE FABRIDAM TYPE INFLATABLE DAM

3.1 HISTORICAL NOTE

Faced with the annual replacement of a timber weir in the Los Angeles River, which was designed to be washed out by floods, a flexible rubber dam on a permanent concrete sill was devised and constructed by Norman M. Imbertson (Water Plant Operating Engineer, Los Angeles Department of Water and Power) and Loring E. Tabor in the latter part of 1957. (Ref. 3c). This prototype dam was 20 feet long, and operated at a height of 5 feet. After perfecting the clamping system and the principle of automatic collapse in flood conditions, they asked Firestone to develop material for a full size dam which was designed to be 130 feet long, 30 feet in circumference, and with 10 feet of bag extended up the sides of the channel at each end. This dam was completed in 1960. The alternative design was a Taintor Gate for $120,000 - but this was rejected because the abutments would cause restriction to flood flows. The Fabridam cost was not stated. The neoprene and nylon fabric was 1/8in. thick and had a tensile strength of 500 lb/in. Automatic deflation was achieved by installing a siphon connecting the water inside of the bag with downstream side of the dam. If the upstream water level built up to a predetermined level the increased pressure primed the siphon which consequently deflated the dam until it lay flat on the concrete sill. Since 1960 Firestone together with Imbertson and Associates has provided material and technical assistance for hundreds of these dams constructed around the world (Refs. 3a,b).

In Australia, seven have been built, five in New South Wales and two in Queensland, six of which are in operation in 1973.

FABRIDAMS UNDER VARIOUS OPERATING CONDITIONS

DIAGRAM 3.1 - PUNCTURED WATER-INFLATED DAM. RUPTURES OF THIS TYPE CAN EASILY BE PATCHED WHILST DAM REMAINS INFLATED.

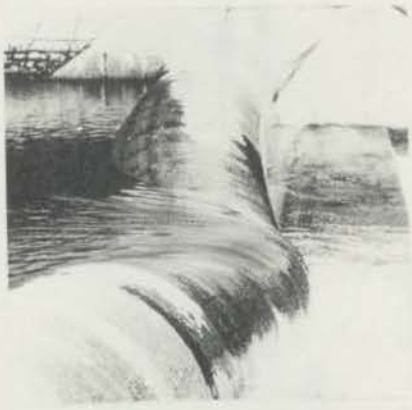

DIAGRAM 3.2 - A VEE-NOTCH ON AN AIR-INFLATED DAM CONCENTRATING THE WATER OVERFLOW. IT IS POSSIBLE FOR A VEE-NOTCH TO OCCUR WHEN $H/h < 1$.

DIAGRAM 3.3 - THE POSSIBILITY OF A SILT LOAD SETTLING ON DEFLATED BAGS SHOULD BE CHECKED IN STRESS CALCULATIONS.

DIAGRAM 3.4 - THE USE OF AN INFLATABLE DAM AVOIDS THE POSSIBILITY OF DEBRIS JAMMING THE GATE. DURING FLOODS FABRIDAMS HAVE PASSED TREES & BOULDERS WITHOUT DAMAGE.

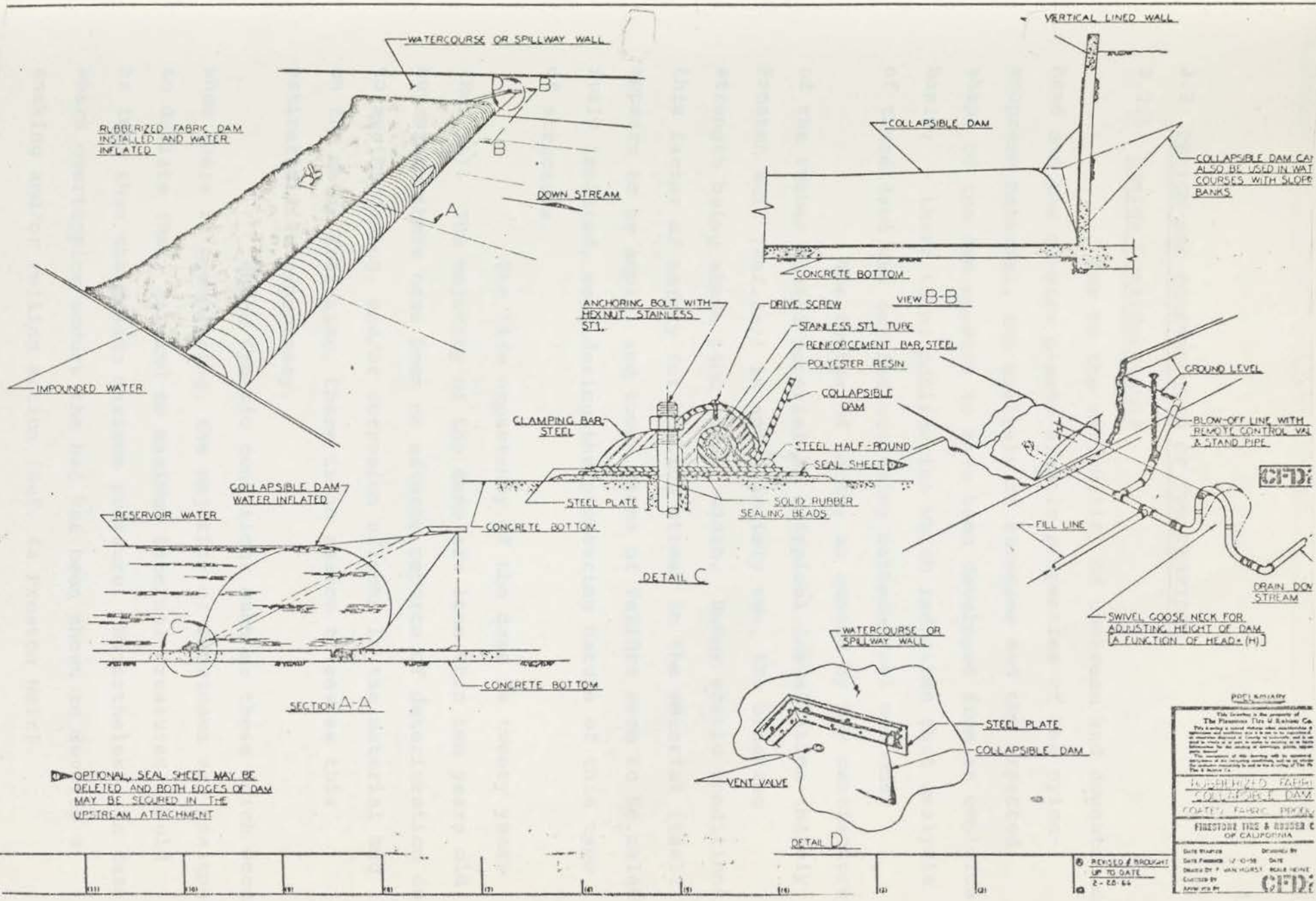

DIAGRAM 3.5 FABRIDAM PLAN – TYPICAL ARRANGEMENT

3.2 DESIGN AND CONSTRUCTION OF THE FABRIDAM

3.2.1 Design Considerations

Due to the variability of upstream and downstream head and the complex plasto-elastic properties of the nylon-neoprene material, the analysis of stresses and the expected shape of the dam appears to have been developed from an empirical basis; - there is no publication which indicates that analysis of these dams was carried out using mathematical methods.

The factor of safety as quoted by the manufacturer, of the rubber coated material in a typical installation (namely Proston Weir (Ref.2a)) is approximately ten, the breaking strength being about 1400 lb/in. width. Under static conditions, this factor of safety for working stress in the material itself appears to be ample, and known cases of failure seem to be relatively isolated, considering the pioneering nature of this type of structure.

The life expectancy of the dams is twenty years (Ref.3A). The majority of the dams are less than ten years old but since there have been no adverse reports of deterioration due to age hardening, and/or corrosion effects in the material and on the metal fastening, there is no reason to revise this estimated life expectancy.

Under dynamic conditions such as these which occur when there is overtopping, the majority of Fabridams are designed to deflate (Ref. 3a) and so maximum internal pressures should be less than the design maximum pressure. Nevertheless, in cases where overtopping occurs the bag has been shown to develop a snaking and/or rolling action (Ref. 4a Proston Weir).

As this rolling action could also occur under conditions of tide or wind waves, there is a fair chance that the dynamic forces generated would be considerably in excess of the design working load and so a high safety factor might be justified if further evidence confirms this speculation.

The designer of such dams, besides applying all constraints normally considered in the design of conventional dams and/or control gates should also consider:-

(i) Availability of power for fluid pumping for bag inflation.

(ii) Availability of inflation fluid.

(iii) Exposure to debris.

(iv) Contamination and freezing of inflation fluid.

Further constraints are listed below, and will be discussed in more detail.

(i) Construction facilities.

(ii) Fabric materials.

(iii) Clamps and anchoring devices.

(iv) Control system.

(v) Design of ends of the bag.

3.2.2 Construction

The Fabridam is usually constructed from a sheet of rubberised fabric folded into a tubular shape, unrolled like a carpet and sealed in place during installation. (See Diags. 3.5 - 3.11). It is fastened to a reinforced concrete slab with structural steel members or clamps and anchor bolts (see Diags. 3.5 and 3.17). Normally a steel cut-off wall is used to keep uplift pressures low and tie the slab into the foundations to prevent scour or seepage.

Where lengths of dam greater than 200 feet are used, it is usual to put in intermediate piers so that:

CONSTRUCTION SEQUENCE OF WATER INFLATED FABRIDAM
ALUMY CK. GRAFTON. N.S.W.

DIAGRAM 3.6 - TIDAL AND FLOOD MITIGATION BARRIER OPERATING AT ALUMY CK. TIDAL WATER (FOREGROUND) IS AT A HIGHER LEVEL THAN THE FRESH. THE POSSIBILITY OF THIS OCCURRING REQUIRED A DOWNSTREAM FLAP TO BE ANCHORED TO THE BASE.

DIAGRAM 3.7 - THE UPSTREAM & DOWNSTREAM CLAMPS HAVE BEEN POSITIONED, AND THE BAG IS MADE READY FOR UNROLLING. NOTE THE SECONDARY FLAPS ON THE BAG. THE SLOPING SIDE WALLS AND TRIANGULAR CONFIGURATION OF THE CLAMPS ENSURES NEAT TYPE 2 ENDS.

DIAGRAM 3.8 - THE OPEN SLEEVE ENDS ARE CUT OFF AND SEALED BY THE CLAMPS.

... CONSTRUCTION ALUMY CK. FABRIDAM

DIAGRAM 3.9 - CLAMPED AND READY FOR INFLATION.

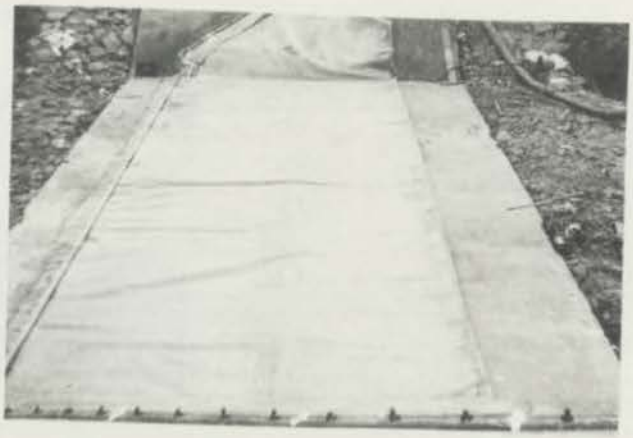

DIAGRAM 3.10 - PARTIAL INFLATION - CHECKING FOR LEAKS.

DIAGRAM 3.11 - FULLY INFLATED ALTHOUGH IT APPEARS TO BE DESIGNED FOR HIGHER UPSTREAM HEADS THAN DOWNSTREAM, THE DAM APPEARED TO FUNCTION SATISFACTORILY WHEN THIS SITUATION WAS REVERSED.

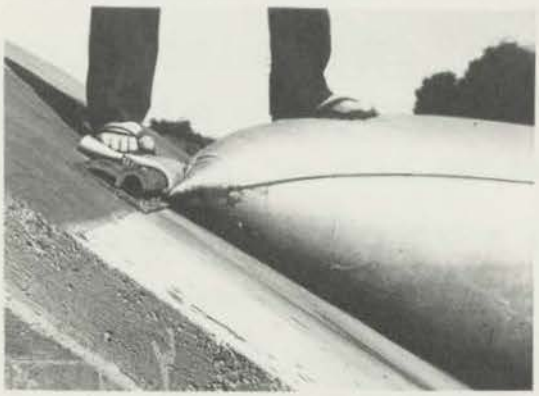

DIAGRAM 3.12 - DETAILED VIEW OF CLAMP CROSS-SECTION.

DIAGRAM 3.13 - A VIEW OF THE TAILORED END CLAMPING JUNCTION AND ASSOCIATED STRESS CONCENTRATIONS. THE PRESSURE RELIEF VALVE ENSURES PROTECTION AGAINST OVER INFLATION.

DIAGRAM 3.14 - THE LARGE CREASES AT THE ENDS OF THE FABRIDAMS. STRESSES ARE PROBABLY DECREASED IN THE CREASE, BUT INCREASED ON THE OTHER SIDE. ALTHOUGH THE BAG APPEARS OVER-INFLATED AT PRESENT WATER MARKS INDICATE EFFICIENCY OF DAM AT HIGH TIDES.

(a) There can be closer control of upstream water level.

(b) If failure of part of the bag occurs the whole length will not be destroyed.

(c) The dam will be more stable should overtopping occur.

3.2.3 Slab and Foundation Forces

The slab should be designed to allow for excess pore pressure and uplift, so that the resultant force due to anchor loads, self weight and friction prevents any overturning moment or sliding movement downstream. For the fully submerged, air inflated case, particular care should be taken to ensure that the buoyant force is less than the dead weight of the bag and concrete slab.

3.2.4 Fabric Materials

The Fabridam fabric is usually constructed of laminations of high strength nylon square woven cloth impregnated with neoprene and coated with hypalon to resist ultra-violet light attack. The material used for the Fabridams is very similar in thickness and content to that used for the side wall of a motor car tyre.

The laminated nylon has a high strength to weight ratio, and the neoprene seals the fabric and provides long-term resistance to weathering and chemical attack.

Some fabric properties, for various plys are given in Table 3.1.

PROPERTIES OF FABRIDAM FABRIC

TABLE 3.1 (REF. 3a).

Construction	Wt/sq yd in.lb	Puncture Resistance	Ultimate Breaking Strength lb/in.
2 ply lt.wt	8.2	200	700
2 ply heavy duty	8.3	370	1400
3 ply heavy duty	10.8	525	1870
4 ply heavy duty	13.3	550	2200

Puncture resistance is measured by Spec. MIL -T- 6396B: it is the force required to rupture a test sample clamped between two 3 inch diameter steel rings with a screw driver point 1/32" x 5/16" forced through the centre of the material at a rate of 12 in/min.

The manufacturer does not give values for the elastic modulus of the material, but Ref. 4a and 12a give values of 300,000 p.s.i. for 4 ply heavy duty material, with no reference to how it was measured. However for the same material, an average value of 33,600 p.s.i. was found in a test where a high deformation electric resistance strain gauge was glued in a central position to side of a specimen measuring 2 inches wide and 8 inches between clamps (Ref.17). The stiffening effect of the strain gauge itself would tend to increase the measured modulus. Despite the difference between results, further review has not led to any doubt about the second result. A question however does arise with respect to the earlier result, as the reported value of the modulus of elasticity for nylon on its own is approximately 300,000 p.s.i. and so for a

composite material containing both rubber and nylon one would expect the modulus to be less.

3.2.5 Clamps and Anchorage System

A working drawing of the Fabridam clamp is shown in Diagram 3.17 below. The usual practice for dams less than five feet high is to clamp both edges of the bag at the upstream edge; in cases where there is a possibility of higher downstream heads than upstream, anchored flaps are attached to the downstream side, as in Diagram 3.15.

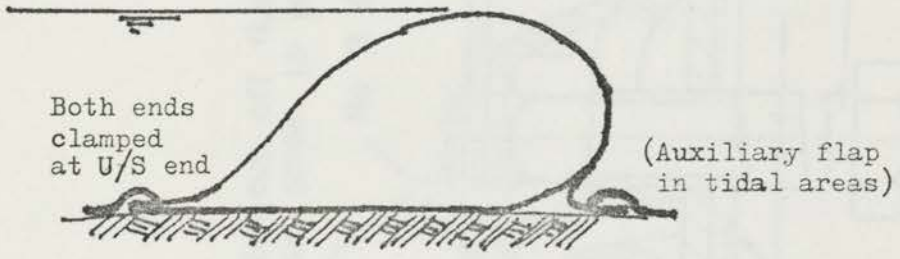

DIAGRAM 3.15 Clamp system for dams less than 5 ft.

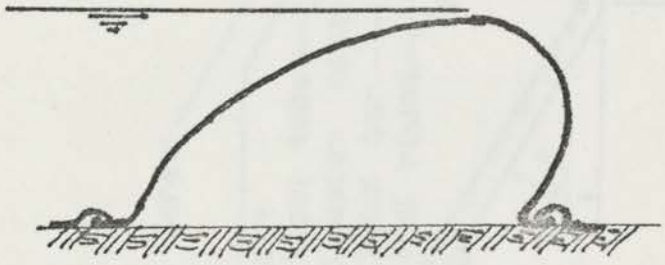

DIAGRAM 3.16 Clamp system for dams higher than 5 ft.

For dams higher than 5 feet, one edge is clamped upstream and the other downstream. Difficulties occurred during the clamping process on the Koombooloomba Fabridam, (Refs. 3 and 13) where the thickness of material to be clamped was increased from 2 and 4 layers due to splicing. Eventually

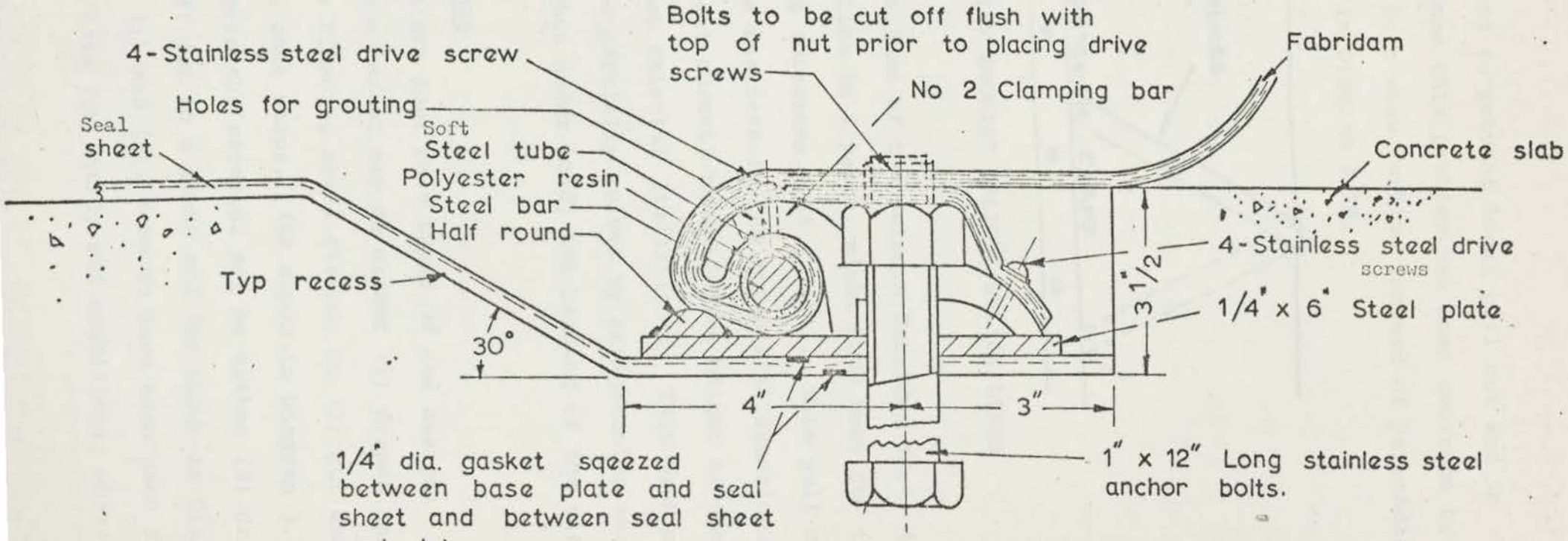

DIAGRAM 3.17 ENLARGED VIEW OF TYPICAL CLAMP DETAILS

larger clamps were used to prevent local pull out and in subsequent installations this problem has been overcome by joining the material in a skew fashion instead of perpendicularly to the clamp line as in Diagram 3.18.

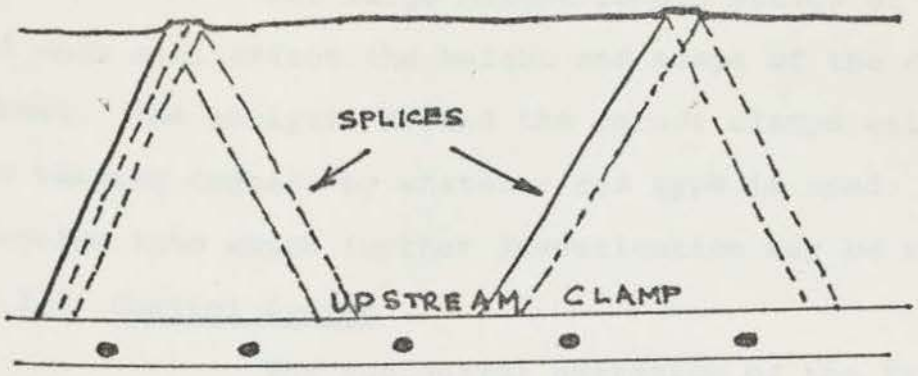

DIAGRAM 3.18 PLAN VIEW SHOWING OBLIQUE SPLICE LINES

The failure of the Belmore Fabridam (Ref. 4a and 18), the second time in 4 years, might have been due to local fabric pull out (Diagrams 3.25 - 3.34). This pull out tendency might be the weakness in the successful functioning of Fabridams, and might curtail the ultimate height of the Fabridam, more so than material limitations. This problem of local pull out may be partially solved by retightening the clamps as the rubber stretches under load, but bending of the clamps must still occur.

3.2.6 Ends of the Bag

There are four main types of end design:-

Sloping Ends: The material may be either (1) draped up the slope and the ends fixed by steel clamps, or (2) cut and formed to a neater cone shape, (as shown in Diagram 3.11).

Vertical Ends: Again the material may be either (3) draped up the side, or (4) cut to a flush end (as shown in Diagram 5.21).

Type (1) and (3), seem to have been used for earlier designs and make for untidy end conditions, whereas (2)

and (4) which are more sophisticated have come into use later on, and are necessary under air inflated conditions to prevent large creasing and ballooning of the ends as occurred in the Model Investigation (Diagram 5.2).

For large height/length ratios of dam, the type of ends will affect the height and shape of the dam along the crest. The analysis around the corner clamps will be complicated to varying degrees by whatever end type is used; this is a problem into which further investigation may be warranted.

3.2.7 Control System

The successful operation of the Fabridam depends on pressure control devices, and in most cases, water level monitoring systems and a pumping system for inflation or deflation of the dam itself.

A wide range of control systems are available, from a simple gravity type fluid feed and automatic siphonic deflation to pump inflation/deflation and valve control, operated from electronic signals obtained by monitoring upstream or downstream waterlevels.

The simplest and most common system for deflation is the inverted "U" syphon which is primed when the upstream waterlevel reaches a predetermined level, which when reached means the dam is then not providing any further useful regulation. This can be seen in Diagram 3.19. Naturally the syphon must be designed so as not to become clogged with weeds or debris. In any case, since allowance must be made for non-calculable effects such as fabric creep, the controls are always made adjustable.

Water is usually favoured as the inflating fluid for smaller dams (height less than 10 feet) and a combination of air/water for larger dams. Where it is necessary to have a small base to height ratio for a short base, or where there is danger of the water inside the Fabridam freezing, air is used.

DIAGRAM 3.19 - OPERATION SEQUENCES OF WATER-INFLATED FABRIDAM

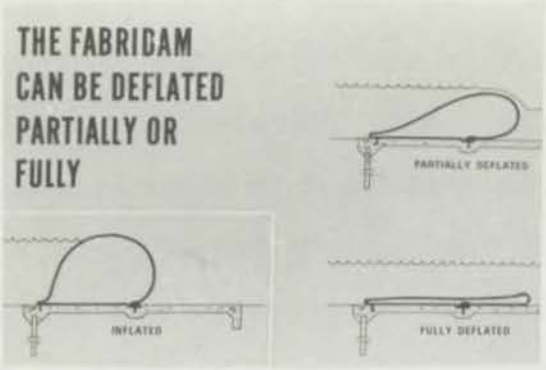

SIPHON OVERFLOW CONTROL

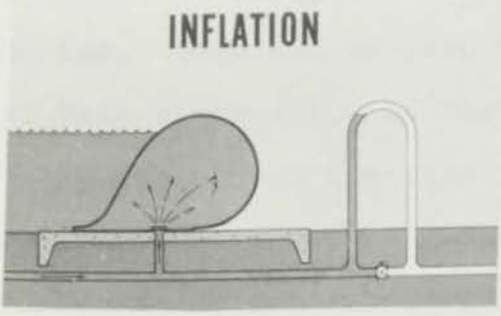

STANDPIPE OVERFLOW CONTROL

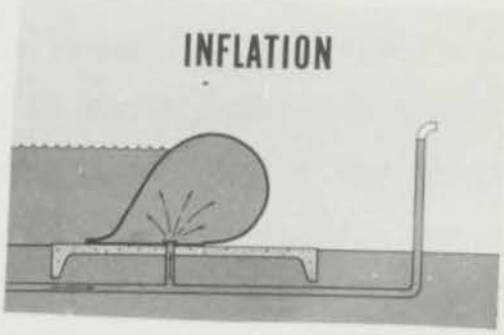

INFLATION PRESSURE (AND HEIGHT) OF DAM IS LIMITED BY HEIGHT OF STANDPIPE.

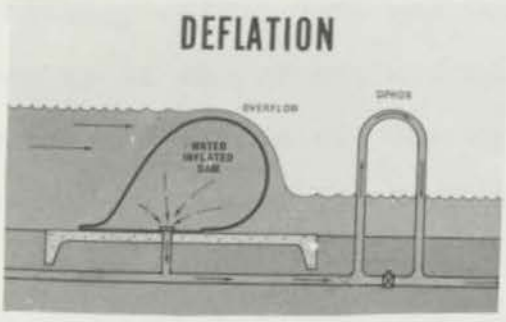

EXTRA PRESSURE DUE TO OVERFLOW CAUSES DAM TO DEFLATE FULLY

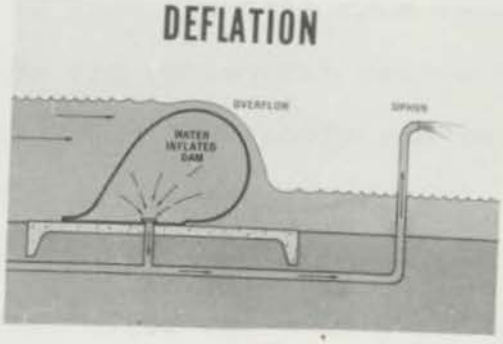

EXTRA PRESSURE DUE TO OVERFLOW CAUSES DAM TO ONLY PARTIALLY DEFLATE.

3.3 FABRIDAMS IN AUSTRALIA

A summary of dimensions and costs of Australian Fabridams are given in Table 3.2 and photographs of some installations are shown in Diagrams 3.20 - 3.24. Usually the base width to height ratio is of the order of 1 to 1½. With the exception of the Belmore dam, which was air/water inflated, all the other dams were water inflated. Also, with the exception of the Belmore dam, the remainder of Fabridams in Australia are working successfully. (A series of photographs documenting the failure of the Belmore dam are shown in Diagrams 3.25 - 3.24).

The N.S.W. Fabridams were built for and costed by the Public Works Department to be 50% less than alternative steel gates, (Ref.4a). Nevertheless it is important to conduct a detailed cost analysis of each case and site before any one system is adopted. This can be seen from the example of the steel radial gate alternative at Para South in South Australia which was built for around the same cost per square foot of dam length by dam height as a Fabridam in N.S.W. or Queensland, (Ref.4b).

3.4 FABRIDAM OF SPECIAL INTEREST

The Mangla Fabridam (Pakistan) appears to be one with features of special interest (Ref.11). This dam, built as a temporary coffer dam, was designed to maintain tail race water-levels so as to prevent hydraulic jumps and subsequent cavitation from forming inside the diversion tunnels during floods and designed to withstand overflows up to 200 cusecs/ft of dam.

While flows were small the inflatable dams (3 sections, each 200 feet wide and 11 feet high) could be deflated, allowing work to be carried out in the tail race structure.

Towards the end of the construction program, one of the bags deflated with overflow at 74 cusecs/ft, and another, one month later, at 95 cusecs/ft, and in view of further damage

TYPICAL FABRIDAM INSTALLATIONS IN AUSTRALIA

DIAGRAM 3.20 - PARTIALLY INFLATED (KINCHELA CK.)

DIAGRAM 3.21 - DEFLATED (KINCHELA CK.)

DIAGRAM 3.22 - CLOSE VIEW OF KINCHELA CK. PARTIALLY WATER-INFLATED FABRIDAM - FLOOD MITIGATION MACLEAY RIVER, N.S.W. - THIS DAM IS DESIGNED TO REMAIN INFLATED DURING THE INTIAL FLOOD PERIOD, THEN ONCE THE BANKS BEGIN TO OVERTOP, THE DAM DEFLATES AND ALLOWS FLOOD WATERS TO ESCAPE INTO A FLOOD PLAIN (BACKGROUND). NOTE THE CONTROL TOWER IN UPPER RIGHT.

DIAGRAM 3.23 - KOOMBOOLOOMBA, FABRIDAM USED FOR INCREASING HEAD FOR A HYDRO-ELECTRIC SCHEME. - A LARGE FLOW DISCHARGING OVER THE CREST, WHILST DAM REMAINS INFLATED.

DIAGRAM 3.24 - A LOG PASSING OVER THE KOOMBOOLOOMBA FABRIDAM. THE OBJECT NUDGES THE DAM THEN WORKS ITS WAY OVER IN A NOTCH FORMED BY ITS OWN WEIGHT.

FEATURES OF SEVEN AUSTRALIAN FABRIDAMS

LOCATION	DATE COMPLETED	LENGTH (FEET)	BASE (FEET) & OPERATING CONDITIONS	FUNCTION	COST OF BASE $	COST OF BAG & CLAMPS $	COST/SQFT OF DAMMED AREA $ (EXCLUSIVE OF BASE)
Koombooloomba Dam - Tully Falls, Qld.	1965	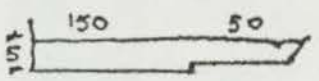		Increasing head and storage for Hydro-electric Scheme	-	$76,000	$76
Proston Weir Stuart River Qld.	1967	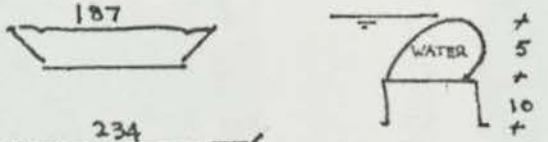		Irrigation	-	Not known	
Tuckombil Richmond River N.S.W.	1966	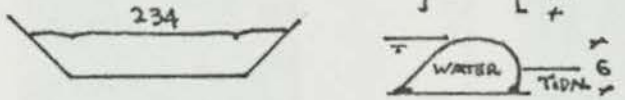		Flood Mitigation	50,000	60,000	43
Kinchela (2) Macleay River N.S.W.	1969	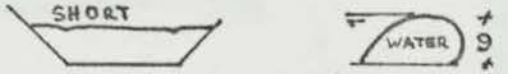		Flood Mitigation	(Total Cost) $29,000 Each		-
Alumy Creek N.S.W.	1969			Irrigation and Flood Mitigation	38,000	25,000	115
Belmore Macleay River N.S.W.	1969	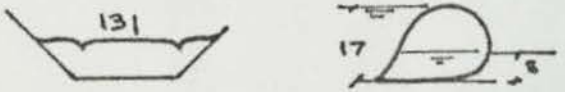		Flood Mitigation	-	80,000	47

AN ECONOMIC COMPARISON OF STEEL RADIAL GATES

Para Sth. South Aust.	1960	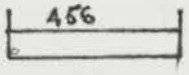		Increased storage	-	44,300	30

TABLE 3.2

BELMORE FABRIDAM FAILURE (1969)

DIAGRAM 3.25 - A VIEW OF FAILURE SHOWING RIPPED FABRIC. FAILURE APPEARED TO HAVE BEEN INITIATED AT RIGHT CORNER OF CLAMP LINES.

DIAGRAM 3.26 - TEAR APPEARED TO PROCEED ALONG BASE CLAMP FOR MORE THAN 100 FT, THEN RUN TRANSVERSELY UNTIL UPSTREAM HEAD LOWERED.

DIAGRAM 3.27 - SECTION OF TORN FABRIC ADJACENT TO WHERE FABRIC PULLOUT OCCURRED.

DIAGRAM 3.28 - STEEL TUBE WITH HOLES USED FOR INJECTION OF EPOXY RESIN VISIBLE. NOTE THE CURVED SECTION WHERE PULLOUT IS BELIEVED TO HAVE INITIATED.

DIAGRAM 3.29 - THE SECTION WHERE PULLOUT OCCURRED NOTE THE CUT EDGES ON EITHER SIDE TO ACCOMMODATE THE CHANGE IN DIRECTION.

BELMORE FABRIDAM FAILURE 1969

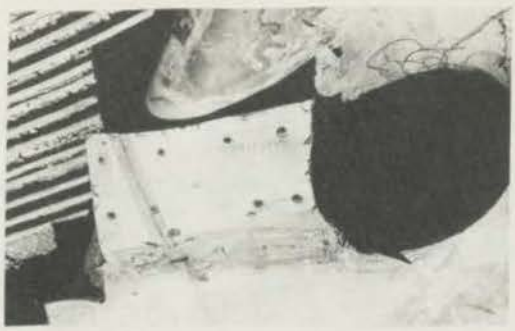

DIAGRAM 3.30 - THE SECTION OF FABRIC WHICH PULLED OUT FROM THE CLAMP.

DIAGRAM 3.31 - THE CORNER SECTION ON THE LEFT HAND SIDE.

DIAGRAM 3.32 - THE LEFT HAND DOWNSTREAM CORNER - OBSERVE THE CONTORTED FABRIC, A POSSIBLE AREA OF STRESS CONCENTRATION.

BELMORE FABRIDAM FAILURE (1973)

DIAGRAM 3.33 - THIS FAILURE STARTED IN THE LEFT-HAND DOWNSTREAM SIDE REGION UNDER A TEST LOAD. IT APPEARED TO RESULT FROM SIMILAR CAUSES TO THESE WHICH CAUSED THE 1969 FAILURE.

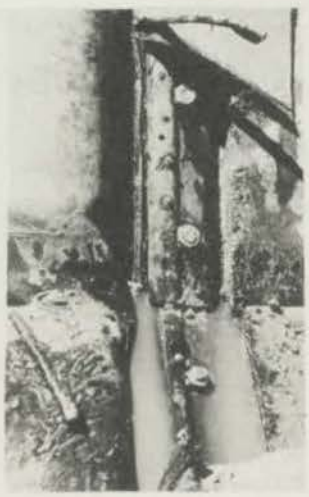

DIAGRAM 3.34 - A VIEW OF SECTION WHERE FABRIC PULLED AND INTERNAL TUBE WHICH HAS PULLED OUT FROM UNDER THE CLAMP.

to the other, the dams were abandoned and replaced by a rock weir (knitted together with steel ropes) which successfully withstood flows of 180 cusecs/ft and velocities of the order of 15ft/2. (Ref. 11).

Prior to the Fabridams construction, a model study was carried out by Baker (Ref.14) and others to investigate its behaviour under continuous overflow, and the more significant of their findings are reported elsewhere in the thesis.

3.5 FAILURES

Besides the failures of the Belmore Fabridam (N.S.W. Australia) and the Mangla Fabridam which were mentioned above, only two other cases of failure have been recorded in the literature:

(i) One of the seven bags in Pennyslvania's (U.S.A.) inflatable dam on the Susquehanna River blew out; failure was attributed to a weak spot in the fabric. (Ref. 5).

(ii) After spring rains and associated debris overtopped the Flandrau Park Dam on the Cottonwood River in Minnesota (U.S.A.) the inflatable bag mounted on the crest was found badly damaged, and needed replacement. (Months later the whole of the dam was washed away in another spring flood). (Ref. 6).

CHAPTER 4 - MATHEMATICAL AND MODEL STUDIES OF INFLATABLE DAMS

4.1 PREVIOUS INVESTIGATIONS

4.1.1 Introduction

Although it would be thought that there would have been many studies carried out and subsequently published on the behaviour of existing Fabridams, or on model and mathematical analyses of these dams only a few papers have been published. Quantitative analyses of the effect of end conditions, of the occurrence of snaking and rolling under overflow conditions, and the effect of surface waves have not been dealt with.

The earliest published report in 1965 found during the present study, is that of Baker (Ref.14) on the inflatable dams used on the Mangla Dam project. A series of tests were made on four models - one eighteen inches wide, and the other three, five feet wide. The paper dealt mainly with the calculation of tension from the experimental shape, the finding of methods of eliminating vibration, and the determination of discharge coefficients. About the same time a model analysis of the Fabridam to be used for crest control on Koombooloomba Dam was made by the Queensland Coordinator General's Department (Ref.13).

The first published mathematical study of the problem was by Anwar (Ref.15) in 1966 in which he analysed forces and shapes for both static and dynamic conditions. Anwar's mathematical results compared well with the results he obtained in a parallel model study. Anwar also calculated discharge coefficients and investigated vibration due to overflow.

In 1969 Harrison (Ref.12) developed a mathematical method of analysis designed for computer, using an iterative process to determine the correct shape of the inflated bag. The method could deal with hydrostatic (that is with no overflow) loadings

with various inflation combinations. The original form of this has been called the Harrison-Newton method to distinguish between it, and a variation developed later in Chapter 7 called the Harrison-Simplex method.

An unpublished study on a test of a model was carried out by Stodulka and Marr in 1970 as part of an undergraduate thesis on "The Design and Behaviour of Inflatable Dams" (Ref. 17). The aim was to compare static shapes and membrane tension of the model with those obtained using Harrison's method. Dynamic overflow cases were also examined and the results were compared with those of Baker and Anwar.

Also in 1969 Ogiwara and others (Ref. 16) made model studies and compared those results with mathematical calculations. Unfortunately full benefit of this work could not be taken because of the difficulty in obtaining an adequate translation of the Japanese in which the paper was written.

The latest mathematical study seems to be that by Binnie (Ref. 23) in 1973 for the analysis of the shape and tension in a water inflated dam with upstream water level at its crest; this appears to be an improved version of Anwar's method. Papers dealing with the construction and behaviour of existing dams in Australia were written by Connor (Ref. 4) on Fabridams in New South Wales and by Wickam (Ref. 4) on the Proston Weir in Queensland. Apart from the largely qualitative investigations of vibration and rolling action (due to the overtopping) of inflatable dams as indicated above, the only quantitative studies of possible relevance have been on the vibrations of less complicated forms of inflatable structures. The inflatable structures for which an in depth study of vibration, deflection,

natural frequencies, and wrinkling has been carried out, are fabric plates (Stroud, Ref. 27 and McComb Ref. 26) air mats, tubular plates, and cylinders, (Leonard and others (Ref. 24) and non-fabric thin walled cylinders and flat sheets, (Stein and Hedgepeth Ref. 25). Unfortunately these analyses did not seem directly applicable to the inflatable dam problem so will not be discussed further.

4.1.2 Previous Mathematical Methods of Analysis of Inflatable Dams

To date, July 1973, it appeared that accounts of four mathematical methods of analysis, - namely those of Anwar (Ref. 15), Harrison (Ref.12), Ogiwarra (Ref.16) and Binnie (Ref. 23), have been published. A brief summary of the conditions analysed and assumptions made in each method has been given in tabular form below. Further comments on the method and problems involved in the Anwar and Binnie Methods and in the Harrison Method follow Section 4.2. Actual computational and quantitative results of the Harrison method will be discussed more fully in Chapter 7.

TABLE 4.1

SUMMARY OF CONDITIONS ANALYSED AND ASSUMPTIONS

ORIGINATOR	YEAR PUBLISHED	CONDITIONS	ASSUMPTIONS
ANWAR	1966	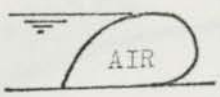	1.(a) Fabric Massless, Inextensible (b) Horizontal base. (c) Downstream fabric tangential to base
		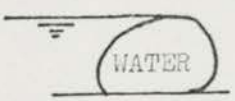	2.(a) As in 1 (b) Vertical component due to wt. of internal water omitted, in calcs
		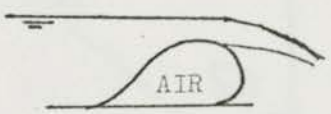	3.(a) As in 1. (b) Water jets off crest.
HARRISON	1969	ALL AIR OR WATER OR 	4.(a) Hydrostatic only. (b) Extensible matl. with mass. (c) Any combination of water levels. (d) On any geometric defined base. (e) Downstream fabric any angle to base.
OGIWARRA et al	1970	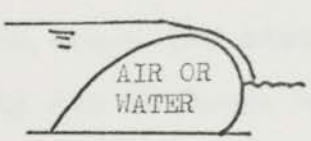	5.(a) As in 1 (b) Static and overflow conditions analysed.
BINNIE	1973	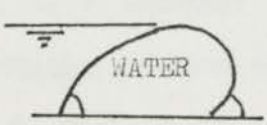	6.(a) As in 1(a) and 1(b). (b) As in 4(e).

NOTE:- aims of all the analyses included theoretical analysis of the shape and tensions.

4.2 ANALYSIS OF INFLATABLE DAMS

4.2.1 General Analysis of Inflatable Structures

From Diagram 4.1 it can be deduced that the tension T, in a flexible massless membrane in equilibrium with the pressure forces only is:

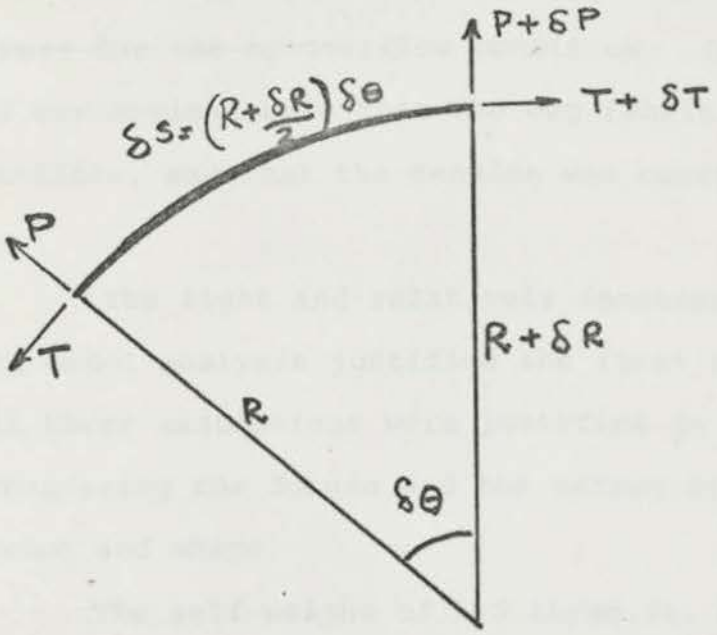

DIAGRAM 4.1 EQUILIBRIUM DIAGRAM

In cases where the analysis consists of coarse nodal elements (such as the analogue method, q.v. Chapter 6, for a typical spacing of 6 inches) the average T and the individual T values around a membrane perimeter differ by less than 4% - (due to the approximation in Eqn. 4.1) - which in many cases is probably an acceptable discrepancy. In the following mathematical methods the membrane tension T has been assumed constant. The implied assumption has been presumably to accept that T is constant, as a convenient working premise, and then to calculate more precise values of T from the primary solution to the membrane shape if desired.

4.3 ANWAR'S MATHEMATICAL METHODS

4.3.1 Introduction and Discussion of Assumptions

Anwar calculated the theoretical shapes of an inflatable dam in air inflated cases for both the no-overflow and the overflow conditions (corresponding to the hydrostatic and hydrodynamic conditions respectively), and in the water-inflated case for the no-overflow condition. In all conditions, the stated assumptions were that the bag fabric was massless and inextensible, and that the tension was constant along the perimeter.

The light and relatively inextensible material used in the model analysis justified the first two assumptions, whereas all three assumptions were justified in the prototype case by considering the forces and the effect of material properties on the tension and shape.

The self weight of 1.5 lb/sq.ft. was negligible when compared to the internal pressure of 600 lb/sq.ft. which was typical of a dam of total perimeter of 80 feet and approximately 20 feet high. From Table 4.2 (Ref.12) the effect of Elastic Modulus and difference in tensions between the upstream and downstream ends of the fabric (for 60 nodes) were also seen to be negligible.

TABLE 4.2 (Ref. 12)

EFFECT OF ELASTIC MODULUS ON TENSION AND SHAPE

ELASTIC MODULUS lb/sq.in	MAX. HT. ft.	AT UPSTREAM CLAMP		AT DOWNSTREAM CLAMP	
		Tension lb/ft.	Slope Deg	Tension lb/ft.	Slope Deg.
30×10^3	21.2	15730	107.1	15790	0.0
30×10^6	19.5	14940	105.2	14950	6.3

Further simplifications considered in the analysis were that the dam was located on a flat slab (as opposed to ogee weir) and the downstream end of the fabric lay tangential to the base. Although these simplifications are reasonable for a first approximation, it should be noted that the tension in the latter condition would be a minimum and allowance be made for appropriate safety factors. For example in case of failure of a pressure release mechanism, the Anwar analysis would become inadequate if the downstream end no longer lay tangential to the base due to an increase in dam height and consequent increase in tension in the membrane.

4.3.2 Analysis of Hydrostatic Case

The no-overflow or hydrostatic case was analysed for a series of internal head to crest height ratios for both air and water inflated cases. The upstream water level was at crest level; this was reasonable in one respect as the designer would usually be interested in the maximum upstream water height for a given internal head; but in another respect according to Harrison (Ref.12) the tension in the fabric could be greater for a lower upstream head as shown in Table 4.3.

TABLE 4.3

DECREASE IN TENSION FOR INCREASED WATER LEVELS IN AIR AND WATER INFLATED CASES

	UPSTREAM HEAD. Ft	TENSION lb/ft
WATER INFLATED Internal Head 35 ft. W.G.	5 19	16120 15055
AIR INFLATED Internal Head 9.3 ft. W.G.	5 20	7600 650

4.3.2(a) Air Inflated Dam

(i) Tension

To obtain the shape and height, and tension in an air inflated dam with upstream waterlevel at crest level, Anwar considered a restricted case where the model was mounted on a horizontal base (as mentioned in 4.3.1) and the membrane (in the vicinity of the downstream clamp) lay tangential to the base.

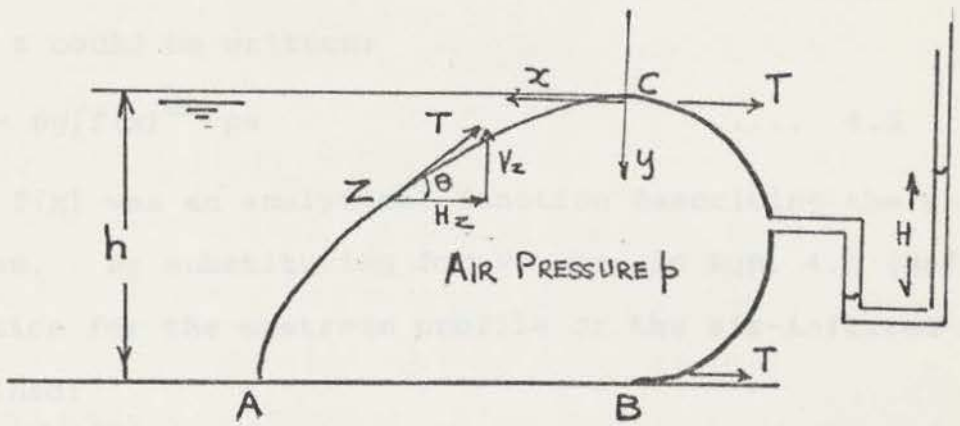

DIAGRAM 4.2 LOADING ON AIR-INFLATED CASE

Although the formula for the tension (Eqn.4.2 below) was used to derive the shape equation, the actual quantitative values of the tensions in the membrane remained unknown until the shape had been theoretically or experimentally obtained. Anwar therefore made the preliminary assumptions regarding shape, as previously mentioned, and as well assumed tension was constant around the membrane.

The value of T was taken as that occurring at the crest: by considering equilibrium through BC or moments about B Anwar obtained the tension formula

$$T = p\frac{h}{2} \qquad \ldots\ldots \quad 4.2$$

where p was the internal air pressure and equal to $\alpha\rho gh$, where α was the proportionality constant and h was the height of the dam.

(ii) Upstream Profile

The differential equation of the shape of the upstream profile was its tangent equation.

This was;

$$\text{Tan } \theta = \frac{dy}{dx} = \frac{Vz}{Hz} \qquad \ldots\ldots \quad 4.3$$

The horizontal component of the tension in the membrane, for unit length at an arbitrary point Z was

$$Hz = \tfrac{1}{2}\alpha\rho gh^2 + \tfrac{1}{2}\rho gy^2 - \alpha\rho ghy \qquad \ldots\ldots \quad 4.4$$

This vertical component for unit length acting at point z could be written;

$$Vz = pg\int f(x)^{dx}\, px \qquad \ldots\ldots \quad 4.5$$

in which f(x) was an analytical function describing the shape of the dam. By substituting for Vz, Hz, in Eqn. 4.3 (Ref.15) an equation for the upstream profile of the air-inflated dam was obtained:

$$\frac{x}{h} = \sqrt{2\alpha}\{2\hat{E}(\sqrt{\alpha}) - \hat{F}(\sqrt{\alpha}) - E\left[\text{arc cos } (\tfrac{\eta}{\alpha}-1), \sqrt{\tfrac{\alpha}{2}}\right]$$

$$+ \tfrac{1}{2}F\left[\text{arc cos}(\tfrac{\eta}{\alpha}-1), \sqrt{\tfrac{\alpha}{2}}\right]\} \qquad \ldots\ldots \quad 4.6$$

in which $\eta = \frac{y}{h}$

F and E were simply shorthand notations for $F(k,\phi) - F(k,\phi_o)$ (which represents the elliptic integral $\int_{\phi_o}^{\phi} \frac{1}{(1-k^2\sin^2\phi)^{1/2}} d\phi$) and for $E(k,\phi) - E(k,\phi_o)$ (which represents the elliptic integral $\int_{\phi_o}^{\phi}(1 - k^2\sin^2\phi)^{1/2} d\phi$) respectively. The circumflexion denoted the integrals were complete. Values for x, for specific values of y were obtained by substitution of values of E and F, tabulated in Abramovitz and Steguns' Handbook (Ref. 28) for $k, 0^\circ(2) \rightarrow 90^\circ$ and ϕ, $0^\circ(5) \rightarrow 90^\circ$ where k and ϕ were equal to arcos $(\eta/\alpha - 1)$ and $\sqrt{\alpha}/2$ respectively.

The solution of the profile equation 4.6 indicated that the base width, a, was dependent on the factor α, and values of the dimensionless parameter $\frac{a}{h}$ could be found as functions of α (noting that here $\alpha = (H-h)/h$ Once the profile was determined, equation 4.2 could be applied and the tension determined.

It was interesting to note here, particular limiting features of the membrane shape. When α was equal to 1, Hz at the upstream anchor point A was zero, and nominally the membrane was vertical there; when α was equal to ½, $Hz = \frac{1}{4}\alpha\rho gh^2$ at A and nominally the membrane lay flat at A.

(iii) Downstream Profile

The downstream profile for the air inflated dam with zero downstream head was a semi circle with diameter h, as the pressure was constant around the membrane.

4.3.2 (b) Water Inflated Dam

(i) Tension

Again the following description of Anwar's derivation was based upon the assumptions:-

(i) The anchor point B occurred the same level as O';

(ii) The membrane lay tangential to the horizontal base at B.

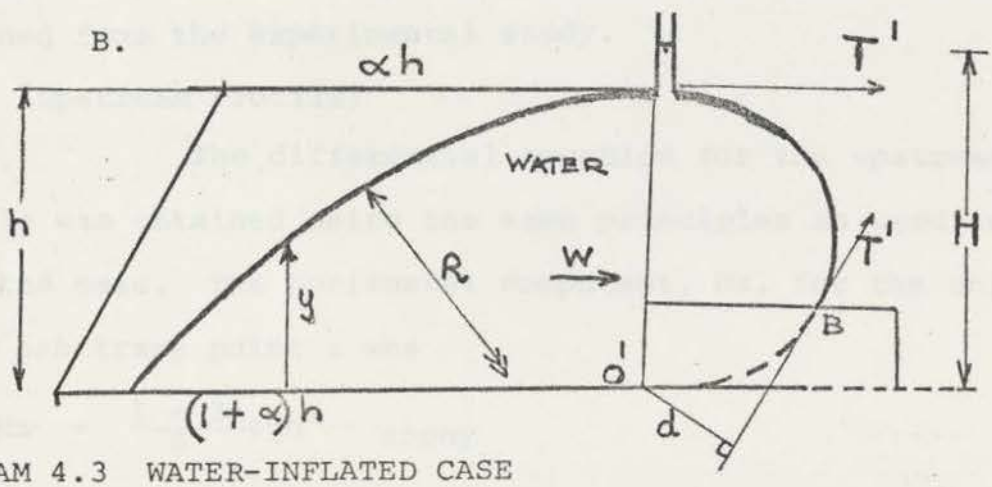

DIAGRAM 4.3 WATER-INFLATED CASE

The step shown in Diagram 4.3 corresponded to the picture of actual solutions obtained by Anwar and was presented

here to indicate a possible inadequacy in his method. The differential water pressure head on the upstream face was equal to αh. Moments were taken about O'; since the horizontal component of the water forces was

$$W = \frac{1 + 2\alpha}{2} \rho g h^2$$

and this had a line of action $(\frac{1 + 3\alpha}{1 + 2\alpha})\frac{h}{3}$ above O', then the tension at the top of the crest was:-

$$T = \frac{(1 + 3\alpha)}{6} \rho g h^2 \qquad \ldots\ldots \quad 4.7$$

In cases where the line of action of the force at B did not pass through O', the extra moment T'd ought to be taken into account. Also in this derivation of tension, Anwar neglected the unbalanced vertical component of moment due to the force

$$V = \rho g \int f(x)\, dx \qquad \ldots\ldots \quad 4.8$$

where f(x) was a function describing the shape of the dam. The effect of this omission which was carried through the remainder of the profile analysis, will be discussed in Section 4.5 where the results are compared with both those of Binnie and those obtained from the experimental study.

(i) (Upstream Profile)

The differential equation for the upstream membrane profile was obtained using the same principles as used in the air-inflated case. The horizontal component, Hz, for the unit length at an arbitrary point z was

$$Hz = \frac{1 + 3\alpha}{6} \rho g h^2 - \alpha \rho g h y \qquad \ldots\ldots \quad 4.9$$

The vertical component for a unit length acting at point z was given by

$$Vz = - \alpha \rho g h x \qquad \ldots\ldots \quad 4.10$$

The tangent θ at the point z of the dam could be written as

$$\frac{dy}{dx} = \tan\theta = -\frac{-\alpha\rho ghx}{\frac{1 + 3\alpha\ \rho gh^2 - \alpha\rho ghy}{6}} \qquad \ldots\ldots\ 4.11$$

Again, operating on this equation the shape of the upstream face was given by the equation of a circle

$$\varepsilon^2 + \eta^2 = \frac{1 + 3\alpha}{3\alpha} \cdot \eta \qquad \ldots\ldots\ 4.12$$

with radius $(1 + 3\alpha)/6\alpha$

$$\varepsilon = \frac{x}{h} \text{ and } \eta = Y/h$$

The fact that the upstream face of a water-filled envelope under hydrostatic conditions had to be a part of a circular cylinder was immediately apparent for the conditions of constant pressure difference and uniform skin tension.

As the tension equation (4.7) was inexact because of the omission of the vertical component, equation (4.12) was also in error. A comparison between this theoretical shape and that of Binnie's will be compared to the experimental shapes obtained by the author in Section 4.5.

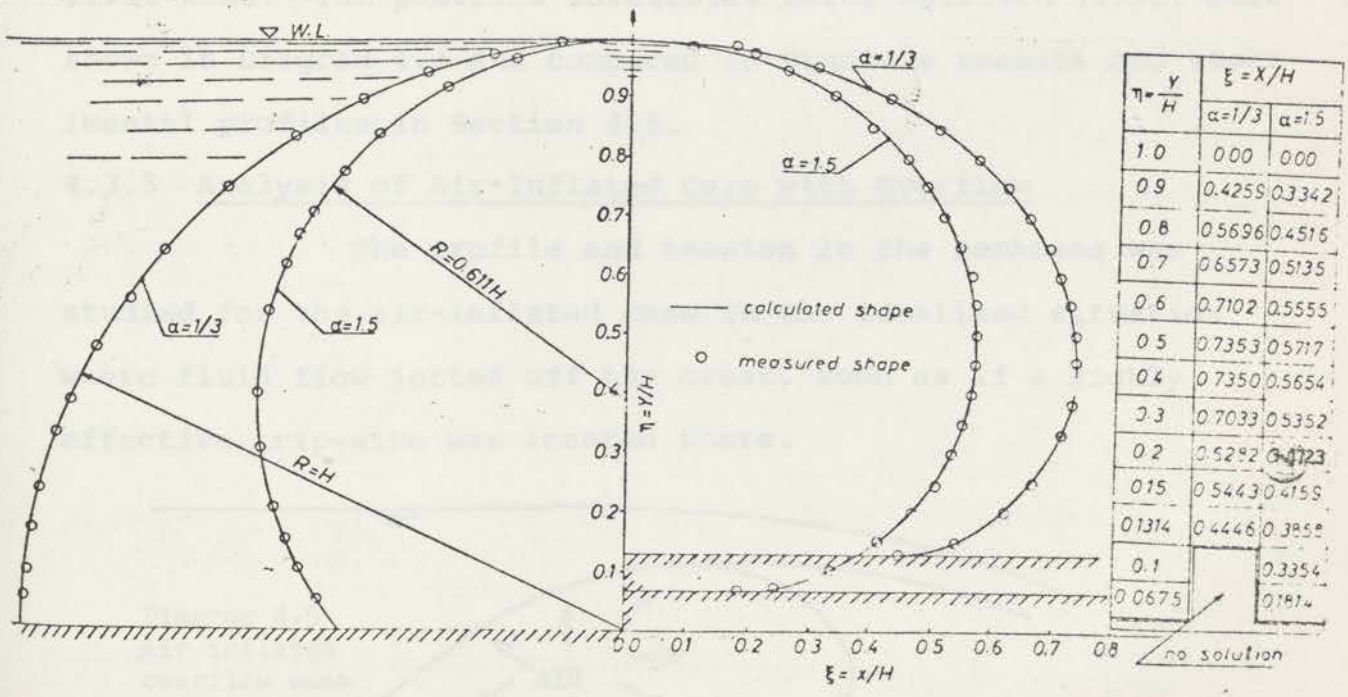

$\eta = \frac{Y}{H}$	$\xi = X/H$	
	α=1/3	α=1.5
1.0	0.00	0.00
0.9	0.4255	0.3342
0.8	0.5696	0.4516
0.7	0.6573	0.5135
0.6	0.7102	0.5555
0.5	0.7353	0.5717
0.4	0.7350	0.5654
0.3	0.7033	0.5352
0.2	0.6292	0.4723
0.15	0.5443	0.4155
0.1314	0.4446	0.3858
0.1		0.3354
0.0675		0.1814

DIAGRAM 4.4 UPSTREAM AND DOWNSTREAM FACE OF WATER-INFLATED DAM

The difference in the Anwar radius was also compared with Binnie's results and experimental values in Table 4.4 for various ratios of internal and upstream heads.

(ii) Downstream Profile

The downstream face profile was obtained from

$$T = P\,R \qquad \ldots\ldots 4.1$$

where T, the tension in the membrane, was given by equation (4.7); P is the pressure on the downstream face which was given by

$$P = \rho g\{(1 + \alpha)h - y\} \qquad \ldots\ldots 4.13$$

and R, the radius of curvature by

$$R = \frac{(1 + y'^2)^{\frac{2}{3}}}{y''} \qquad \ldots\ldots 4.14$$

Substituting for T, P and R, a final solution may be written

$$\varepsilon + C_2 = \sqrt{2\alpha_1 + \delta}\; E(k_1\phi) - \frac{\delta}{\sqrt{2\alpha_1 + \delta}} F(k_1\phi) \qquad \ldots\ldots 4.15$$

in which E and F were the elliptic integrals of the second and first kind. The profiles calculated using equation (4.15) were shown in Diagram 4.4 and compared to Binnie's results and experimental profiles in Section 4.5.

4.3.3 Analysis of Air-Inflated Case with Overflow

The profile and tension in the membrane was studied for the air-inflated case in the idealized situation where fluid flow jetted off the crest, such as if a highly effective trip-wire was located there.

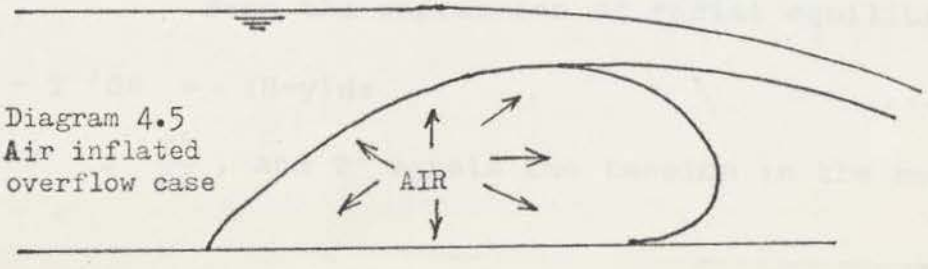

Diagram 4.5
Air inflated overflow case

The theoretical approach then, was essentially the same as in Section 4.32(a), except that allowances were made in the analysis of the upstream profile for velocity and static pressures due to an increased head. The resulting equation was non linear and had to be solved numerically using a digital computer.

[The velocity or dynamic pressure is assumed to have the form of a power series with parabolic shape. The constant s, determined from boundary conditions, were shown experimentally to be governed by a curve of dynamic pressure which approached the water surface height above the upsteam clamp.]

4.4 BINNIE'S MATHEMATICAL METHOD

4.4.1 Introduction

Binnie (Ref.23) observed the misclose at the downstream base clamp in Anwar's solution (Diag.4.4) for the water-inflated case. By using a different approach to Anwar's, Binnie derived equations describing relations between the internal pressure and height and the base width and the length of the curved perimeter of the water inflated dam on a horizontal base with upstream head at crest level.

Whereas the Binnie solutions did not appear to exhibit miscloses for high ratios of internal to upstream heads, a misclose occurred at the crest for low values of internal to upstream head ratios and where the downstream fabric end lay tangential to the base. These miscloses will be shown in Diagrams 4.7 and 4.8 Section 4.5.

4.4.2 Downstream Profile Analysis

From the expression of radial equilibrium,

$$- T^2 d\theta = (H-y)ds \qquad \ldots\ldots \quad 4.16$$

where $T^2 = \frac{T^1}{\rho g}$, and T^1 equals the tension in the membrane, an

expression for the downstream profile not unlike Anwar's, was derived and shown below.

The abscissa of the curve was given by the expression

$$\frac{x}{T} = F(k,\emptyset)-F(R,\emptyset_o)-2\{E(k,\emptyset)-E(k,\emptyset_o)\} \quad \ldots\ldots \quad 4.17$$

where F, and E were elliptic integrals of the 1st and 2nd kind respectively and k and $\emptyset$ were constants to simplify the equation. k and $\emptyset$ are connected by the expressions,

$$k = \{\frac{H^2}{4T^2} + \cos \frac{^2\alpha^1}{2}\}^{\frac{1}{2}} \quad \ldots\ldots \quad 4.18$$

$$\text{and } k \sin \emptyset = \cos \tfrac{1}{2}\theta \quad \ldots\ldots \quad 4.19$$

where α^1 was the downstream fabric angle, and when

$$\theta = 0$$

$$k \sin \emptyset_1 = 1 \quad \ldots\ldots \quad 4.20$$

$$\text{and } \theta = \alpha^1$$

$$K \sin \emptyset_o = \cos \tfrac{1}{2} \alpha^1 \quad \ldots\ldots \quad 4.21$$

The ordinate of this curve was given by

$$\frac{Y}{T} = 2k (\cos \emptyset_o - \cos \emptyset) \quad \ldots\ldots \quad 4.22$$

Associated expressions included the total distance s measured from the downstream clamp to the crest and was given by

$$S/_T = \int_{\emptyset_o}^{\emptyset} \frac{1}{(1 - k^2 \sin^2 \emptyset)^{\frac{1}{2}}} d\emptyset \quad \ldots\ldots \quad 4.23$$

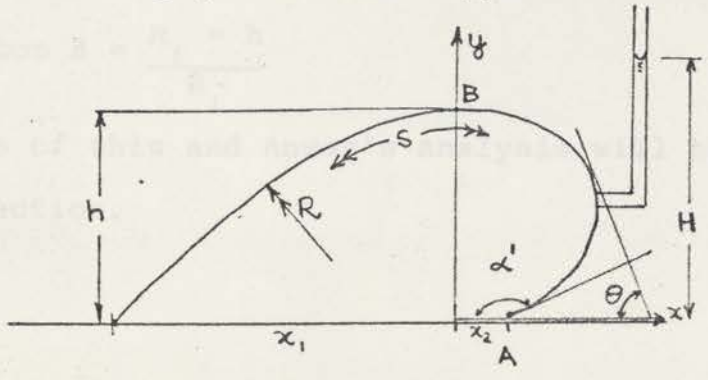

DIAGRAM 4.6 LOADING ON WATER-INFLATED CASE

In these cases compared with those considered experimentally the downstream fabric edge lay flat along the base so

$\alpha = 180^{o}$, and equation (4.18) reduced to

$$k = \frac{H}{2T} \qquad \ldots\ldots \quad 4.24$$

and from equation (4.21), $\phi_o = 0$.

To obtain the values of constants such as k and T for a particular case of known height and pressure ratio, the boundary conditions

$y = h$, and $\phi_o = 0$, $\phi = \phi_1$

were substituted into equation (4.22) to obtain ϕ_1 from

$$\frac{h}{H} = (1 - \cos \phi_1) \qquad \ldots\ldots \quad 4.25$$

Once ϕ_1 was known, k was obtained from equation (4.20) and T from equation (4.24).

4.4.3 Upstream Profile Analysis

The equation of the upstream side was an arc of constant radius because of the constant pressure difference (H-h). Its radius

$R_1 = -\frac{ds}{d\theta}$ was given by

$$\frac{T}{R_1} = \frac{H}{T} - \frac{h}{T} \qquad \ldots\ldots \quad 4.26$$

derived from equation (4.16), and the length of membrane between the crest and anchor point was given by

$$\frac{S_1}{T} = \frac{R_1}{T}\beta \qquad \ldots\ldots \quad 4.27$$

where $\cos \beta = \frac{R_1 - h}{R_1}$ $\qquad \ldots\ldots \quad 4.28$

Results of this and Anwar's analysis will be discussed in the next section.

4.5 COMPARISONS BETWEEN ANWAR'S AND BINNIE'S ANALYSIS, AND EXPERIMENTAL RESULTS (for the water inflated case)

4.5.1 Upstream Profile Comparisons

As the radius of the upstream curve was easily calculable the values of radius R are shown in Table 4.4 for several ratios of internal/upstream head $\frac{H}{h}$ for cases where downstream fabric edge lay flat on a horizontal base.

TABLE 4.4

COMPARISON OF RADII OF UPSTREAM PROFILES OF WATER-INFLATED DAMS BY ANWAR, BINNIE, AND EXPERIMENTALLY

H/h	R/H	R/h	R(FT)	
1.14	1.72	1.96	2.8 ± .1	E (FROM EXP. MODEL)
	1.50	1.72	-	A (ANWAR METHOD)
	2.00	2.26	3.2	B (BINNIE METHOD)
1.26	0.98	1.24	2.0 ± .1	E
	0.95	1.19	-	A
	1.14	1.44	2.3	B
1.38	0.83	1.15	2.0 ± .1	E
	0.68	0.94	1.7	A
	0.89	1.20	2.2	B
1.60	0.56	0.88	1.8	E
	0.49	0.78	1.6	A
	0.58	0.93	1.9	B
1.72	0.46	0.79	1.7 ± .1	E
	0.43	0.74		A
	0.50	0.86	1.8	B

From Table 4.4 it can be seen that neither Anwar's results (which were obtained from formulae neglecting the vertical component of water weight) nor Binnie's results (assumed correct) agree with the experimental results. However Binnie's results agreed more closely with the experimental results for higher internal heads than Anwar's results which were closer to the experimental results for lower internal heads.

4.5.2 Downstream Profile Comparisons

Profiles of only two experimental cases with ratios of H/h equal to 1.38 and 1.60 were compared with profiles calculated by the Binnie method, for the same ratios.

The results Anwar obtained for $\frac{H}{h}$ equal to 1.33 were compared with the above results for $\frac{H}{h}$ equal to 1.38 and it was assumed for the purposes of comparison (namely to show the step misclose obtained by Anwar) that the difference in shape between the Anwar 1.33 case and Anwar 1.38 case would be small when compared to the difference in shape between the Anwar 1.33 and the 1.38 experimental shape.

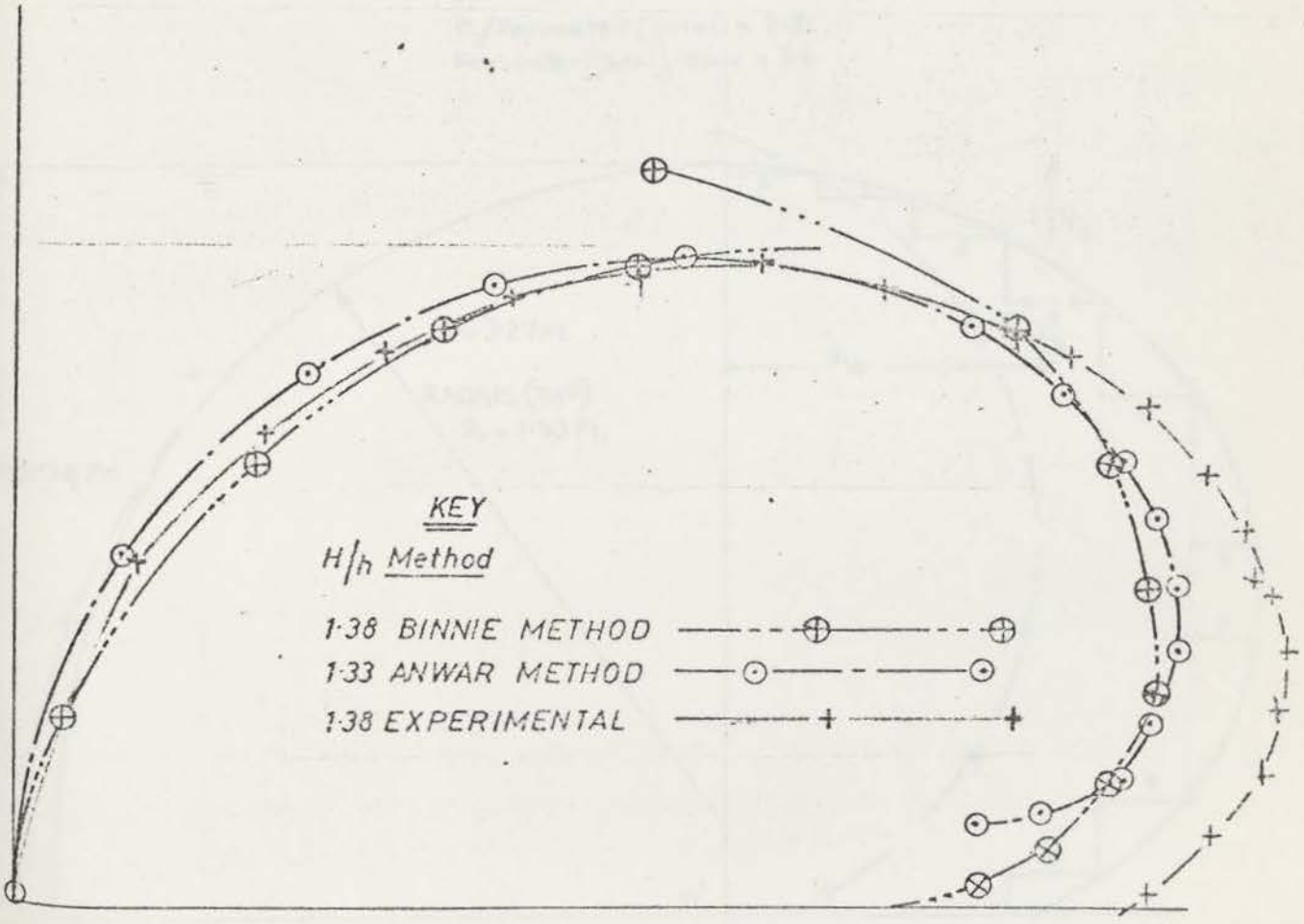

SCALE 1:6

DIAGRAM 4:7 COMPARISON OF PROFILES FOR WATER - INFLATED CASE.

The shapes calculated here, by the Binnie method, were for much lower values of H/h (<2) than those shown by Binnie in his paper (Ref.23). These higher values, ranging between 2.3 and 23.0, are much greater than usual for actual inflatable dams.

The profile shapes were obtained as outlined by Binnie observing the special inversion formulae (in 17.4.15 and 17.4.16 on page 593 in Abramowitz and Steguns Handbook Ref.28) which had to be substituted in cases where k<1.

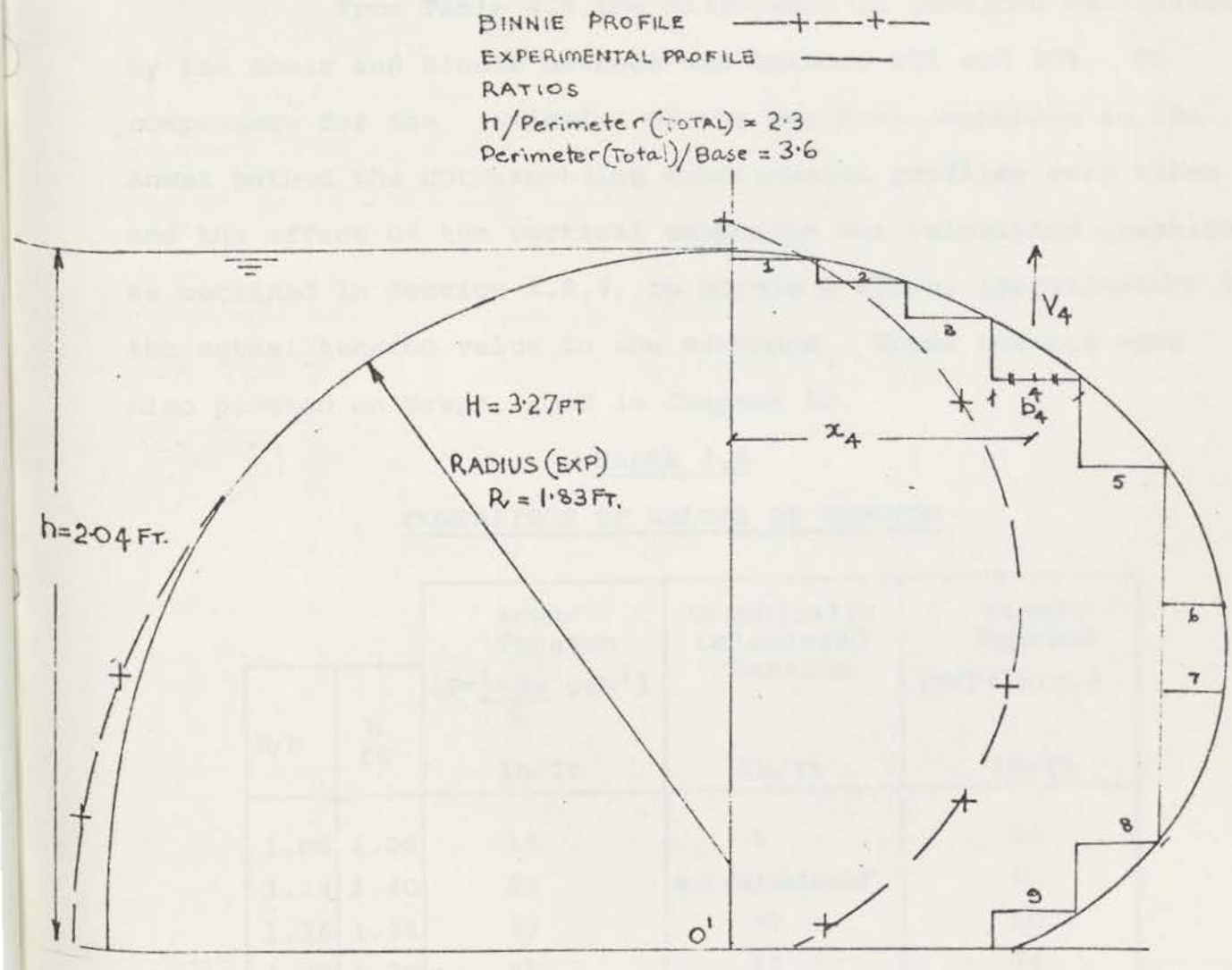

DIAGRAM 4.8 A COMPARISON OF THE EXPERIMENTAL MODEL PROFILE AND THAT CALCULATED BY BINNIE FOR $^{H}/_{h}$ = 1.60. (The D/S Experimental Profile is divided into Segments for the Graphical Calculation of Tension. See Section 4.5.4.)

As can be seen from the profiles in Diagrams 4.7 and 4.8 the agreements between both sets of theoretical results were poor. In the profile by the Binnie method there was a misclose between the upstream and downstream curves at the crest, whilst there was a misclose in the Anwar profile at the downstream anchor point.

4.5.3 Comparison of Values of Tension Derived from the Binnie and Anwar Analyses.

From Table 4.5 the difference in tensions calculated by the Anwar and Binnie methods was between 10% and 20%. To compensate for the omission of the vertical component in the Anwar method the corresponding experimental profiles were taken and the effect of the vertical component was calculated graphically as outlined in Section 4.5.4, to obtain a closer approximation to the actual tension value in the membrane. These results were also plotted on Graph. 10.2 in Chapter 10.

TABLE 4.5

COMPARISON OF VALUES OF TENSION

H/h	h ft	Anwar Tension ($T=\frac{1+3\alpha}{6}\rho g h^2$) lb/ft	Graphically Calculated Tension lb/ft	Binnie Tension ($T=T^{1^2}\rho.g.$) lb/ft
1.06	1.06	14	9	21
1.14	1.40	29	Not Calculated	40
1.26	1.58	47	37	60
1.32	1.70	59	71	74
1.38	1.78	70	67	87
1.60	2.04	122	137	143
1.72	2.12	148	141	170

4.5.4 Graphical Calculation of Tension in Fabric for Water-Inflated Case

Calculations of tension for a typical case are outlined below. The vertical component of force was added to the horizontal component due the horizontal moment as calculated by Anwar (Eqn.4.7) as shown

$$T = \frac{-\Sigma V_n X_n}{h} + \left(\frac{1+3\alpha\varrho gh^2}{6}\right) \qquad \ldots\ldots \quad 4.29$$

where Vn is the vertical force at n and X_n is the horizontal distance from O' in feet as shown in Diagram 4.8 for segment n = 4. Sample calculations are shown in Table 4.6 over.

Columns 1, 2, 3, and 4 list the segment number (n) the moment arm (X), the width of segment n, (b) and the height of n above the base (h_n) in feet respectively. Column 5 is the average difference between internal head and upstream head at n. When multiplied by the width b, the density of water α (lb/ft^3) and the moment arm X, the moment (lb.ft/ft.)is obtained (Column 6). Dividing the sum of column 6 by the height of the dam h gives the additional tension due to the vertical component.

TABLE 4.6

SAMPLE TABLE OF GRAPHICAL CALCULATIONS FOR TENSION

Col. No. 1	2	3	4	5	6
n	x(ft.)	b(ft.)	h_n(ft.)	$H-\left(\frac{h_{n+1}+h_n}{2}\right)$ ft.	5.b.γ x. (lbft/ft.)
1	0.13	0.25	2.04	1.23	+ 2.38
2	0.38	0.25	2.02	1.28	+ 7.51
3	0.63	0.25	1.95	1.36	+13.29
4	0.88	0.25	1.86	1.50	+20.66
5	1.13	0.25	1.67	1.73	+30.33
6	1.33	0.17	1.41	2.06	+28.53
7	1.33	0.17	0.31	2.74	-38.10
8	1.13	0.25	0.11	3.06	-53.63
9	0.88	0.25	0.00	3.21	-43.98

Σ - 33.01 lbft/ft.

From Eqn. 4.29

$$\therefore T = + \frac{33.01}{2.04} + 121.3 = 137 \text{ lb/ft.}$$

for the water inflated case $H/h = 1.60$.

4.5.5 Summary of Comparison Between Anwar and Binnie Methods

Neither of the analyses could easily be applied to the case where one starts off with a known perimeter and base because it would be necessary to first develop a set of dimensionless profiles and then determine the optimum solution by interpolation.

In view of the poor agreement between the theoretical and the experimental profiles at low values of internal/upstream head, and the need for specialist mathematician assistance to solve what appeared to be formidable equations, the Anwar and Binnie methods are not recommended for use in the average design office.

4.6 HARRISON - NEWTON METHOD

4.6.1 Introduction

This method was developed to analyse inflatable dams for loadings due to any combination of upstream and downstream water levels under hydrostatic conditions with air, or water, or a combination of both as the dam inflation fluid.

The two basic assumptions were:-

(i) The behaviour of the three-dimensional structure was represented by a two-dimensional transverse section of unit width.

(ii) The perimeter was composed of a finite number of small straight elements, and the loads acted on the joints.

No restriction was made on the extensibility or mass of the membrane itself, or the geometry of the base, and it would not be difficult to include properties such as flexibility of the fabric if it was thought necessary (e.g. in the case of a steel mesh fabric). The membrane was specified by its base length and the unstretched curved perimeter together with its thickness, and elastic modulus, as shown in Diagram 4.9. The loads acting on the membrane were the upstream water head, the internal and downstream water head, the membrane weight, and the gauge pressure of internal air, or the gauge pressure of the internal water at its highest point.

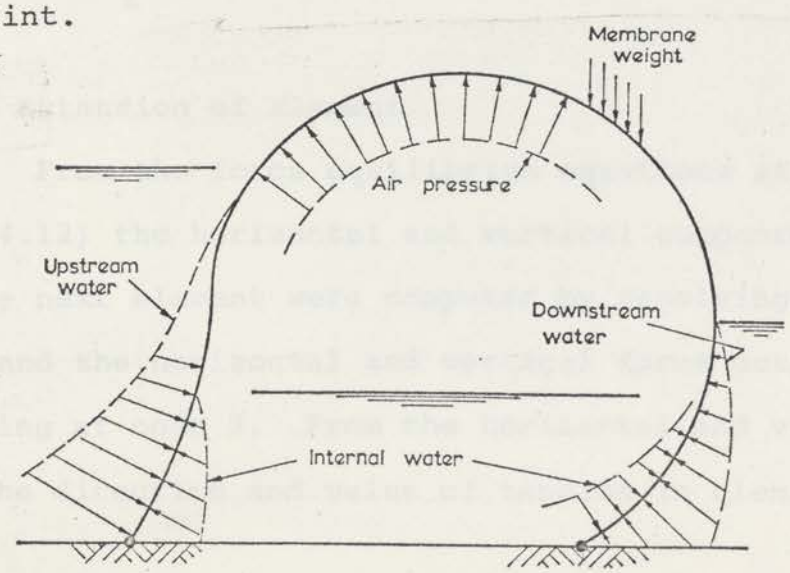

DIAGRAM 4.9 Forces acting on a membrane dam

4.6.2 Method of Obtaining Profile and Tension

To obtain the profile, and tension in the membrane, the membrane was divided into N segments, which ended at N + 1 nodes or joints. The forces acting on a typical node are shown in Diagram 4.10.

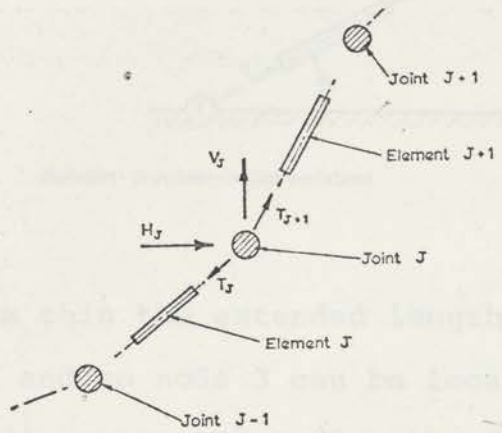

. Finite element analysis element and node forces

DIAGRAM 4.10

The new length, due to the extension (caused by the tension) and the guessed angle determined the position of node 2 (Diagram 4.11).

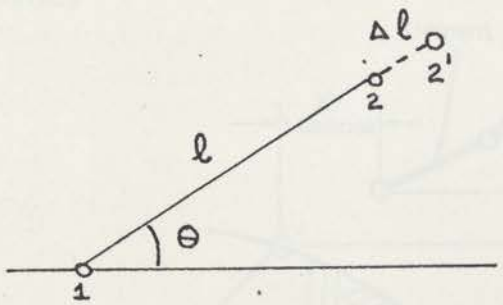

DIAGRAM 4.11 Extension of Element

From the force equilibrium equations at node 2, (see Diagram 4.12) the horizontal and vertical components of tension in the next element were computed by resolving the tension in element 1 and the horizontal and vertical force acting on element 1 acting at node 2. From the horizontal and vertical components, the direction and value of tension in element 2 can be calculated.

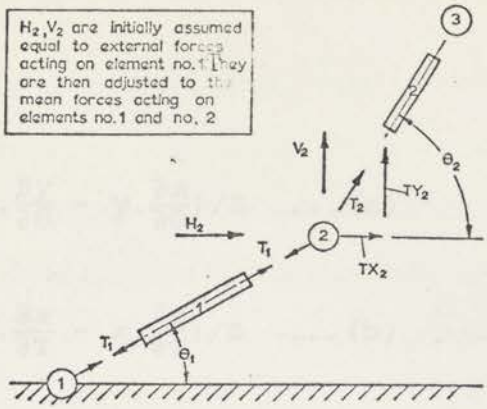

DIAGRAM 4.12 Solution process—initial variables

From this the extended length and direction of element 2 is known and so node 3 can be located. To obtain a more accurate value of direction and angle, the forces on node 2 are recomputed as acting over half of element 1 and 2 and so a better estimate of node 3 can be made.

This procedure was carried on around the whole membrane. At the end of the perimeter length there was a 'misclose' (as in Diagram 4.13) between the end of the fabric and the specified anchor point.

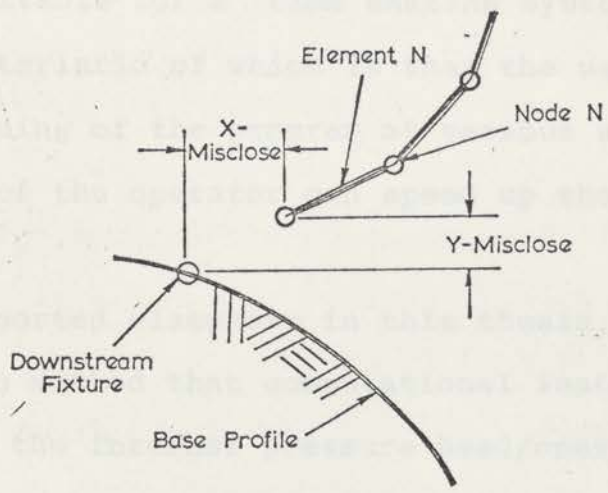

DIAGRAM 4.13 Solution process—calculated miscloses

The misclose could be reduced by carrying out two more numerical analyses for slightly varied values of first, the initial tension, and then, the initial angle. Using the Newton iteration technique (Ref.12) the initial values of tension and angle were corrected.

$$T(\text{improved}) = T - [x.\frac{\partial y}{\partial \theta} - y.\frac{\partial x}{\partial \theta}]/Z \quad \ldots(a)$$

$$\theta(\text{improved}) = \theta - [y.\frac{\partial x}{\partial T} - x.\frac{\partial y}{\partial T}]/Z \quad \ldots(b)$$

$$\text{where } Z = \frac{\partial x}{\partial T}.\frac{\partial y}{\partial \theta} - \frac{\partial y}{\partial T}.\frac{\partial x}{\partial \theta} \quad \ldots(c) \quad \ldots\ldots \quad 4.30$$

The improved values of T and θ were obtained by using the above equations. This would be repeated until the misclose was reduced to the desired value.

Further information on the method and full details of the flow chart for the computer program were given by Harrison in Ref. 12.

4.6.3 Application and Results

The Harrison method did not need a high storage capacity, and was suitable for a 'time sharing system' computer, - the essential characteristic of which is that the user is permitted to interrupt the running of the program at various stages, where intuitive decisions of the operator can speed up the solution process.

As reported elsewhere in this thesis, it was found in using the Harrison method that computational instability could occur in cases where the internal pressure head/crest height ratio was low. This is the sort of case in which the designer is most likely to be interested. Also, difficulty in convergence was experienced if the angle between the downstream end of the membrane and the base was zero.

Due to these difficulties, the Harrison method was altered from the Newton based method of solution, to an improved method called the Simplex method discussed in Chapter 7. To differentiate between the two analyses, the original Harrison program was called the "Harrison - Newton" and the new programme was called the "Harrison- Simplex."

In general the Harrison - Newton method produced theoretical solutions with a much better agreement to experimental results than did either Binnie's or Anwar's methods. A comparison of various experimental results and those obtained from the corresponding Harrison analysis is made in Chapter 7.

4.7 CONCLUSION OF ANALYSIS

4.7.1 Practical Suitability of the Harrison - Newton and Anwar - Binnie Methods.

Unfortunately, all the methods of analysis required care and time to apply them successfully for design, even for the simplest cases. Probably, for the one-off analysis, Anwar's or Binnie's method was better. However, Harrison's method, apart from appearing more accurate, once the computer programme was working, was many times more simple to apply than Anwar's and could be adapted to a wide range of possible loadings, and material properties. Unless a great deal of intuitive ability and understanding of the problem to choose good initial values of tension and upstream angle were used, much valuable time, both of operator and computer, could be wasted.

4.8 SUMMARY OF PREVIOUS MODEL TESTS OF INFLATABLE DAMS

4.8.1 Introduction

Several models of bag dams have been built by independent investigators as well as by Fabridam-Firestone. Published reports on four models only have been found and their findings as well as those of an unpublished report by Stodulka and Marr are summarised below.

The Koombooloomba model (Ref.13) and the Mangla Dam Model (Ref.14) were built chiefly to study dynamic overflow behaviour in actual prototype dams which were subsequently constructed The Anwar model (Ref.15) and the Ogiwara Model (Ref.16) were built to obtain experimental data on both static and dynamic effects for comparison with the results of theoretical calculations. The Stodulka-Marr model (Ref.17) was built to confirm the Harrison analysis; it was specially designed so that the model ends would conform in shape to the rest of the bag, and so the whole bag would behave as a slice of a uniform structure.

Summaries of physical dimensions of previous model tests and of their functions are given in Tables 4.7 and 4.8 respectively.

PREVIOUS MODEL COMPARISONS

MODEL NAME & INVESTIGATOR	YEAR	MODEL SCALE	MODEL DIMENSIONS (INCHES)	MAX. DESIGN, DISCHARGE CU.SECS/FT.	PERIMETER OF MODEL (INCHES)	MODEL MATERIAL	MATERIAL WEIGHT (lb/sq.yd)
KOOMBOOLOOMBA CREST FABRIDAM Co-ord. Gen. Public Works, Q'land.	1965	1:50	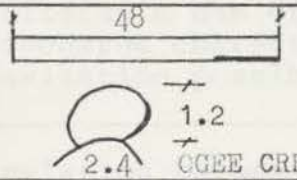	370	-	1. Uncoated nylon. 2. Neoprene coated nylon	.15 .41
MANGLA DAM FAB-RIDAM Brit. Hydromech. Res. Assoc.	1964 1st series 2nd series	1:20 1:20 1:24 1:24	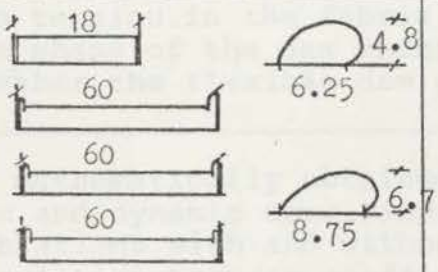	170	23.5 27.8	Rubberized cloth	-
ANWAR MODEL Hyd. Res. Station Wallingford England	STATIC 1966 OVERFLOW		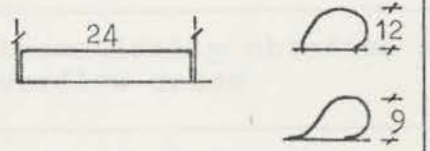	-	-	Polythene (.01 in. thick) U.T.S. 11 to 24 lb/in.	.44
OGIWARRA MODEL JAPAN	1969	-	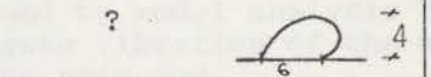	-	-	Polythene?	-
STODULKA-MARR UNIVERSITY OF SYDNEY, N.S.W.	1970	-	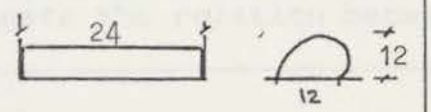	-	38	Neolon fabric	.41

TABLE 4.7

SUMMARY OF MODEL FUNCTION AND ASPECTS CONSIDERED

MODEL NAME	Purpose of Model Test.
KOOMBOOLOOMBA	(a) To examine hydraulic behaviour and stability of inflatable dam. (b) " " inflatable dam effect on spillway and dissipator. (c) " " discharge characteristics. (d) " " cavitation possibility.
MANGLA	(a) To find the relation between discharge and upstream water level. (b) " " the tension in the fabric and the forces on the foundation. (c) " " the shape of the dam under high flows. (d) " " whether the flexible dam would be stable, under operation.
ANWAR	(a) To compare mathematically obtained shapes with those of model data under static and dynamic conditions both with air or water only. (b) To test vibrations with and without trip rod. (c) To test a relation between coeff. of discharge and flow.
OGIWARA	(a) To test mathematically obtained shapes with those of model data for static and overflow cases
STODULKA-MARR	(a) To compare the shapes obtained by the Harrison computer method with those obtained by model analysis for static cases. (b) To investigate vibration of the model under overflow conditions with and without trip rod. (c) To investigate the relation between coeff. of discharge and flow.

TABLE 4.8

4.9 FINDINGS OF KOOMBOOLOOMBA MODEL STUDY

4.9.1 Introduction

Two models, (one of lightweight fabric, and the other of heavier coated fabric) were constructed to study the effect of overflow on a Fabridam installed on the top of an ogee spillway.

The actual bag dam was designed to automatically deflate when the upstream head was about 3 feet above the 5 foot high crest; this was equivalent to a 5000 cusec (or 30cusec/foot) flood. However, the behaviour of the model was investigated for a fully inflated condition with a 75000 cusec flood.

Although the models of the Fabridam were less than two inches high, (corresponding to a prototype dimension of 5 feet) detailed and useful observations were made. The main features of these are summarized below, in Section 4.9.2. The slow heave observed at 75000 cusecs, (which would have increased as the inflation pressure decreased) would probably not have been observed on a larger diameter model with the same or less length, as these effects were dependent on the diameter/length ratio.

4.9.2 Behaviour of Fabridam Model with Overflow

(a) Vibration and Amplitude

Table 4.9 summarises the vibration observed under various flows ranging between 5000 and 75000 cusecs (prototype) for the fully inflated case. Ventilation of the nappe removed any evidence of vibration, and entrapped air pockets inside the model were observed to cause localized disturbances. These two effects were observed for all flows. For the fully deflated case both models exhibited only slight vibration.

(b) Effect of Inflatable Dam on Spillway

The flow down the main dam face was not disturbed by the Fabridam under any conditions.

For a maximum flow of 75,000 cusecs without the bag dam, the maximum negative pressure head developed just downstream from the crest was 5 feet of water. With the inflated bag dam, maximum negative pressure head was 15 feet.

Ventilation of the nappe considerably reduced the negative pressures in all cases.

(c) Effect on Flood Discharge

The effect of the inflatable dam on flood discharge for the same upstream head above the crest, was:-

No bag dam Flow = 75000 cusecs

Fully deflated dam Flow = 74000 cusecs

Fully inflated dam Flow = 52500 cusecs

	FLOW (PROTOTYPE) cusecs					
	5000		45000		75000	
Fabric Type	Lt.Wt.	Coated	Lt.Wt.	Coated	Lt. Wt.	Coated
VIBRATION (Freq.Hz.)	3	Not observed	5	3	10	6
AMPLITUDE (inches) (Prototype Dimensions)	Not observed		1-2	1	3	3
SLOW HEAVE (Freq.Hz.)	Not observed		Not observed		.5	1
AMPLITUDE (inches) (Prototype Dimensions)	"	"	"	"	12	3

TABLE 4.9 VIBRATION OF KOOMBOOLOOMBA MODEL

4.10 MANGLA BAG DAM MODEL

4.10.1 Introduction

At first an 18 inch wide model (1/20 scale) with preformed ends was supplied by Firestone. As it was felt this model might not reproduce the ventilation of the nappe a second model 5 feet wide with material draped up the vertical side walls was built.

For a second series of tests, two more five feet long models, the ends of which were more closely tailored to those of the prototype, were constructed, with the aim of studying the discharge coefficients and the dam's behaviour over a wider range of conditions. A description of the investigations into discharge coefficients, tension, shape of model and vibration analysis are given below in sections 4.10.2 to 4.10.5 respectively.

4.10.2 Discharge Coefficients: (Cd).

Discharge coefficients were evaluated by dividing the discharge/ft x $\frac{1}{\sqrt{2g}}$ by the square root of the mean value of the water head above the crest. The coefficient had values varying from 0.4 at low heads up to 0.5 at maximum discharge. The varying of internal pressure, the attachment of a trip-wire and a small rise in the tail-water of 10% to 20% of the crest height had no measurable effect on the discharge coefficients.

On the second series of tests carried out with a model built to a 1/24 linear scale of the prototype, differential bulging was not evident, as it was in the earlier series, however, the coefficient of discharge, ranging from less than 0.4 to about 0.5, agreed well with values obtained from the earlier models.

4.10.3 Tension in the Fabric and the Effect of Vibration

Estimates of tension, T, in the fabric were made using the same relation as given by equation 4.1:

$T = P R$ where P = Pressure Differential

and R = Radius of Curvature

Pressure due to water flowing over the crest was difficult to measure, so it was assumed that streamlines between the crest and free water surface had a radius of curvature that varied linearly between that of the crest and the free water surface above it. Since these two curvatures were measurable, the lowering of pressure at the crest of the dam due to curvature of the streamlines and hence the tension in the fabric could be calculated.

Tensions were also determined by the use of strain gauges bonded to the fabric near the upstream clamp, where the bending of the fabric was usually least. The strain gauge was calibrated by submerging the model and varying the pressure inside the model. These strain gauge measurements of tension gave values somewhat higher than those calculated from the profiles. This was probably because of the bending action of the fabric, which was not allowed for.

It was observed that raising the tailwater, or decreasing the excess internal pressure diminished the tension. The investigators also concluded that it would be better to place the strain gauges on the neutral axis to eliminate bending effects.

In the second series of tests, a pressure tapping was bonded to the fabric inside the dam, to measure pressure differences across the crest of the model. This allowed the $T = PR$ formula to be used directly.

For both series, the mean tensions in the full scale fabric working under similar conditions were assumed to be proportional to the square of size, and this relation was justified by the present findings.

The increase and decrease of mean tension due to vibration effects, were calculated with the aid of signals from the strain gauges, or alternatively by determining the dynamic

loadingsassociated with the frequency of the vibration and displacement of the fluid, and thence calculating the fabric tension due to this value.

4.10.4 The Shape of the Model Dam

As the discharge over the crest increased, the profile of the model changed due to the reduced pressure around the curved crest. The amounts by which the profiles increased in height are largely dependent on the length of the models, the degree and manner in which the ends are fixed, and whether the downstream edges are anchored to the base or not.

For a 100,000 cusec discharge (Prototype), the central profile of the various models increased in height from between 9% (for the 5ft model with draped ends) to 25% (for the 18" model with preformed ends).

4.10.5 Vibration (or Flutter) and Stability Analysis

At relatively low heads over the crest of the model, and with normal internal pressures the model was stable and tension practically constant. When the discharge was increased, the 5 foot model would vibrate at normal internal pressures and the fluctuations in tension were very large.

This vibration could be stopped and the fluctuations in tension reduced by various means including:-

(i) Touching the model with a hand.

(ii) Artificial aeration of the nappe with compressed air.

(iii) Stiffening the model by attaching rods to it.

(iv) Doubling the normal internal pressure.

(v) Fitting a flexible 'tripwire' causing nappe ventilation.

The last of these methods proved the most practicable so a one eighth inch diameter tripwire was placed in the optimum position - horizontally along the downstream face of the dam just below the crest. The tripwire ventilated the nappe up to a discharge of

100,000 cusecs, above which the cavity became drowned. The optimum position of the tripwire was found to be just below the top of the crest. Doubling the size of the tripwire had little effect.

By introducing a small quantity of air into the dam, the vibrations were only slightly reduced. Also, no appreciable improvement in ventilation was obtained by fixing a pier (at the centre of the model) with two holes in the sides, opposite the tripwires, and connected to the atmosphere through the top of the pier.

4.11 ANWAR'S MODEL

4.11.1 Introduction

As mentioned in the discussion of Anwar's method of analysis (Section 4.3) his model results agreed closely with his theoretical calculations. Although the ends were preformed, it was not stated whether they were clamped or fixed to the sides or not. If the ends were not clamped, one would have expected leakage to occur in the air inflated cases where $H/h < 1$ (see Section 4.10).

Various experimental results are summarized in the sections below.

4.11.2. Coefficient of Discharge, and Vibration (Flutter) Behaviour of the Air and Water Inflated Model

The dimensionless coefficient of discharge was found from the formula $Cd = \frac{q}{\sqrt{2g}\, h^{1\ 3/2}}$

(where h^1 is the upstream height of water above the crest of the bag dam). Cd was found to vary between 0.40 for low flows to 0.50 for high flows and between .38 and .46 for the air and water inflated cases, respectively.

For the range of internal pressures investigated it was found that Cd had lower values for lower internal pressures. This was because the dam crest is broader under these conditions. In addition the values of Cd were slightly lower (approximately 5%) in cases where a tripwire was used to aerate the nappe.

Skin vibration observed under overflow conditions was evidently due to varying pressures caused by oscillations of the downstream water-levels in a partly ventillated or unventillated nappe. Observations showed the air-inflated dam was prone to skin vibration which started at the mid-point of the upstream face when the upstream water height/crest height ratio was 1.25 and reached the crest when the ratio was 1.7. The vibrations increased in magnitude for lower internal pressures.

The skin vibrations were considerably reduced by the positioning of a $^{3}/_{8}$inch diameter tripwire near the crest; the tripwire behaved effectively, provided the nappe was sufficiently ventilated to allow the jet to spring clear.

Similar effects were observed in the overtopped water-inflated cases.

4.12 STODULKA-MARR MODEL

4.12.1 General Description

The model shape was that of a cylinder (see Diag. 4.15) with plane ends flexible enough to enable large deformations to take place and so minimize the constraints exerted by the ends on deformations occurring elsewhere along the length of the cylinder. The model fitted within a perspex channel 2 feet wide and had a perimeter of 3.2 ft. The ends, which were parallel with the sides of the channel were formed of a very flexible and readily extensible membrane of air-cured latex rubber solution, a few thousandths of an inch thick (Diagram 4.14). The cylinder membrane was made of flexible Neolon fabric with a single longitudinal join.

1970 STODULKA-MARR MODEL STUDY

DIAGRAM 4.14 - COLLAPSED, DEFLATED BAG SHOWING FLEXIBILITY OF ENDS.
P = INTERNAL AIR PRESSURE (W.G. INCHES
Hu= UPSTREAM WATER LEVEL (INCHES)
Hd= DOWNSTREAM WATER LEVEL (INCHES).

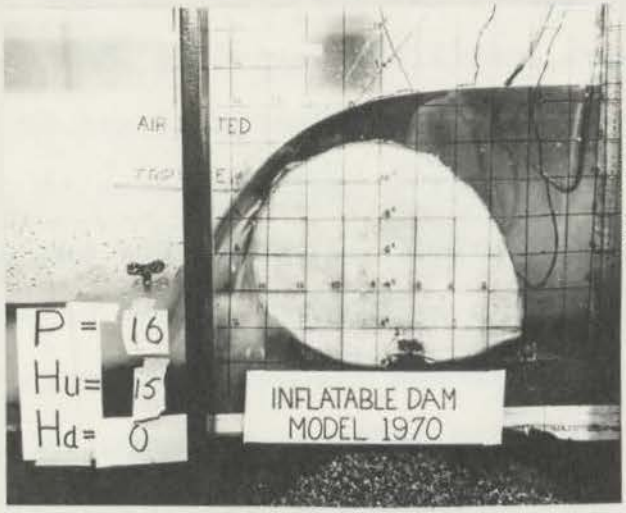

DIAGRAM 4.15 - SIDE VIEW OF AIR INFLATED DAM WITH TRIP WIRE. THE AERATED NAPPE IS A CONSIDERABLE FACTOR IN THE REDUCTION OF VIBRATION. SO AS NOT TO STIFFEN THE BAG THE TRIP-WIRE IS NOT ATTACHED TO THE BAG BUT SUPPORTED BY WIRE FROM THE SIDES OF THE CHANNEL. DUE TO THE LARGE DIAMETER OF THE DAM, A VEE NOTCH WAS NOT OBSERVED. INSTEAD THE SIDES OF THE BAG WOULD COLLAPSE WHEN P/Hu < 1, STARTING FROM THE UPSTREAM CLAMP. THE CLAMP DEVICE IS VISIBLE IN THE BOTTOM LEFT-HAND CORNER.

DIAGRAM 4.16 - A WATER-INFLATED CASE WITHOUT TRIP-WIRE. COMPARE THE SQUAT SHAPE OF THE WATER INFLATED CASE TO THAT OF AIR. ALSO NOTE THE TURBULENCE FREE WATER AND THE LOCATION OF THE STRAIN GAUGES ON THE DOWNSTREAM FACE. THE OVERFLOWING WATER IS SEEN TO CLING TO THE DOWNSTREAM FACE.

The model was attached to a concrete base upstream and downstream along its length, through which two $^{5}/_{8}$ inch diameter brass rods would pass. The brass rods were in turn fed through and 'locked' by inch by inch aluminium channels. These details are shown in Diagram 4.15. No difficulties or distortion in the fabric were experienced in clamping the bag parallel and perpendicular to the flow.

The advantage of the above system was that the sealing of the ends of the model was independent of the clamps. A minor but very practical additional advantage was that the bag could be easily detached from the concrete base if necessary.

An unsatisfactory feature however, was that the bag fabric was not connected tangentially to the base as would be the case in typical prototype dams. This meant there would be significant discrepancies when the model shapes were compared to the shapes computed by other methods.

4.12.2 Instrumentation and Experimental Control

A view of the experimental model set up can be seen in Diagrams 4.14 - 4.16. Two tappings were located in one of the ends to enable water and air to be supplied and internal pressures measured. The upper profile of the central section only was measured using a single pointer profile gauge. As mentioned earlier the section measured was representative of the rest of the bag, as end effects were negligible. A reasonable measurement precision (to within ± 0.05 inches) was obtained, even under conditions of overflow and consequent vibration.

Strains, from which tensions were to be determined, were measured from a pair of strain gauges located centrally on the model, in a transverse and longitudinal direction to the flow. These tension values were compared with those calculated using the radii of curvature obtained from profile and pressure measurements. To determine maximum and minimum tensions which occur during overflow and subsequent vibration conditions, the strain gauge signals were fed through an amplifier to an ultraviolet light galvanometer recorder. Typical recordings for different flows were similar to those shown in Diagrams 5.31 to 5.35.

Vibration was reduced by the placing of a tripwire - a solid brass rod one eighth inch diameter, - across the width of the bag on the downstream face, below the crest. The tripwire was not rigidly fastened to the bag, so the longitudinal and vertical stiffening effect on the bag should have been negligible.

4.12.3 Results of Stodulka-Marr Study

(a) Discharge Coefficients Cd.

Cd varied from 0.25 to 0.4 (in equation $Cd = \frac{q}{\sqrt{2g}\, hc^{3/2}}$) for a range of low flow to a moderate flow of 0.8 cusec/ft. Discharge coefficients were found for cases where inflation was by air, water and by air plus water. The discharge coefficients were accurate to ± 10% which is consistent with the scatter in the values on the graph (Diagram 4.17).

(b) Tension in the Membrane

The tension in the membrane at the crest of the bag dam was calculated by multiplying the measured radius of curvature at the crest and the difference in pressure across the fabric at that point.

In these results, the accuracy was about ± 5% for static cases, and ± 15% for dynamic cases. No attempt was made to measure the external pressure for overflow cases and the effect of neglecting the decrease in radial acceleration would be to undervalue the tensions by about 5%.

The results of electric resistant strain gauges (E.R.S.G.) were likely to need correction to allow for membrane curvature, but whatever the effects of membrane curvature, they were masked by creep effects, temperature effects, and hysteresis in the fabric. To eliminate curvature effects on strain readings, it would be best to take the mean value from a pair of gauges, one on each side of the fabric.

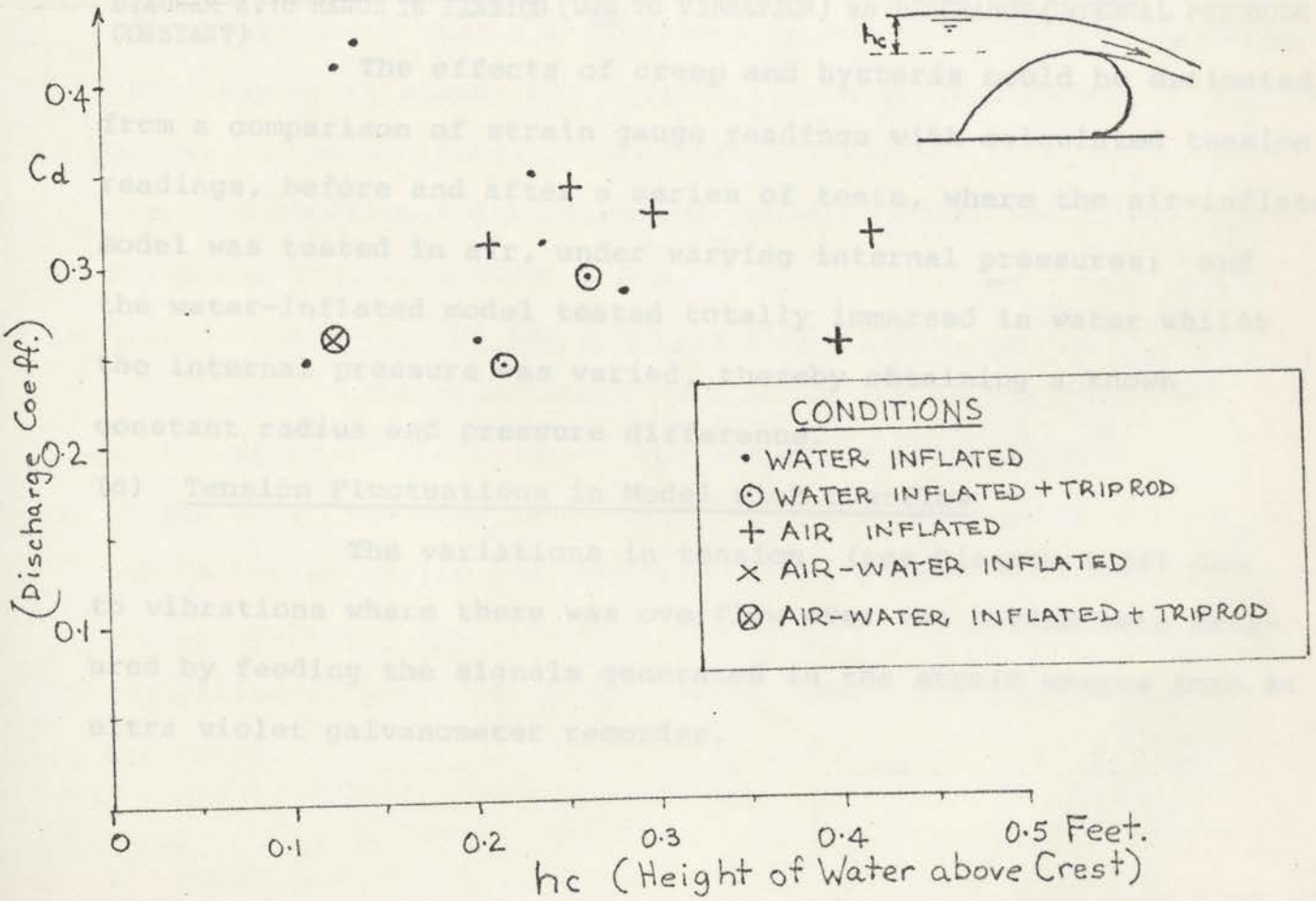

DIAGRAM 4.17 DISCHARGE COEFFICIENT vs HEIGHT OF WATER ABOVE CREST

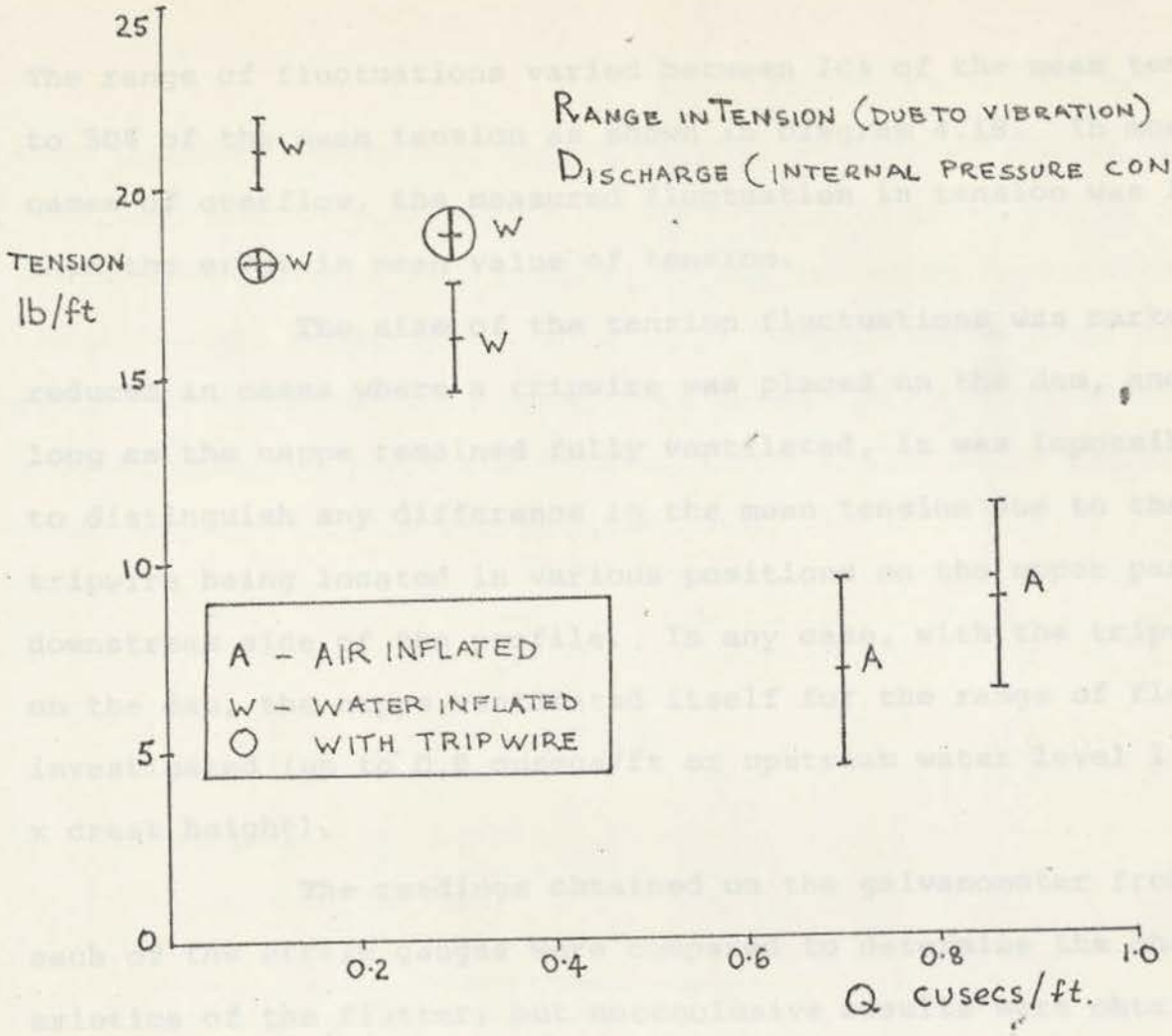

DIAGRAM 4.18 RANGE IN TENSION (DUE TO VIBRATION) vs DISCHARGE (INTERNAL PRESSURE CONSTANT)

The effects of creep and hysteris could be estimated from a comparison of strain gauge readings with calculated tension readings, before and after a series of tests, where the air-inflated model was tested in air, under varying internal pressures; and the water-inflated model tested totally immersed in water whilst the internal pressure was varied, thereby obtaining a known constant radius and pressure difference.

(c) Tension Fluctuations in Model with Overflow

The variations in tension, (see Diagram 4.18) due to vibrations where there was overflow over the bagdam were measured by feeding the signals generated in the strain gauges into an ultra violet galvanometer recorder.

The range of fluctuations varied between 10% of the mean tension to 50% of the mean tension as shown in Diagram 4.18. In most cases of overflow, the measured fluctuation in tension was less than the error in mean value of tension.

The size of the tension fluctuations was markedly reduced in cases where a tripwire was placed on the dam, and as long as the nappe remained fully ventilated, it was impossible to distinguish any difference in the mean tension due to the tripwire being located in various positions on the upper part of downstream side of the profile. In any case, with the tripwire on the dam, the nappe ventilated itself for the range of flows investigated (up to 0.8 cusecs/ft or upstream water level 1.25 x crest height).

The readings obtained on the galvanometer from each of the strain gauges were compared to determine the characteristics of the flutter, but noconclusive results were obtained. It was expected for example that the amplitude may be a function of curvature and that the vibration on the upstream and downstream sides may be in phase, but because of the limited number of strain gauges it was not possible to determine whether this was so or not, and additional investigation would be justified to carry out a further test in a wider flume.

4.12.4 Discussion of the Stodulka-Marr Model

The major model deficiency (which was envisaged at the start of the program) was the large height/length ratio of the dam. The effects of this deficiency were particularly noticeable in static and overflow cases, because when the inflating pressure was low, the ends tended to collapse, allowing large quantities of water to escape between the walls and the ends of the model.

The large height to length ratio also probably restrained any rolling or heaving action as the friction, which could not be eliminated by lubrication, on the ends prevented them from readily moving backwards or forwards under dynamic conditions. This large height/length ratio also prevented the model from lying flat in the fully deflated case. Another deficiency was the dissimilar base fastening compared with typical Fabridam clamps (Diag. 4.19).

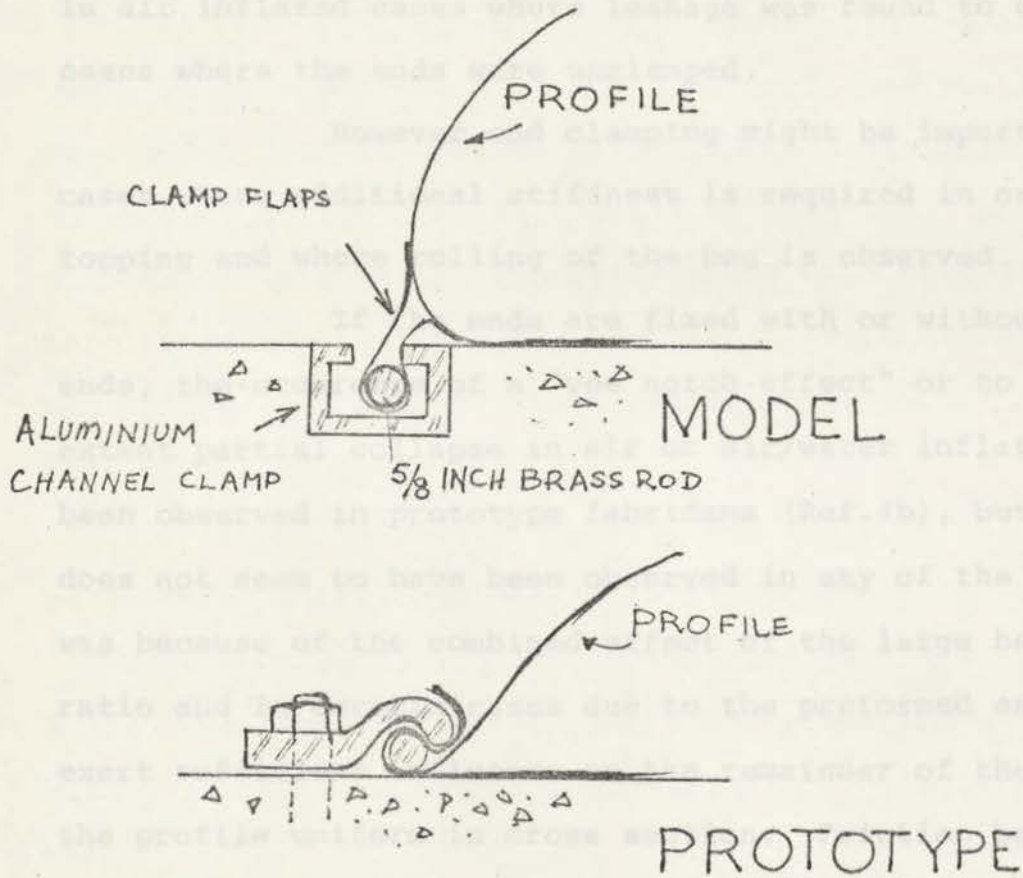

DIAGRAM 4.19 CLAMP DETAIL IN MODEL AND PROTOTYPE

Even so, it was interesting to note that in nearly all cases the upper profile measured from the model corresponded closely with the profile obtained by the Harrison method.

4.13 RESULTS OF MODEL STUDIES AND DISCUSSION OF END EFFECTS

Every model gave results matching to some degree the results obtained from one or other of the analytical methods.

Study of the effects of end conditions seems to have been neglected in all models constructed to date. The clamping of the ends to the vertical walls of the flume in water inflated (or in air inflated cases where $H/h > 1$), where no leakage occurs does not appear to be as important, as when $H/h < 1$ in air inflated cases where leakage was found to occur in the cases where the ends were unclamped.

However end clamping might be important in all cases where additional stiffness is required in cases of overtopping and where rolling of the bag is observed.

If the ends are fixed with or without preformed ends, the occurence of a "vee notch effect" or to a certain extent partial collapse in air or air/water inflated cases, has been observed in prototype fabridams (Ref.4b), but this effect does not seem to have been observed in any of the models. This was because of the combined effect of the large height/length ratio and in certain cases due to the preformed ends which would exert sufficient influence on the remainder of the model to keep the profile uniform in cross section. Friction between the ends and wall of the flume also tended to keep the model uniform in cross section. This lack of investigation into the vee notch effect and end conditions was yet another reason for deciding to build a longer and larger model. The account of this model occurs in the next Chapter.

CHAPTER 5 - MODEL ANALYSIS

5.1 INTRODUCTION

It was decided to build two models, both larger and longer than the 1970 Stodulka-Marr Model to reduce further the effects of end restraints, and also have the clamping system conform more closely to that of the prototype.

The aim of the model analysis was to study the shape profiles under static load conditions and compare these to the profiles calculated by maethematical analysis.

The second, longer model with a smaller height/length ratio would allow the "vee notch effect" (Ref.4b) Section 5.6 to be studied, and in dynamic cases it was anticipated the tendency of rolling action (Ref.4a), could be observed. However, whereas a range of interesting vibration modes were observed, none could be classified distinctly as 'rolling'. This may have been due to the height/length ratio still being too large.

5.2 DESIGN OF TANK

To enable the proposed dam model to be built on a platform, off the concrete floor if necessary, a tank was constructed eighteen feet long, eight feet wide and five feet high (Diagram 5.5). The size of the tank would allow the model to be constructed with its long axis either longitudinaly or transversally across the tank.

A six inch diameter inlet pipe, capable of supplying up to three cusecs, was installed as shown in Diagrm 5.5. It was envisaged that turbulence generated by this asymmetry could be overcome if it arose. The interior of the tank was lined with malthoid, and the joints were heat sealed and covered with 'Pabco Bitupave' for water-proofing.

DIAGRAM 5.1 - INSTRUMENTATION USED FOR PROFILE AND WATER LEVEL MEASUREMENT.

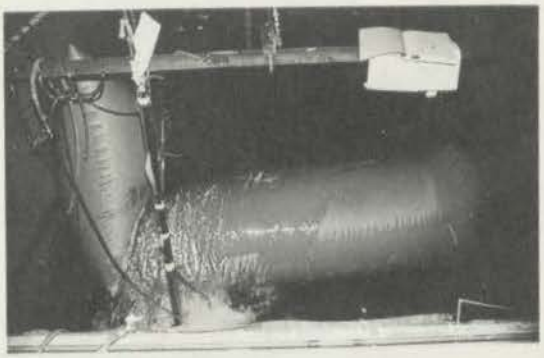

DIAGRAM 5.2 - AN AIR-INFLATED DAM WITH A POPPED END. A LARGE AMOUNT OF WATER ESCAPED BETWEEN THE DAM AND CORNER OF THE WALL AND FLOOR.

DIAGRAM 5.3 - A METAL GUARD WAS PLACED OVER EACH END TO PREVENT THE ENDS FROM POPPING OUT. FROM THE PHOTOGRAPH IT CAN BE SEEN THE DAM IS UNIFORM IN CROSS-SECTION WITH ONLY SLIGHT LEAKAGE.

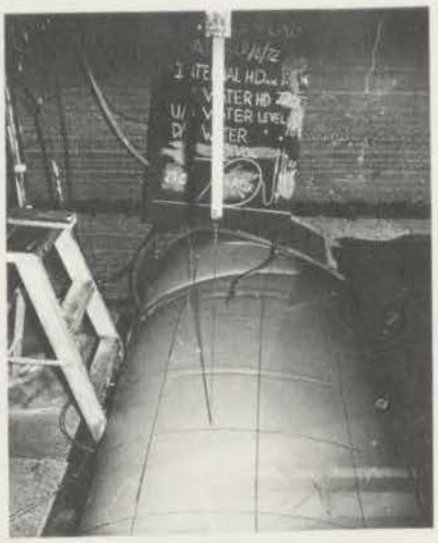

DIAGRAM 5.4 - A WATER-INFLATED DAM. APART FROM ONE OR TWO CREASES APPEARING NEAR THE ENDS, THE DAM BEHAVED UNIFORMLY.

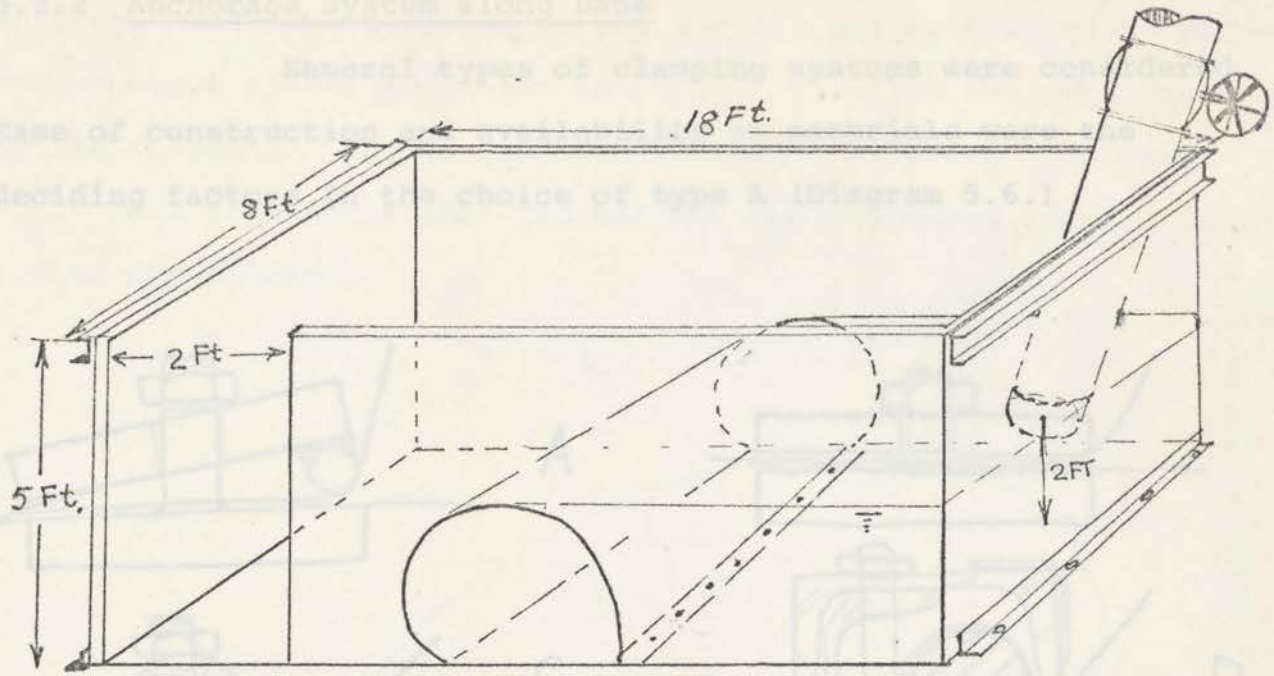

DIAGRAM 5.5 EXPERIMENTAL TANK

5.3 Construction of the Models

5.3.1 Introduction

The major aspects considered in building the two models were the type of clamps to be used and the method of construction of the bags.

Both models were similiar in construction and instrumentation, but any minor differences are discussed in Section 5.5.

5.3.2 Anchorage System along Base

Several types of clamping systems were considered. Ease of construction and availability of materials were the deciding factors in the choice of type A (Diagram 5.6.)

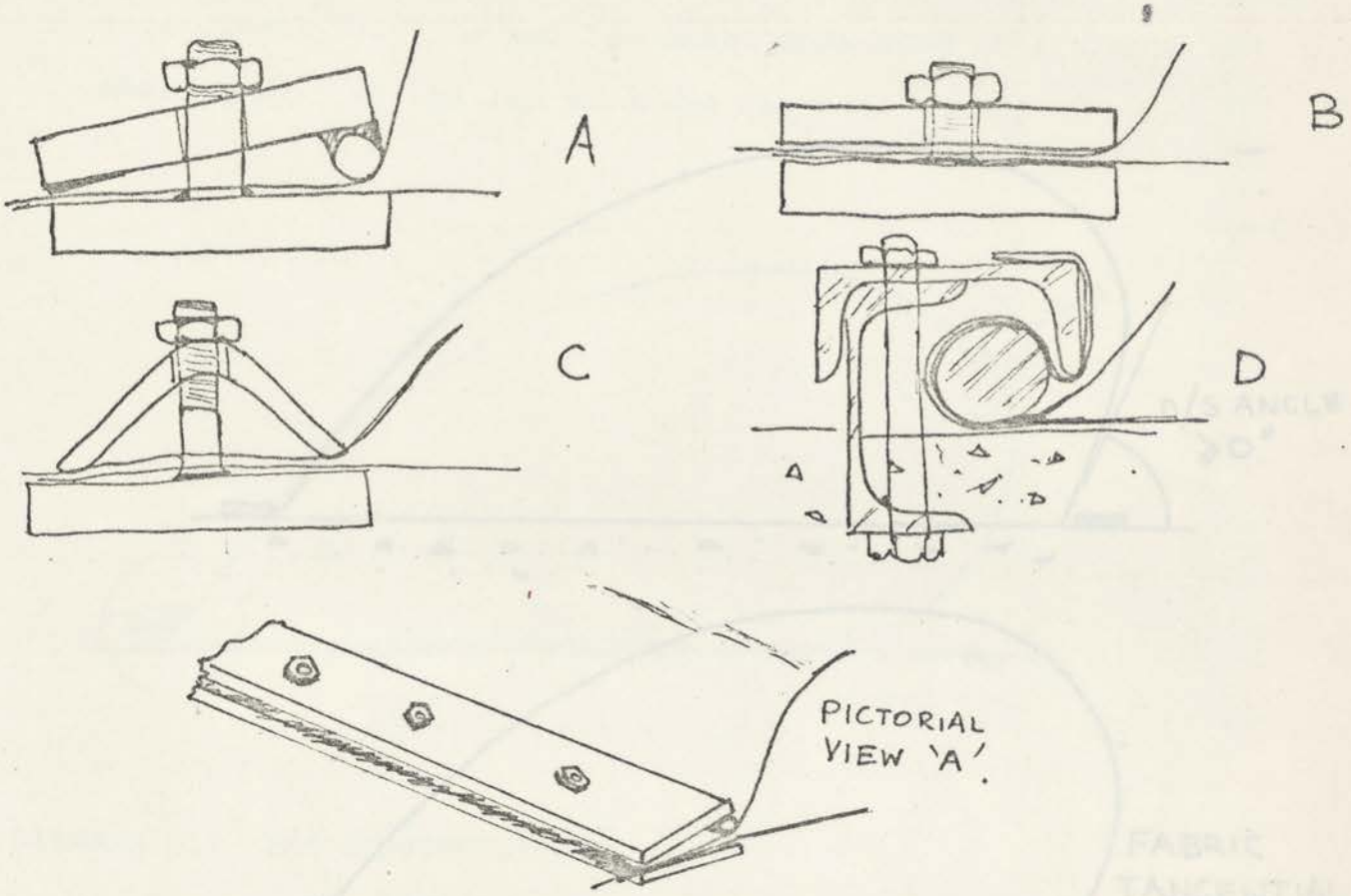

DIAGRAM 5.6 CLAMPING SYSTEMS

Type A consisted of a small bar, welded to the edge of a flat bar such that the clamp could provide sufficient force onto the membrane to stop slip, without cutting the fabric. Type A worked satisfactorily for the duration of the tests. No slip of the fabric was observed. The other types of clamping bar were rejected because of excessive machining and assembly time required (as in Case C and D) and/or exposing the fabric to a cutting edge and stress concentrations in the fabric in the vicinity of the clampingstuds, (as in case B).

To allow the model to be studied under a large variety of internal head/height ratios it was decided not to fix the downstream base contact of the perimeter but rather to allow the perimeter to lie tangential to the base at all times, as shown in Diagram 5.7. This also meant that the tension was a minimum for any particular crest height.

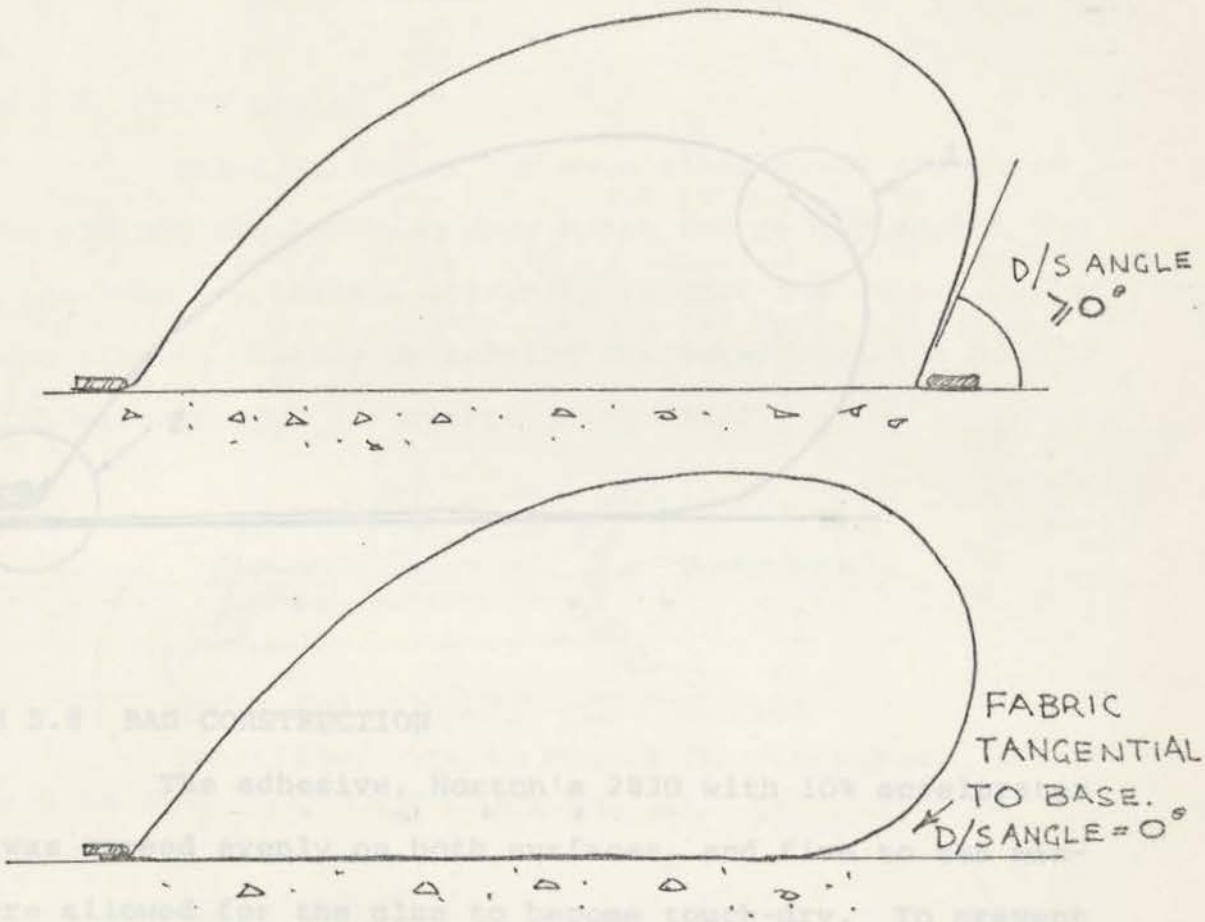

DIAGRAM 5.7 DOWNSTREAM CLAMP REGION

5.3.3. Bag Construction

(a) General Construction Technique

The bag for the first model was made by gluing two sheets of PVC coated scrim mesh each 52 inches wide together as a lap join (inset 1 in Diagram 5.8), then gluing the remaining edges together to complete the bag, as a glue tension join (inset 2). The smaller model consisted of a single sheet only, so the lap join was omitted.

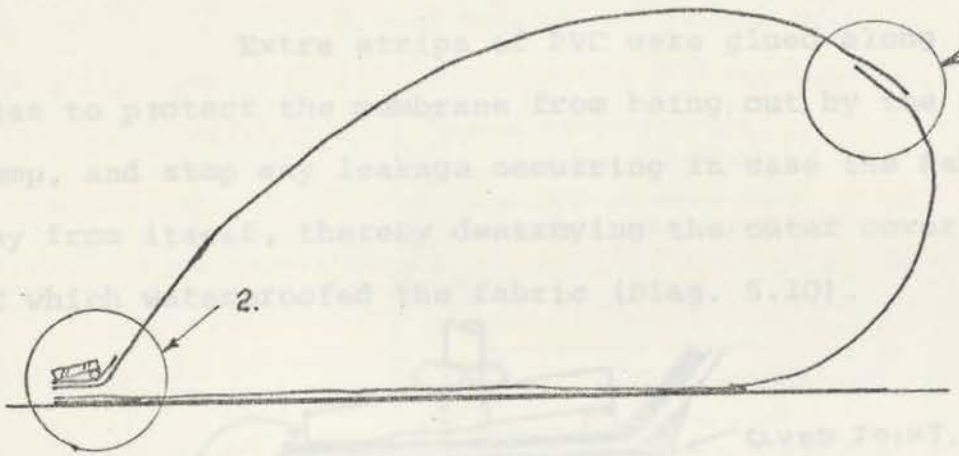

DIAGRAM 5.8 BAG CONSTRUCTION

The adhesive, Norton's 2830 with 10% accelerator added, was spread evenly on both surfaces, and five to ten minutes were allowed for the glue to become touch-dry. To prevent wrinkles occurring as the surfaces were brought together, an inert material, like polythene, was placed between the touch-dry surfaces, and then, as the polythene was carefully pulled out and back over itself, hand pressure was applied to the newly joined part.

Before the third and final pair of edges were sealed, four valves (of the type shown in Diag. 5.9) were inserted: one on the crest, one near the base, and two on the downstream face. These valves were for connections to control and measure the internal pressure.

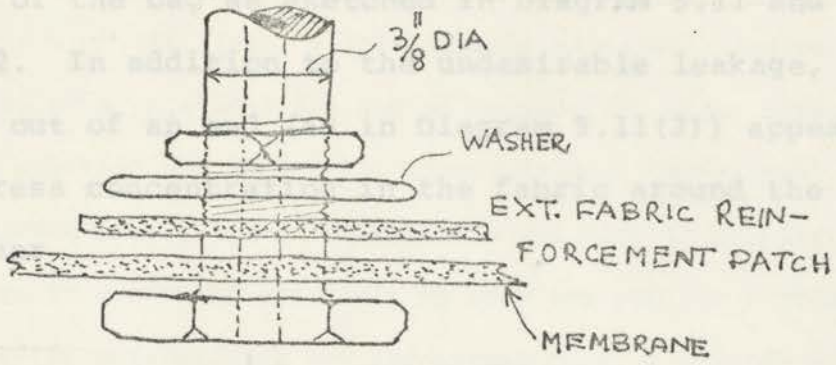

DIAGRAM 5.9 VALVE DESIGN

Extra strips of PVC were glued along the three edges to protect the membrane from being cut by the anchor clamp, and stop any leakage occurring in case the fabric pulled away from itself, thereby destroying the outer covering of PVC which waterproofed the fabric (Diag. 5.10).

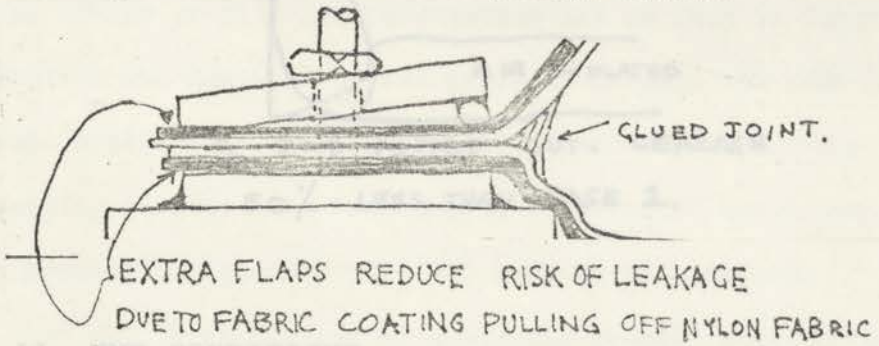

DIAGRAM 5.10 U/S CLAMP FABRIC DETAIL

(b) End Design

The ends of the large model bag were cut so that the model was 6-8 feet longer than the width of the channel. It was intended to clamp this extra length of bag vertically up the sides of the channel. However this was unnecessary in most cases, as it was found easier and more effective, especially in the water inflated cases, to tuck the ends back inside the bag.

No leakage past the ends occurred in water inflated cases nor in air inflated cases, where the internal air pressure was greater than the upstream head. For air inflated cases where

the internal air pressure was less than the upstream head, there was leakage of up to 2 cusecs (for an upstream head of around 30 inches) around the edges, and a tendency for the ends to pop out of the bag as sketched in Diagram 5.11 and seen in Diagram 5.2. In addition to the undesirable leakage, this type of popping out of an end (as in Diagram 5.11(3)) appeared to cause a stress concentration in the fabric around the end of the clamp bar.

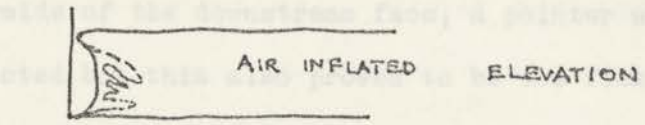

1. END TUCKED AND FOLDED IN.

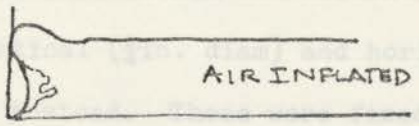

2. END ABOUT TO POP OUT

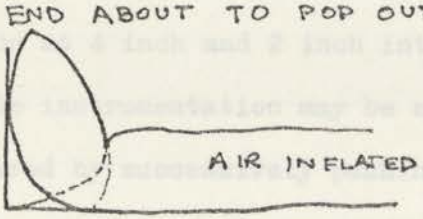

3. END POPPED OUT. LEAKAGE 50% LESS THAN CASE 1.

DIAGRAM 5.11 END CONDITIONS

In a successful attempt to prevent the ends from popping out, a pair of sheet metal guards were clamped to the floor and placed over the ends of the model (see Diagrams 5.17 - 5.20) in a loose fashion.

Attempts were also made to apply negative pressures (with the aid of a vacuum pump) to the ends of the model, but not enough was done to indicate whether or not the proposal would work satisfactorily. Alternatively, by shortening the ends, it may have been possible to reduce the size of this popping out effect, or eliminate any tendency for the ends to pop out at all.

5.4 INSTRUMENTATION

5.4.1 Larger Model

(a) Profile Measurement

At first, a continuously adjustable device was tried in the form of a pointed brass rod to measure the upper surface both in the vertical and horizontal direction in a transverse plane. This device proved to be too flexible and slow to operate. In addition it was found difficult to keep the pointer vertical. To measure the underside of the downstream face, a pointer with a right angle was constructed but this also proved to be too flexible and inaccurate.

The previous method was discontinued in favour of using a series of vertical ($\frac{1}{4}$in. diam) and horizontal ($\frac{1}{8}$in. diam.) brass measuring rods instead. These were fixed in the horizontal and vertical direction at 4 inch and 2 inch intervals respectively; (a view of the profile instrumentation may be seen in Diagram 5.1). The profile was measured by successively pushing the rods onto the membrane until they were just touching, and then recording the outstanding length. The rods proved to be stiff and adjustable for a reasonable accuracy of $\pm$ 0.5 inch to be attained.

With the aim of achieving greater accuracy of measurement, especially where the profile was under water, a strip of conductive silver paint was brushed onto the section of profile to be measured, to enable the operator to observe a torch globe light up when contact was made with the bag. (See Diag. 5.1). Although a length of multistrand wire was shunted in parallel with the paint and connected at 4 inch intervals, the resistance of the paint was still too high and as it would have been too time consuming to apply it thickly enough to extend its limited range, this idea was abandoned.

(b) Pressure Measuring Devices

To ensure that internal air pressures remained reasonably constant and counteract any leakage during a test, it was at first thought that a constant pressure device would be required. However as no leakage was observed, such a device was unnecessary.

The pressure of air and of internal water head in the bag were measured by a water manometer and piezometer, (with free end connected to the atmosphere) respectively, as shown in Diagram 5.3. Under static loading of both air and water inflated cases, pressure was measured to $\pm$ 0.1 in. water gauge, and under dynamic conditons pressure was measured to $\pm$ 0.5 in. water gauge.

(c) Strain and Vibration Instrumentation

For the analysis of flutter and rolling action a number of Electric Resistance Strain Guages were glued onto the fabric - 2 pairs, a quarter of the bag length from the side, and another 2 pairs half way along the length, one set being in the middle of the downstream face and the other in the middle of the upstream face. The gauges of each pair were placed perpendicularly and longitudinally to the flow.

The gauges were bonded to the PVC using "Cynoacrilyte" (an Eastman Kodak Product) and were waterproofed with a thin coating of rubber "Latex" solution. Anything stiffer than either of these adhesives would result in the pulling out of the fine wires leading to the gauges because of the large changes in curvature which occurred. The signals received from the gauges were passed through a Pekel strain gauge bridge and into an amplifier and galvanometer. Results will be discussed later in Section 5.6.3 and shown in Diagrams 5.31 to 5.35.

5.5 CONSTRUCTION - INSTRUMENTATION OF SMALL MODEL

Both the construction method and instrumentation used for the large model was repeated in the small model, with the exception of the following:-

(i) A single sheet of material, 48" wide was used for the construction of the small model so the need for a lap join as in Diagram 5.8 was eliminated.

(ii) A single pointer profile measurer was used to measure the upper profile in the small model.

(iii) The need for guards (as in Diagrams 5.17-5.20) was eliminated as the stresses caused by the popped ends were not as critical in the small dam model as they were in the larger model (Diagram 5.12).

VEE NOTCH EFFECT IN SMALL MODEL AIR-INFLATED MODEL

DIAGRAM 5.12 - A VIEW OF THE POPPED END.

DIAGRAM 5.13 - TUCKED IN END WITH OVER-FLOW. A SERIES OF VERTICAL RIPPLES IS SEEN ON DOWNSTREAM FACE.

DIAGRAM 5.14 - A NOTCH IS BEGINNING TO DEVELOP WITH AN INCREASE IN FLOW AND REDUCTION IN AIR PRESSURE.

DIAGRAM 5.15 - ... AND TRAVELS TO AN END, RESULTING IN TOTAL COLLAPSE. FLOW 2·5 cusecs.

DIAGRAM 5.16 - VEE-NOTCH PERSISTS DUE TO WEIGHT OF WATER ON COLLAPSED FABRIC.

VEE NOTCH EFFECT IN LARGE MODEL

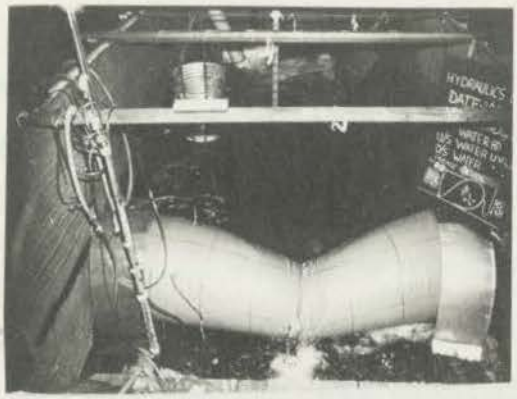

DIAGRAM 5.17 - SMALL VEE-NOTCH FORMED WHEN H/h - ½. THE INLET PIPE CAN BE SEEN IN THE BACKGROUND: PRESSURE CONTROL TUBES ARE ON THE LEFT.

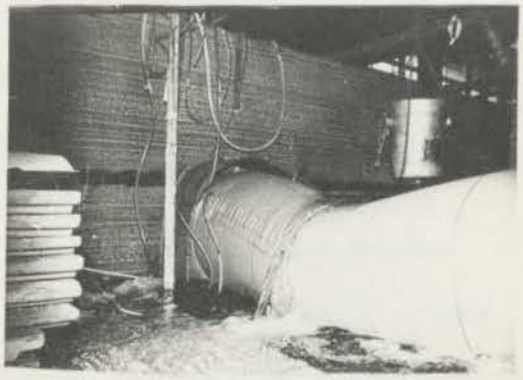

DIAGRAM 5.18 - SIDE VIEW OF VEE-NOTCH H/h - ½.

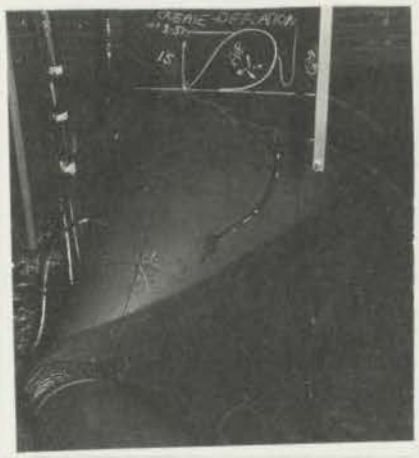

DIAGRAM 5.19 - LARGE VEE-NOTCH AT H/h - 1/3.

DIAGRAM 5.20 - H/h - 1/3, NOTE THE POPPED END ON THE RIGHT CONTAINED BY THE GUARD

DIAGRAM 5.21 - TUCKED IN END IN AIR-INFLATED DAM, NOTE THE LEAKAGE AROUND THE END.

5.6 BEHAVIOUR OF MODEL AND RESULTS

5.6.1 Static Tests

The behaviour and cross section profiles of the models were investigated for several combinations of upstream head and internal air, air/water or water pressures.

The upstream, downstream water level and the internal pressure, were recorded for a range of upstream heads between zero, and crest level. The profile of a typical cross section was measured and plotted for three values of upstream water level, namely, upstream water level of zero, an intermediate value, and one at crest level, keeping the volume of fluid inside the dam constant.

The data for the profiles and various pressure conditions was recorded in three Pen Carbon books. The books and the profiles plotted are available on request. The design curves for static conditions, discussed and graphed in Chapter 10, were obtained from these results.

The profiles were recorded and the tension in the fabric was calculated from the Anwar method (details in Section 4.3) by the graphical method (Section 4.5.4) and in certain cases by the Binnie method (Section 4.4), the Analogue method (Chapter 6) and the Harrison method (Section 4.6). Each set of results were compared with each other and discussed in Chapters 7 and 8. Experimental profiles were compared with those obtained by the Analogue method and the Harrison - Simplex method wherever applicable and these will be further discussed in Chapters 6 and 7 respectively.

5.6.2 Model Behaviour when H/h <1 and Vee-Notching

(a) Description and Conditions in which a Vee-Notch Would Form.

An interesting and partly unexpected aspect of the

OVERFLOW OF LARGE MODEL

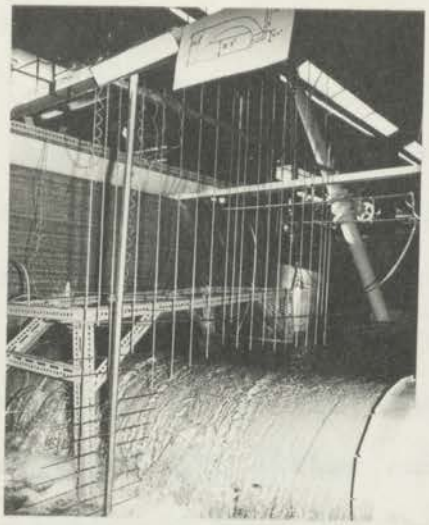

DIAGRAM 5.22 - OVERFLOW WITHOUT A TRIPROD.

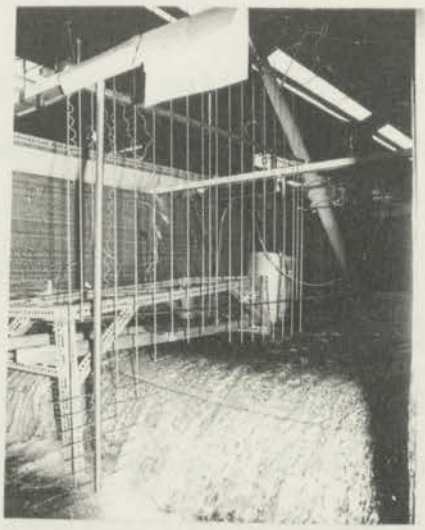

DIAGRAM 5.23 - WATER-INFLATED DAM. OVERFLOW WITH A TRIP ROD, PROBABLY TOO SMALL AND TOO HIGH TO TOTALLY SEPARATE THE FLOW FROM THE DOWNSTREAM FACE. NOTE THE LARGE AMOUNT OF TURBULENCE WHICH MADE INTERPRETATION OF STRAIN GAUGE RECORDINGS DIFFICULT TO INTERPRET. (FLOW 0·32 cusecs/ft.)

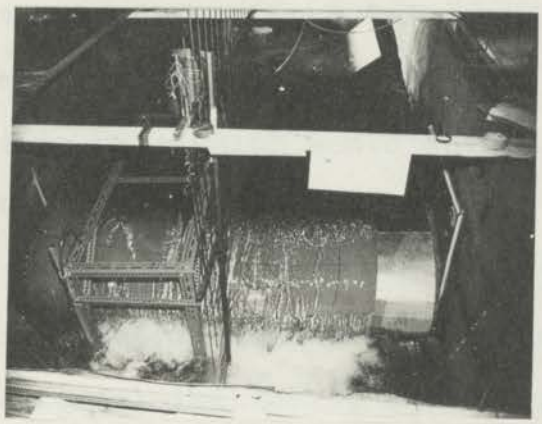

DIAGRAM 5.24 - DOWNSTREAM VIEW OF OVERFLOW WITHOUT A TRIPROD. THERE IS SOME FLOW SEPARATION VISIBLE DUE TO THE JOIN IN THE FABRIC.

DIAGRAM 5.25 - WATER INFLATED DAM WITH TRIP ROD CAUSING PARTIALLY AERATED NAPPE. (FLOW 0·22 cusecs/ft.)

study was the unstable behaviour in the form of three dimensional 'vee-notch' exhibited in conditions where $H/h < 1$ for air or air/water inflated cases, and seen in Diagrams 5.12 to 5.21.

Vee-notching takes the form of a solid revolution of a parabolic cusp, the angle between the surfaces at the crest gradually opening out towards the upstream clamp. The notch may occur anywhere along the length of the dam or at either end. It is usually formed half way along the length, and would either remain there or travel towards either end, or even disappear again when the upstream head was lowered. Application of a physical force was also found to initiate a vee-notch for values of $H/h < 1$ which may or may not disappear on removal of the force.

In cases where the ends were fixed and to a certain extent preformed it was deduced from observation that a vee-notch was more likely to occur and have a greater horizontal curvature effect, than in cases of free flexible ends which would deform more closely to the rest of the dam.

It was observed that the minimum possible internal head before notching occurred, without application of external initiating forces, was approximately $h/2$ where h is the value of upstream water height at crest level. This value corresponded to the theoretical value derived by Anwar, (Section 4.3) for the case where the angle between the fabric and base at the upstream clamp was just zero in the uniform profile case, as well as for the case where the fabric lay flat for some proportion of the total perimeter in the uniform case. Once the notch had formed

and as the internal air pressure was reduced further by allowing air to escape, the values of internal head/upstream water level (at notch crest height) also decreased as shown in Diagram 5.26 below.

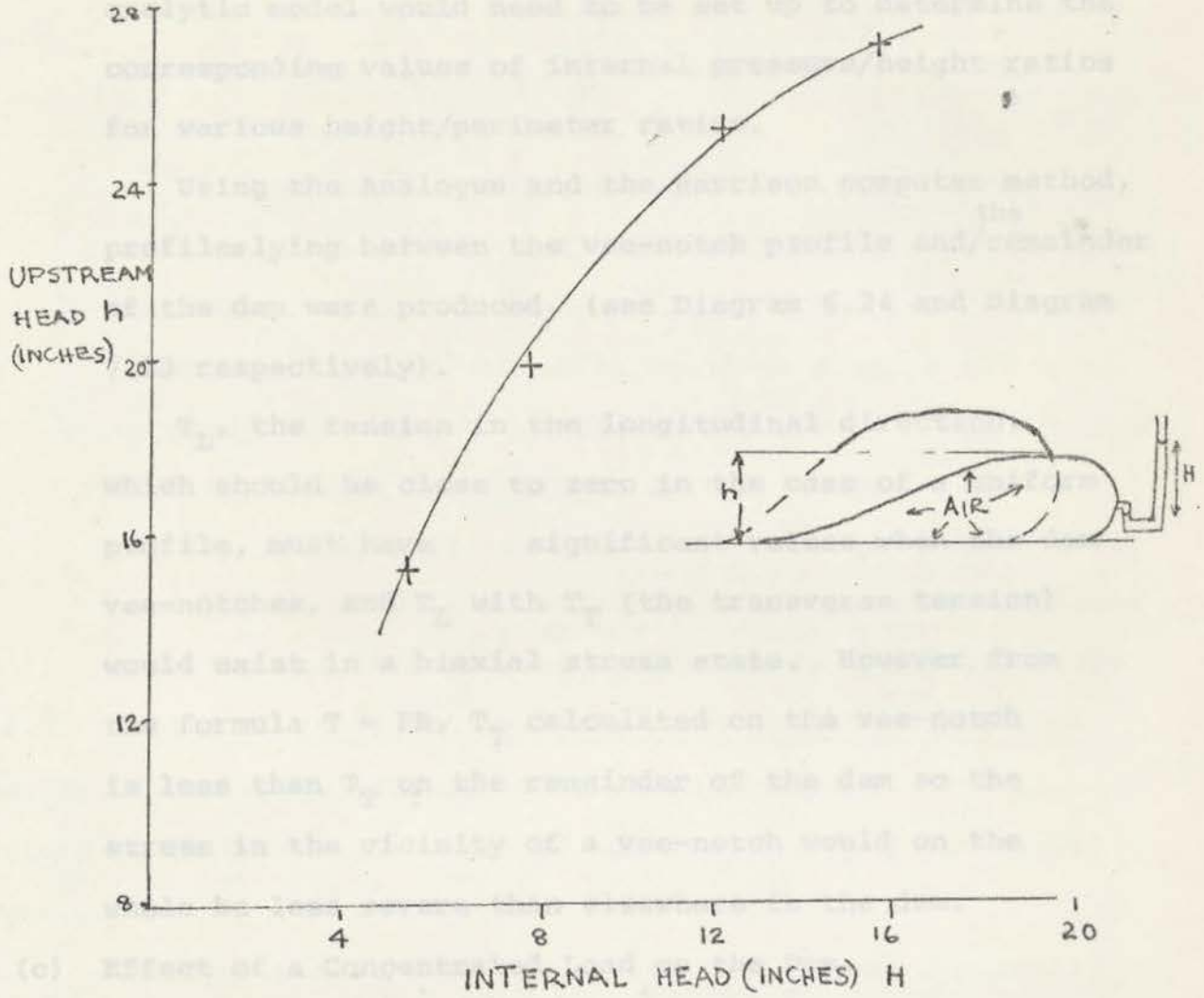

DIAGRAM 5.26 RELATION BETWEEN H/h FOR v-NOTCH

The values of internal pressure/height ratio and height/perimeter ratio at which it was possible for a vee notch to exist were uncertain as it was not possible to determine how its occurrence depended on the volume of the internal fluid, the height/length ratio, the compressibility of the fluid, and/or the height of the upstream head.

(b) Analysis of Dam affected by Vee-Notch

From the description of the vee-notch effect it can be appreciated that quite a complex three dimensional analytic model would need to be set up to determine the corresponding values of internal pressure/height ratios for various height/perimeter ratios.

Using the Analogue and the Harrison computer method, profiles lying between the vee-notch profile and the remainder of the dam were produced, (see Diagram 6.24 and Diagram 7.13 respectively).

T_L, the tension in the longitudinal direction, which should be close to zero in the case of a uniform profile, must have significant values when the dam vee-notches, and T_L with T_T (the transverse tension) would exist in a biaxial stress state. However from the formula $T = PR$, T_T calculated on the vee-notch is less than T_T on the remainder of the dam so the stress in the vicinity of a vee-notch would on the whole be less severe than elsewhere in the dam.

(c) Effect of a Concentrated Load on the Dam.

Although it is known that water inflated fabridams of medium size and under areasonable internal pressure height ratio could easily support a man, it would be very dangerous to attempt to stand on an air or air-water inflated fabridam operating under critical inflation pressures (with $H/h < 1$) with a maximum upstream head. The sudden vee-notch effect and/or partial collapse of the dam could result in enveloping the man and washing him off the crest. A similar effect would occur if a large tree trunk were washed onto the crest of dam, resulting in a probable loss of a large quantity of water.

For a cursory examination of the effect of a concentrated load on an air-water inflated dam, a 10 lb steel weight and then a 20 lb one was placed on the crest. In this particular case the weights settled into the crest compressing the air until they 'rested' at the internal water level.

To draw any conclusions from this study several more tests on various inflation combinations and pressures would need to be carried out. Again a complex three dimensional analytical model would need to be set up to study this effect. Although a study of a concentrated load applied to the Analogue system (Chapter 6) was not carried out, it is assumed the Analogue system could probably be used in an approximate analysis once various experimental factors were determined from a model study.

5.6.3 Results of Vibration Analysis under Dynamic Conditions

Results on the whole were not conclusive because of several factors which caused interference and distortion of the output signal.

The interference was so bad that it was impossible to determine accurately the magnitude of any of the quantities such as frequency and variation of stress in the fabric. These factors are described below.

(i) Surface Wave Effect

The surface waves vibrated the strain gauge wires sufficiently in some cases to mask any dam vibration, and appeared as a high frequency fuzz on the U.V. recordings (Diagram 5.31).

(ii) Vortices around the Wires

Vortices around the wires would increase the masking effect described in (i) above.

CASES OF OVERFLOW OF WATER-INFLATED DAM
(Small Model)

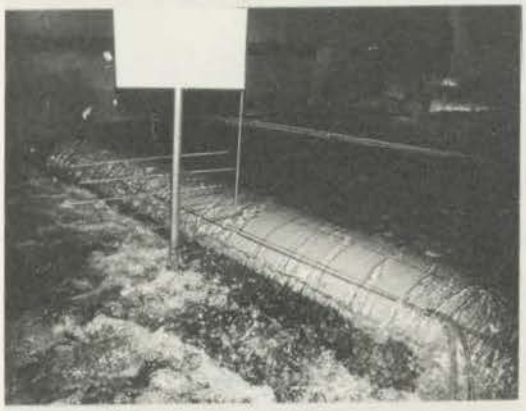

DIAGRAM 5.27 - PARTIALLY AERATED NAPPE DUE TO TRIPROD.

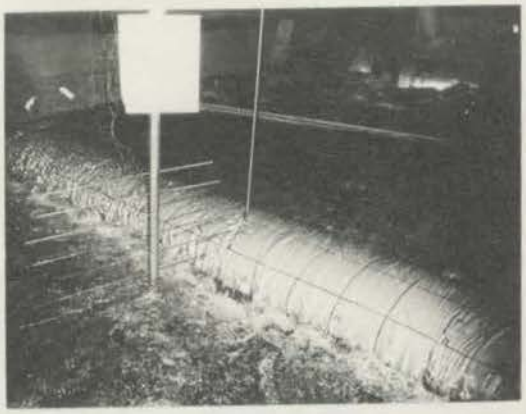

DIAGRAM 5.28 - OVERFLOW WITHOUT TRIPROD. A SERIES OF VERTICAL WAVES OR RIPPLES WERE SEEN TO TRAVEL BACKWARDS AND FORWARDS ACROSS THE DOWNSTREAM FACE. THESE WERE NOT AFFECTED BY ATTACHING VERTICAL DIVIDERS (POLYTHENE HOSE) ALONG THE WIDTH OF THE DAM.

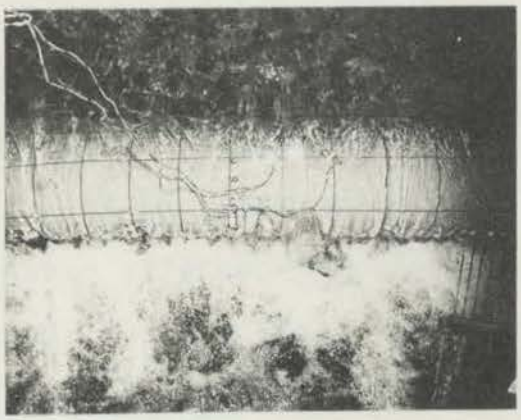

DIAGRAM 5.29 - VIEW OF OVERFLOW PATTERN FROM ABOVE WITHOUT TRIPROD. OBSERVE THE VERTICAL WAVES ON THE DOWNSTREAM EDGE WHICH TRAVELLED BACKWARDS AND FORWARDS AND MAY HAVE INITIATED THE ROLLING ACTION OBSERVED AT PROSTON WEIR.

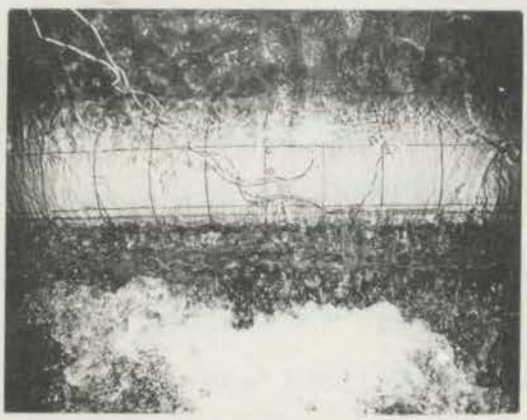

DIAGRAM 5.30 - VIEW OF OVERFLOW WITH TRIPROD. VERTICAL WAVE EFFECT APPEARS TO HAVE BEEN REDUCED.

(iii) Transverse Oscillation of Water

Transverse oscillation of water across the dam, probably due to a combination of waves and vibration of the model, also would add to the vibration of the wires and the fuzz. (Diagram 5.29).

(iv) Oscillation of Dam

This motion being the main interest was made up of several modes of vibration, namely:-

(a) Backwards and forwards due to water breaking off the downstream profile unevenly.

(b) Transverse vibration or rolling action due to oscillation of water waves along the crest.

(c) Mechanically induced vibration (as shown in Diagram 5.33).

Examples of each of the phenomena are shown below in Diagrams 5.31 to 5.35.

By positioning the S.G. on the inside of the model bag the effect of surface waves (which would, nevertheless, be a property of prototype reservoirs) would be eliminated. Due to the lack of time and the extra analysis which an indepth study of dynamic effects would involve, further modifications to the apparatus and the idea of placing the S.G. internally was abandoned.

Also the inlet capacity and/or the length/diameter ratio of the dam was insufficient to induce a snaking or rolling effect even in the smaller model (diameter/length ratio of 1/12 of Proston Weir where a rolling motion was observed with a diameter/length ratio of about 1/30).

Again, the exact effect of a trip rod seemed to be difficult to determine. Although several profiles were drawn for various conditions of overflow, these have not been reproduced here as it was decided to only describe the overflow and behaviour qualitatively.

U.V. RECORDING OF STRAIN FLUCTUATION UNDER OVERFLOW CONDITIONS.

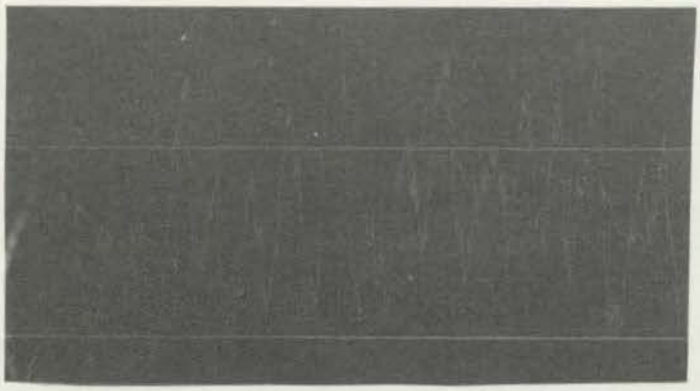

DIAGRAM 5.31 - LARGE MODEL, WATER INFLATED FLOW. 0.22 CUSECS/FT. NO TRIPROD.

	FUZZ	BACK AND FORTH	ROLLING
FREQ. C/S	60-80	2.5	1.2
AMPLITUDE (CM)	0.3	9.0	2.5

(STRAIN GAUGE PARALLEL TO FLOW)
NOTE: FUZZ (DUE TO TURBULENCE) SUPERIMPOSED ON BACK AND FORTH VIBRATION AND ROLLING VIBRATION.

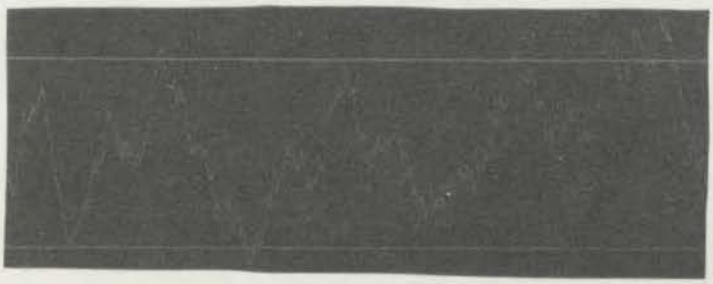

DIAGRAM 5.32-LARGE MODEL, CONDITIONS AS ABOVE, WITH TRIPROD.

	FUZZ	BACK FORTH
FREQ. C/S	75	2-4
AMPLITUDE (CM)	0.6	7-4

AMPLITUDE IS REDUCED DUE TO TRIPROD.

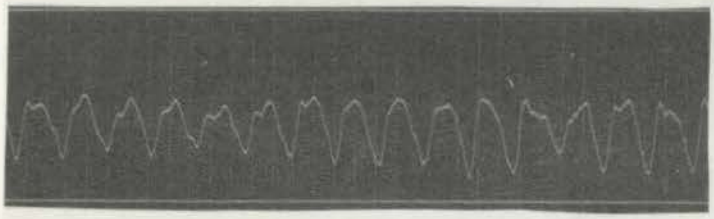

DIAGRAM 5.33-SMALL MODEL, WATER INFLATED, INTERNAL HEAD =23INCHES MECHANICALLY VIBRATED BY HAND IN LONGITUDINAL DIRECTION. (STRAIN GAUGE TRANSVERSE TO FLOW CAUSES AMPLITUDE TO BE REDUCED BY HALF)

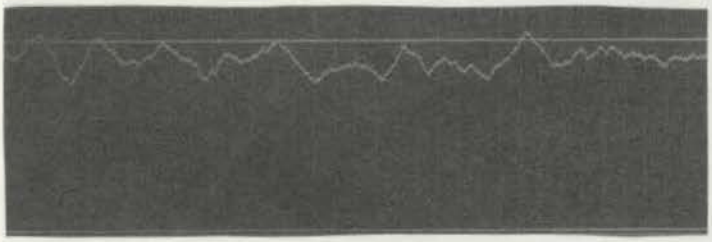

DIAGRAM 5.34- AS IN 5.33 EXCEPT FLOW 0.32 CUSECS/FT. WITH TRIPROD.

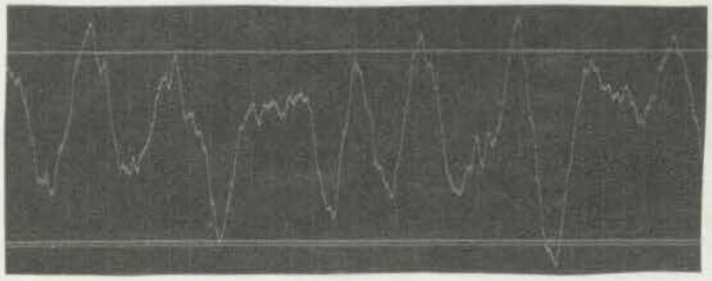

DIAGRAM 5.35- AS IN 5.34 EXCEPT STRAIN GAUGE PARALLEL TO FLOW, AND BAFFLE PLATE INSTALLED TO REDUCE TURBULENCE. THIS WAS OBSERVED TO HAVE REDUCED THE AMPLITUDE.

5.7 MODEL DEFICIENCIES AND APPROACH TO FURTHER TESTS

Although the model behaved satisfactorily, several minor changes could have facilitated the recording of data and improved performance. These included inserting perspex sides to observe end effects, and raising the dam model onto an elevated base, which would have facilitated recording the downstream profile and eliminated tail water problems in overflow cases. The perspex sides would also reduce end friction but due to the length of the model had only negligible effect in any case.

Surface wave effects on strain gauge readings (as already mentioned in section 5.6) could be eliminated by inserting the strain gauges inside the model.

The study could have been extended by making provision for end and downstream clamping.

CHAPTER 6 - THE CORD ANALOGUE METHOD OF ANALYSIS

6.1 DESCRIPTION

As a reaction to the problems which occurred in analysing and evaluating the iterative computer method developed by Harrison (see Chapter 4.6, and 7) an alternative, possible simple methodswas devised.

This method was a physical system where a number of point loads, approximately simulating hydrostatic loading over parts of the membrane were attached to a cord simulating the membrane (see Diagram 6.1).

The Analogue method was surprisingly simple to apply, requiring no knowledge of computer methods or specialized mathematics, and using only inexpensive simple apparatus. Whatever the loading conditions and the initial profile, one was certain of obtaining a reasonably accurate result, relatively quickly. The shape and tension obtained by the Analogue method corresponded well with those obtained from the experimental model, and generally agreed with those of the Harrison analysis (Chapter 7 and Diagram 6.17). In fact, the Analogue method has possible application in any situation where there are non-uniform loadings applied to any membrane structure which may be analysed two-dimensionally.

6.2 PROCEDURE AND APPARATUS

6.2.1 Calculation and Application of Loads

Initially, a cord equal in length to the membrane perimeter, but reduced to a suitable scale and arranged in any semi-ovular shape which it is thought the actual membrane shape might take, was used to trace the shape onto a sheet of graph paper. Of course the base length of the analogue shape would equal that of the full-sized dam reduced by the linear scale factor.

CORD ANALOGUE METHOD-TYPICAL CASES

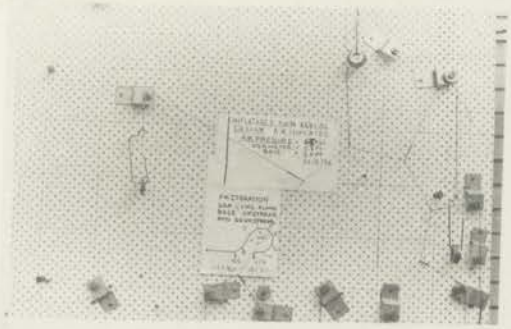

DIAGRAM 6.1 - THE ANALOGUE METHOD PRODUCED A PROFILE EQUIVALENT TO A VEE NOTCH IN A PROTOTYPE DAM. FOR H/b < 1. TENSION IN THE MEMBRANE IS GIVEN BY THE AVE. LOAD ON THE U/S AND D/S ENDS. INITIALLY MAX. U/S CREST LEVEL AND LOCATION OF DOWNSTREAM CLAMP WERE UNKNOWN.

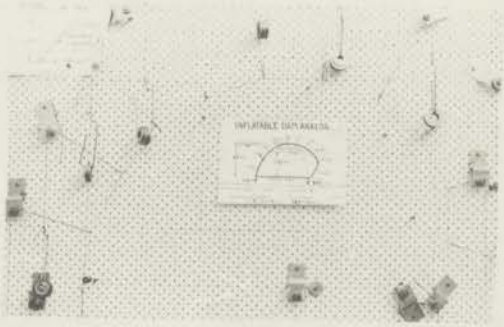

DIAGRAM 6.2 - THE ANALOGUE METHOD CAN ANALYSE A WIDE VARIETY OF LOADINGS, AS IN THIS AIR-WATER INFLATED CASE.

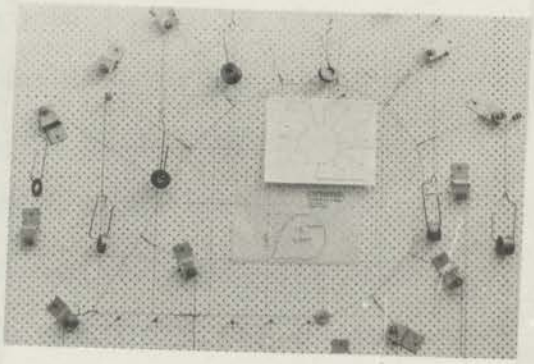

DIAGRAM 6.3 - AIR INFLATED DAM (INTERNAL PRESSURE 0.76 PSI AND U/S HEAD 2.43 FT.). THE CORD IS CONTINUOUS UNLIKE THE MAJORITY OF THE OTHER CASES WHERE THE ENDS TERMINATE AT THE U/S AND D/S END RESPECTIVELY.

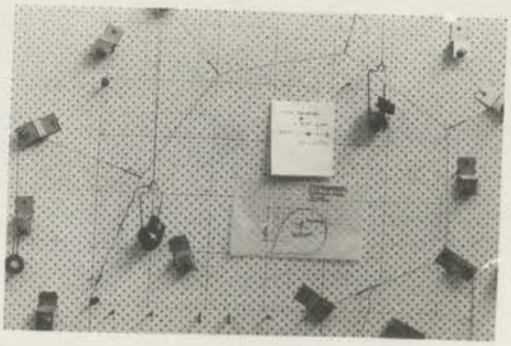

DIAGRAM 6.4 - AS ABOVE EXCEPT CORD IS NOT CONTINUOUS AND THE NODES HAVE BEEN REDUCED TO 5 FOR COMPARISON PURPOSES.

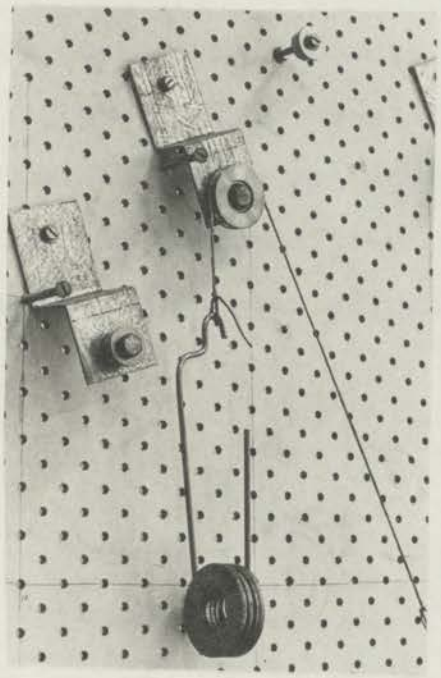

DIAGRAM 6.5 - CLOSE VIEW OF LOADED ⌐ BRACKET AND TYPE OF BALL BEARING RACE USED. THE BRACKET ENSURES THE LOAD, OR STRING DOES NOT DRAG ON THE PEG BOARD.

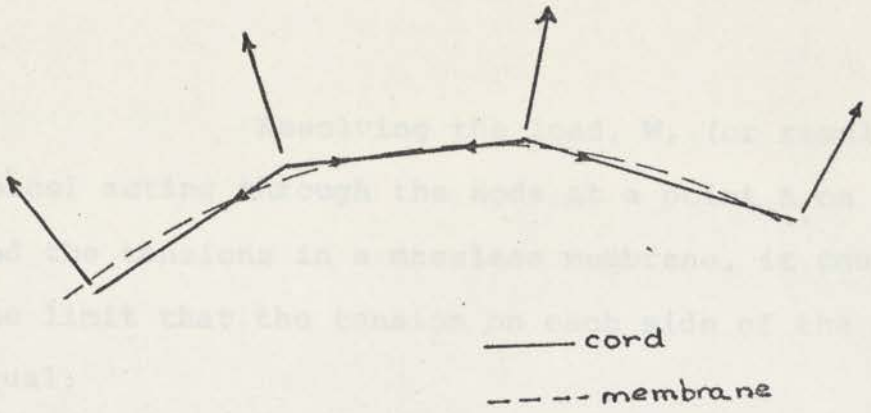

DIAGRAM 6.6 FORCES ACTING ON CORD ANALOGUE

The loads were calculated as acting perpendicularly to the cord, taken to act through the node for practical reasons, and at a given node was equal to the net force due to the internal and external average pressure acting over half a segment length on each side of the node. Typical values are shown in Table 6.2. Where hydrostatic loading occurred, the pressures on the membrane were most conveniently found graphically as indicated in Diagram 6.7.

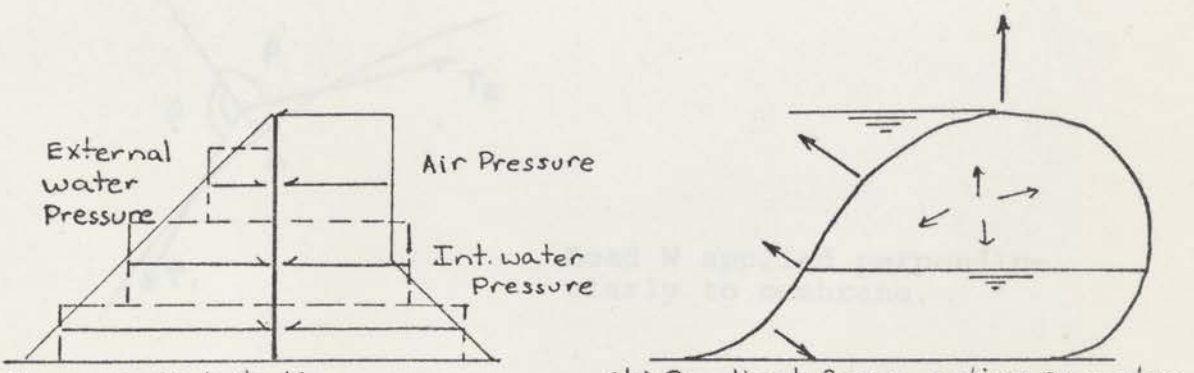

DIAGRAM 6.7

From the analysis (in Section 6.3.2) the maximum error in tension due to assuming the load acted through the mid-point between two nodes, rather than through the force centroid, was less than 5% and this was less than the error involved in the physical positioning of the load itself.

Resolving the load, W, (or resultant pressure force) acting through the node at a point A on Diagram 6.8, and the tensions in a massless membrane, it could be seen in the limit that the tension on each side of the node would be equal.

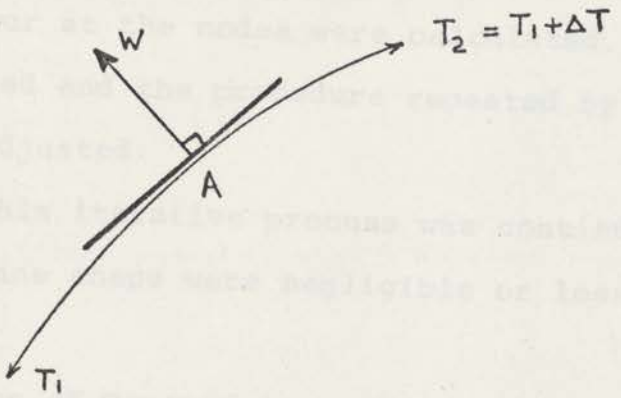

DIAGRAM 6.8 FORCE ON AN ELEMENT

When transferred physically onto the perimeter cord, the curved surface of the prototype membrame was simulated by a series of straight chords as shown on Diagram 6.1 and 6.9.

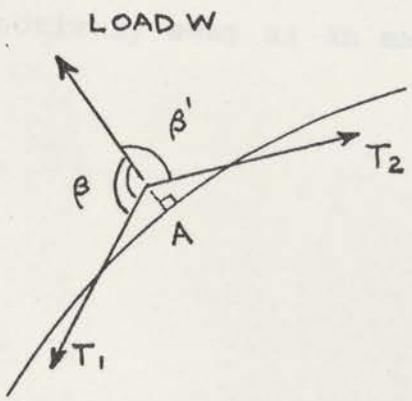

Load W applied perpendicularly to membrane.

DIAGRAM 6.9 LOAD ON A NODE

So that T_1 was as nearly equal to T_2 as possible, it was desirable to have the angles β^1 and β as nearly equal as possible, such that the load string bisected the perimeter cord.

Once set up a polaroid photograph was usually taken to record the profile and this made it easier to scale the resultant shape onto a graph. From the graph the loads which should occur at the nodes were calculated. The revised loads were applied and the procedure repeated by which the cord shape was adjusted.

This iterative process was continued until variations in membrane shape were negligible or less than a specified limit.

6.2.2 Calculation of Tension in Membrane

When all the loads were applied, the upstream and downstream ends of the perimeter cord were eased and the cord adjusted back into the same perimeter length (if any movement had occurred) by increasing or decreasing the forces at the ends of the perimeter cords. When finally adjusted these end forces would equal the upstream and downstream membrane tensions respectively seen, as an example, in Table 6.1.

Alternatively, the membrane tensions at the nodes were calculated using the equations following.

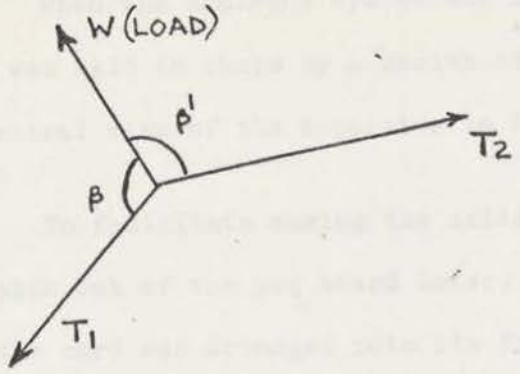

DIAGRAM 6.10 RELATION BETWEEN LOAD, TENSION AND BISECTED ANGLE

Resolving parallel to the load W,

$$T_1 \cos (180 - \beta^1) + T_2 \cos (180 - \beta) = W \quad \ldots \quad \ldots \quad 6.1$$

Resolving perpendicular to W,

$$T_1 \sin (180 - \beta^1) = T_2 \sin (180 - \beta) \quad \ldots \quad \ldots \quad 6.2$$

Also, if $\beta \doteq \beta^1$ it was shown in Section 6.3.1 that the mean value of T_1 and T_2 was approximately equal to value of tension calculated by using the mean of β^1 and β, which simplifies the calculation to

$$T_{(mean)} = \frac{W}{2 \cos (180 - \frac{\beta^1 + \beta}{2})} \quad \ldots \quad \ldots \quad 6.3$$

The mean tensions were then averaged and it was shown in Section 6.3.1 that the value obtained by the above method corresponded, within experimental error, to the mean value of the upstream and downstream tension calculated by the simpler method described first, so it was decided to use the simpler method.

6.2.3. General Description of Apparatus

When the Analogue system was in operation, the membrane cord was held in shape by a series of weights as seen from a general view of the apparatus in Diagram 6.1.

To facilitate making the initial set up, screws (which were taken out of the peg board later) were set out, around which the cord was arranged into its first approximate shape. String instead of wire was used for the cord, as wire tended to kink. The weights, applied at approximately 6 inch intervals and such as to bisect the node angle (see Section 6.2.4), were attached to the cord by means of small wire hooks and pieces of string, which were passed over ball bearings to minimize friction (see Diagram 6.5).

In addition, as shown in Diagram 6.5 the ball bearing races were attached to "⅂" sections which in turn were bolted to the peg board. The ⅂ section prevented any part of the cord system from dragging on the peg board. It was possible to rotate the ⅂ section for fine adjustment so ensuring the load bisected the cord angle at the point of loading.

It was decided to mount the system on a vertical peg board instead of horizontal, as it was found that the adjustment of load directions was easier if everything lay in the plane of gravity.

6.3 POSSIBLE ERRORS

6.3.1 Discussion

Several influences such as approximations of pressure forces and their positioning could contribute to possible errors in answers obtained using the cord analogue. To estimate the error involved in the approximations several checks and counter checks were carried out.

The first series of checks was based on answers found using the cord analogue for cases where the shape was already known experimentally, namely an air-water inflated case and an air only inflated case.

From the analysis below it appears that it would be reasonable to assume that differences in, for example, height or base and tension when compared to experimental profiles and other methods of analyses, of $< 5\%$ would be good agreement and differences of $< 10\%$ would be fair. From a design aspect, the height of the dam, with water at crest level is specially significant and so reference will usually be made to this aspect in comparisons of shapes.

Tables 6.1 and 6.2 below summarize the tensions as calculated by equations in Section 6.2.2 (for the air-water case) and compares the average of these tensions to that obtained by averaging the U/S and D/S end forces. The average tension at a node was also nearly equal (within a few percent) to the tension calculated by averaging the bisected angles.

TABLE 6.1

SUMMARY OF TENSION DATA FOR AIR-WATER INFLATED CASE

SEGM'T LENGTH INS. COL.1	NODE NO. COL.2	TENSION (LBS.) T_1 COL.3	T_2 COL.4	T(mean) $(T_1+T_2)/2$ COL.5	T(from mean angle) COL.6	ANGLE θ_1 COL.7	θ_2 COL.8	θ(mean) $=(\theta_1+\theta_2)/2$ COL.9.
5.6	0							
7.3	1	1.42	1.44	1.43	1.48	100.5	102.5	101.5
5.9	2	2.32	2.32	2.32	2.38	92.0	97.3	94.6
6.0	3	1.81	1.81	1.81	1.82	96.0	97.3	96.6
6.1	4	1.86	1.84	1.85	1.85	101.5	95.0	98.2
6.0	5	1.65	1.62	1.64	1.64	103.4	98.0	100.7
6.4	6	1.55	1.62	1.58	1.66	94.0	107.7	100.9
6.0	7	1.85	1.92	1.88	1.89	94.2	105.0	99.6
6.3	8	1.72	1.75	1.73	1.74	99.0	104.0	101.5
5.8	9	1.99	2.10	2.05	2.04	97.5	109.0	103.3
5.3	10	2.01	2.00	2.00	1.98	110.0	108.2	109.1
2.0	11	3.43	3.53	3.48	3.54	88.0	103.4	95.7
	12							

TABLE 6.2

COMPARISON OF AVERAGE TENSION VALUES

AVE. T(MEAN) (COL.5)	AVE. T. (COL.6)	AVE. END TENSIONS $(T_0+T_{12})/2$
1.88 LB.	2.00 LB.	1.91 $\pm$ .30 LB.

Several aspects which affected the results to varying degrees are discussed below:-

1. Correct load positioning.
2. Friction between load hook and perimeter cord, and unequal bisecting angles affecting tension and curvature (Diagram 6.11).
3. Friction between load string and ball bearing race, and the variation of tension around the membrane.
4. Miscellaneous errors due to
   (a) load accuracy,
   (b) extension in the cord and
   (c) graphical calculation.
5. Number of nodes.

6.3.2 Correct Load Positions

The maximum possible error in positioning a load in a six inch segment through the mid point was -2% for an air inflated case, (Appendix II) and -3% for a water inflated case. However the human error in locating the load could be ± ¼" or 4% which superseded the previous possible error. The worst possible error in tension due to this ± 4% would also be about ± 4% as lowering or raising all the loads by a given amount would be the same as decreasing or increasing the pressure difference by approximately the same amount (in the worst case).

The effect of position error of the nodes of say 4% of H and on minimum radius of curvature of 8 inches would have a < 1% effect on the radius of curvature. As the curvature increases the error would become even less.

6.3.3 Friction Effect

Attempts were made at reducing the friction by replacing the hook with a rolling pulley and cradle, but this combination only partially reduced the friction. It was felt that the extra trouble of using the cradle with or without a ball bearing race was not warranted, as by carefully and successively adjusting the load directions by eye, a reasonable order of accuracy of an average of ± 7° off centre was obtained.

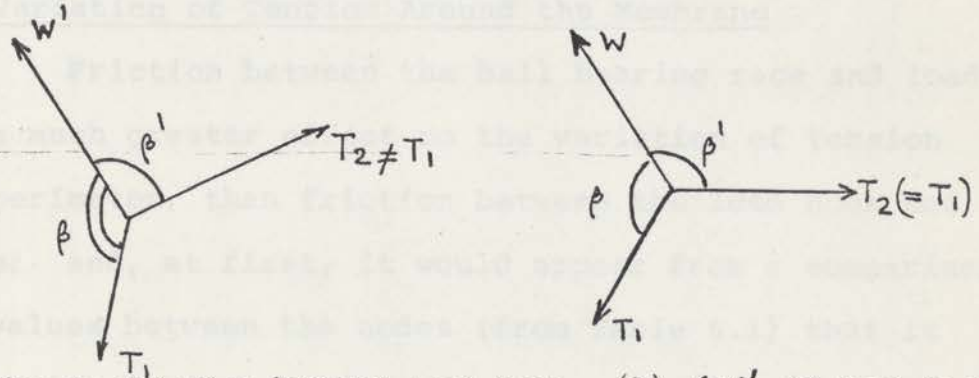

(a) $\beta \neq \beta'$ due to friction between load hook and membrane.

(b) $\beta = \beta'$ if load hook friction zero.

DIAGRAM 6.11 FRICTION BETWEEN LOAD HOOK AND PERIMETER CORD

The worst possible error in tension, for an eccentricity of angle of 15° for the smaller curvature (8 ins radius), was < 5%. This would cause (as indicated in Section 6.3.2), an error in curvature < 1%. However, calculations tab-

ulated in Table 6.1 which indicated the probable effect of differences in the bisected angles of up to 15°, only caused differences in tension of about 2 to 3%.

The friction effect was most serious at the ends of the perimeter where the curvature was large, as a small error in orientation of the applied load had a relatively large effect on the tension there of up to 5%.

Also, as the difference between the average tension on either side of the node and the tension calculated by using the average angle was negligible (< 2%) as seen from Table 6.1 it was felt that it was acceptable to use the average angle and consider the tension on either side of the node as equal.

6.3.4 The Variation of Tension Around the Membrane

Friction between the ball bearing race and load string had a much greater effect on the variation of tension around the perimeter, than friction between the load hook and the membrane; and, at first, it would appear from a comparison of tension values between the nodes (from Table 6.1) that it was unacceptable to simply take the average tension in the membrane to equal the average of the upstream and downstream tension.

To justify the simple method of calculating the membrane tension by taking it as the mean of the end forces on the cord, the tensions in each segment were calculated, using equation 6.1 and 6.2, and average values compared in Table 6.2. From the Table the difference between the methods is less than 3% probable, and this is considerably less than the error due to the possible friction and curvature effect of the cord around the end roller supports of ±0·30 lb in 1.91 lb for example, or approximately 15%.

Considering this friction effect and by using equations 6.1 and 6.2 to calculate the tension, it will be seen that from Table 6.2 the two values of tension calculated between any two nodes differed by an average of 13%.

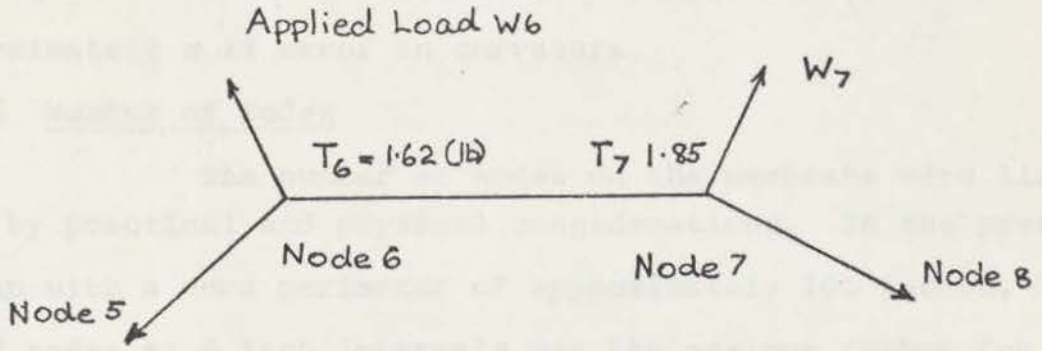

DIAGRAM 6.12 TYPICAL EXAMPLE OF UNEQUAL TENSION IN MEMBRANE DUE TO FRICTION IN PULLEY

The magnitude of this difference in each segment seemed to vary from node to node depending on whether the final membrane movement was out or in, which in effect, increased or decreased the applied load.

This effect was not as serious as one would have at first thought, as the calculated inequalities in tension in successive cord perimeter segments seemed to cancel each other, or average out, as seen in Table 6.1.

In general, the results show that the percentage difference of 10% between upstream and downstream tension at the ends was less than the percentage difference of the tensions around the perimeter and their average value.

6.3.5 Miscellaneous Errors

For the series of tests conducted, extension of the cord, the experimental error in total perimeter length of < 1% and the resultant effect on tension and curvature were all considered negligible.

Errors due to limits of readings of graphical plot and subsequent calculations were estimated to be of the order of 4%, and errors in load values were less than 3%, causing a 4% and 3% error in tension respectively, and each approximately a 1% error in curvature.

6.3.6 Number of Nodes

The number of nodes on the membrane were limited by practical and physical considerations. In the present set up with a cord perimeter of approximately 100 inches, 12 to 13 nodes at 6 inch intervals was the maximum number for convenience.

Initially it was feared too many nodes might cause instability in calculations as occurred with too many nodes in the Harrison analysis but these fears turned out to be groundless.

Another effect of an increase in the number of loads could be an increase in the error in the perimeter cord tension due to the friction between the load string and the ball bearing race; but as was mentioned previously, these effects usually appeared to be largely self-cancelling, and it was generally considered that the use of more nodes would result in more accurate results.

On a cord perimeter of about 100 inches a segment length of 6 inches between nodes seemed to be satisfactory. A comparison between the results with a set up using 5 nodes (12 inch spacing) and one using 12 nodes (6 inch spacing) was made and the results were shown in Diagrams 6.3, 6.4 and 6.13. The general shapes can be seen to be similar, but the 5 node model seems to be too coarse in areas where the curvature varies rapidly.

Results in shape and tension when compared to other analyses (e.g. in Section 6.4) and an analysis of experimental reliability seemed to bear out that a set-up with more than 12 nodes would only marginally increase the accuracy.

TABLE 6.3

COMPARISON OF TENSION FOR ANALYSIS USING 5 AND 12 NODES

METHOD OF OBTAINING TENSION	TOTAL PERIM. (feet)	BASE WIDTH (feet)	NO. OF NODES.	TENSION (lb/ft) CALCULATED UPSTREAM VALUE	CALCULATED DOWNSTREAM VALUE	AVERAGE
ANWAR from EXP. PROFILE	8.5	2.0	-	-	-	132
HARRISON -SIMPLEX	8.5	2.0	60	119	142	130
ANALOGUE	8.5	2.0	5 12	114 114	135 114	125 114

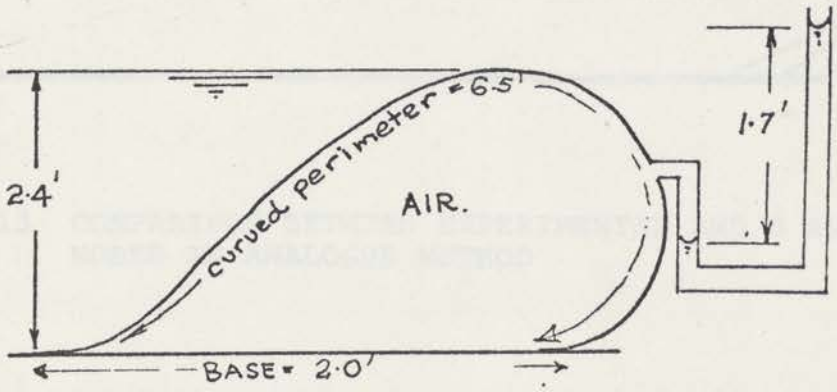

For convenience the analogue and experimental shapes for a case using 5 and 12 nodes respectively are compared here but more detail (in an example in Section 6.4.1) on the method of calculating values of tension is given below.

The Harrison - Simplex computer plot was not graphed as it lay between the two shapes - namely experimental and analogue.

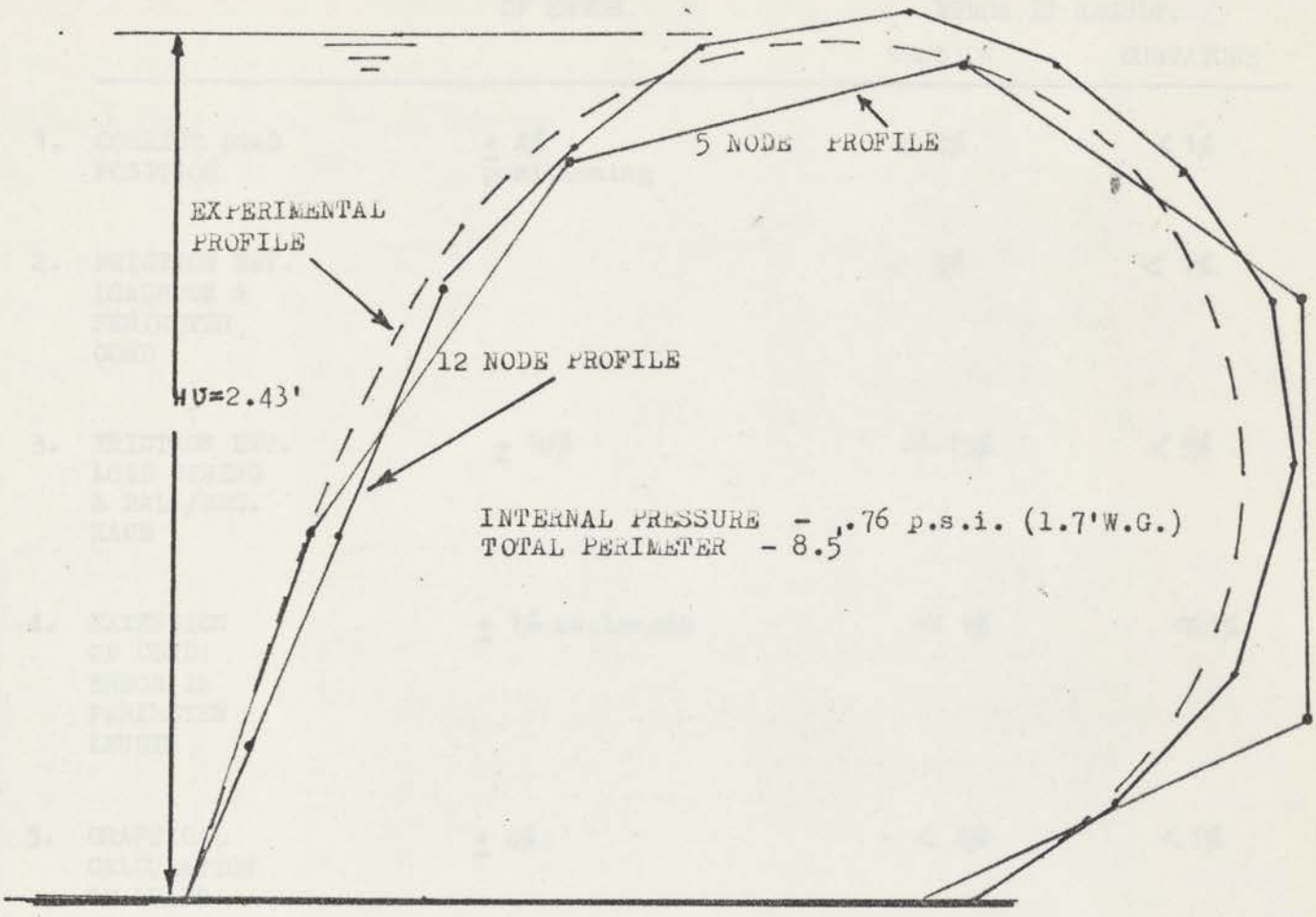

DIAGRAM 6.13 COMPARISON BETWEEN EXPERIMENTAL AND 5 AND 12 NODES IN ANALOGUE METHOD

SUMMARY OF EFFECTS OF EXPERIMENTAL ERRORS ON RESULTS

	ASPECT	MAGNITUDE OF ERROR.	MAX. POSSIBLE ERROR IN RESULT. TENSION	CURVATURE
1.	CORRECT LOAD POSITION	± 4% positioning	< 4%	< 1%
2.	FRICTION BET. LOADHOOK & PERIMETER CORD		< 5%	< 1%
3.	FRICTION BET. LOAD STRING & BALL/BRG. RACE	± 10%	10–15%	< 3%
4.	EXTENSION OF CORD: ERROR IN PERIMETER LENGTH	± 1% in length	≪ 1%	≪1%
5.	GRAPHICAL CALCULATION OF LOADS	± 4%	< 4%	< 1%
6.	WEIGHING OF LOADS	± 3%	< 3%	< 1%

From a comparison of experimental results of tension and shape, the error in each appeared to be within ± 10% and ± 5% respectively.

6.4 SHAPE VERIFICATION STARTING WITH KNOWN SHAPE

6.4.1 An Example in which the Method of Calculation is shown

The accuracy obtainable using the Analogue method was further tested by comparing its results with experimental values in several cases for which scale model experimental results were known.

A measured profile (shown in Diagram 6.14 below) was taken from the experimental model analysis (discussed in Chapter 5) and perimeter was divided into 6 inch segments.

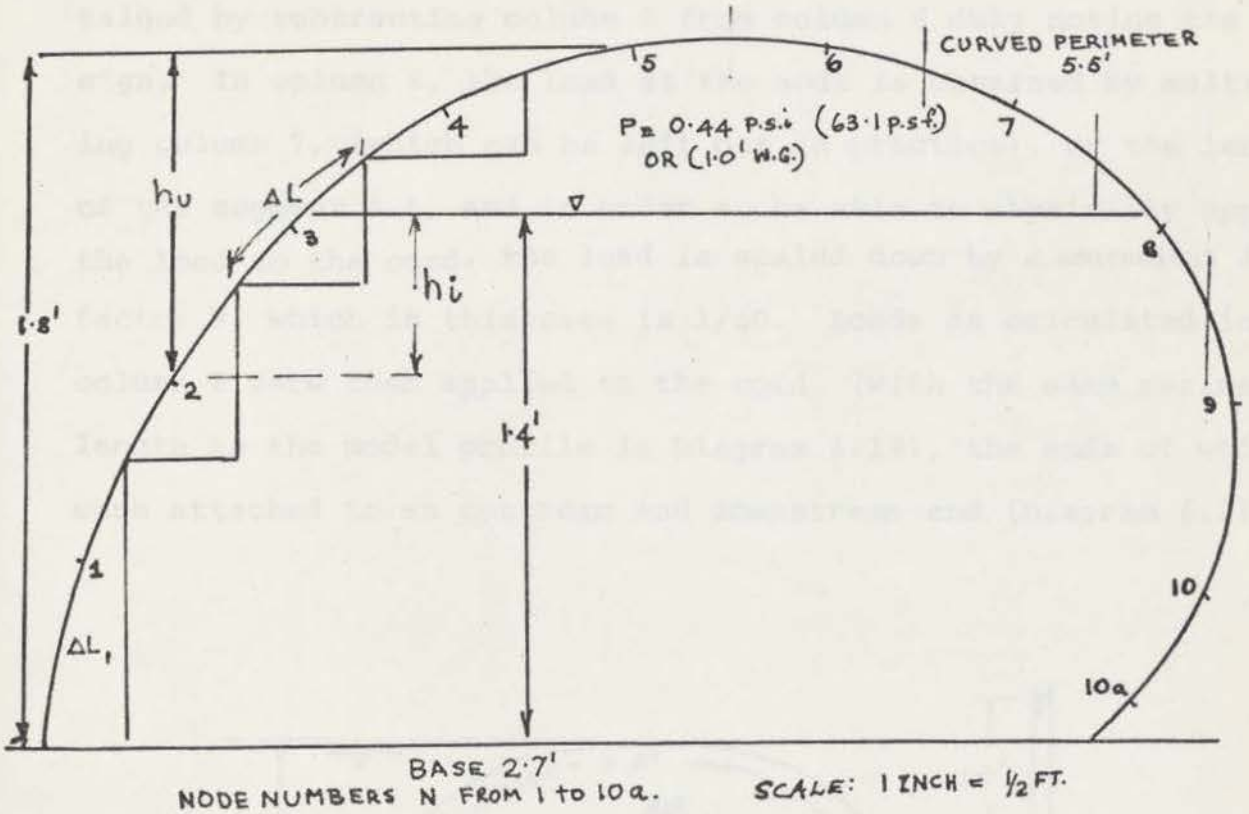

DIAGRAM 6.14 LOADING ON AIR-WATER INFLATED CASE

Since the profile was known, the loadings on it were immediately calculable. Values in columns 1 to 8 in Table 6.4 were successively calculated as described below.

N, Δ L, and H_u and H_i in columns 1 - 4 respectively were defined in Diagram 6.14 and represent the node number, the length between midpoints of successive segments, and the depths of the node in question below the internal and external water levels. Column 5 is the difference in water head between the internal head and external head multiplied by the water density, and represents the average water pressure at the particular node/ft width of fabric. Column 6 is the internal air pressure in p.s.f. and acts uniformly over the internal surface/foot width of fabric. The resultant average pressure at a particular node is given in column 7 which is obtained by subtracting column 5 from column 6 duly noting the sign. In column 8, the load at the node is obtained by multiplying column 7, (which can be left out in practice), by the length of the segment Δ L, and in order to be able to physically apply the load to the cord, the load is scaled down by a convenient load factor F, which in this case is 1/50. Loads as calculated in column 8 were then applied to the cord, (with the same perimeter length as the model profile in Diagram 6.14), the ends of which were attached to an upstream and downstream end (Diagram 6.2)

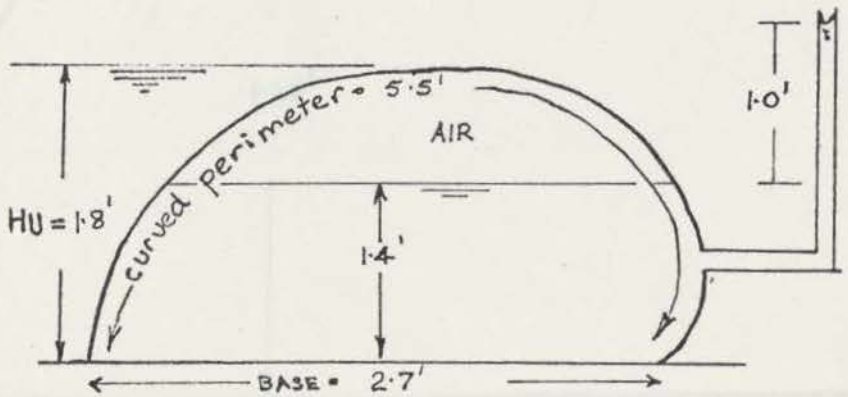

TABLE 6.4

ANALOGUE COMPUTATION – LOAD CALCULATION FOR PROFILE VERIFICATION OF AIR-WATER INFLATED CASE

*F = 1/50 (Scaling Factor)

NODE	L (FT)	hu (FT)	hi (FT)	WATER PRESS (LB/FT^2)	AIR PRESS (LB/FT^2)	AVE. PRESS. (LB/FT^2)	APPLIED LOAD (LB) 7 x 2 x F*
COL.NO. 1	2	3	4	(3-4)γ 5	6	(5+6) 7	8
1	0.40	1.40	0.46	25.0	63.1	88.1	0.57
2	0.57	0.86	0.10	25.0	63.1	88.1	0.38
3	0.50	0.45	–	21.9	63.1	85.0	0.42
4	0.50	0.15	–	9.4	63.1	72.5	0.53
5	0.50	0.03	–	2.0	63.1	65.1	0.61
6	0.50	–	–	–	63.1	63.1	0.63
7	0.50	–	–	–	63.1	63.1	0.63
8	0.50	–	0.10	6.2	63.1	69.3	0.69
9	0.50	–	0.50	31.2	63.1	94.3	0.94
10	0.50	–	1.10	68.6	63.1	131.7	1.30
11	0.12	–	1.25	75.0	63.1	138.1	0.70

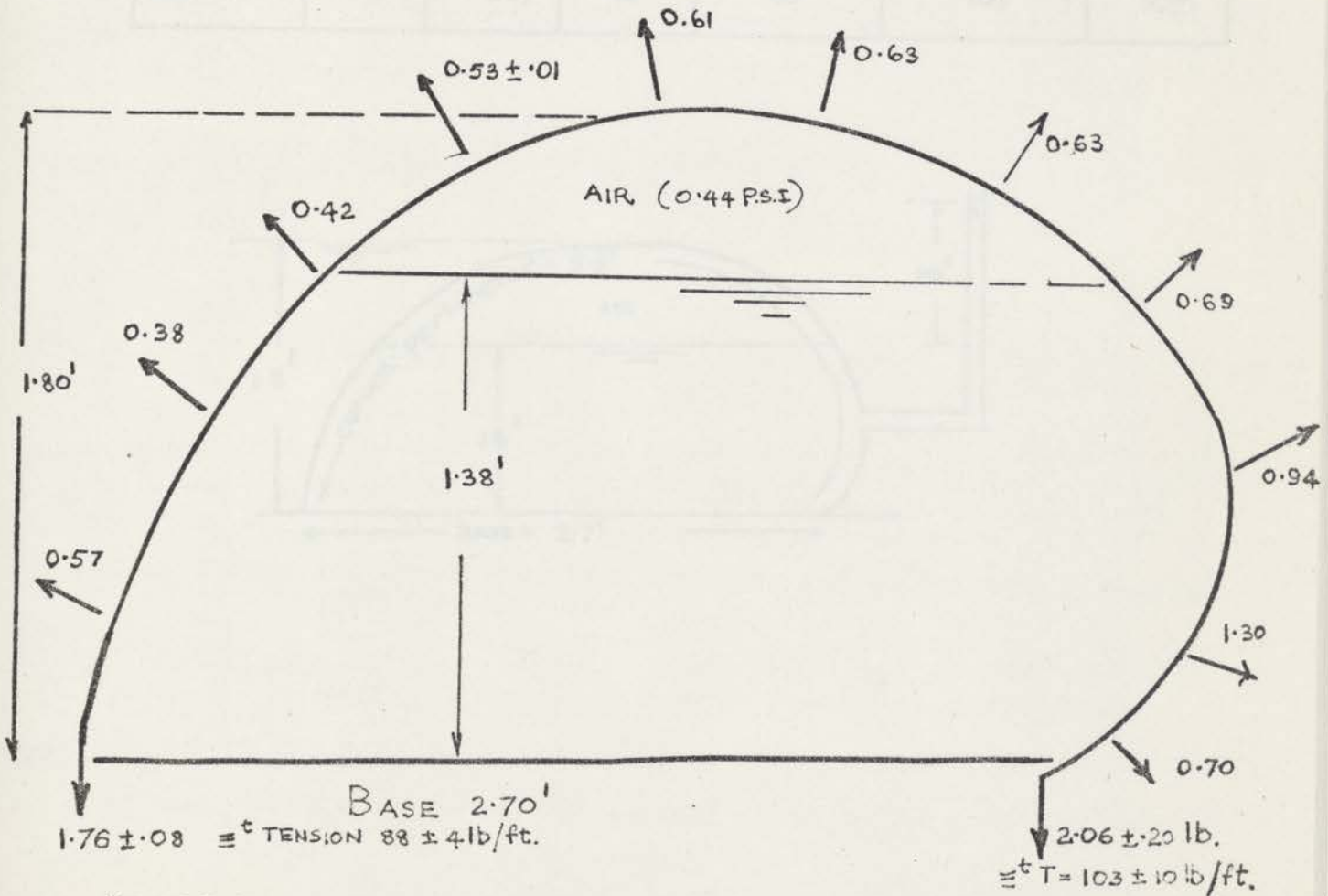

DIAGRAM 6.15 LOAD DISTRIBUTION AROUND PERIMETER.

The values of tension, and shape obtained were in good agreement (w.r.t. height and shape of the dam) with those obtained using other methods of solution, and with the experimental model (Diagram 6.16).

TABLE 6.5 COMPARISON OF TENSION OF AIR-WATER INFLATED CASE

METHOD OF OBTAINING TENSION	TOTAL PERIM. (feet)	BASE WIDTH (feet)	NO. OF NODES	TENSION (lb/ft)		
				CALCULATED UPSTREAM VALUE	CALCULATED DOWNSTREAM VALUE	AVERAGE
ANWAR from EXP. SHAPE	8.2	2.7	-	-	-	78
GRAPHICAL	8.2	2.7	-			103
HARRISON SIMPLEX	8.2	2.7	60	84	99	92
ANALOGUE	8.2	2.7	12	88	103	95±7

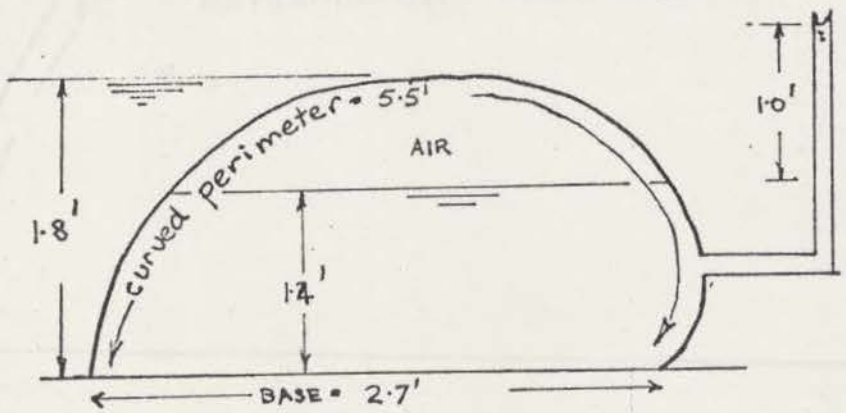

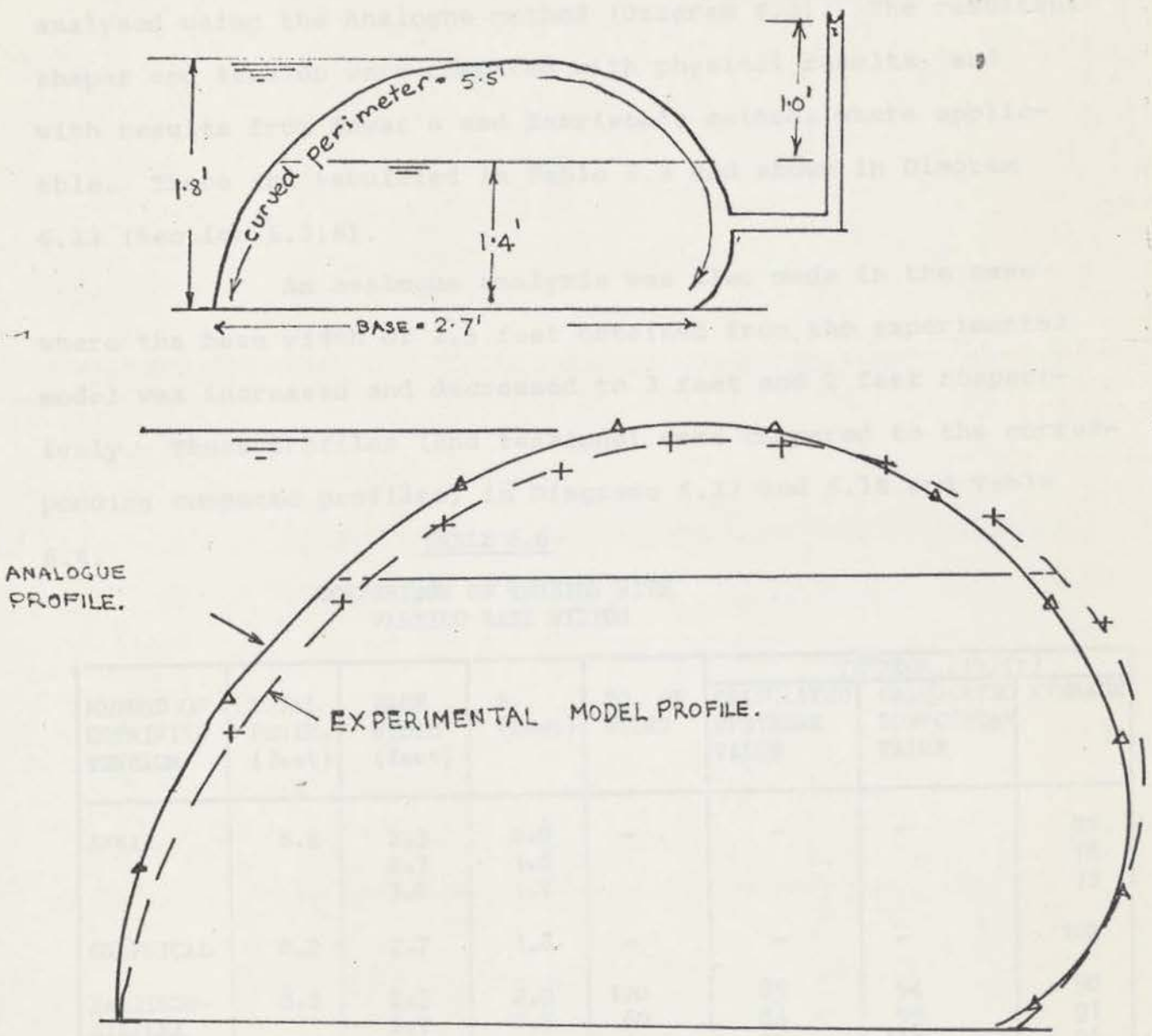

DIAGRAM 6.16 COMPARISON BETWEEN ANALOGUE AND EXPERIMENTAL PROFILE FOR AIR-WATER CASE

As expected, no second adjustment was required to the loads and profile since the starting positions for these analogue calculations were based on existing experimental values.

6.4.2 Results of Other Cases

Using the Analogue method to check a known profile.

Besides analysing the air/water inflated experimental case, an experimental case of an air inflated dam was analysed using the Analogue method (Diagram 6.3). The resultant shapes and tension were compared with physical results, and with results from Anwar's and Harrison's methods where applicable. These are tabulated in Table 6.3 and shown in Diagram 6.13 (Section 6.3.6).

An analogue analysis was also made in the case where the base width of 2.3 feet obtained from the experimental model was increased and decreased to 3 feet and 2 feet respectively. These profiles (and tensions) were compared to the corresponding computed profiles, in Diagrams 6.17 and 6.18 and Table 6.6.

TABLE 6.6

COMPARISON OF TENSION WITH VARYING BASE WIDTHS

METHOD OF OBTAINING TENSION	TOTAL PERIM. (feet)	BASE WIDTH (feet)	h (feet)	NO. OF NODES	TENSION (lb/ft) CALCULATED UPSTREAM VALUE	CALCULATED DOWNSTREAM VALUE	AVERAGE
ANWAR	8.2	2.3	2.0	-	-	-	87
		2.7	1.8				78
		3.0	1.7				72
GRAPHICAL	8.2	2.7	1.8	-	-	-	102
HARRISON-SIMPLEX	8.2	2.3	2.0	120	85	94	90
		2.7	1.8	60	84	99	91
		3.0	1.7	20	80	112	96
ANALOGUE	8.2	2.3	2.0	12	75±4	82±4	78± 7
		2.7	1.8	12	88±4	103±10	95± 7
		3.0	1.7	12	109±10	103±10	106± 7

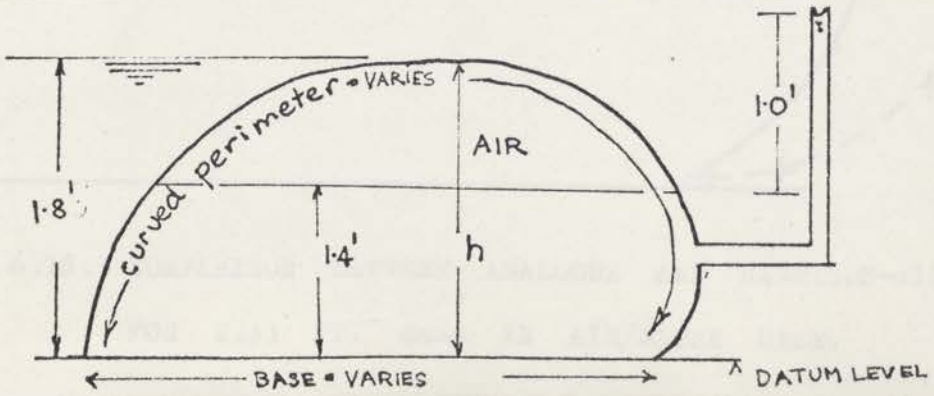

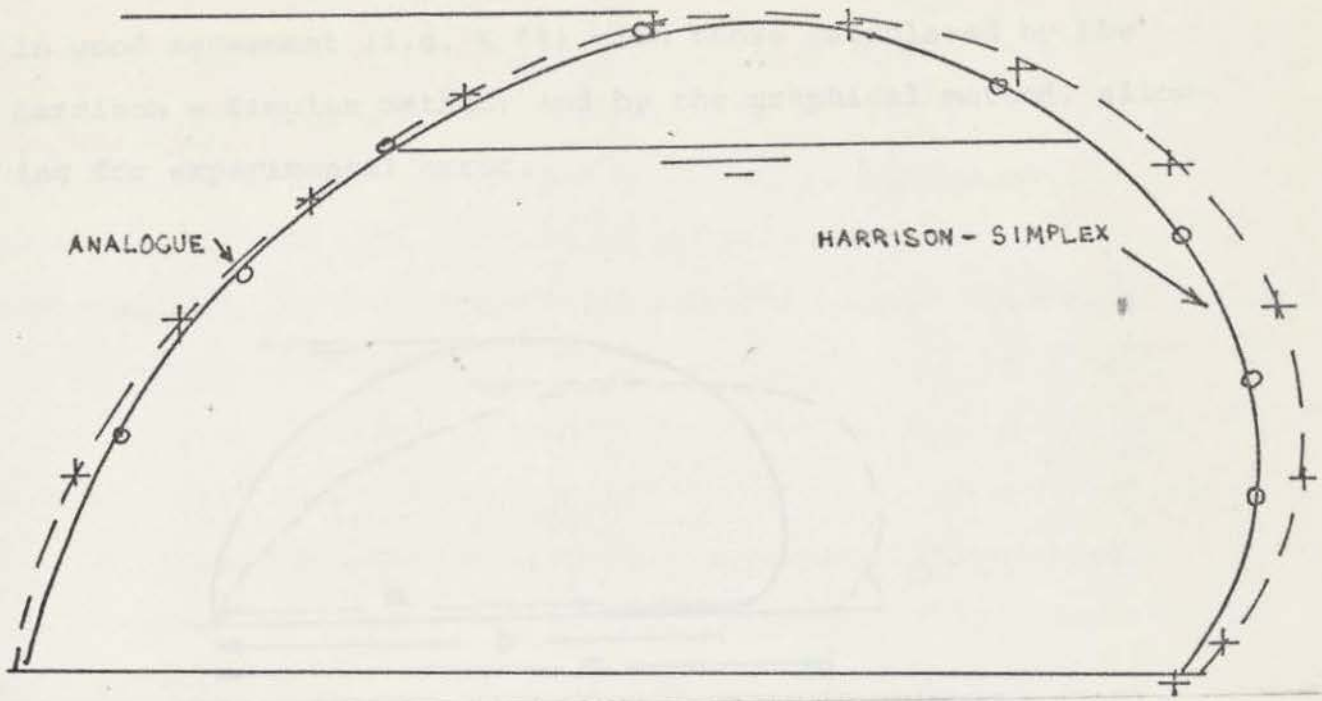

DIAGRAM 6.17. COMPARISON BETWEEN ANALOGUE AND COMPUTER HARRISON - SIMPLEX METHOD FOR 3 FT. BASE IN AIR / WATER CASE.

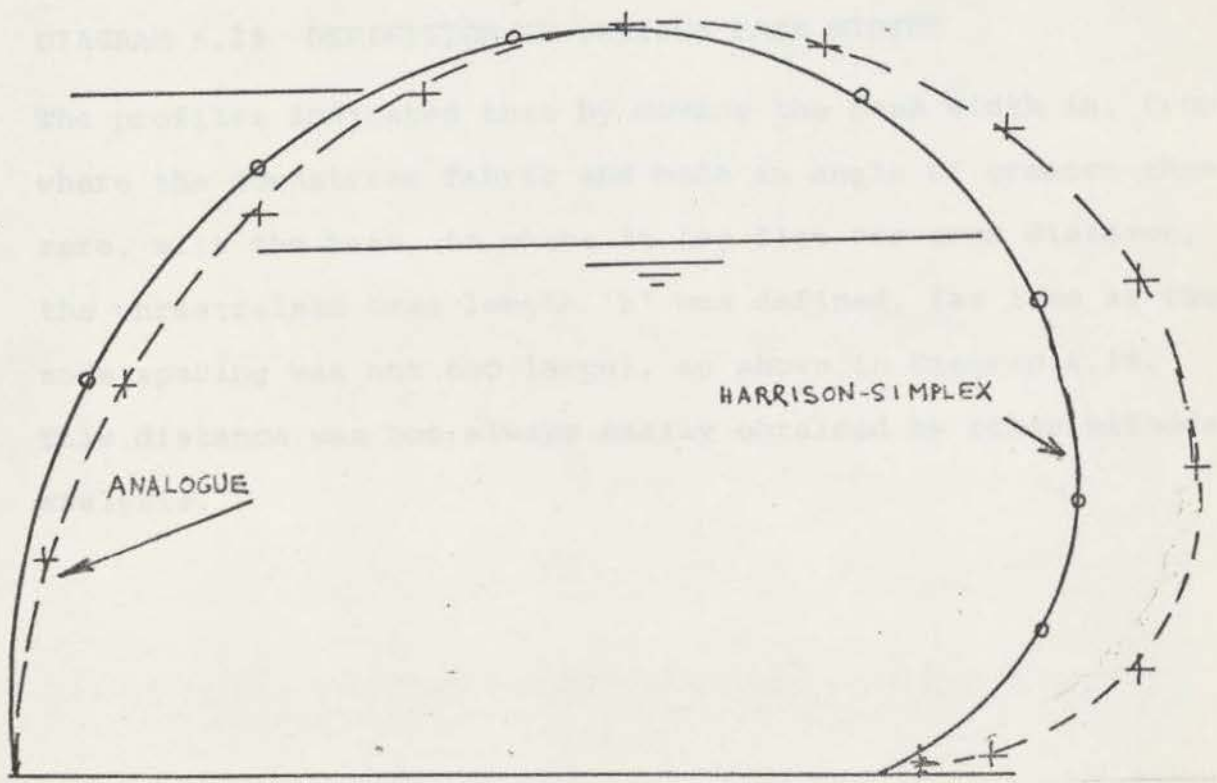

DIAGRAM 6.18. COMPARISON BETWEEN ANALOGUE AND HARRISON-SIMPLEX FOR 2.33 FT. BASE IN AIR/WATER CASE.

Tensions calculated by the Analogue method were in good agreement (i.e. < 5%) with those calculated by the Harrison - Simplex method, and by the graphical method, allowing for experimental error.

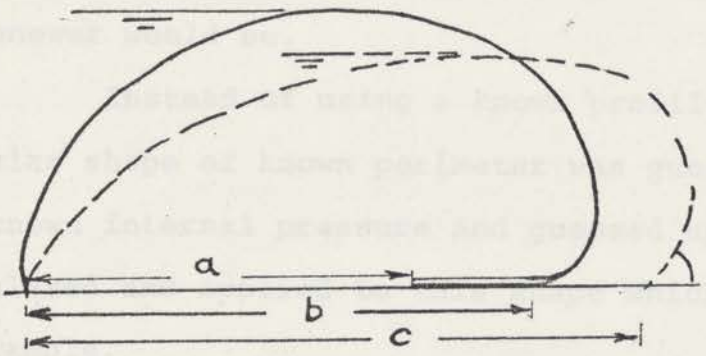

b - unrestrained base.

a = shorter base width than unrestrained width b.

c = physically restrained base for same internal pressure and total perimeter, and upstream water height at crest level.

DIAGRAM 6.19 DEFINITION OF VARIOUS BASE WIDTHS

The profiles indicated that by moving the base width in, from where the downstream fabric end made an angle of greater than zero, with the base, to where it lay flat for some distance, the unrestrained base length 'b' was defined, (as long as the node spacing was not too large), as shown in Diagram 6.19. This distance was not always easily obtained by other methods of analysis.

6.5 PREDICTION OF SHAPE (where the analysis starts with a guessed shape, with unknown exact values of upstream head at crest level and unknown base width).

After a reasonable degree of confidence was obtained in verifying several 'known' cases, the Analogue method was easily applied in cases where one had only a rough idea of what the answer would be.

Instead of using a known profile to start from, a semi-ovular shape of known perimeter was guessed and the loads, due to a known internal pressure and guessed upstream head, were calculated and applied to this shape which was water-inflated in this example.

The method of calculation of node forces was the same as in the previous example in 6.4.1 and differed only in that more than one set of calculations (Tables 6.7 and 6.8) was required to reach the convergence desired.

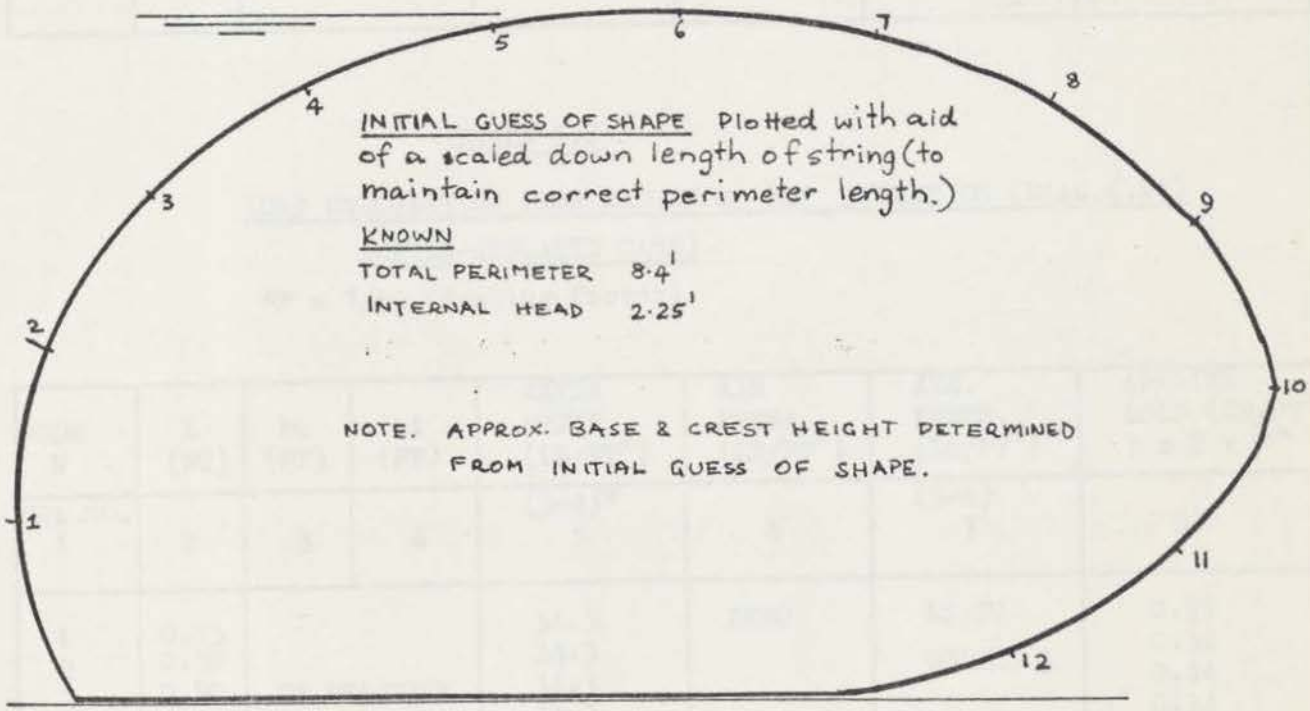

DIAGRAM 6.20 GUESSED PROFILE FOR UNKNOWN WATER-INFLATED PROFILE

TABLE 6.7

LOAD CALCULATION FROM 1ST GUESSED PROFILE (DIAG.6.21)

(WATER-INFLATED CASE).

*F = 1/50 (Scaling Factor).

NODE N	L (FT)	hu (FT)	hi (FT)	WATER PRESS (LB/FT^2)	AIR PRESS (LB/FT^2)	AVE. PRESS. (LB/FT^2)	APPLIED LOAD (LB) 7 x 2 x F*
COL.NO. 1	2	3	4	(3-4)Y 5	6	(5-6) 7	8
1	0.75			28.1	ZERO	AS IN	0.42
2	0.50	IN PRACTICE		28.1	ZERO	COLUMN 5.	0.28
3	0.50	COL. 5 CALC.		28.1	ZERO		0.28
4	0.50	IN ONE STEP.		28.1	ZERO		0.28
5	0.50			28.1	ZERO		0.28
6	0.50			28.1	ZERO		0.28
7	0.50			31.2	ZERO		0.31
8	0.50			39.3	ZERO		0.39
9	0.50			59.9	ZERO		0.60
10	0.50			89.9	ZERO		0.90
11	0.50			115.4	ZERO		1.16
12	0.50			131.04	ZERO		1.31

TABLE 6.8

LOAD CALCULATION FROM RESULT OF 1ST ITERATION (DIAG.6.21)

(WATER-INFLATED CASE)

*F = 1/50 (Scaling Factor).

NODE N	L (FT)	hu (FT)	hi (FT)	WATER PRESS. (LB/FT^2)	AIR PRESS. (LB/FT^2)	AVE. PRESS. (LB/FT^2)	APPLIED LOAD (LB/FT^2) 7 x 2 x F*
COL.NO. 1	2	3	4	(3-4)Y 5	6	(5-6) 7	8
1	0.75			34.3	ZERO	AS IN	0.51
2	0.50			34.3		COLUMN 5.	0.34
3	0.50	IN PRACTICE		34.3			0.34
4	0.50	COL. 5 CALC.		34.3			0.34
5	0.50	IN ONE STEP.		34.3			0.34
6	0.50			34.3			0.34
7	0.50			44.3			0.44
8	0.50			60.4			0.60
9	0.50			90.5			0.90
10	0.55			121.7			1.34

Values of tension are given in Table 6.9, and the experimental and best computer shapes are compared in Diagram 6.22.

TABLE 6.9

COMPARISON OF TENSION FOR WATER-INFLATED CASE.

METHOD OF OBTAINING TENSION	TOTAL PERIM. (feet)	BASE WIDTH (feet)	NO. OF NODES.	TENSION (lb/ft) CALCULATED UPSTREAM VALUE	CALCULATED DOWNSTREAM VALUE	AVERAGE
ANWAR FROM EXP. PROFILE	8.4	2.9	-	-	-	58
GRAPHICAL	8.4	2.9	-	-	-	71±4
HARRISON-SIMPLEX	8.4	2.9	120 20	73 60	84 94	78 77
BINNIE	8.4	2.9	-	-	-	74
ANALOGUE 1 st.cycle 2 nd.cycle	8.4	2.9	12	46 80	88 100	67 90

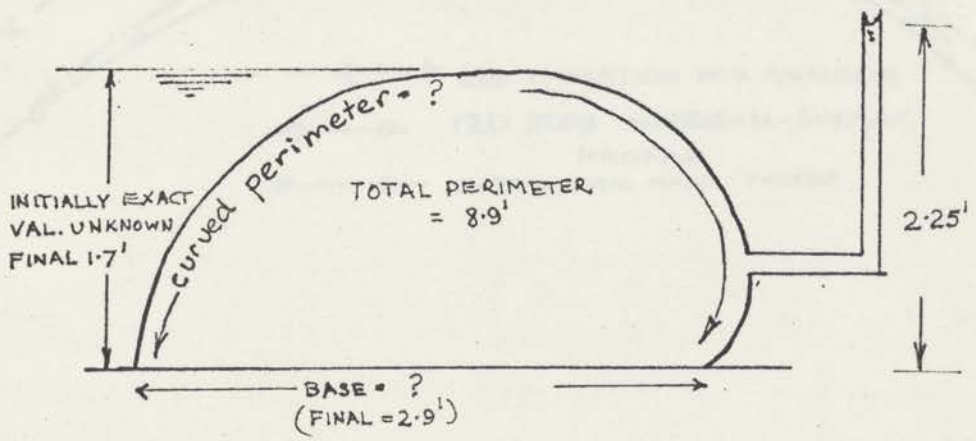

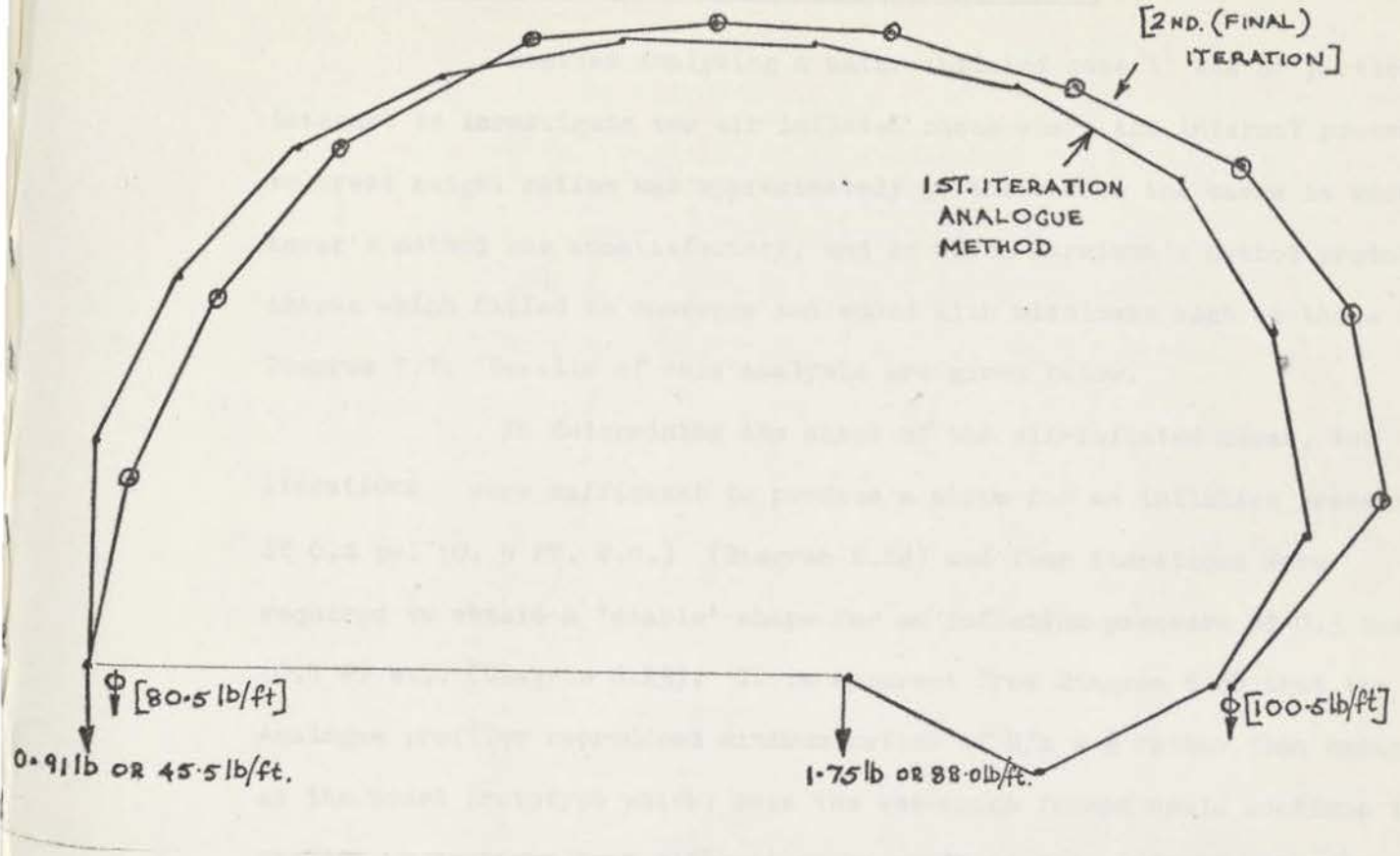

DIAGRAM 6.21 RESULTS OF GUESS AND 1ST ITERATION FOR WATER-INFLATED CASE

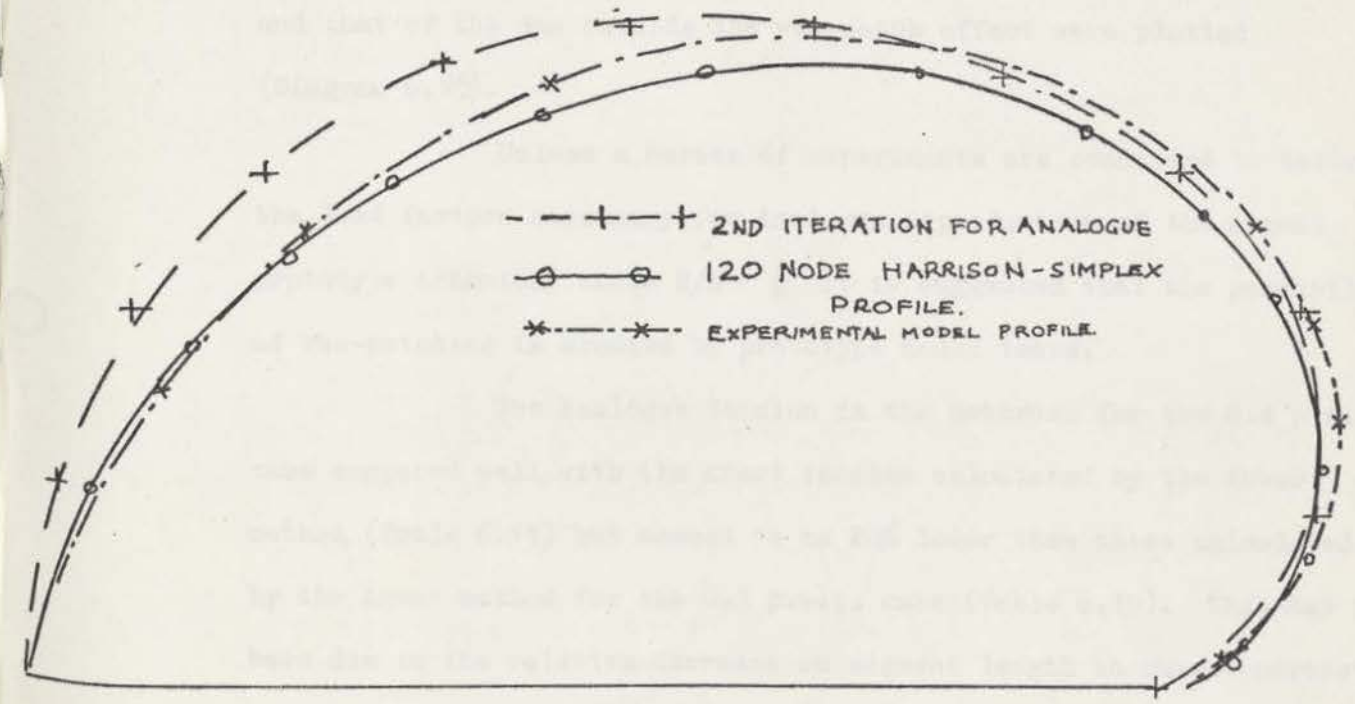

DIAGRAM 6.22 COMPARISON OF 2ND ANALOGUE ITERATION, EXPERIMENTAL PROFILE AND HARRISON PROFILE.

6.5.2 Further Results of Shape Prediction Analysis

Besides analysing a water-inflated case it was of particular interest to investigate two air inflated cases where the internal pressure to crest height ratios was approximately $\frac{1}{2}$; these were the cases in which Anwar's method was unsatisfactory, and in which Harrison's method produced shapes which failed to converge and ended with miscloses such as those in Diagram 7.7. Results of this analysis are given below.

In determining the shape of the air-inflated cases, two iterations were sufficient to produce a shape for an inflation pressure of 0.4 psi (0. 9 FT. W.G.) (Diagram 6.24) and four iterations were required to obtain a 'stable' shape for an inflation pressure of 0.3 p.s.i. (0.7 FT W.G. (Diagram 6.23). It is apparent from Diagram 6.25 that the Analogue profiles reproduced minimum ratios of $H/h = \frac{1}{2}$ rather than behave as the model prototype which, once the vee-notch formed would continue to support an upstream head with ratios as small as 1/3. (Diagram 5.26). The shapes obtained by the Analogue method straddled those from the model analysis in the case where both the profile for the vee-notch and that of the dam outside the vee-notch effect were plotted (Diagram 6.25).

Unless a series of experiments are conducted to determine the load factors necessary for Analogue reproduction of the actual prototype behaviour where $H/h \doteq \frac{1}{2}$ it is suggested that the possibility of vee-notching is studied by prototype model tests.

The analogue tension in the membrane for the 0.4 p.s.i. case compared well with the crest tension calculated by the Anwar method (Table 6.11) but seemed to be 20% lower than those calculated by the Anwar method for the 0.3 p.s.i. case (Table 6.10). This may have been due to the relative increase in segment length to curved perimeter ratio.

TABLE 6.10

COMPARISON OF TENSION FOR

AIR-INFLATED CASE (INTERNAL HEAD = 0.7 FT W.G., (0.3p.s.i))

METHOD OF OBTAINING TENSION	TOTAL PERIM. (feet)	BASE WIDTH (feet)	NO. OF NODES	TENSION (lb/ft)		
				CALCULATED UPSTREAM VALUE	CALCULATED DOWNSTREAM VALUE	AVERAGE
Anwar (from Analogue Shape)	8.3	3.0	-	-	-	29
Analogue	8.3	3.0	12	24	24	24

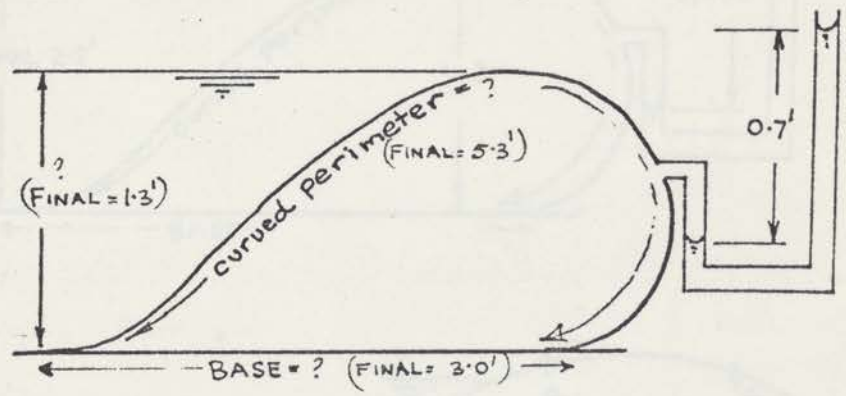

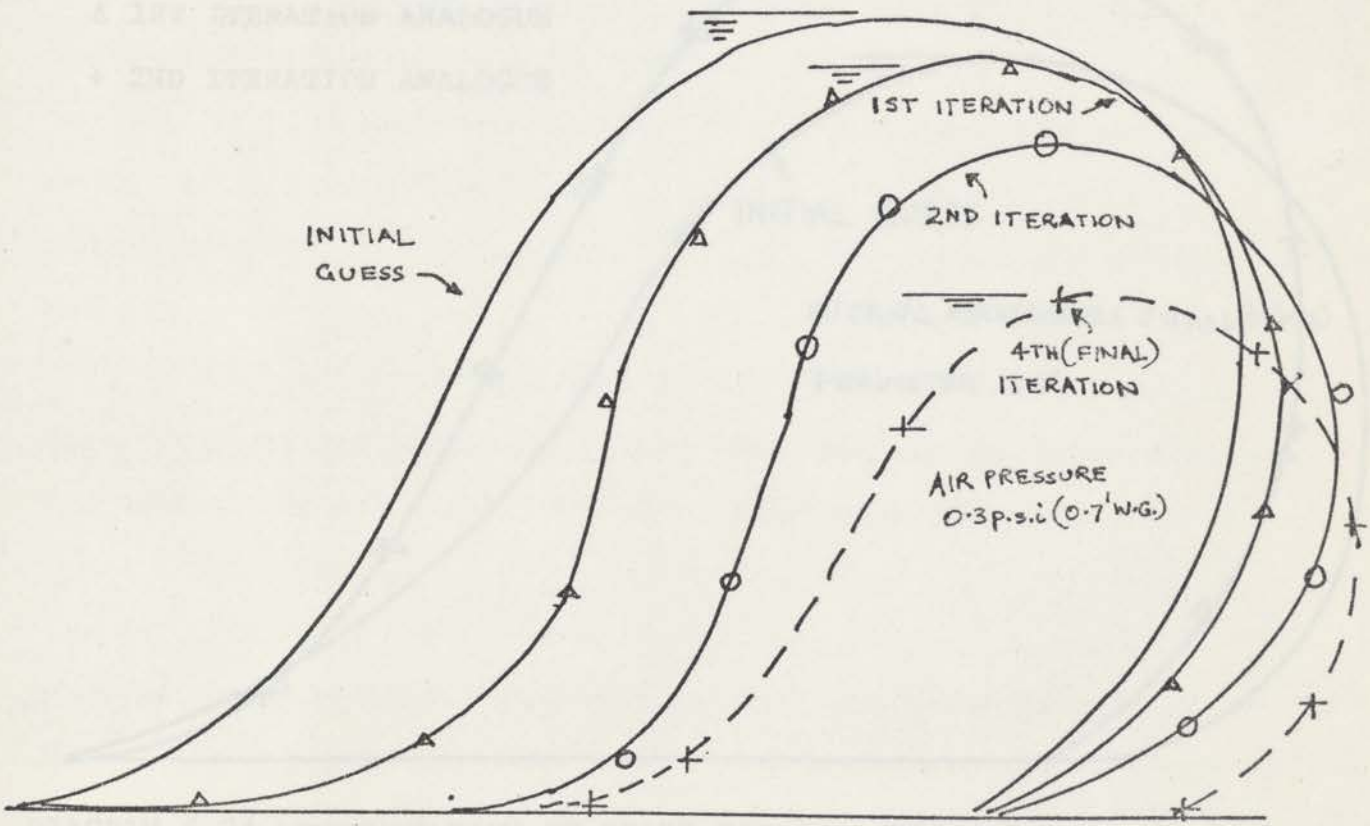

DIAGRAM 6.23 ITERATIONS FOR AIR-INFLATED CASE

TABLE 6.11

COMPARISON OF TENSION FOR

AIR-INFLATED CASE (INTERNAL HD = 0.9 ft W.G. (0.4 p.s.i.)

METHOD OF OBTAINING TENSION	TOTAL PERIM. (feet)	BASE WIDTH (feet)	NO. OF NODES	TENSION (lb/ft)		
				CALCULATED UPSTREAM VALUE	CALCULATED DOWNSTREAM VALUE	AVERAGE
ANWAR (FROM ANALOGUE SHAPE)	8.7	2.6	-	-	-	63
ANALOGUE (2ND ITERATION)	8.7	2.6	12	68	64	66

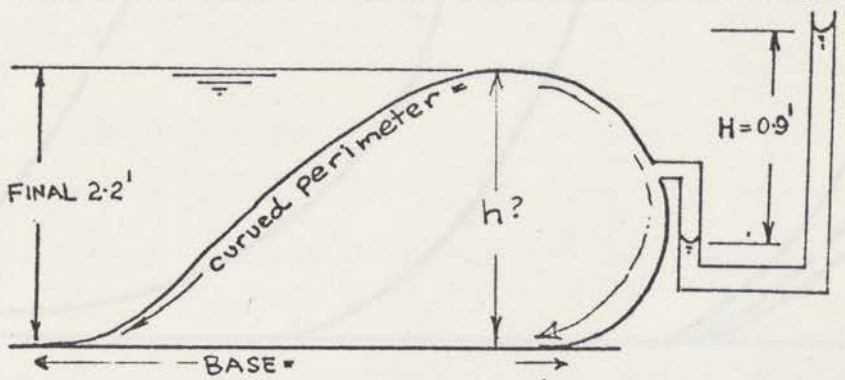

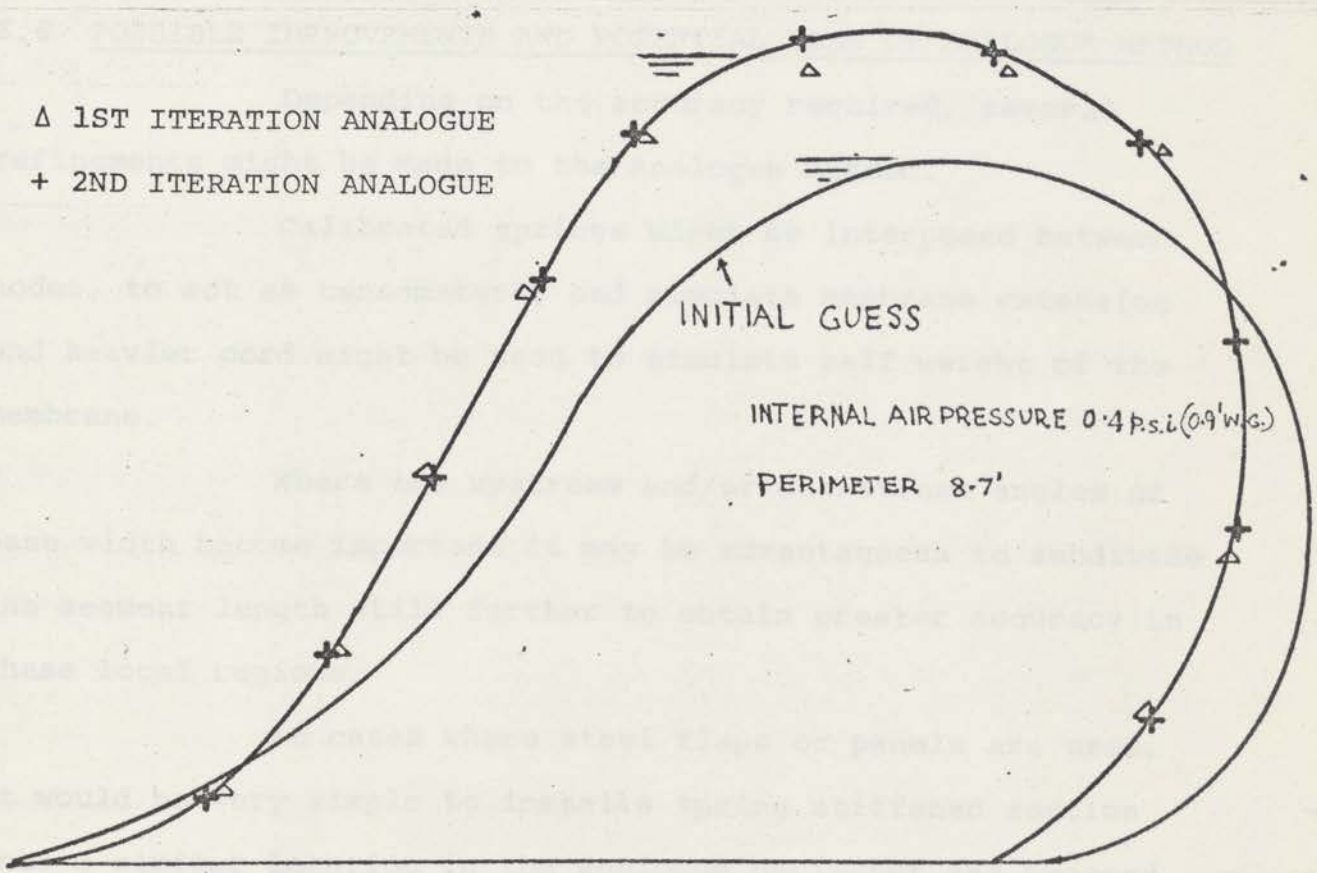

DIAGRAM 6.24 DETERMINATION OF SHAPE FOR AIR-INFLATED CASE (0.9 Ft. W.G.

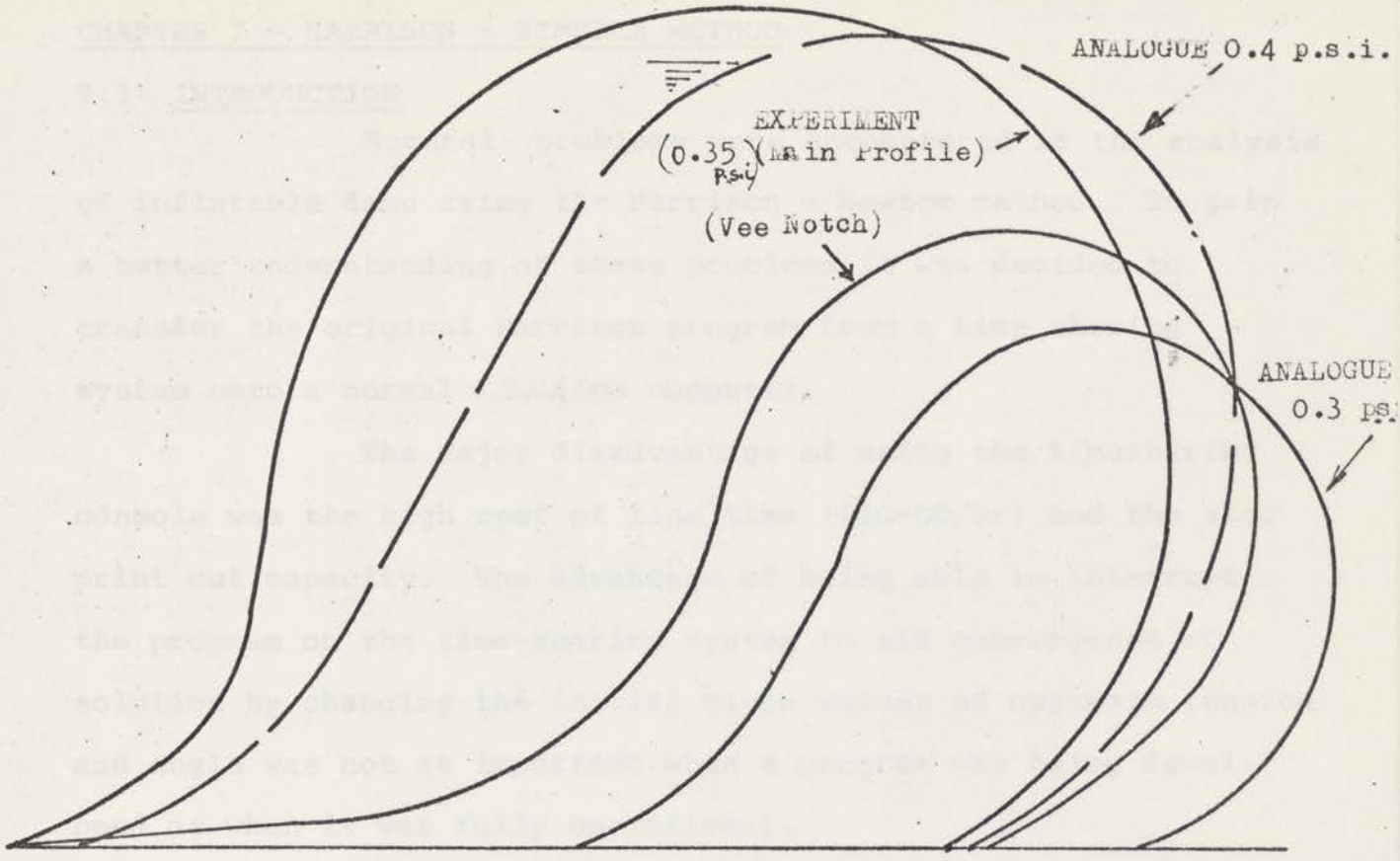

DIAGRAM 6.25. COMPARISON OF AIR-INFLATED PROFILES FOR LOW H/h

6.6 POSSIBLE IMPROVEMENTS AND POTENTIAL USES OF ANALOGUE METHOD

Depending on the accuracy required, several refinements might be made to the Analogue method.

Calibrated springs might be interposed between nodes, to act as tensometers, and simulate membrane extension and heavier cord might be used to simulate self weight of the membrane.

Where the upstream and/or downstream angles or base width become important it may be advantageous to subdivide the segment length still further to obtain greater accuracy in these local regions.

In cases where steel flaps or panels are used, it would be very simple to installa spring stiffened section into a similar location in the analogue perimeter and proceed as for the ordinary case.

CHAPTER 7 - HARRISON - SIMPLEX METHOD

7.1 INTRODUCTION

Several problems were encountered in the analysis of inflatable dams using the Harrison - Newton method. To gain a better understanding of these problems it was decided to transfer the original Harrison program from a time sharing system onto a normal C.D.C.6600 computer.

The major disadvantage of using the timesharing console was the high cost of line time ($10-00/hr) and the slow print out capacity. The advantage of being able to interrupt the program on the time-sharing system to aid convergence of solution by changing the initial given values of upstream tension and angle was not as important when a program was being developed as when it was fully operational.

7.2 PROBLEMS ASSOCIATED WITH THE HARRISON ANALYSIS AND THEIR ATTEMPTED SOLUTION AND OTHER ALTERATIONS

7.2.1 Introduction

Several minor changes and improvements were progressively carried out on the original program but the overall effect of these still did not markedly improve the results. Iteration of the solution was improved by changing the Newton method of iteration (discussed in Section 4.6) to the Simplex method which will be described below in Section 7.3 as the Harrison - Simplex method. Again the above minor changes were applied and these mostly had similar effects. Unless the effect of a minor improvement on the original Harrison - Newton method differed from the effect on the Harrison - Simplex, it will not be discussed again under the Harrison - Simplex description, even though applied.

The final version of the Harrison - Simplex program enabled a profile to be obtained in graph form starting with a pair of guessed values of tension and angle with more than 100% discrepancy compared with the correct values. This was very useful in those cases of particular interest to designers: - namely with the dam about to be overtopped, with low H/h ratio, and with the base defined a few % less than the unrestrained base width.

7.2.2 "Overflow Stop"

In many cases during computation there was a print out suggesting that the crest level was below the upstream water level whereupon the original program would ask for a new set of guessed values of tension and angle. When this occurred in cases based on experimental results it was apparent that the program was not completely satisfactory. Also in these cases the time-sharing program failed to give the value of the final iterated tension and angle, and misclose, so no indication as to whether to increase or decrease the new values was available.

In cases where the dam was overtopped a conditioned 'GO TO' statement was introduced to enable the programme to continue. (See Appendix I(vi) statement No. 170 to 180). If the top part of the profile of the dam flattened out to a gradient between 0.0 and 0.2, and the level of water was higher than the corresponding value of y, the analysis would continue as if the water level was equal to the value of the y ordinate of the node the adjacent segment of which had a gradient between 0.0 and 0.2.

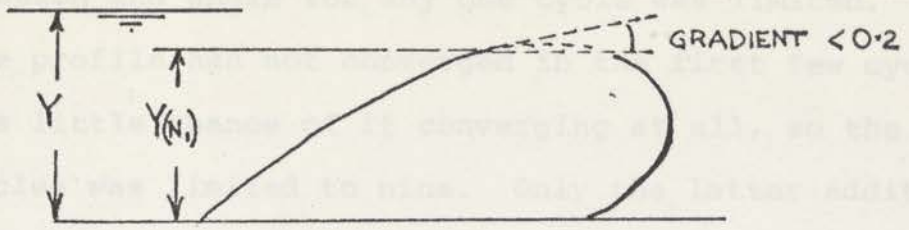

DIAGRAM 7.1 ANALYSIS CONTINUES FOR WATER LEVEL = $Y(N_1)$ EVEN THOUGH Y > CREST HEIGHT

As the segment tensions and profile up to node N_1 had been calculated for a waterlevel of $Y > Y(N_1)$ some element of error had been introduced. However $\frac{Y - Y(N_1)}{Y} \times 100\%$ was of the order of a few percent which had negligible effect and in any case the value of waterlevel could be adjusted in the next run, if desired.

7.2.3 Graphical Representation of Results

To save several hours plotting a graph of each profile result, a graph subroutine GRADAM was added. (Appendix I, towards end of program). This enabled the computer to plot the profile co-ordinates after they had been calculated to the required scale. Since point location was printed using the line and character change spacing, precision of the plot on the graph was limited to ± 1/10" respectively.

7.2.4 Divergence Stop

A major problem in the Harrison - Newton program was divergence of the misclose after a few iterations. (See Chapter 4 Section 4.6. for a description of the analysis and Diagrams 7.2 and 7.7). The reasons for this divergence are discussed in more detail in Section 7.3.

To slow the rate of divergence of the misclose and so possibly allow the diverging calculations to reverse and

start converging, the maximum variation of the new values of tension and angle for any one cycle was limited. However if the profile had not converged in the first few cycles, there was little chance of it converging at all, so the number of cycles was limited to nine. Only the latter addition was successful in preventing needless expenditure and also prevented the misclose oscillating about unacceptable values without converging any further.

7.2.5 Reduction of Computation Time

To reduce computation time, without markedly affecting the results, the material fabric was taken as massless and inextensible. In addition the base was taken as horizontal.

7.2.6 Inner Do Loop

Even after previous alterations had been effected, the problem of "non-convergence" still existed. The results, in the form of graphed profiles, showed some profiles looped around in most unusual shapes with no similarity to those derived experimentally.

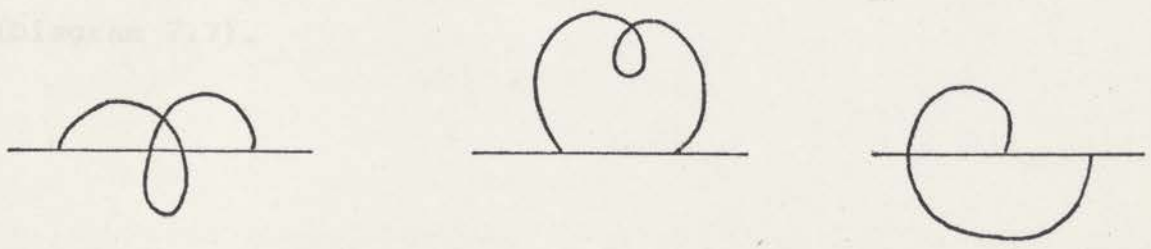

DIAGRAM 7.2. EXAMPLES OF INSTABILITY

To further reduce the computation time and cost and possibly improve the stability, it was decided to take out the inner do loop which was inserted to recalculate the tension between nodes more accurately once the approximate position of

the last node and direction of the next segment had been calculated, (as described in Section 4.6). This had two unexpected effects.

The first effect was that the profiles for certain conditions would converge more frequently than before.

The second effect was that the tension increased around the perimeter from the upstream side to the downstream side (in certain cases by as much as 100% above the upstream value) whereas before, the calculated tension varied only by a few percent. As the number of nodes increased from 20 to 120 the difference in tension around the curved perimeter decreased. An average of the upstream and downstream values would equal the value of tension in the membrane (assumed constant) as calculated previously.

7.2.7 Tension T set to a Constant Valve

To compensate for the varying tension in Section 7.2.6. above, it was decided to set the tension constant, either after the first few nodes or immediately, but the effect in terms of instability, was as bad as, or worse than before, so was rejected (Diagram 7.7).

7.3 CHANGE FROM NEWTON TO SIMPLEX ITERATIVE METHOD

As more cases were studied, it became increasingly apparent that a major weak spot in the analysis was the Newton iterative method. The successful operation of the Newton method, and the ultimate solution was dependent on the value of the misclose. If the downstream end of the membrane lay flat along the horizontal base and the misclose or the denominator, tended to zero, (see Diagram 7.3. below),

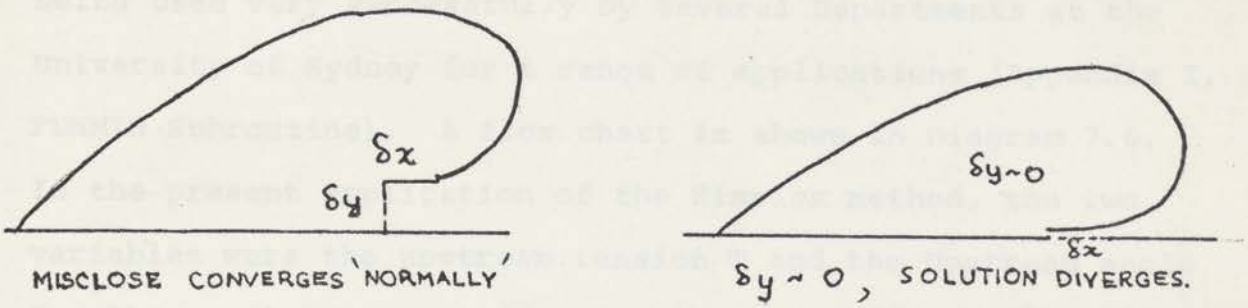

DIAGRAM 7.3. MISCLOSE EFFECT

the new value of tension T might tend to infinity: as might be deduced from the formula,

$$T^1 = T - \left| \left(x\frac{\partial y}{\partial \theta} - y\frac{\partial x}{\partial \theta} \right) \Big/ \left(\frac{\partial x}{\partial T}\frac{\partial y}{\partial \theta} - \frac{\partial y}{\partial T}\cdot\frac{\partial y}{\partial \theta} \right) \right|$$

where T was the original tension value.

This divergence effect, the sensitivity of stability for low values of internal to upstream head ratios, and the sensitivity of the choice of the initial guessed values of T and Θ making it difficult and expensive to do a systematic search through a series of values (inserted by a series of data cards) for a single case, induced the author to investigate and search for a more satisfactory method which combined both a search and solution potential.

Such a method, called the 'Simplex Method', was found and successfully applied to this particular problem.

7.3.2 The Simplex Method Subroutine

The purpose of the subroutine was to solve the values of N independent variables by minimising the dependent function. The method was described in Nelder and Mead's paper in Reference 19, but the important aspects as applied to the Harrison program are outlined below.

The subroutine was developed by D. Herbertson - Evans (Ref.20) and modified by G. Kipp (Reference 20) and is being used very successfully by several Departments at the University of Sydney for a range of applications (Appendix I, FUNMIN Subroutine). A flow chart is shown in Diagram 7.6. In the present application of the Simplex method, the two variables were the upstream tension T and the Upstream angle θ. These values were initially guessed, as before (Chapter 4.6) and the misclose calculated, In this case however the two values of tension and angle were successively changed by a predetermined percentage, and the miscloses were calculated again. The worst misclose was selected and a new set of T and θ were produced by reflecting the triangle away from the worst misclose.

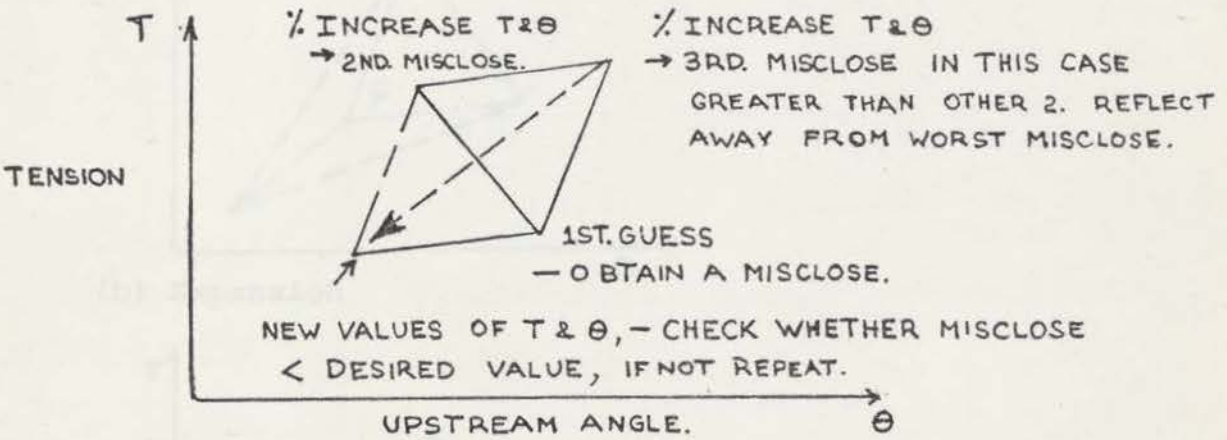

DIAGRAM 7.4 SIMPLEX METHOD

If these values of tension were plotted against angle, a series of triangles would be obtained (Diagram 7.4).

7.3.3 The Principle of The Simplex Method

Referring to Diagram 7.5 let Yi be the value of the misclose at a point Pi, and let h be the suffix such that Yh = max (Yi) and l the suffix Yl = min (Yi). Further $\bar{P}$ was the centroid of the triangle joining the points and (Pi Pj) was the distance between Pi and Pj. At each stage Ph was rejected and a new point tried, (trying a pair of values of T and Θ) by using one of the following operations - reflection, expansion, or contraction shown below. This was continued until the misclose was reduced to the specified limit.

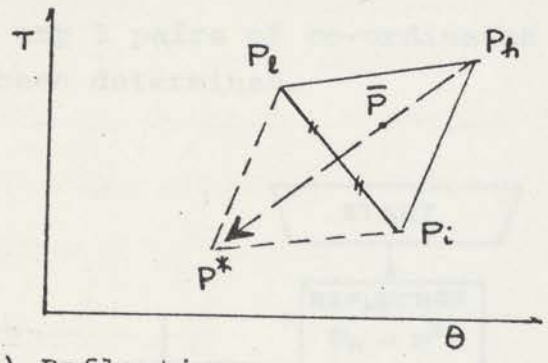

(a) Reflection

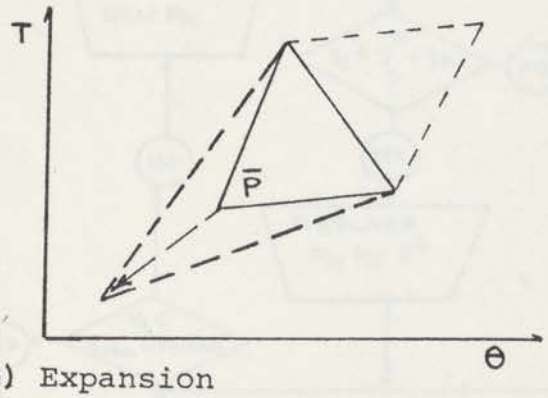

(b) Expansion

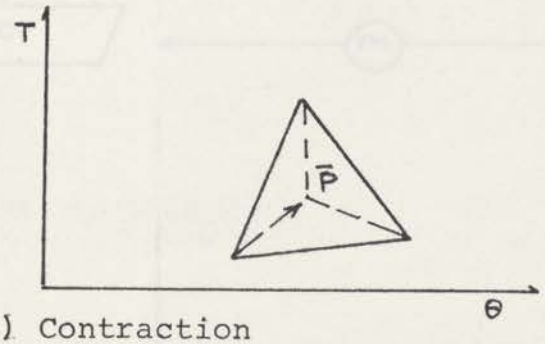

(c) Contraction

DIAGRAM 7.5 SIMPLEX PROCESS

The operations were specified as follows:-

The reflection point of Ph was denoted by P*. Each of its coordinates was calculated by an equation,

$$P^* = (1 + \alpha)\,\overline{P} - \alpha Ph$$

where α is the reflection coefficient.

An expansion point was found as

$$P^{**} = \gamma P^* + (1 - \gamma)\,\overline{P}$$

where γ ($>\ell$) was the expansion coefficient.

A contraction point was found as

$$P^{**} = \beta\, Ph + (1 - \beta)\,\overline{P}$$

The contraction coefficient lay between 0 and 1

The process started off with a reflection once any 3 pairs of co-ordinates and any 3 corresponding miscloses had been determined.

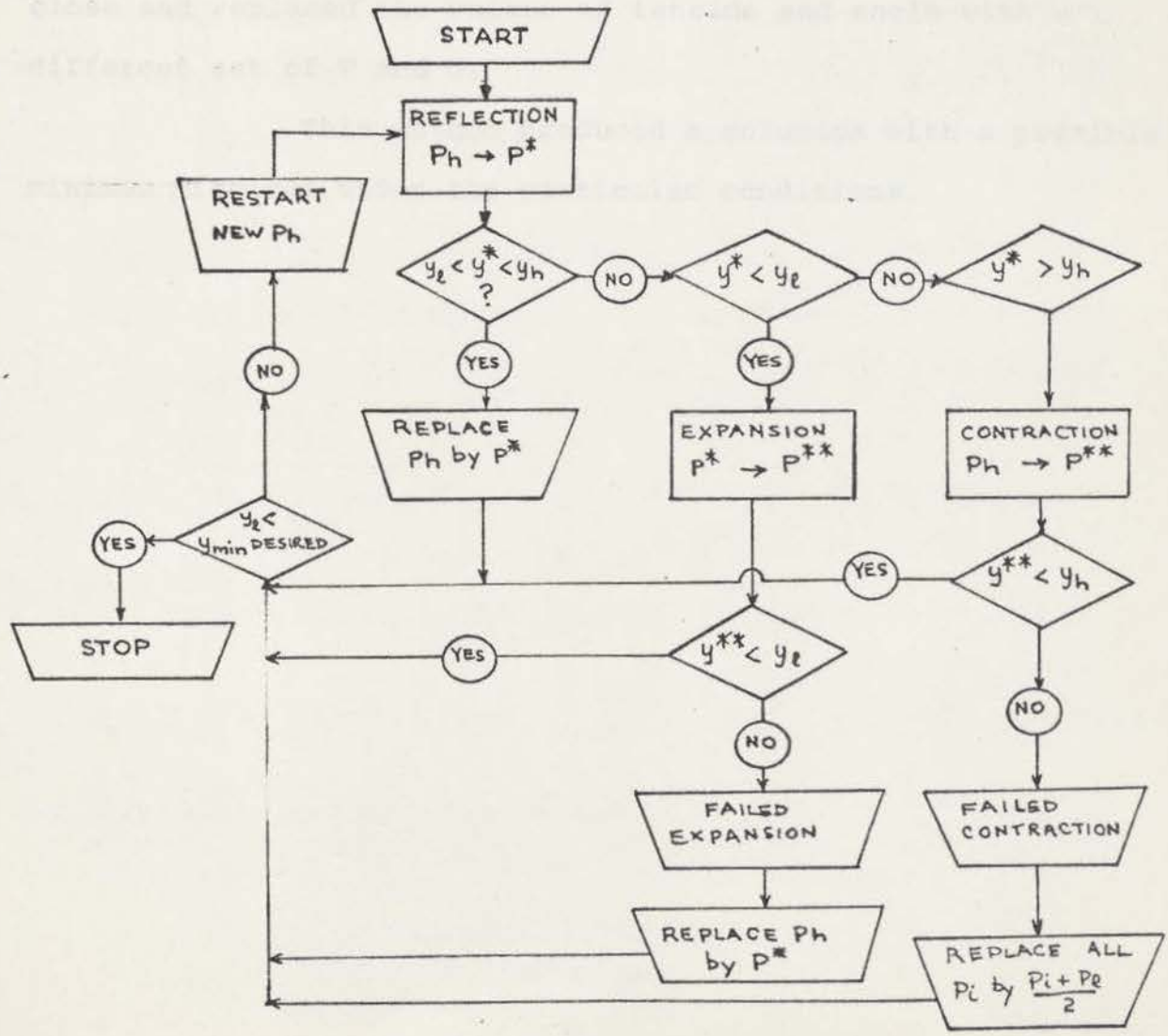

DIAGRAM 7.6 SIMPLEX FLOWCHART

Nelder and Mead (Reference 19) had tried several ratios and combinations of coefficients and recommended the best and simplest to be

$\alpha = 1$, $\beta = \frac{1}{2}$, and $\gamma = 2$.

However it was thought that a more efficient system (with direct engineering application) would be to weight the ratios according to the centroid of the miscloses rather than the geometric centroid calculated from the co-ordinates of P.

This process of triangle flip-flopping was repeated either until the difference between the two smallest miscloses was no less than the desired value, or the smallest misclose was less than the smallest value specified.

Convergence was pretty well assured for most functions because the system physically rejected the worst misclose and replaced the values of tension and angle with a different set of T and Θ.

This method produced a solution with a possible minimum misclose under the particular conditions.

7.4 RESULTS

As can be seen from the graphs the profile shapes corresponded closely to those obtained experimentally. Generally the closeness of fit of the profiles improved as the number of nodes were increased. Instability prevailed where the head differential between upstream and downstream was small, or where upstream and downstream heads were zero.

Tension values compared well with those obtained by other methods and were within the range of error when compared with those calculated by the Analogue Method and Graphically.

A few interesting graphs have been selected from a series of approximately 250 cases which were analysed (and will be available for inspection on request). The intention here is to indicate trends resulting from changes to the various parameters which affected the results. These parameters included the number of nodes, the ratio of the curved perimeter and base width and the physical loading conditions acting on the dam.

A description of the main features of each graph follows below.

Diagram 7.7. This diagram shows typical profiles in which the computer analysis failed to converge, as well as a comparison between a 60 node profile and the experimental profile for the conditions shown on the diagram.

Several cases of instability occurred when the Tension 'T' around the perimeter was set constant. Another common cause of instability before the Newton program was altered to the Simplex program, was when initial guessed values of T and θ (Tension and upstream angle respectively) were not close enough to the actual values.

EXAMPLES OF INSTABILITY AND COMPARISON OF WATER-INFLATED PROFILES BETWEEN EXPERIMENT AND COMPUTER

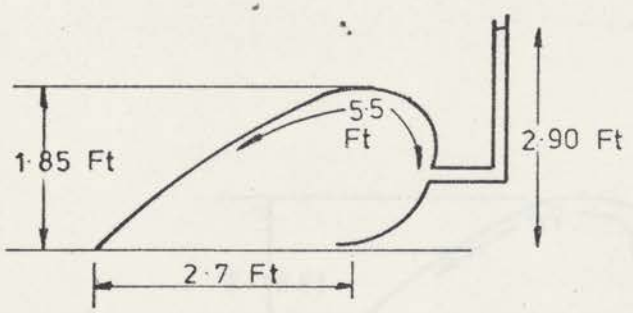

$(H/h = 1.57)$

RESULTS FOR 60 NODES

- o GUESS TOO LARGE (FINAL PROGR
- \+ CONSTANT TENSION
- × AVERAGE TENSION 115 lb/Ft
  UPSTREAM ANGLE 97°

SCALE 1:6

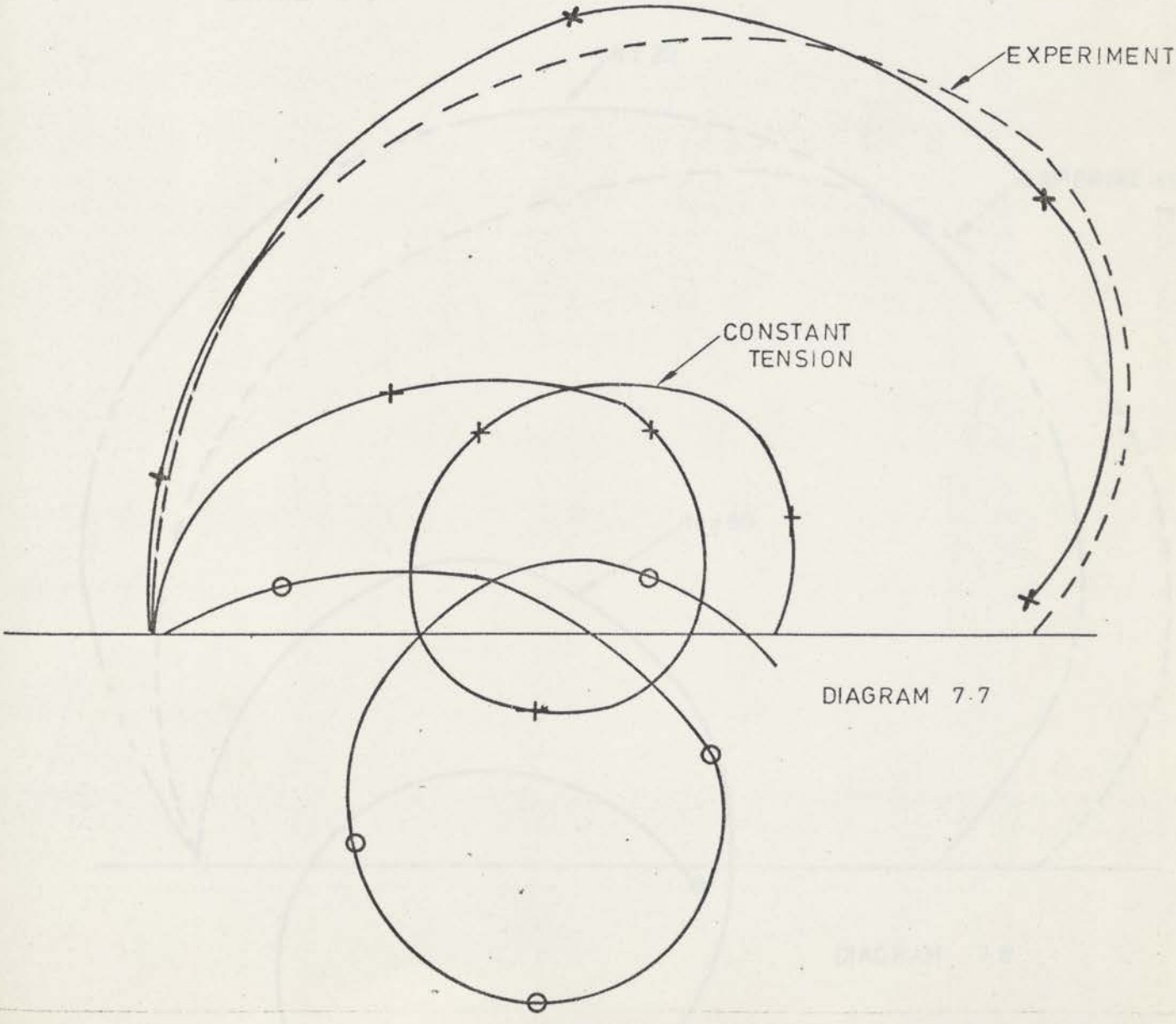

DIAGRAM 7·7

COMPARISON BETWEEN 20 AN 60 NODES AND EXPERIMENTAL PROFILES FOR WATER INFLATED CASE.

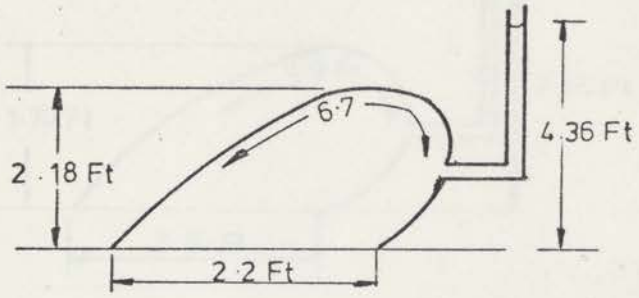

SCALE 1:6

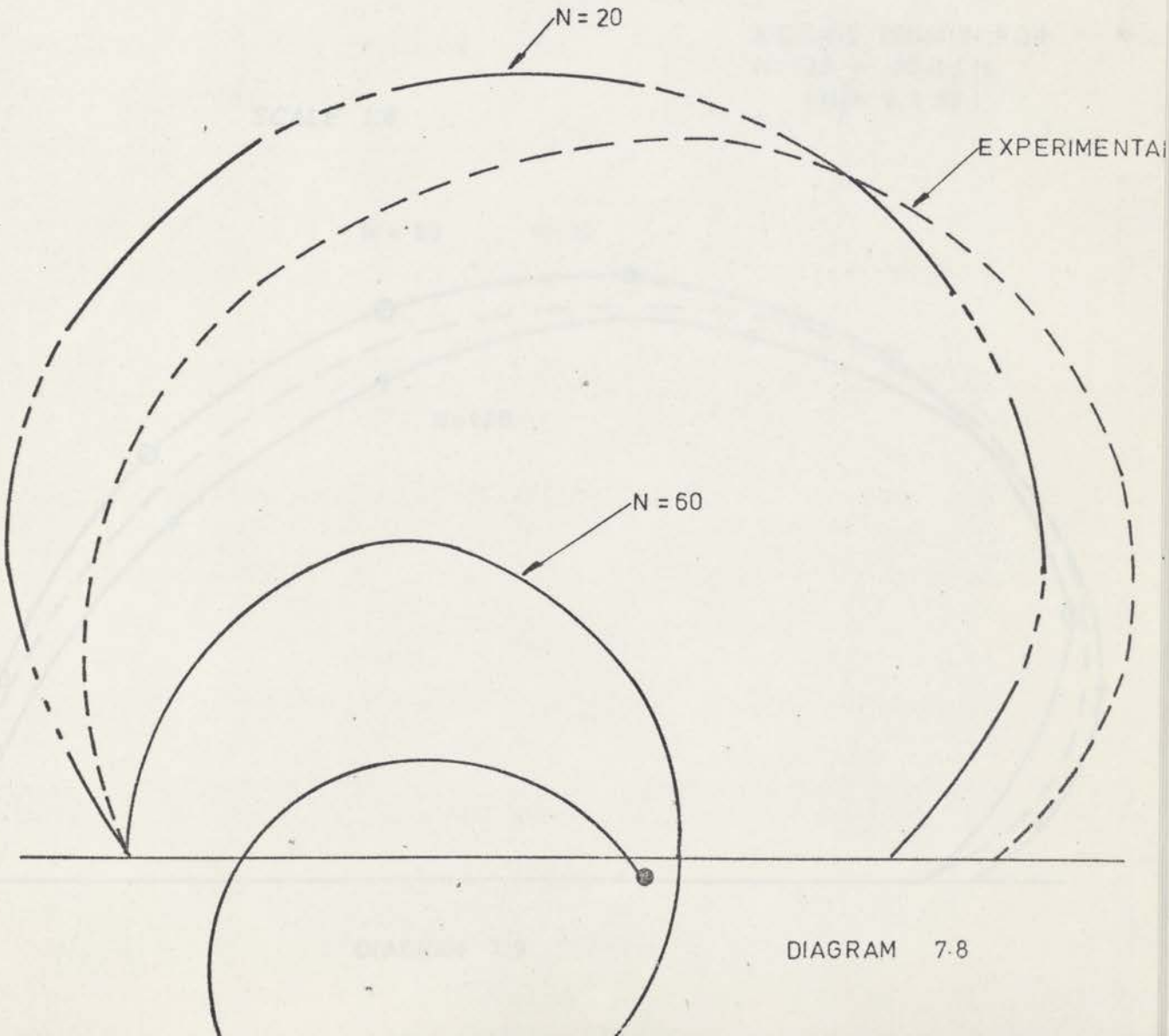

DIAGRAM 7·8

COMPARISON BETWEEN PROFILES FOR 20, 60 AND 120 NODES FOR WATER INFLATED CASE. COMPARE THE SIMILARITY BETWEEN. THE SHAPE FOR 20 NODES, AND THE EXPERIMENTAL SHAPE WITH THAT OF THE ANALOGUE PROFILE FOR 12 NODES. (Diag 6·22).

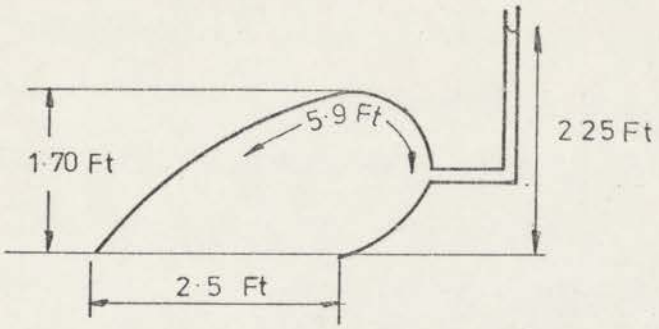

AVERAGE TENSION FOR
N=120 — 70 lb/ft
(H/h = 1·32)

SCALE 1:6

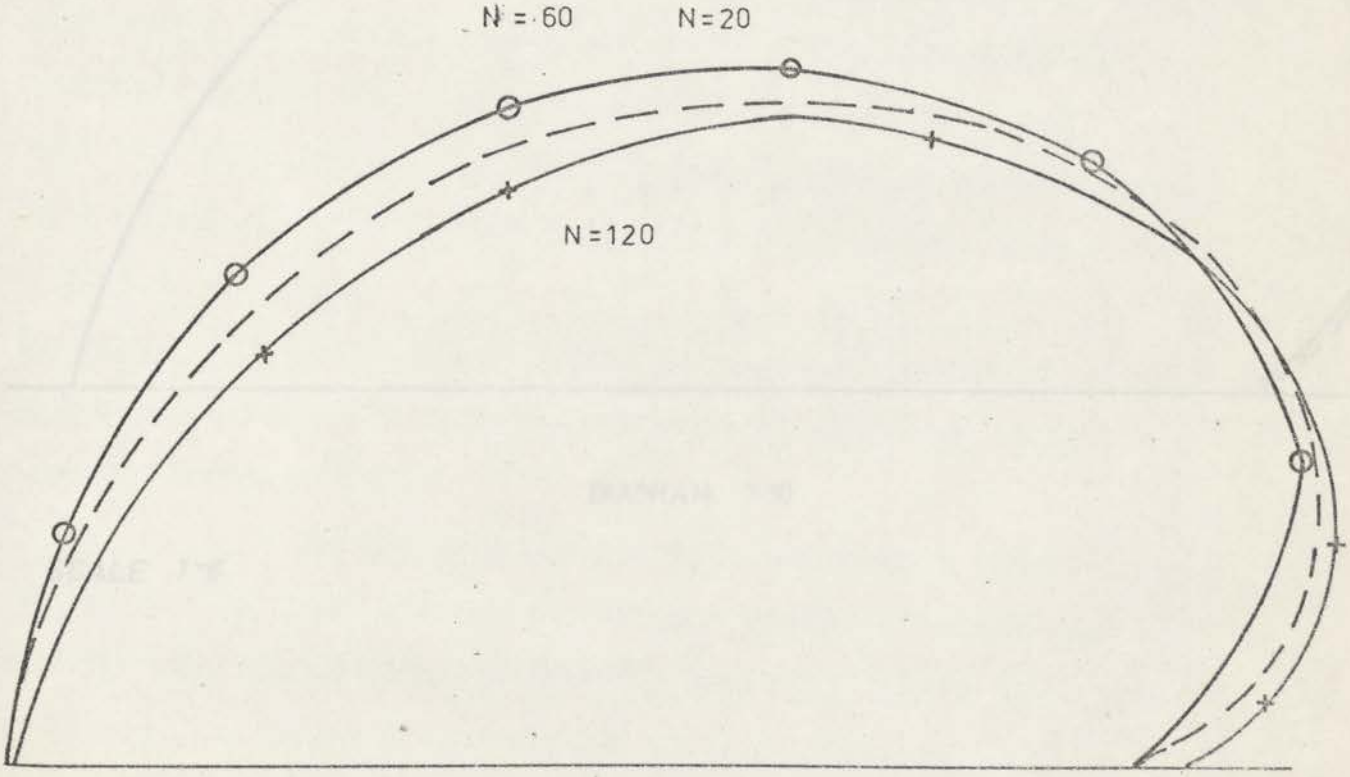

DIAGRAM 7·9

COMPARISON BETWEEN 20 NODE COMPUTER PROFILE AND EXPERIMENTAL PROFILE.

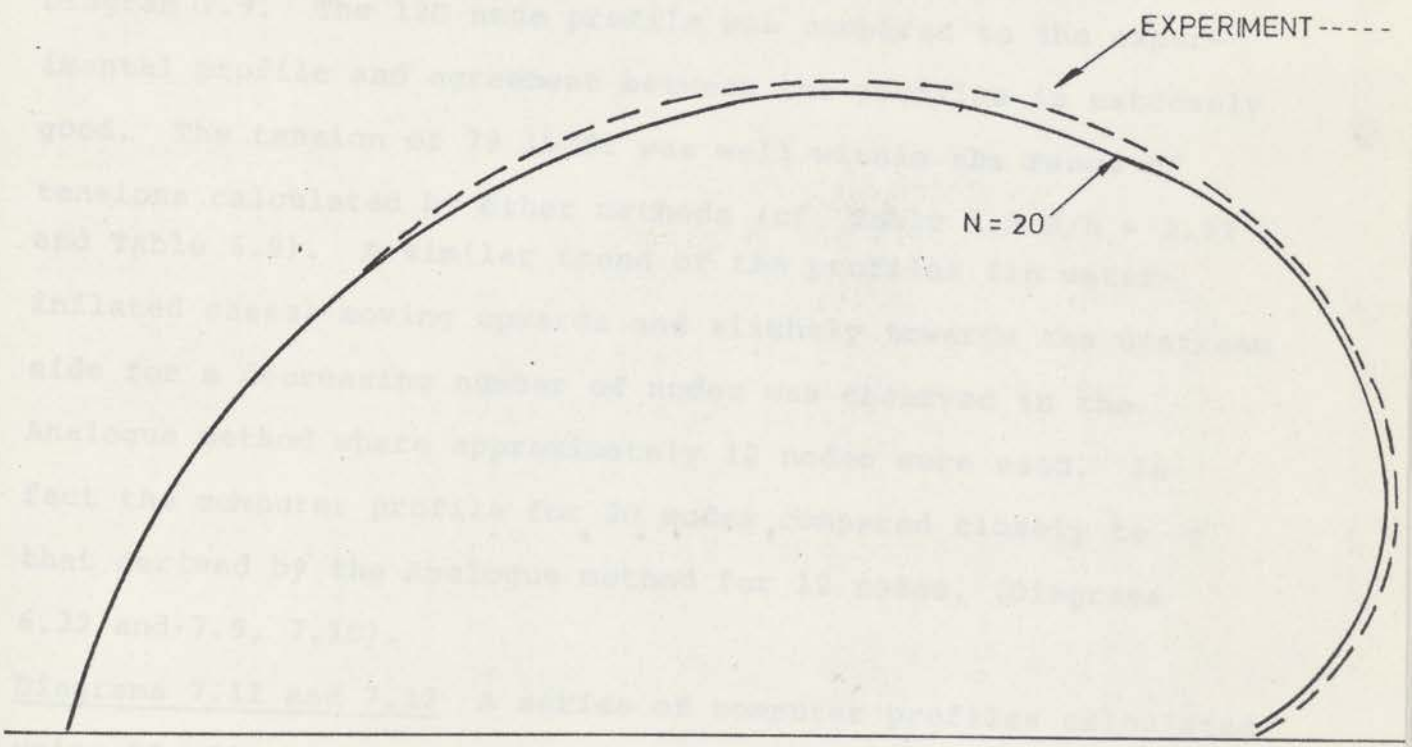

DIAGRAM 7.10

SCALE 1:6

The shape derived by the computer analysis which did converge, compared closely to the experimental shape as seen in the diagram, and the tension of 115 lb/ft was within the range calculated by the various methods.

Diagram 7.8 As demonstration of the instability which could occur without warning, a stable profile calculated using 20 nodes and an unstable profile calculated using 60 nodes are compared in Diagram 7.8 with the experimental shape. Apart from the number of nodes all other parameters were equal.

Diagrams 7.9 and 7.10 A comparison between profiles using 20, 60 and 120 nodes was made for a water inflated case in Diagram 7.9. The 120 node profile was compared to the experimental profile and agreement between the profiles is extremely good. The tension of 79 lb/ft was well within the range of tensions calculated by other methods (cf Table 4.5 H/h = 1.32 and Table 6.9). A similar trend of the profiles (in water-inflated cases) moving upwards and slightly towards the upstream side for a decreasing number of nodes was observed in the Analogue method where approximately 12 nodes were used. In fact the computer profile for 20 nodes compared closely to that derived by the Analogue method for 12 nodes. (Diagrams 6.22 and 7.9, 7.10).

Diagrams 7.11 and 7.12 A series of computer profiles calculated using 20, 60 and 120 nodes were compared with each other for the air-inflated case.

As the number of nodes increased a trend (opposite to that described above) of the profiles moving upwards and towards the upstream side was observed. Again the 120 node profile compared closely to the experimental profile.

COMPARISON OF PROFILES BETWEEN 20, 60, 120 NODES FOR AIR-INFLATED CASE.

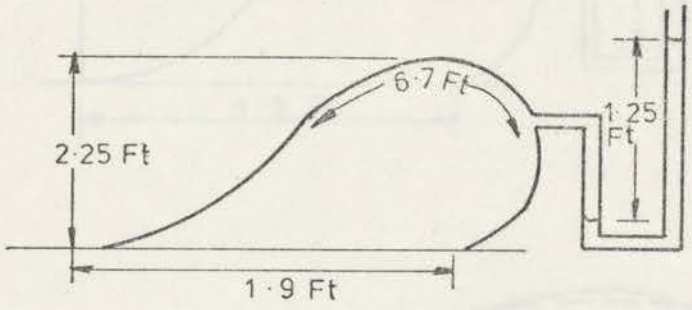

SCALE 1:6

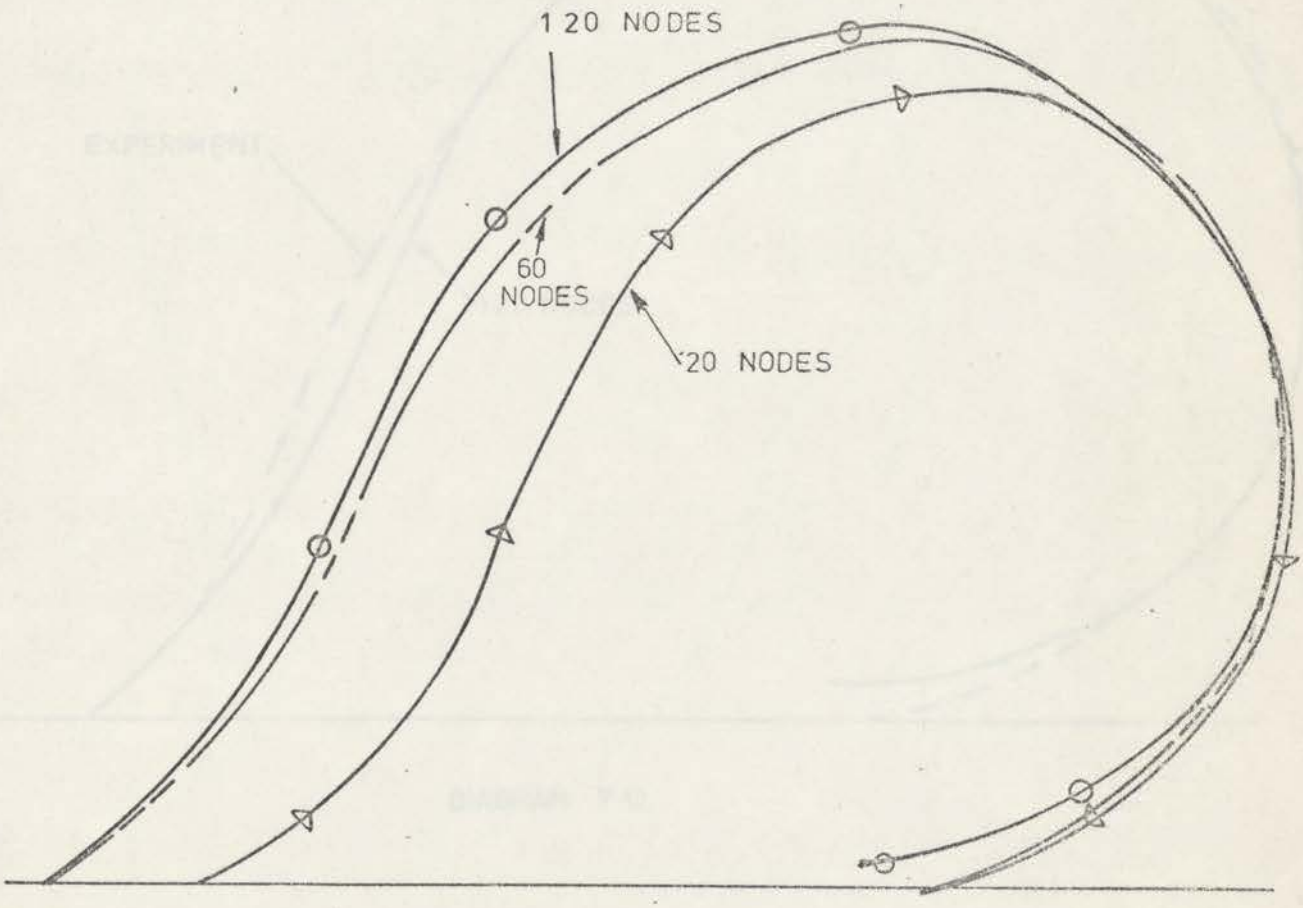

DIAGRAM 7·11

COMPARISON BETWEEN EXPERIMENT PROFILE AND COMPUTER PROFILE FOR 120 NODES. (AIR-INFLATED CASE).

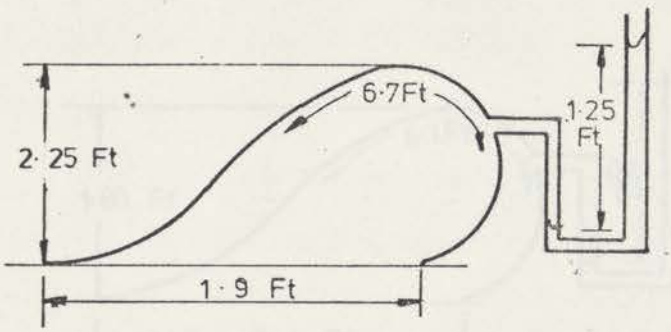

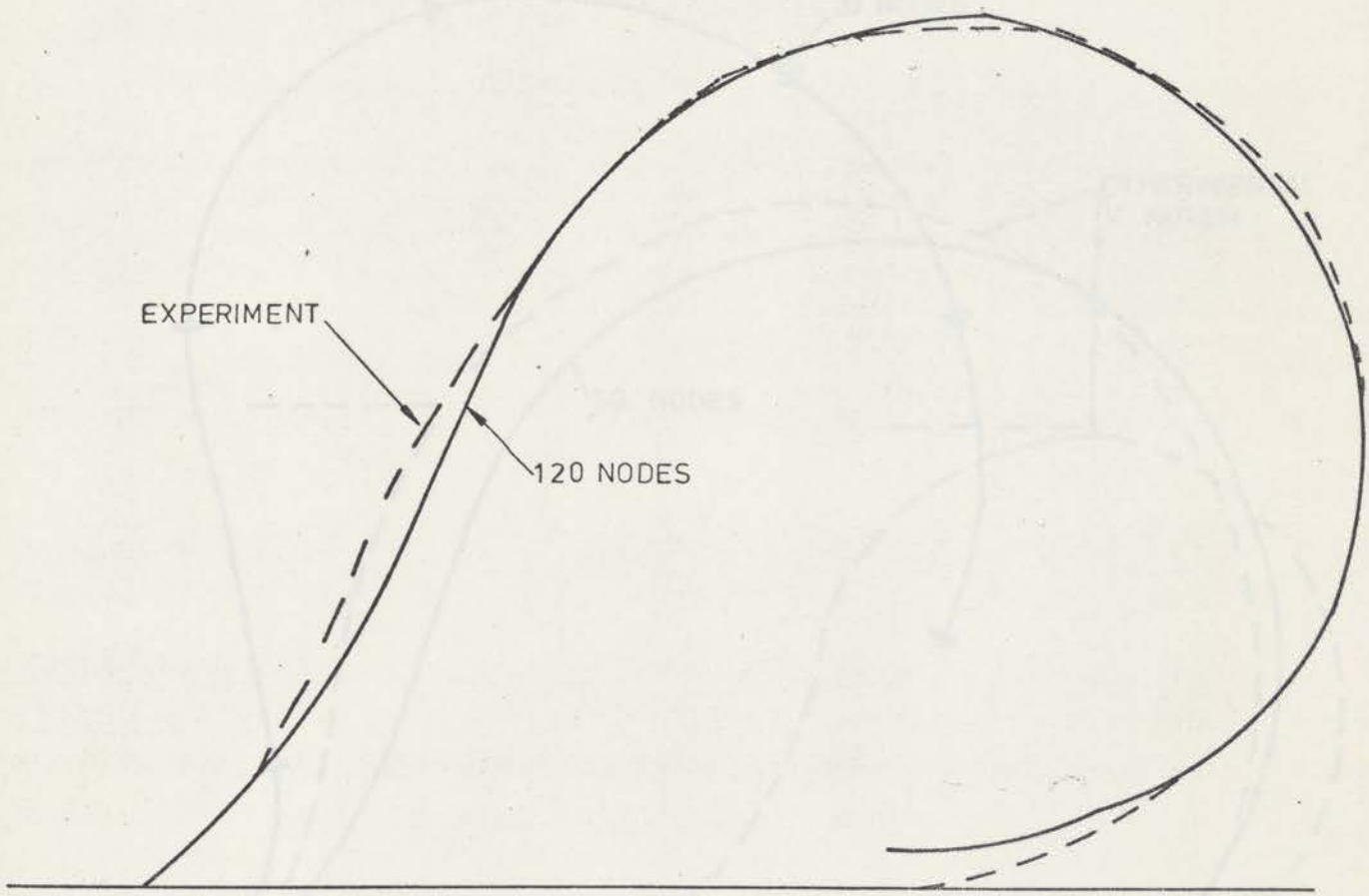

DIAGRAM 7·12

EXAMPLE OF INSTABILITY AND PROFILE WHICH CONVERGED AND COMPARISON WITH EXPERIMENTAL VEE-NOTCH AIR-INFLATED CASE.

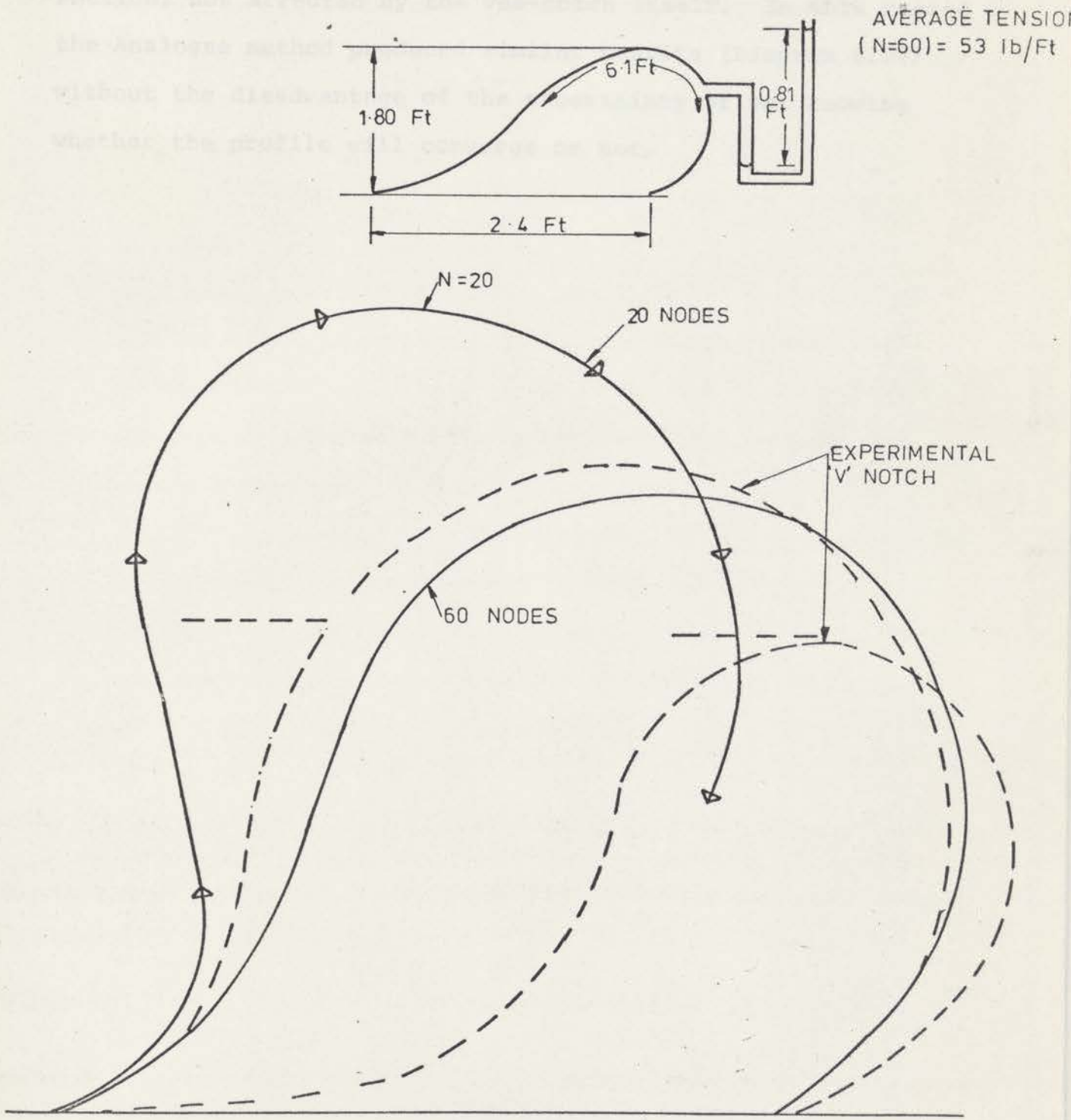

DIAGRAM 7·13

Diagram 7.13 Instability of profiles (similar to the typical example shown in Diagram 7.13) was experienced more often than not in air-inflated cases where $H/h \doteq \frac{1}{2}$. When a case did converge it lay between the experimental profiles of the vee notch and that of the section of the dam uniform in section, not affected by the vee-notch itself. In this regard the Analogue method produced similar results (Diagram 6.24) without the disadvantage of the uncertainty of not knowing whether the profile will converge or not.

7.5 SUMMARY AND IMPLICATIONS

Although the Newton iterative method was changed to the Simplex method profile looping still occurred, but much less frequently. The looping was more prone to occur in conditions where the profile was divided into 60 nodes instead of 20, and low ratios of internal to upstream head. It is well known that there are forms of quadratic equations which are not well conditioned, and it was likely that a similar difficulty could occur with regard to the solution of 60 non-linear simultaneous equations.

No method of solving or predicting this inherent problem was found. A check for looping (which was not carried out) would have been to test whether the co-ordinates of the last and 2nd last nodes lay within a segment length of any of the nodes between the N-3rd and 1st node. If it was about to loop, the analysis could have been restarted using either a decreased number of nodes or a new set of values of T or θ.

Although it would have been nice to be able to continue analysi by investigating the optimum number of nodes that were necessary to 'stabilize' the profile, it was considered an expensive luxury to proceed without a very clear idea of where the trouble was precisely.

CHAPTER 8 - COMPARISON OF METHODS OF ANALYSIS

8.1 COMPARISON OF METHODS

A summary of methods of shape and tension analysis is given below in Table 8.1 wherein comparisons of modes of solution, difficulties, assumptions, usefulness and efficiency are outlined.

TABLE 8.1

SUMMARY OF CONDITIONS ANALYSED AND ASSUMPTIONS

ORIGINATOR	YEAR PUBLISHED	CONDITIONS	ASSUMPTIONS
ANWAR	1966	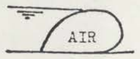	1. (a) Fabric Massless, Inextensible (b) Horizontal base. (c) Downstream fabric tangential to base
		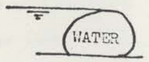	2. (a) As in 1 (b) Vertical component due to wt. of internal water omitted, in calc
		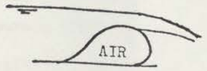	3. (a) As in 1. (b) Water jets off crest.
HARRISON	1969	ALL AIR OR WATER 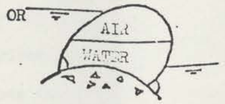	4. (a) Hydrostatic only. (b) Extensible matl. with mass. (c) Any combination of water levels. (d) On any geometric define base. (e) Downstream fabric any angle to base.
OGIWARRA et al	1970	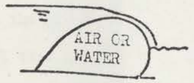	5. (a) As in 1 (b) Static and overflow conditions analysed.
BINNIE	1973	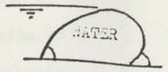	6. (a) As in 1(a) and 1(b). (b) As in 4(e).
HARRISON-SIMPLEX		As for 4	7. (a) As in 1(a), (b) (b) As in 4(c), (d)
ANALOGUE		As for 4	8. (a) As in 4.

SUMMARY OF PROPERTIES OF METHODS IN SHAPE AND TENSION* ANALYSIS.

Principle of Method	Mode of Solution.	Number of Iterations required for acceptable answer	No. of Nodes req'd for acceptable answer	Ease of solution. Advantages. Disadvantages.	DETERMINATION OF PARAMETERS Crest height, max. upstream head, Base width, Perimeter.	CALCULATION OF TENSION *
1 and 2. Shape defined by a series of non linear differential equations, which were set up from principles of equilibrium. Involves solving Elliptic Integrals.	1 and 2. Mathematical tables. 3. Digital Computer.	Not acceptable.	Not acceptable.	1 and 2. Involved mathematical process for solution generally difficult. Does not lend itself to design. 2. Misclose in shape. 3. As for 1.	1 and 2. Trial and Error process of complex method.	1. Simple and accurate for air. 2. Neglected unbalanced vertical forces on D/S side.
4. Finite element solution of a series of independent n on linear simultaneous equations solved step by step on computer. New values selected by Newton Iterative Method. 5. Solution of integral equations.	Computer. Initial values of T,θ guessed.	If > 5 solution is oscillating or diverging.	The greater number of nodes the greater chance of instability or divergence. 20 nodes for general picture. 60 nodes indicates approx. location of D/S clamp. 120 nodes gives as much accuracy as desired.	Reasonably good accuracy if converged Suitable for analysis or design. Unstable where H/h low, or when U/S head nearly equal to D/S head. Solution not difficult once program working.	4. Trial and Error. Considerably less difficult than 1 and 2, due to automatic nature of solution. Solution terminated if overtopped. Base width not accurately defined if actual D/S edge lay outside estimated base width.	Tension accurate if solution converged. Variation bet U/S and D/S negligible.
6. As in 1 and 2.	As in 1 and 2.	Not Applicable.	Not Applicable.	As for 1 and 2. Misclose in shape for (low?) H/h.	As for 1 and 2.	Tension correspondingly higher than in 2. (also due to misclose?)
7. As in 4 except values selected by Simplex iterative method.	As in 4.	∝ 15 for miscloses of 1% or less.	As in 4.	As for 4, but greater stability and more chance of convergence especially for low H/h and for a wider range of guessed values of T and θ than 4.	7. As for 4, although solution continued if initial upstream head overtopped. Base width more accurately defined.	As in 4. Inner do loop removed-caused T to increase between U/S and D/S clamps. Ave. T = to 4. More chance of converging.
8. Analogue solution Hydrostatic loads replaced by a series of weights applied at points around membrane. Converging iterative solution from guessed shape.	String, peg board and series of weights.	2 in stable cases; 4 in unstable cases.	5 nodes gave a reasonable solution. 12 nodes good.	Simplest of design. Solution method consistently supplies correct results without requisite degree of skill required by above.	8. Trial and Error, Parameters determined from Perimeter and internal head.	Accuracy of Tension not as good as 4. Critically dependant on 1st. and last node.

* Graphical solution of tension gave more accurate value than 2 or 5.

IMPROVEMENTS

(a) Possibly have greater number of nodes around U/S and D/S clamp.
(b) Program to iterate max. U/ head.
(c) Program to detect non-convergance early.

(a) As for 7(a).
(b) Add weights to allow self wt. of membrane.
(c) Put in solid members to simulate Buijze Type for analysis.

CHAPTER 9 - TYRE TUBE MODEL OF A MULTI TOROID DAM

9.1 INTRODUCTION

A series of experiments was conducted to evaluate the efficiency of using a number of inflated toroidal tubes mounted alongside each other to form a dam as shown in Diagram 9.1. The toroids used in the present tests were secondhand inner tubes from lorry tyres.

The behaviour of the dam formed in this manner was observed under several varying conditions of inflation pressures and flow conditions. It was thought that:-

(i) The tubes would stay in line.

(ii) Only minor leakage would occur.

(iii) The tubes would be a practical and economical solution for temporary damming of rectangular channels with water depths up to the diameter of the largest inner tubes commercially available.

The behaviour of the air-water inflated case was close to the anticipated behaviour, but when the tubes were inflated with air only, and also to some extent when water-inflated, expectations (i) and (ii) above were not met.

Although the present tests did not confirm the original expectations, it is felt that with a more ingenious arrangement a satisfactory system could be achieved.

The details of the present experimental layout and results of various combinations of inflation medium are given below.

TYRE TUBE DAM MODEL

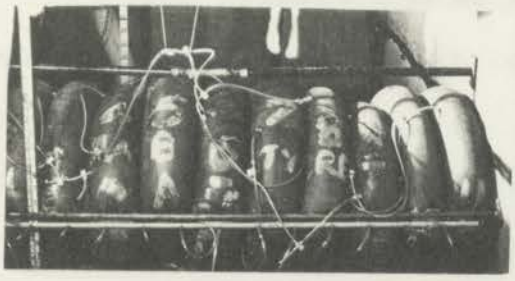

DIAGRAM 9.1 - AIR INFLATED - (ZERO U/S HEAD, INTERNAL HEAD ~ 3 FT WG.) SHOWING FAIRLY REGULAR INFLATION PATTERN.

DIAGRAM 9.2 - AIR-INFLATED (U/S HEAD = 2.8 FT; INTERNAL HEAD = 3.7 FT WG.) SHOWING SHEET AND CUSP FLOW UNDER TUBES, AND TUBES UPLIFTED AGAINST TOP BAR.

DIAGRAM 9.3 - WATER-INFLATED UNDER LOW INTERNAL HEAD. U/S HEAD = 0.8 FT - VERY LITTLE LEAKAGE.

DIAGRAM 9.4 - WATER-INFLATED UNDER LOW INTERNAL HEAD, BEING OVERTOPPED.

DIAGRAM 9.5 - AIR-WATER INFLATED. (U/S HEAD = 2.2 FT) THE DRAPED POLYTHENE SHEET IS REDUCING THE CUSP LEAKAGE.

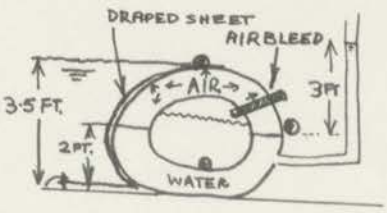

9.2 EXPERIMENTAL PROCEDURE

9.2.1 Test Set Up

The primary aim of the first series of experiments was to have simplicity in construction and operation of the multi-tube dam.

Three steel pipes were placed, as shown in Diagram 9.6 to anchor the eleven tubes across the channel, and to prevent them individually or collectively moving downstream. The internal pipe was placed at the lowest point so that the deflated tubes would provide as little resistance to the flow as possible. To allow for removal and replacement of tubes, the pipes on the inside and on top of the tubes, were in two pieces, each cantilevered from the sides and only partially spanning half the width of the tank. The pipes acted as sleeves for two smaller diameter pipes which could be slipped back and forth across the gap.

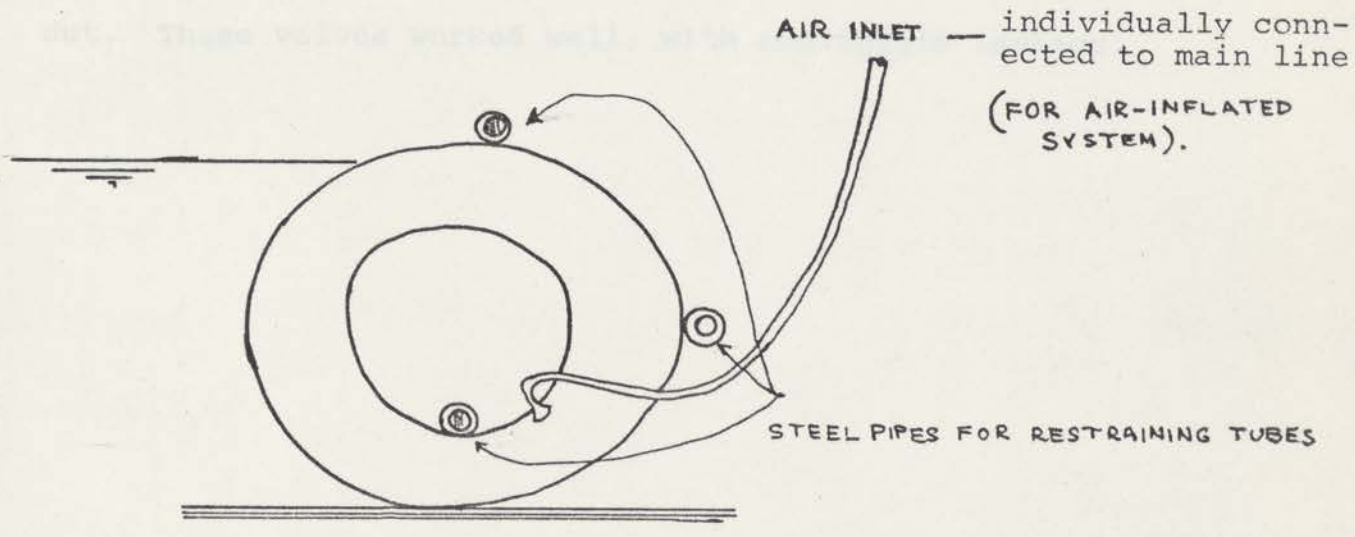

DIAGRAM 9.6 GENERAL ARRANGEMENT

9.2.2 Inflation System

The tubes were inflated using air only, water under low and high pressure, and a combination of air and water.

For the air inflated case the original air inlets were connected, using short one to two feet long p.v.c. hose ¼" internal diameter, to a common air pressure pipe. The air pipes were all interconnected although behaviour would have been more uniform had they been individually connected to a common source.

To enable the use of both air and water or just water, a second valve was added to the top of each tube as an air bleed, and the original air inlet valve became the water inlet. This additional valve, made from a 2-BA bolt with a 1/16" diameter hole drilled through its centre, was pushed head first into a hole in the tube (made with a red hot length of 1/8" brass rod) and kept in place by a washer and nut. These valves worked well, with negligible leakage.

9.3 GENERAL BEHAVIOUR

9.3.1 Tube Behaviour

Several aspects of tube behaviour were similar for all modes of inflation.

Generally, the tubes moved up and forward under a rising upstream head, maintaining a cylindrical shape, instead of appearing tear dropped due to the high pressure acting on the inflation fluid (up to twice the upstream head, (Diagrams 9.1, 9.2 and 9.9 - 9.13).

Once the tubes had been overtopped, a general reordering occurred wherein the tubes rose up a few inches and seemed to reduce the leakage through the cusps. This effect may have been due to the air trapped inside the toroids. This trapped air may not have entirely been eliminated even in the cases where it was allowed to escape by inserting a 2" diameter P.V.C. hose into the toroidal space (see Diagrams 9.9 - 9.13).

One or two of the tubes seemed to be slower inflating than their neighbours (Diagram 9.9) which may have been due to a number of factors:

(a) Not all the tubes were of uniform size, and uniform rubber thickness.

(b) Pressure losses varied along the inlet pipe.

(c) Leaky valves and tubes.

(d) Once the size difference became relatively great, the larger tube would dominate the smaller one.

The effect of this differential filling was not significant except that it was 'nice' to have all the tubes of the same size. If an individual tube deflated due to a puncturing or valve malfunction, the remaining tubes tended to redistribute themselves and the gap was considerably reduced. In practical

operations a few deflated spares could be interposed at intervals and could be inflated to help make good the failure of any of the original tubes.

9.3.2 Leakage

Leakage of varying degree was observed in the form of cusp leakage (in all cases) (Diagram 9.7) and in the form of sheet flow (in the air inflated case due to tube uplift).

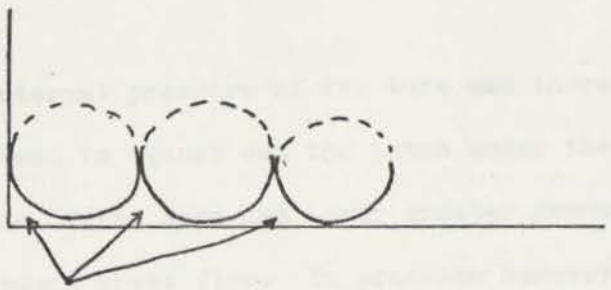

DIAGRAM 9.7 CUSP LEAKAGE

No leakage was observed to occur between the tubes themselves, even with internal pressures as low as that of upstream water level.

Several devices to reduce the leakage were tried and except for one will be described below in Section 9.4.

In the case of the low pressure water inflated tubes, and the air-water inflated tubes a polythene sheet was draped over the upstream side of the tubes and one edge clamped to the base. This proved to be effective in partially reducing the cusp leakage (Diagrams 9.3 - 9.5).

9.4 BEHAVIOUR OF AIR-INFLATED TUBES

The first series of tests used air to inflate the tubes, as this was the simplest inflation medium to control. The major deficiency of this system was the excessive leakage and uplift forces which had to be resisted by the anchor pipes (shown in Diagram 9.2). Leakage was at the rate of $\frac{1}{4}$ cusec/foot for an upstream head of 3 to $3\frac{1}{2}$ feet.

Two unsuccessful modifications were tried to reduce the leakage:-

1. (a) The internal pressure of the tube was increased to twice the upstream head to squash out the tubes under the lower bar to reduce the size of the gaps and apply greater downward force on the base to reduce sheet flow. In practice however the extra force only negligibly reduced the leakage, and as the anchorage system was overloaded any attempt to further increase the pressure was abandoned.

   (b) Sand-cement mortar was poured around the tube base at a medium inflation pressure to fill in the cusp gaps. Although this greatly reduced the cusp leakage, the sheet flow persisted. Since there would also be increased probable maintenance problems in keeping the base free from gravel and debris, it was decided that the disadvantages were too great.

As the use of air inflated tubes arranged as described above appeared to be unsatisfactory it was decided to investigate the water-inflated case described in the next section.

9.5 BEHAVIOUR OF WATER-INFLATED TUBES.

At first a series of tests were conducted with the tubes under a high internal pressure of 5 ft. water gauge. The accompanying photographs, Diagrams 9.9 - 9.13 indicate the behaviour of the water-inflated tubes under high pressure for various conditions.

When it was found that the tubes tended to collapse because the weight of water in the upper half was too heavy for the tubes to support themselves, it was decided to conduct another series of tests on low pressure water-inflated tubes, in which the internal pressure was only marginally higher than the height of the dam (as shown in Diagrams 9.3 and 9.8).

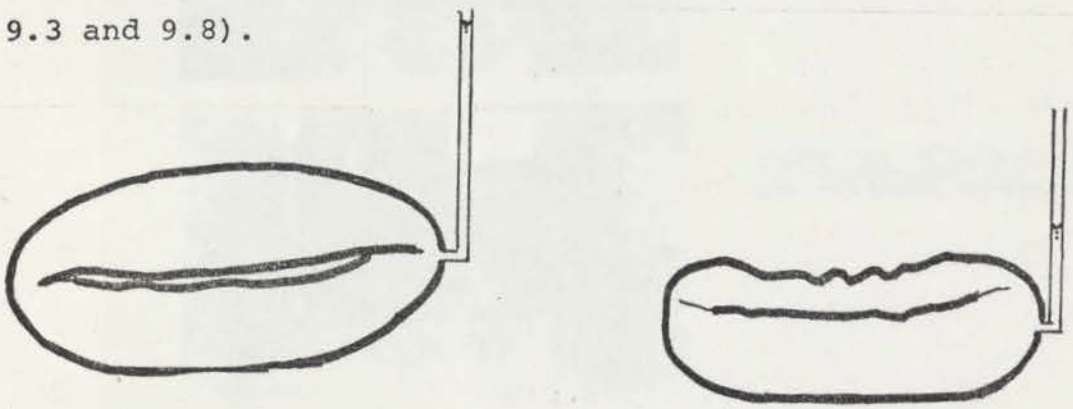

DIAGRAM 9.8 HIGH AND LOW PRESSURE WATER-INFLATED TUBES.

The volume of inflating was considerably reduced, just so the tubes were standing up on edge 1.3 ft. high or about 1/3rd of their normal air-inflated height. The behaviour of the low pressure water-inflated tubes is shown in Diagrams 9.3 and 9.4.

Sheet flow was eliminated and cusp leakage, in the water-inflated cases was considerably reduced when compared to the air-inflated case.

WATER-INFLATED TYRE TUBE DAM MODEL UNDER VARYING CONDITIONS OF UPSTREAM HEAD

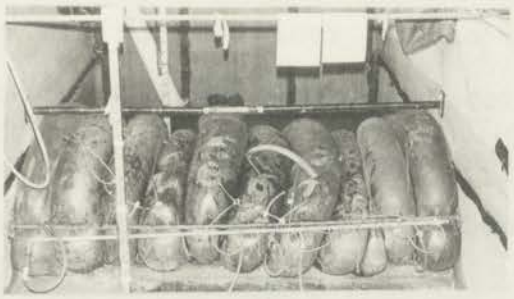

DIAGRAM 9.9 - INTERNAL HEAD 5 ft, U/S=0
NOTES: 1. A 1 INCH PVC HOSE WAS INSERTED TO ALLOW AIR TO ESCAPE FROM INSIDE THE TOROID.
2. THE WATER-INFLATED TUBES APPEAR TO BE IRREGULARLY INFLATED.

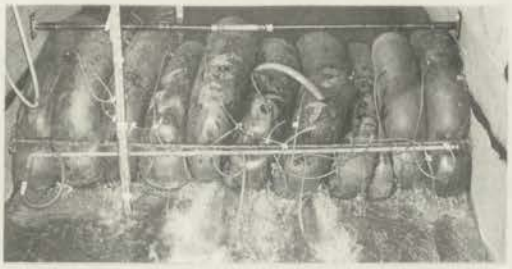

DIAGRAM 9.10 - CUSP LEAKAGE OCCURRING BETWEEN TUBES NEAR CENTRE AT U/S HEAD OF 2 FT.

DIAGRAM 9.11 - AT U/S HEAD OF 2.8 FT FLOW OVERTOPS LOWER TUBES. 1 INCH PVC HOSE STILL DISPELLING TRAPPED AIR.

DIAGRAM 9.12 - OVERFLOW WITH U/S HEAD AT 3.0 FT. PVC TUBE DISPELLING WATER.

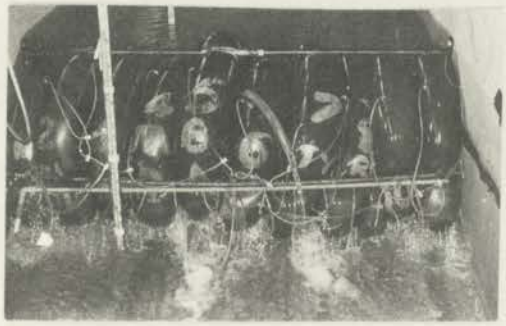

DIAGRAM 9.13 - ONCE AIR HAD BEEN DISPELLED FROM TOROID, TUBES APPEARS TO HAVE REDISTRIBUTED THEMSELVES AND SLIGHTLY HIGHER, AND LEAKAGE APPEARS TO BE LESS THAN BEFORE.

It was envisaged problems in automatic inflation due to the unequal inflation volumes in each tube could be overcome. However further investigation would need to be carried out to determine behaviour of the tubes under inflation conditions once they had been disordered.

To gain the full height potential of the tubes it was decided to try a combination of both air and water described in the next Section.

9.6 BEHAVIOUR OF AIR WATER-INFLATED TUBES

An air water combination of about equal volumes was tested (Diagram 9.5).

This system incorporated the advantages of nearly full height as with the air-inflated case, and no sheet flow and reduced cusp leakage due to the self weight of the tubes. The air pressure head was about 4 ft. of water in all tests.

Under conditions of maximum upstream water level of about 3.3 ft. the system worked well. Leakage which was slight compared to the air inflated case, was approximately 0.1 cusec/ft. (due to the cusp effect between tubes) as shown in Diagram 9.5).

9.7 CONCLUSION AND SUGGESTED IMPROVEMENTS

The air-water inflated tubes appeared to be the most feasible system and warrant further investigation.

As it was intended that the study of the rubber tube dam was only to sample its possibilities, there was no extensive testing to optimize the internal air and/or water ratio and fluid pressures, or to reduce the cusp leakage problem.

Improvements which would allow the air and/or water inflated system to be of practical use in irrigation schemes and other uses, where no other alternative might be feasible included:-

(i) Each tube anchored individually and an anchored sheet draped over the tubes (Diagram 9.14). This would reduce cusp leakage and possibly enable punctured tubes to be replaced.

(ii) Each tube separately connected directly to a common inflation source, so ensuring a more uniform height of individual tubes.

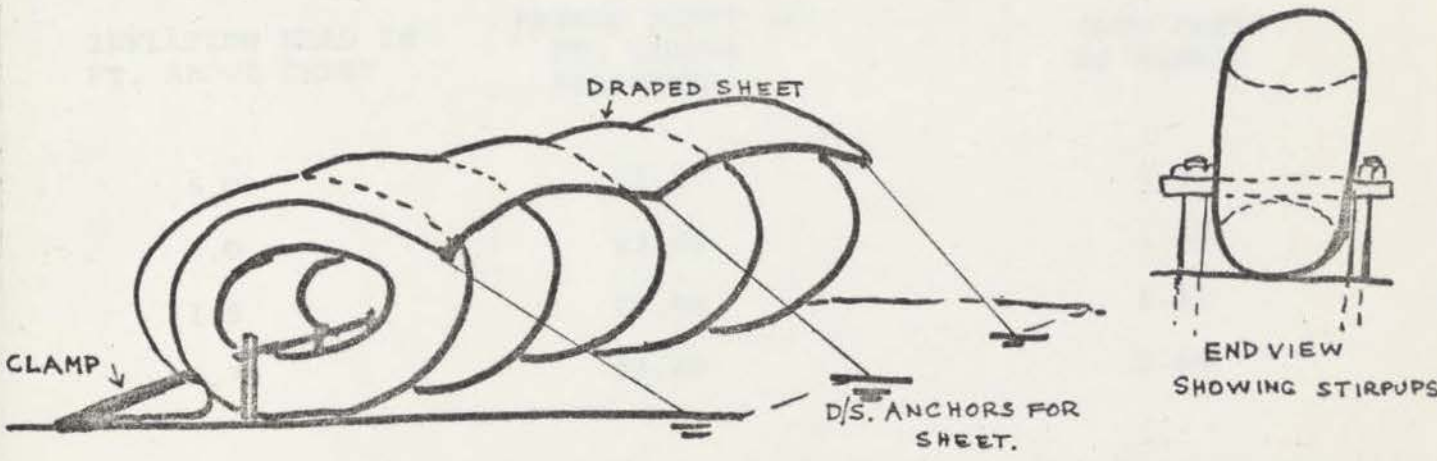

DIAGRAM 9.14 MODIFIED SYSTEM OF ANCHORING AND SEALING TUBE DAM

CHAPTER 10 - DESIGN GRAPHS

10.1 INTRODUCTION

Several dimensionless parameters were calculated from data obtained from the experimental model, extrapolated and filled out by data from computer calculations, and plotted onto several graphs shown on pages 174 - 182.

Although relations such as that between cost ratio of the fabric' and the inflation head for the Proston Weir which was required to support an upstream head of 5 ft. (Table 10.1), appear to have been investigated (Ref. 4a.) it is hoped that these graphs enable an inflatable dam to be designed with reasonable accuracy, by relating important aspects such as total perimeter, base width, tension in the fabric, maximum design upstream head and internal pressure. Alternatively, given the allowable tension of the fabric (Table 3.1) and the dam perimeter, the graphs allow the other variables to be quickly determined.

TABLE 10.1 RELATION OF PERIMETER TO INFLATION HEAD FOR 5 FT. HIGH WATER-INFLATED FABRIDAM.

INFLATION HEAD IN FT. ABOVE CREST	FABRIC WIDTH IN FT. (TOTAL PERIMETER)	COST RATIO OF FABRIC
5.0	21.0	1.0
3.0	23.46	1.12
1.5	27.60	1.31
0.75	34.40	1.64

In conjunction with known cost factors, the graphs automatically lend themselves to optimization of materials.

A design example for a dam 20 ft. high follows in Section 10.4

10.2 LIMITATIONS OF DESIGN GRAPHS

The parameters were calculated for dams on a flat horizontal slab with maximum upstream head, and downstream head and angle, zero.

In the cases where:-

(a) There is a curved base and the upstream and downstream clamp lines of the dam may not be level, e.g. Ogee Weir.

(b) Where a series of stiff panels are located along the perimeter (Buijze type dam), or

(c) Where a series of loadings are applied, which are not covered by these design graphs, and/or more accuracy is required.

It is recommended that the Analogue method be used, or the Harrison-Simplex Computer method as described in Chapter 6 and 7.

In cases where there are steps along the dam base, or sloping sides, a 3 dimensional model analysis may be required. The graphs can not be reliably used for conditions where instability occurs, namely at low air pressures, as the effect of stiffness of the whole dam must be considered. For the above conditions and for the overflow and consequent vibration condition it is recommended a model analysis is conducted.

The self weight of the fabric and its extensibility were ignored. However if the modulus, and tension, in the fabric are known, the stretched perimeter length can easily be calculated by the designer.

WATER INFLATED CASE

PERIMETER / BASE VS INTERNAL/UPSTREAM HEAD RATIOS

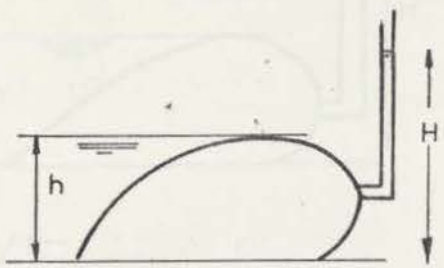

BASE (B)
PTOTAL = CURVED PERIMETER + BASE

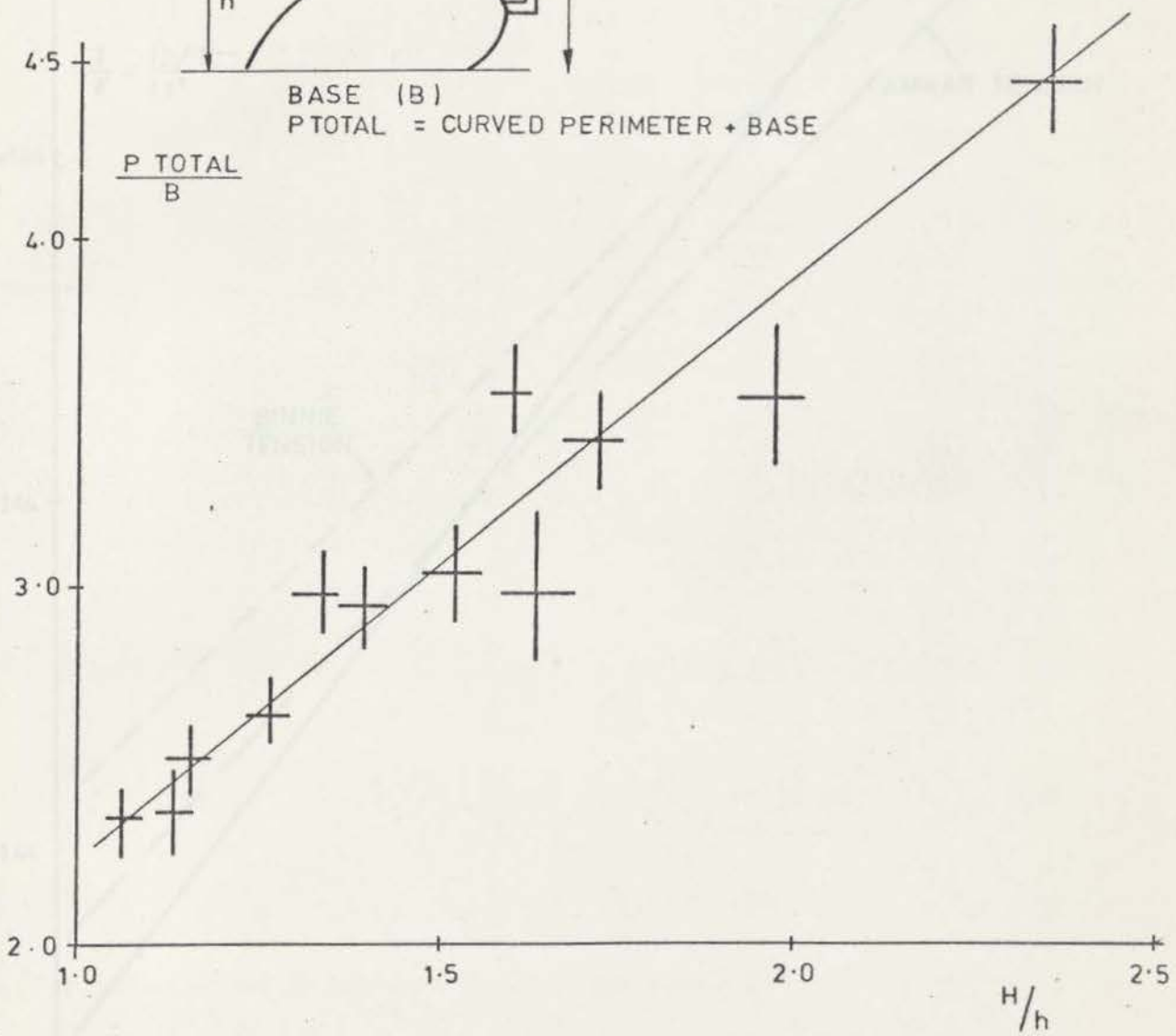

GRAPH 10·1

WATER INFLATED CASE

TENSION (T)* AND INTERNAL HEAD DIVIDED BY UPSTREAM WATER HEAD

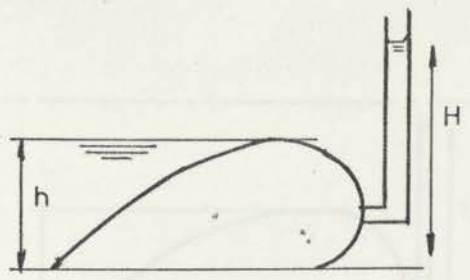

$\frac{T}{\gamma} = \frac{lb/ft}{ft^2}$

ANWAR TENSION

BINNIE TENSION

·4×144

·3×144

·2×144

·1×144

0

1·0

1·5

2·0

2·5

H/h

*NOTE. TENSION CALCULATED BY GRAPHICAL METHOD

GRAPH 10·2

WATER INFLATED CASE
PERIMETER AND INTERNAL HEAD

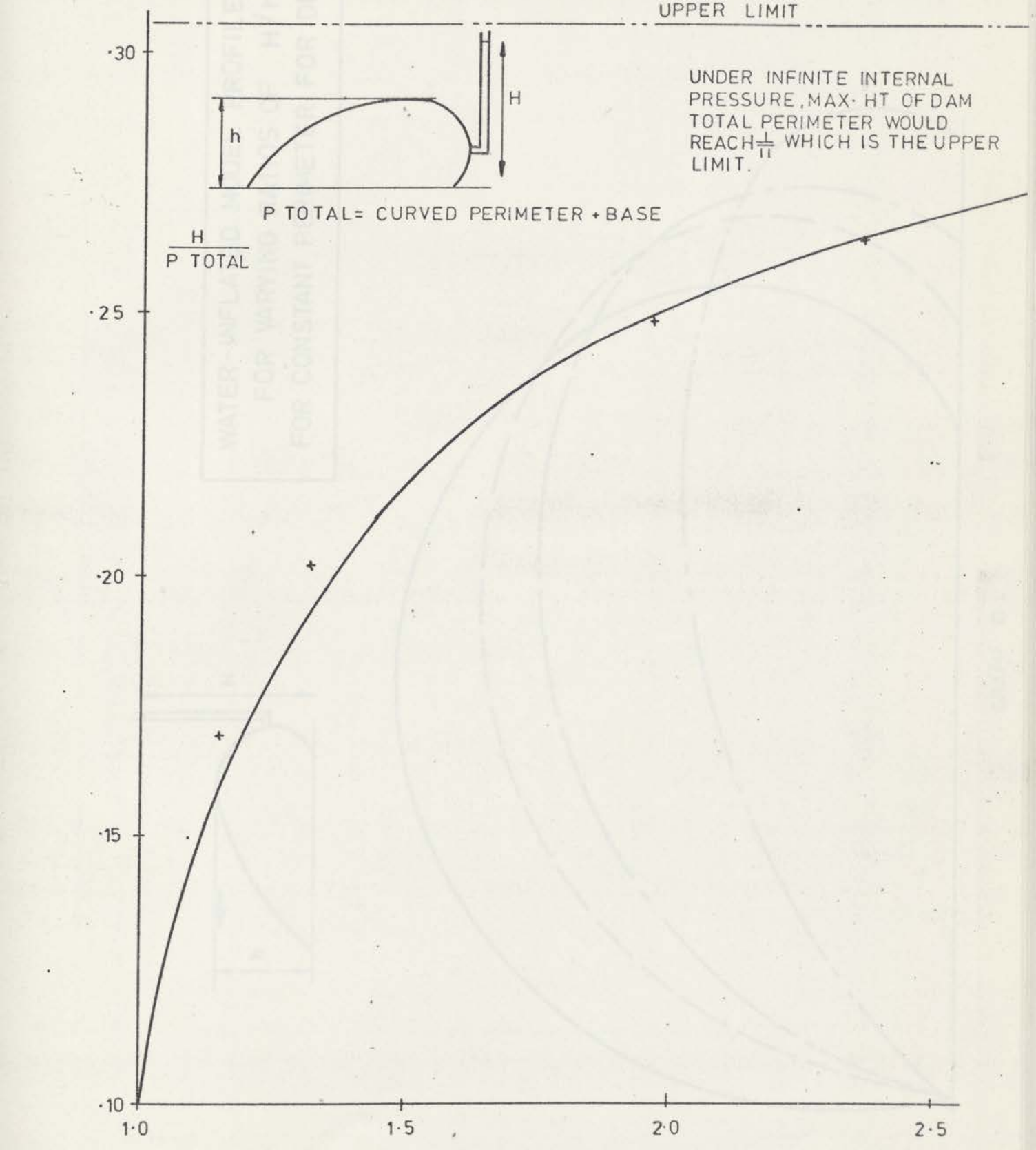

GRAPH 10·3

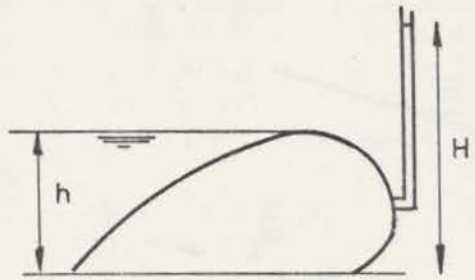

WATER-INFLATED MODEL PROFILES
FOR VARYING RATIOS OF H/h
FOR CONSTANT PERIMETER FOR DESIGN

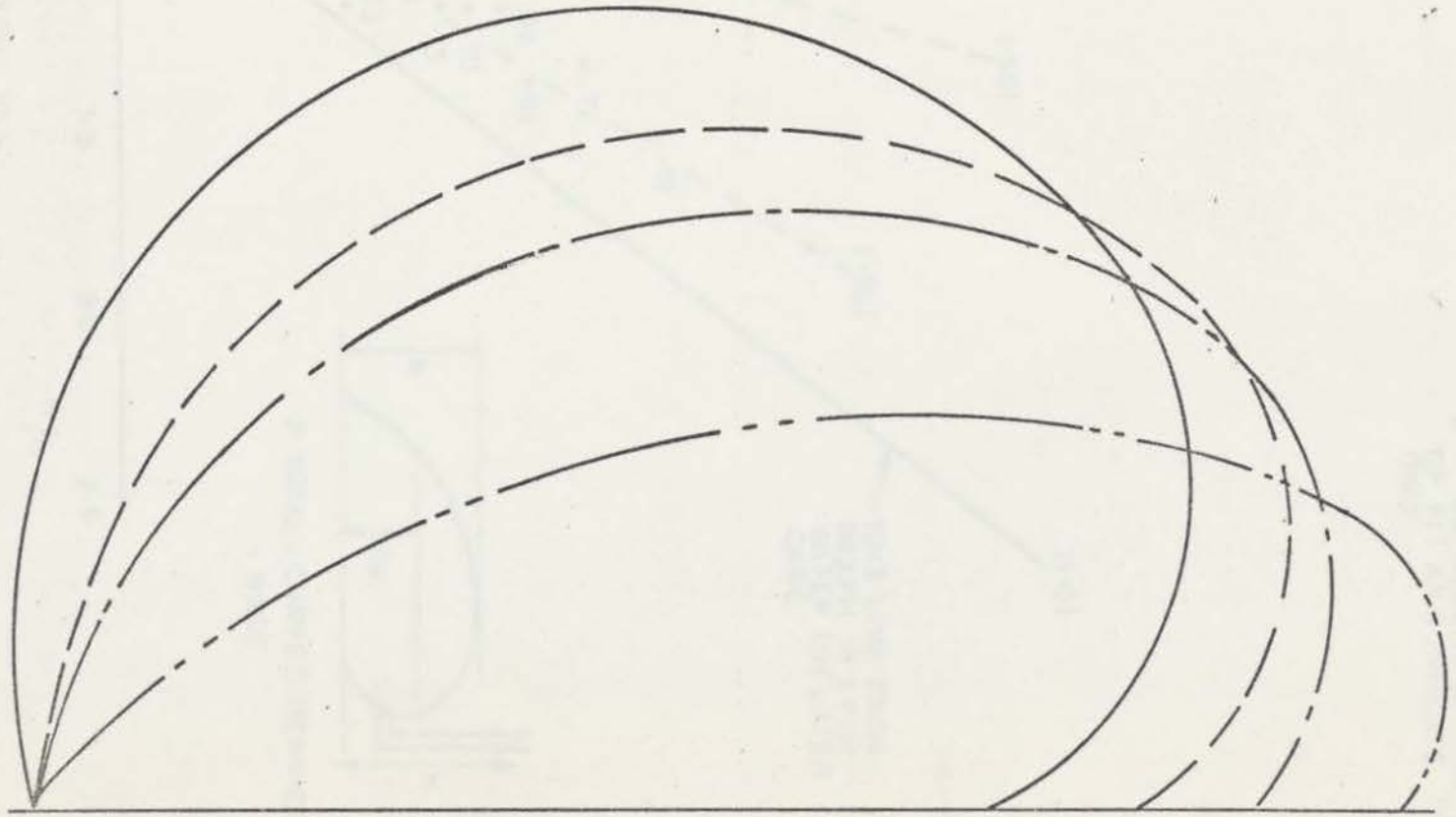

GRAPH 10·4

AIR, AIR-WATER., WATER INFLATED CASES
PERIMETER/BASE VS INTERNAL/UPSTREAM HEAD RATIOS

NOTE : 1. FIGURES BESIDE EXPERIMENT. POINTS DENOTE $\frac{Hw}{h}$ RATIOS

2. --- REPRESENT APPROX. LINES OF FIT AND INDICATE TREND ONLY.

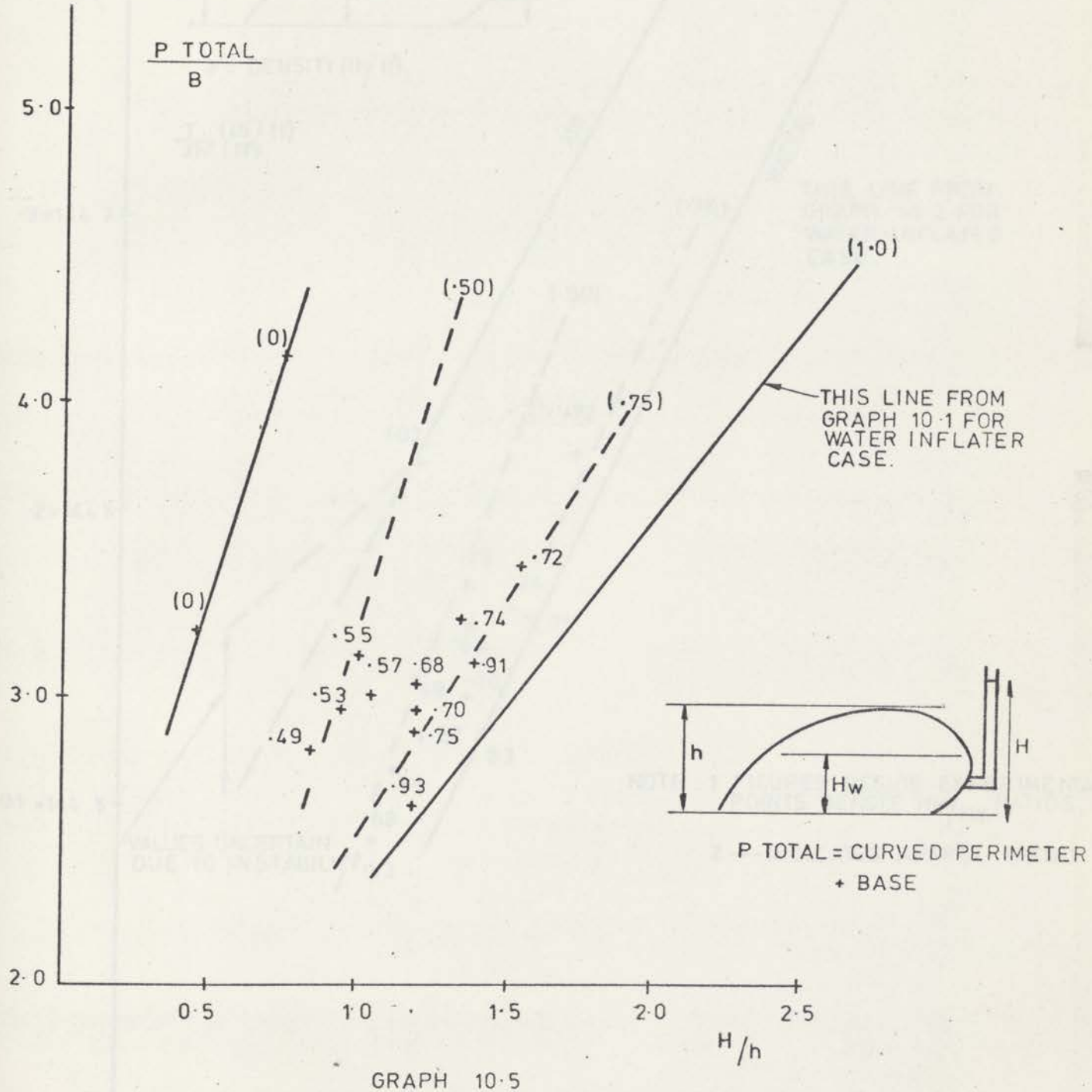

GRAPH 10·5

AIR AIR-WATER, WATER-INFLATED CASES TENSION T* AND INTERNAL HEAD DIVIDED BY UPSTREAM WATER HEAD

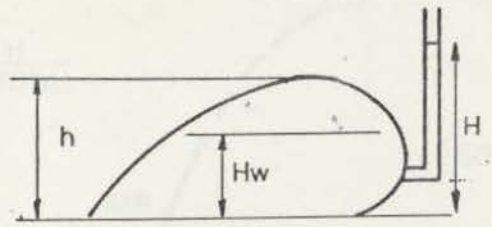

γ = DENSITY (lb/ft³)

$\frac{T}{\gamma h^2}$ (lb/ft) / (ft²)

·4×144 γ

·3×144 γ

·2×144 γ

0·1×144 γ

0

0·5

1·0

2·0

2·5 H/h

(0)

(1)

AIR

WATER

(·75)

(·50)

THIS LINE FROM GRAPH 10·2 FOR WATER-INFLATED CASE.

(0)

·72

·75

·74

·91

·68

·49

·70

·57

·93

·55

·68

·53

VALUES UNCERTAIN DUE TO INSTABILITY

NOTE : 1. FIGURES BESIDE EXPERIMENTAL POINTS DENOTE Hw/Hm RATIOS.

2.---INDICATES APPROX. TREND.

* TENSION FROM GRAPHICAL METHOD AND HARRISON METHOD

GRAPH 10·6

AIR, AIR-WATER, WATER INFLATED CASES PERIMETER AND INTERNALHEAD

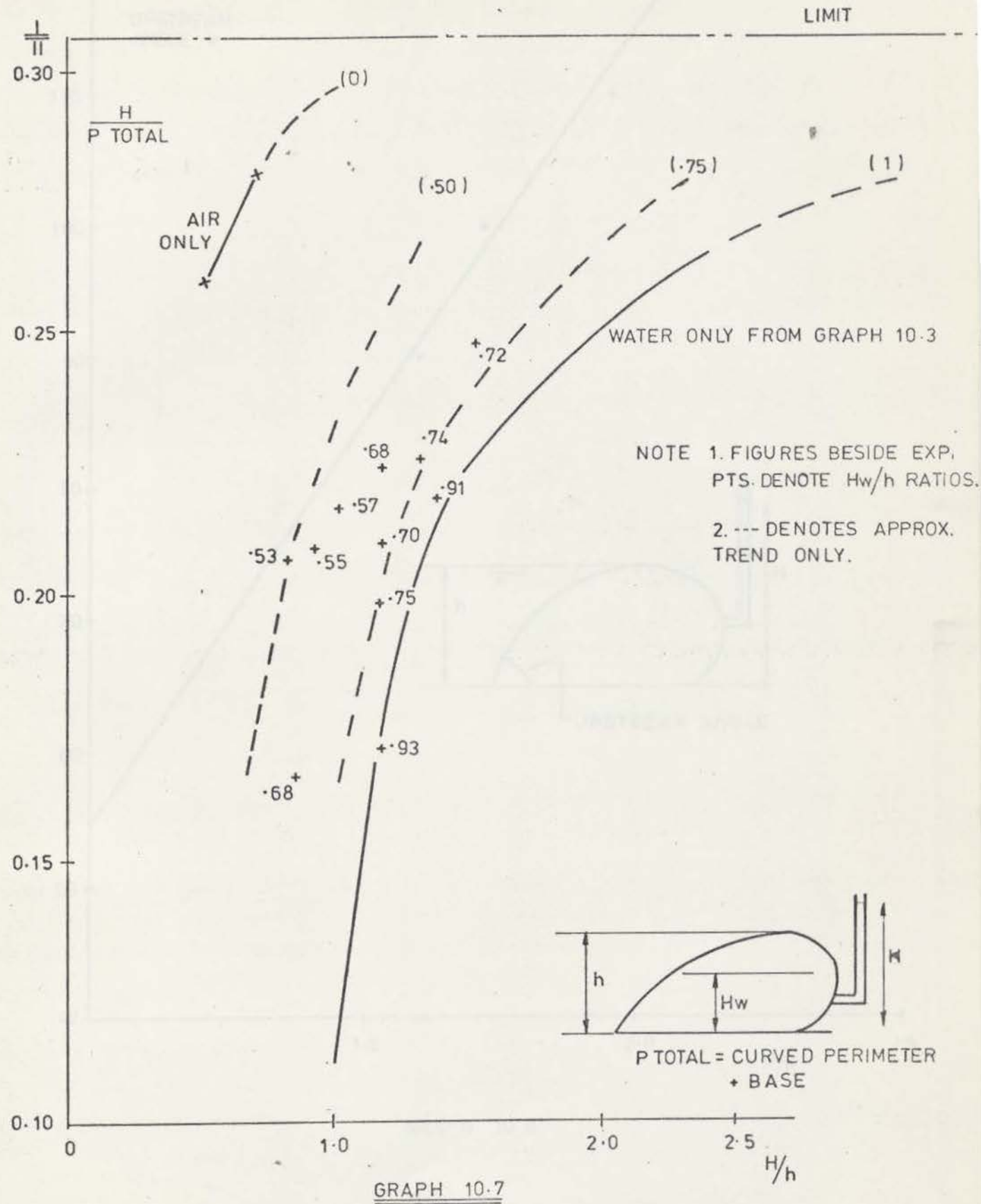

GRAPH 10·7

WATER INFLATED CASE
UPSTREAM ANGLE FOR MAX UPSTREAM HEAD AND VARYING INTERNAL HEAD
(D/S ANGLE = 0)

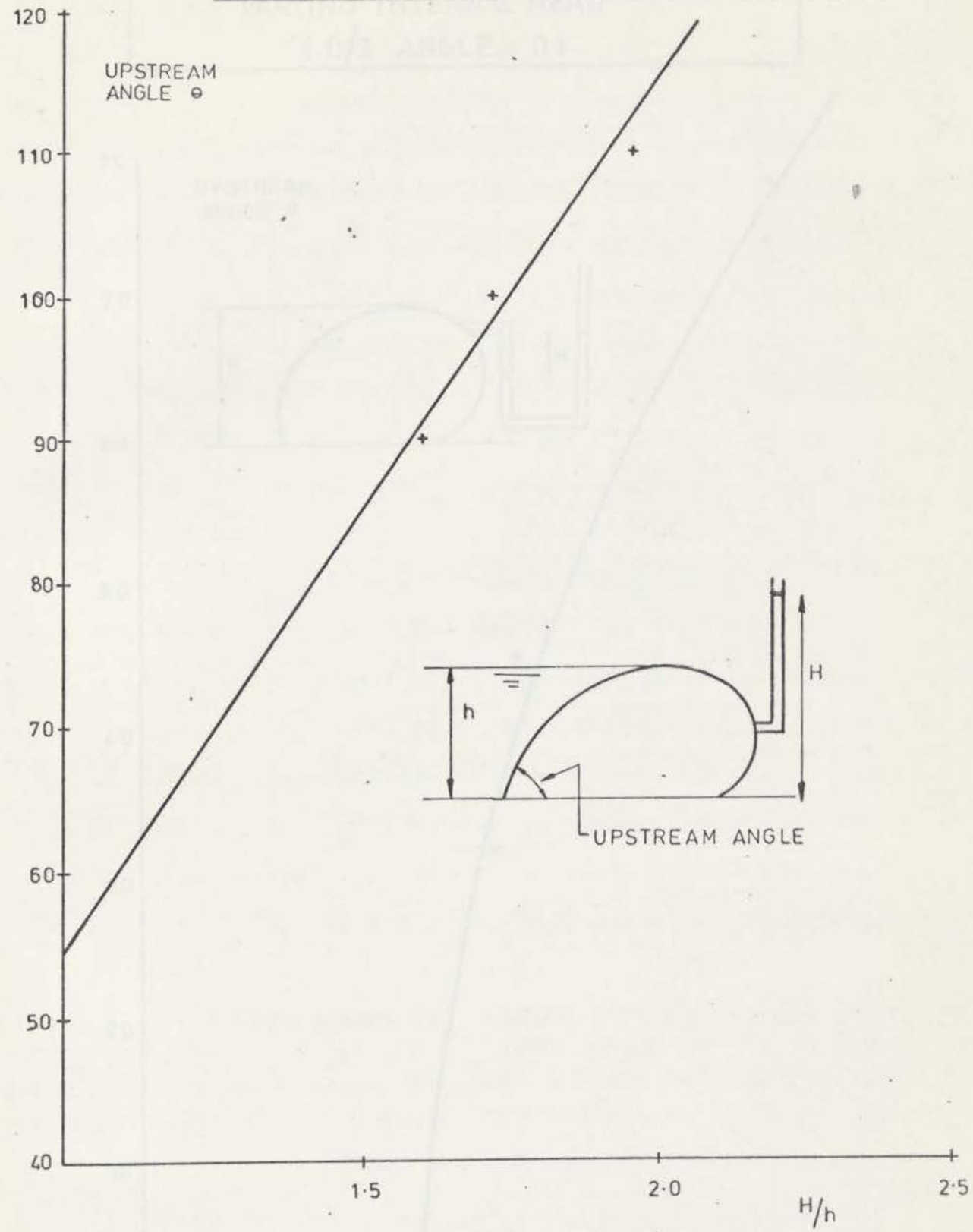

GRAPH 10·8

AIR INFLATED CASE
UPSTREAM ANGLE FOR MAX U/S HEAD AND VARYING INTERNAL HEAD
(D/S ANGLE = 0)

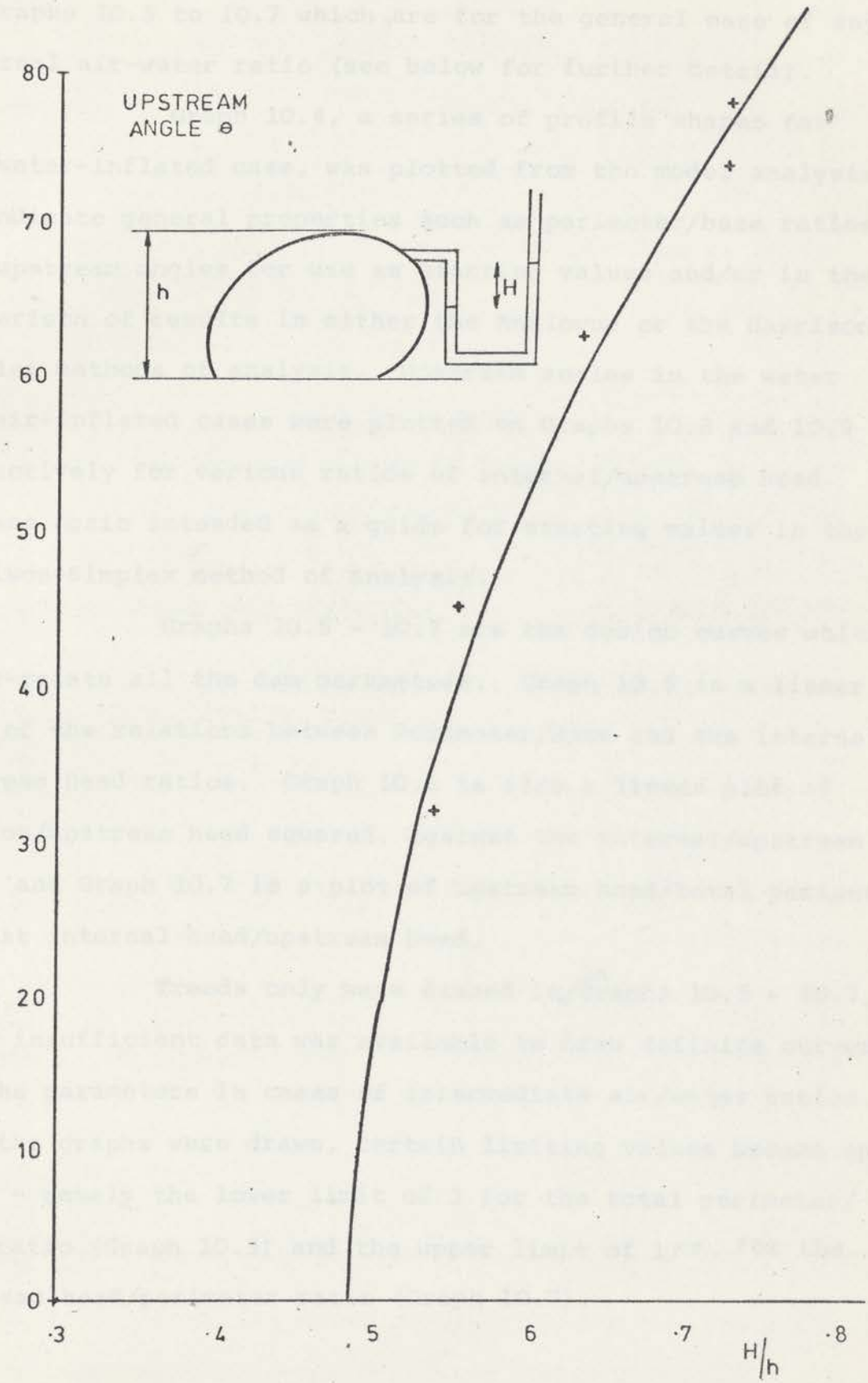

GRAPH 10·9

10.3 DESCRIPTION OF GRAPHS

Nine graphs were drawn. Graphs 10.1 to 10.3 are for the design of water-inflated cases and were repeated in Graphs 10.5 to 10.7 which are for the general case of any internal air-water ratio (see below for further detail).

Graph 10.4, a series of profile shapes for the water-inflated case, was plotted from the model analysis to indicate general properties such as perimeter/base ratios and upstream angles for use as starting values and/or in the comparison of results in either the Analogue or the Harrison-Simplex methods of analysis. Upstream angles in the water and air-inflated cases were plotted on Graphs 10.8 and 10.9 respectively for various ratios of internal/upstream head and are again intended as a guide for starting values in the Harrison-Simplex method of analysis.

Graphs 10.5 - 10.7 are the design curves which inter-relate all the dam parameters. Graph 10.5 is a linear plot of the relations between Perimeter/Base and the internal/upstream head ratios. Graph 10.6 is also a linear plot of tension/upstream head squared, against the internal/upstream head, and Graph 10.7 is a plot of upstream head/total perimeter against internal head/upstream head.

Trends only were dashed in on Graphs 10.5 - 10.7, where insufficient data was available to draw definite curves for the parameters in cases of intermediate air/water ratios. Once the graphs were drawn, certain limiting values became apparent - namely the lower limit of 2 for the total perimeter/base ratio (Graph 10.5) and the upper limit of $1/\pi$ for the upstream head/perimeter ratio (Graph 10.7).

10.4 WORKED EXAMPLES USING DESIGN GRAPHS

As an example of the use of the graphs consider the design of a dam 20 ft. high. (h = 20 ft).

(a) Assuming the dam is air-inflated

H/h (for stability) > 1.0

From Graph 10.6 Tension

$T = 12600$ lb/ft.

From Graph 10.7 Perimeter (Total) (h given as 20 ft.)

$P_{(Total)} \doteq \frac{20}{.3} \sim 67$ ft.,

and from Graph 10.6 Base width,

$B = 12.5$ ft.

(b) For a water-inflated dam assuming the same allowable tension of 12600 lb/ft., a value of H/h of 1.65 is obtained from Graph 10.6.

From Graph 10.7 Perimeter,

$P(Total) = 20 \times 4.4 = 86$ ft.,

and from Graph 10.5 the Base

$B = 27$ ft.

(c) Assuming the allowable tension is only 7500 lb/ft. and the dam is water inflated:- it is required to find the internal/upstream head ratio, the Perimeter and base.

From Graph 10.6,

$H/h = 1.25$

and from Graph 10.7, Perimeter

$P(Total) = \frac{20}{0.18} = 110$ ft.

From Graph 10.6 Base

$B = \frac{110}{2.6} = 43$ ft.

From the above examples it can be seen how easy it is to operate the parameters using the Graphs.

CHAPTER 11 - FINAL DISCUSSION AND CONCLUDING REMARKS ON THE STUDY OF INFLATABLE DAMS

11.1 DISCUSSION OF RESULTS PERTAINING TO THE FABRIDAM TYPE INFLATABLE DAM

11.1.1 Introduction

This present study was primarily concerned with the analysis and behaviour of the Fabridam type inflatable dam under static conditions.

11.1.2 Discussion of an Alternative System

A review of the construction, operation and behaviour of existing inflatable dams was carried out. From this review, and from the analytical and experimental model investigations into the behaviour of conventional Fabridam type inflatable dams, it appears that a more efficient concept for the form of the bag would be as a complete bag without longitudinal ends clamped to the base and water inflated. The water inflated bag would rely on its own weight as well as a series of restraining straps for stability (Diagram 11.1).

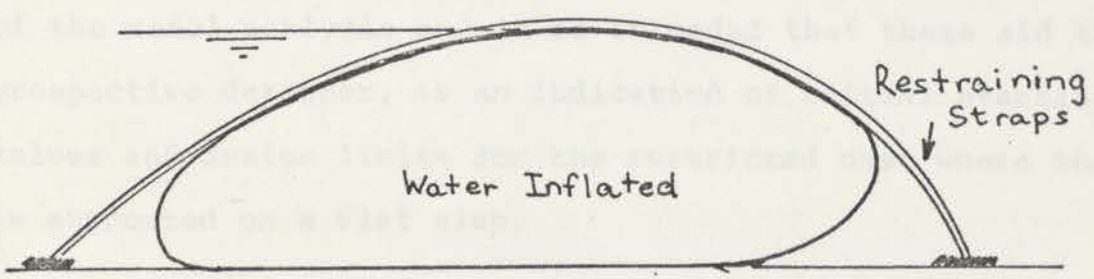

DIAGRAM 11.1 STRAPPED BAG

This system would eliminate the problem of pullout of ends from the anchors and thereby more fully utilize the overall loop tensile strength of the bag because it appears bag joins are stronger than clamp connections.

11.1.3 Analysis of Inflatable Dams

Several methods of analysis of the Fabridam inflatable dam were investigated.

Each method exhibited advantages and disadvantages - nevertheless the Analogue method seemed to be the simplest and most likely to consistently produce an answer closely corresponding to the experimental model profiles and producing similar values of tension as the mathematical analyses within experimental error.

The Harrison - Simplex computer method was satisfactory in cases of moderately high internal head to upstream water level ratios, and less satisfactory in cases of low ratios when difficulties in convergence were experienced. Analysis could mostly, but not always be improved when the tension and shape were firstly closely approximated, for instance by model analysis.

Other methods of analysis by Anwar and Binnie appeared to produce miscloses at low internal to upstream head ratios and so appeared to be unsatisfactory.

11.1.4 Design Graphs

A series of graphs were drawn from the results of the model analysis and it is intended that these aid the prospective designer, as an indication of initial starting values and design limits for the restricted case where the dam is supported on a flat slab.

11.1.5 Vee Notching and Vibration Analysis

The formation of the vee-notch in air-inflated cases was described qualitatively. Until exact conditions for its formation can be determined, it is recommended that water inflated dams be used in cases where vee-notching could have deleterious effects.

Vibration of the models was again only studied qualitatively and it appears that the factors affecting frequency and amplitude could be analogous to those of vibration of a column, important factors being the inflation fluid (water-lower frequency and amplitude than air) and crest height/length ratio (the higher the ratio the higher the frequency and lower the amplitude). Other factors which it is assumed would affect the vibration characteristics are whether the ends are clamped to the walls and/or whether the downstream edge is clamped.

Two distinct modes of vibration were observed, one due to the nappe breaking free at low tail water conditions, and a longitudinal rolling action which tended to occur as the water level above the crest increased appreciably, irrespective of tail water conditions.

11.2 TYPES OF INFLATABLE DAM OTHER THAN FABRIDAM TYPE

11.2.1 Buijze and Mesnager Types

Other types of inflatable dams such as the Buijze Steel Panel type and the Mesnager - Parachute type were briefly described and merit consideration for application where conditions warrant their use.

In the case of the Buijze type, the steel panels provide positive protection against river traffic, and would tend to reduce vibration in case of wind waves, with the disadvantage of increased maintenance and complexity of construction. Whereas the Mesnager type dam would be suitable for deep water purposes where the bottom may be uneven and it is required to dam a relatively small head differential.

An alternative proposal derived from the Mesnager type dam is a single impervious sheet attached to a single large diameter float, as shown in Diagram 11.2.

The advantage would be that only one set of anchors need be provided, and this system clearly warrants further investigation.

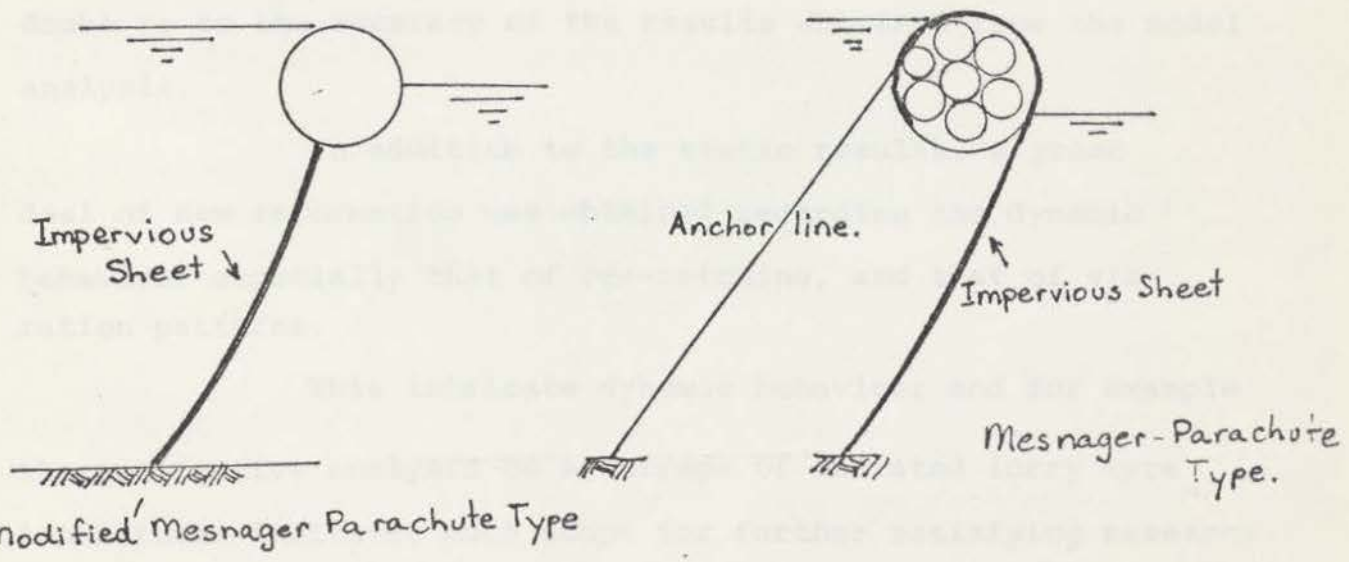

DIAGRAM 11.2

11.2.2 Tyre Inner Tube Type

A preliminary investigation was carried out into the feasibility of constructing a barrage consisting of a series of inner-tubes from lorry tyres. As the study was largely qualitative no positive conclusions could be drawn other than that this system warrants further investigation.

11.3 CONCLUSION

Several aspects of the analysis and behaviour of inflatable dams have been investigated.

Sone of the more important aspects resulting from the investigation were the Analogue method, the modifications (by way of the Simplex-Iterative method) made to the Harrison computer method and the negative conclusions reached regarding the Binnie and Anwar methods of analysis. The model analysis under static conditions played a major part in providing profile shapes which were essential in the comparison of the results obtained mathematically. Great care was taken in the model analysis to make the model conform as closely to a prototype Fabridam as possible and there is no doubt as to the accuracy of the results obtained from the model analysis.

In addition to the static results, a great deal of new information was obtained regarding the dynamic behaviour especially that of vee-notching, and that of vibration patterns.

This intricate dynamic behaviour and for example the qualitative analysis on a barrage of inflated lorry tyre inner tubes indicates much scope for further satisfying research both from the analytical and practical points of view.

REFERENCES

1. Proceedings 1st Colloquim on Pneumatic Structures, University of Stuttgart, Germany, 1967.

2. Nimmo, W., Technical Aspects of a Visit to Europe.

3(a) Imbertson-Firestone, "The Fabridam" Sales Publication, (1966).

3(b) Imbertson-Firestone, "The Fabridam" Sales Publication, (1970).

3(c) Imbertson, N.M., "The Automatic Collapsible Membrane Type Rubber Dam and its Uses" Content of Paper presented at the A.S.C.E. Science Convention, Nevada, June 20-21.

4(a) Connor and Wickam, "Queensland and N.S.W. Fabridams" Journ. Aust. Nat. Committee on Large Dams, No. 29, pp.54-74, (1969).

4(b) Connor and Wickam, "Discussion of 4(a)" Journ. Aust. Nat. Committee on Large Dams, No. 30, (1969).

5. Anon., "Pennsylvania's Inflatable Dam Blowout" E.N.R., June 26, p.1 (1969).

6. Anon., "Flandrau Park Dam Failure" E.N.R., May 5, p.15 (1969).

7. Anon., "Dutch Inflatable Weir" Engineering, Sept. 19, p.313 (1969).

8. Anon., "Dutch Inflatable Weir" Vredestein Press Service, Aug. (1969).

9. Buijze, Private Communication, (1970).

10. Anon., "English Inflatable Weir" Engineering, Sept. 19, p.313 (1969).

11. Binnie et al., "Mangla Engineering" I.C.E. Proc. Vol.38, p.455, p.469, (1967).

12. Harrison, H.B., "The Analysis and Behaviour of An Inflatable Membrane Dam Under Static Loading", Research Report No. R.123 Uni. of Sydney, (1969).

13. Shepherd et al., "The Fabridam Extension on Koombooloomba Dam in Tully Falls Hydroelectric Power Project" Journ. I.E. Aust. Vol. 41, No. 1-2. (1969).

14. Baker et al., "Model Tests on a Proposed Flexible Fabric Dam for the Mangla Dam Project - Pakistan", R.R. 803, 827 British Hydromech., Res. Assoc. (1966)

15. Anwar, H.O. "Inflatable Dams", Proc. A.S.C.E. HY3 (1967).

16. Ogiwara et al., "The Shape of the Rubber Dam", Proc. Japan S.C.E., No.179, (1970). (In Japanese).

17. Stodulka and Marr, "The Design and Uses of Inflatable Dams", Unpublished Honours Thesis, University of Sydney, (1970).

18. Deleted.

19. Nelder and Mead, "A Simplex Method for Function Minimisation", Computer Journal Vol.7, p.308- et seq (1965).

20. Herbotson, D. and Evans, Private Communication (1973).

21. Kipp, G., "Private Communication" (1973).

22. Schofield, A., "A Parachute to Tame the Tide" New Scientist, Oct. 8, pp.66-68, (1970).

23. Binnie, A.M. "Theory of Flexible Dams Inflated by Water Pressure" Journ. of Hydraulic Research. Vol.11, No.1. 1973.

24. Leonard et al., "Structural Considerations of Inflatable Re-entry vehicles" N.A.S.A. T.N.D.-457.

25. Stein and Hedgepeth, "Analysis of Partly Wrinkled Members", N.A.S.A. T.N. D-813.

26. McComb, "A Linear Theory of Inflatable Plates of Arbitrary Shape" N.A.S.A. T.N. D-930.

27. Stroud, "Experimental and Theoretical Deflection and Natural Frequencies of an Inflatable Fabric Plate. N.A.S.A. T.N. D.931.

28. Abramowitz and Steguns, "Handbook of Mathematic Tables"

29. Deleted.

30. Binnie et al. "Inflatable Weir Used During Construction of Mangla Dam", Proc. I.C.E., (Nov), Paper No.7655 (1973).

HARRISON - SIMPLEX PROGRAM FOR THE ANALYSIS OF INFLATABLE DAMS

(FORTRAN IV C.D.C. 6600)

1. DATA.

```
      PROGRAM INFDAM (INPUT,OUTPUT,TAPE5=INPUT,TAPE6=OUTPUT)
      REAL ANGLE,TANGLE,ERROR,XMIS,YMIS,SL,  RAG,V(202),H(202),T(202)
      REAL D,DL,HU, HI, HD, P, TG,AG
      REAL X(202),Y(202)
      DIMENSION XY(2),DX(2)
      EXTERNAL LOADAM
      COMMON /BLOK7/X,Y,NS,NJ,T,AG,TG/ BLOK8/XY/BLOK9/D,DL,HU,HI,HD,P
C
C
C
      DO 1310  II=1,4
      WRITE(6,20)
   20 FORMAT(///24H INFLATABLE DAM ANALYSIS)
      WRITE(6,21)
   21 FORMAT(/20H INPUT THE BASE DATA)
      WRITE(6,22)
   22 FORMAT(/31H X-COORD. OF DOWNSTREAM FIXTURE)
      WRITE(6,80)
   80 FORMAT(///23H INPUT THE LOADING DATA)
      WRITE(6,90)
   90 FORMAT(/22H UPSTREAM HEAD IN FEET)
      WRITE(6,100)
  100 FORMAT(/22H INTERNALPHEAD IN FEET)
      WRITE(6,110)
  110 FORMAT(/24H DOWNSTREAM HEAD IN FEET)
      WRITE(6,120)
  120 FORMAT(/29H INTERNAL AIR PRESSURE IN PSI)
      WRITE(6,125)
  125 FORMAT(/67H GUESSED VALUES FOR UPSTREAM TENSION AND ANGLE (LB/FT
     2 AND DEGREES)
      READ(5,11)D,HU,HI,HD,P,TG,AG
      WRITE(6,11)D,HU,HI,HD,P,TG,AG
   11 FORMAT(5F6.2,2F9.2)
      WRITE(6,30)
   30 FORMAT(//24H INPUT THE MEMBRANE DATA)
      WRITE(6,50)
   50 FORMAT(/39H UNSTRETCHED MEMBRANE PERIMETER IN FEET)
        DL=8.5-D
      WRITE(6,11)DL
      WRITE(6,70)
   70 FORMAT(//37H NOMINATE NUMBER OF MEMBRANE SEGMENTS)
      NS=60
      WRITE(6,13)NS
   13 FORMAT(I3)
   12 FORMAT(2F9.2)
      XY(1)=TG
      XY(2)=AG
      DX(1)=XY(1)/10.0
      DX(2)=XY(2)/10.0
       CALL FUNMIN(LOADAM,XY,DX,2,.001, CONV,COUNT)
       CALL PRINTD
       CALL GRADAM
 1310 CONTINUE
      STOP
       END
```

```
      SUBROUTINE FUNMIN(FUN,X,DX,N,ACC,CONV,COUNT)
C*************************************************************************
C
C       SUBROUTINE FUNMIN
C
C       PURPOSE
C          MINIMIZE A FUNCTION OF N VARIABLES
C
C       USAGE
C          CALL FUNMIN(FUN,X,DX,N,ACC,CONV,COUNT)
C
C       DESCRIPTION OF PARAMETERS
C          FUN  - NAME OF FUNCTION FUN(X) TO BE MINIMIZED
C                 CONTAINS THE MINIMUM VALUE OF FUNCTION ON EXIT
C          X    - INPUT VECTOR OF N INITIAL VALUES OF VARIABLES
C                 OUTPUT VECTOR OF VARIABLES CORRESPONDING TO THE
C                 MINIMUM VALUE OF FUN
C          DX   - INPUT VECTOR OF N INITIAL INCREMENTS OF VARIABLES
C                 OUTPUT VECTOR OF STANDARD DEVIATIONS OF VARIABLES FOR
C                 BEST (N+1) ESTIMATES OF  THE MINIMUM OF FUN
C          N    - THE NUMBER OF VARIABLES  (TYPE INTEGER)
C          ACC  - INPUT PARAMETER SPECIFYING THE MAXIMUM STANDARD
C                 STANDARD DEVIATION ALLOWED IN THE BEST (N+1) ESTIMATE
C                 OF THE MINIMUM VALUE OF FUN
C          CONV - LOGICAL OUTPUT VARIABLE WHOSE VALUE IS .TRUE. IF
C                 ACCURACY IS LESS THAN ACC AND NUMBER OF ESTIMATES
C                 CONSIDERED IS LESS THAN 100*N, OTHERWISE .FALSE.
C
C          COUNT- INTEGER OUTPUT VARIABLE CONTAINING THE NUMBER OF
C                 SIMPLEX REPLACEMENTS REQUIRED TO OBTAIN THE MINIMUM
C       REMARKS
C          CALLING PROGRAM MUST SPECIFY
C                 EXTERNAL FUNCTION NAME
C
C       SUBROUTINES REQUIRED
C          REPLAS - SUPPLIED
C          NEW    - SUPPLIED
C
C       METHOD
C          DESCRIBED IN ≠A SIMPLEX METHOD FOR FUNCTION MINIMISATION≠
C                 BY J.A. NELDER AND R. MEAD, COMPUTER JOURNAL VOL 7
C                 1965, P. 308. A FLOW CHART IS SUPPLIED FROM WHICH THIS
C                 SUBROUTINE IS CONSTRUCTED.
C
C*************************************************************************
C
      DIMENSION X(N), DX(N), XS(20), XSS(20)
      COMMON /BLOK1/ YS,YSS /BLOK2/ Y(20),VHI /BLOK4/ XX(20,20)/LOT/ -
      INTEGER V, COUNT, VLO, VNHI  ,VHI
      LOGICAL CONV
     INTEGER IV
     INTEGER FUNEV

      J = N
C
C  FIND (N+1) INITIAL SIMPLEX VERTICES, GIVING (N+1) ESTIMATES OF FUN
C
     FUNEV=0
     DO 110 V = 1,N
      X(V) = X(V) + DX(V)
     DO 100 I = 1,N
  100  XX(V,I) = X(I)
      Y(V) = FUN(X)
     FUNEV=FUNEV+1
     X(V) = X(V) - DX(V)
  110  CONTINUE
```

2. Cont.

```
      WRITE(6,2200) (Y(IV),IV=1,N)
 2200 FORMAT(1H ,5HY(V)=,3(1PE10.3))
      DO 115 I = 1,N
  115  XX(N+1,I) = X(I)
       Y(N+1) = FUN(X)
      FUNEV=FUNEV+1
      WRITE(6,2201) Y(N+1)
 2201 FORMAT(1H ,7HY(N+1)=,1PE10.3)
       COUNT = 0
       NONG = N + 1
C
C  FIND VERTICES GIVING HIGHEST(YHI), NEXT HIGHEST (YNHI) AND LOWEST
C  (YLO) ESTIMATES
C
  120  YLO = 1.0E20
       YHI = -YLO
      DO 140 V = 1,NONG
       YV = Y(V)
       IF (YV .GE. YLO) GOTO 130
       YLO = YV
       VLO = V
  130  IF (YV .LE. YHI) GOTO 140
       YHI = YV
       VHI = V
  140  CONTINUE
       YNHI = YLO
      DO 150 V = 1,NONG
      YV = Y(V)
       IF (V .EQ. VHI .OR. YNHI .GE. YV) GOTO 150
      YNHI = YV
       VNHI = V
  150  CONTINUE
      WRITE(6,2230) YLO
 2230 FORMAT(1H ,4HYLO=,1PE10.3)
      WRITE(6,2231) YHI
 2231 FORMAT(1H ,4HYHI=,1PE10.3)
      WRITE(6,2232) YNHI
 2232 FORMAT(1H ,5HYNHI=,1PE10.3)
C
C  REFLECT HIGHEST ESTIMATE IN CENTROID OF REMAINING VERTICES TO
C  OBTAIN A NEW ESTIMATE YS AT VERTEX PS
C
      DO 160 I = 1,N
  160  XSS(I) = XX(VHI,I)
       CALL NEW (XS, VHI, 2.0, -1.0, XSS)
       YS = FUN(XS)
      FUNEV=FUNEV+1
C
      WRITE(6,2048) (XS(I),I=1,N)
 2048 FORMAT(1H ,3HXS=,3(2X,F12.7))
      WRITE(6,2203) YS
 2203 FORMAT(1H ,3HYS=,1PE10.3)
C
C  IF YS IS LESS THAN YLO, EXPAND FURTHER FOR ANOTHER ESTIMATE YSS
C
       IF (YS .GE. YLO) GOTO 190
       CALL NEW(XSS,VHI, -2.0,  3.0, XS)
       YSS = FUN(XSS)
      FUNEV=FUNEV+1
C
      WRITE(6,2047) (XSS(I),I=1,N)
 2047 FORMAT(1H ,5HXSS1=,3(2X,F12.7))
      WRITE(6,2204) YSS
```

```
C2204 FORMAT(1H ,5HYSS1=,1PE10.3)
      IF (YSS - YLO) 240, 250, 250
C
C  EXPANDED ESTIMATE IS UNSATISFACTORY. CONTRACT FOR A NEW ESTIMATE
C
  190  IF (YS .LE. YNHI) GOTO 250
       IF (YS .GE. YHI) GOTO 200
       CALL REPLAS (1, XS)
       YHI = YS
  200  DO 210 I = 1,N
  210  XS(I) = XX(VHI,I)
       CALL NEW (XSS, VHI, 0.5, 0.5, XS)
       YSS = FUN(XSS)
      FUNEV=FUNEV+1
C
      WRITE(6,2046) (XSS(I),I=1,N)
 2046 FORMAT(1H ,5HXSS2=,3(2X,F12.7))
      WRITE(6,2205) YSS
 2205 FORMAT(1H ,5HYSS2=,1PE10.3)
C
C  IF YSS IS STILL NOT LESS THAN YLO, REPLACE ALL VALUES BY AN
C  ≠AVERAGE≠
C
       IF (YSS .LE.YHI) GOTO 240
      DO 230 V = 1,NONG
      DO 220 I = 1,N
       DUM = 0.5*(XX(V,I) + XX(VLO,I))
       XX(V,I) = DUM
       XS(I) = DUM
  220  CONTINUE
       IF (V .EQ. VLO) GOTO 230
       Y(V) = FUN(XS)
      FUNEV=FUNEV+1
  230  CONTINUE
C
      WRITE(6,2042)
 2042 FORMAT(1H ,32HREPLACE ALL VALUES BY AN AVERAGE)
      WRITE(6,2043) (XS(I),I=1,N)
 2043 FORMAT(1H ,3HXS=,3(2X,F12.7))
       GOTO 260
  240  CALL REPLAS (2, XSS)
       GOTO 260
  250  CALL REPLAS (1, XS)
C
   INCREASE REPLACEMENT COUNT AND CHECK STANDARD DEVIATION FOR
C  CONVERGENCE
C
  260  COUNT = COUNT + 1
      WRITE(6,2044) COUNT
 2044 FORMAT(1H ,/,6HCOUNT=,I3)
      WRITE(6,2049) FUNEV
 2049 FORMAT(1H ,6HFUNEV=,I3)
C
      IF (FUNEV.LT.200) GOTO 99
      RETURN
C
   99  YS=0.0
       YSS = 0.0
      DO 270 V = 1, NONG
       YV = Y(V)
       YS = YS + YV
       YSS = YSS + YV*YV
  270  CONTINUE
       ANON = NONG
       IF (YSS/ANON-(YS/ANON)**2.GT.ACC*ACC.AND.COUNT.LT.100*N) GOTO 12(
```

```
C
C  CONVERGENCE HAS OCCURRED IF THE STANCARD DEVIATION OF THE ESTIMATES
C  OF FUN IS LESS THAN ACC OR IF THE COUNT OF THE NUMBER OF ESTIMATES
C  IS LESS THAN 200*N
       CONV = COUNT .LT. 100*N
C
C  FIND STANDARD DEVIATION OF VARIABLES SPECIFYING THE BEST (N+1)
C  ESTIMATES OF FUN AND STORE IN DX.
C
      DO 290 I = 1,N
       YS = 0.0
       YSS = 0.0
      DO 280 V = 1,NONG
       XXVI = XX(V,I)
       YS = YS + XXVI
       YSS = YSS + XXVI*XXVI
  280  CONTINUE
       DX(I) = SQRT(ABS(YSS/ANON -(YS/ANON)**2))
  290  CONTINUE
C
C  PLACE VARIABLES FOR MINIMUM FUN IN X
C
       YLO = 1.0E20
      DO 310 V = 1,NONG
       YV = Y(V)
       IF (YLO .LE.YV) GOTO 310
       YLO = YV
      DO 300 I = 1,N
  300  X(I) = XX(V,I)
  310  CONTINUE
      YSS=FUN(X)
      WRITE(6,2004)COUNT,(X(I),I=1,N),(DX(I),I=1,N),YSS,CONV
 2004 FORMAT(1H ,2X,I3,6(2X,F12.7),2X,1PE10.3,2X,L6,/)
C
C  EXIT WITH ARRAY X CONTAINING THE PARAMETERS FOR MINIMUM FUN, AND
C  ARRAY DX CONTAINING THE STANDARD DEVIATIONS OF PARAMETERS
C
      RETURN
      END
      SUBROUTINE NEW(ANEWX,NDUDV,CBAR,CI,XI)
       COMMON   /BLOK4/ XX(20,20) /LOT/ N
       DIMENSION ANEWX(20), XI(20)
       INTEGER V
       NUT = N  + 1
       AN = N
      DO 30 I = 1,N
       XBAR = 0.0
      DO 20 V = 1,NUT
   20  IF (V .NE. NDUDV) XBAR = XBAR + XX(V,I)
       XBAR = XBAR/AN
       ANEWX(I) = XBAR*CBAR + XI(I)*CI
   30  CONTINUE
      RETURN
      END
      SUBROUTINE REPLAS (NSTAR,ANEWX)
       COMMON /BLOK1/ YS,YSS /BLOK2/ Y(20),VHI /BLOK4/ XX(20,20)/LOT/ N
       DIMENSION ANEWX(20)
       INTEGER VHI
      DO 10 I = 1,N
   10  XX(VHI,I) =ANEWX(I)
       IF (NSTAR .EQ. 1) GOTO 20
       Y(VHI) = YSS
       GOTO30
   20  Y(VHI) = YS
   30 RETURN
      END
```

3. LOADAM SUBROUTINE. (CALCULATES LOADING, TENSION AND ANGLES IN INFLATABLE DAM.) (vi).

```
      REAL FUNCTION LOADAM
      REAL ANGLE,TANGLE,ERROR,XMIS,YMIS,SL,  RAG,V(202),H(202),T(202)
      REAL D,DL,HU, HI, HD, P, TG,AG
      REAL GRADT
      REAL X(202),Y(202)
      DIMENSION XY(2)
      COMMON /BLOK7/X,Y,NS,NJ,T,AG,TG/BLOK9/D,DL,HU,HI,HD,P/BLOK10/H,V
      TG=XY(1)
      AG=XY(2)
      X(1)=0.0
      Y(1)=0.0
      SL=DL/FLOAT(NS)
      NJ=NS+1
C
C
  130 IC=1
  140 T(1)=TG
      RAG=3.14159265*AG/180.0
      X(2)=SL*COS(RAG)
      Y(2)=SL*SIN(RAG)
      IL=1
      IH=1
      DO 1 I=3,NJ
  141 J=I-1
      K=1
      L=J+K-1
      H(J)=-P*144.0*(Y(L)-Y(J-1))/FLOAT(K)
      V(J)=P*144.0*(X(L)-X(J-1))/FLOAT(K)
C
C
      IF(Y(J)-HI) 150,160,160
  150 H(J)=H(J)-62.5*(HI-Y(J))*(Y(L)-Y(J-1))/FLOAT(K)
      V(J)=V(J)+62.5*(HI-Y(J))*(X(L)-X(J-1))/FLOAT(K)
C
  160 IF(IH)200,200,170
  170 IF(Y(J).GE.HU) GOTO 190
       IK=NS/3
      IF(J.LT.IK) GOTO 180
      GRADT=(Y(J)-Y(J-1))/(X(J)-X(J-1))
      IF(GRADT.GE.0.0.AND.GRADT.LE.0.2)GOTO 182
  180 H(J)=H(J)+62.5*(HU-Y(J))*(Y(L)-Y(J-1 ))/FLOAT(K)
      V(J)=V(J)-62.5*(HU-Y(J))*(X(L)-X(J-1))/FLOAT(K)
      GOTO 210
C
  182 WRITE(6,183) Y(J),J,GRADT
  183 FORMAT(/23H DAM OVERTOPPING Y(J)=,F6.2,4H J=,I2,8H GRADT=,F6.2)
C
C
C
  190 IH=0
  200 IF(Y(J)-HD)205,210,210
  205 H(J)=H(J)+62.5*(HD-Y(J))*(Y(L)-Y(J-1))/FLOAT(K)
      V(J)=V(J)-62.5*(HD-Y(J))*(X(L)-X(J-1))/FLOAT(K)
C
C
C
C
  210 TX=-H(J)+T(J-1)*(X(J)-X(J-1))/SL
      TY=-V(J)+T(J-1)*(Y(J)-Y(J-1))/SL
C
C
  219 TANGLE=TY/TX
      ANGLE=ATAN(TANGLE)
      T(J)=SQRT(TX*TX+TY*TY)
C
```

```
C
C
  211 DELX=SL*COS(ANGLE)
      DELY=SL*SIN(ANGLE)
      IF(TX)212,212,215
  212 DELX=-DELX
      DELY=-DELY
  215 X(I)=X(J)+DELX
      Y(I)=Y(J)+DELY
    1 CONTINUE
      XMIS=X(NJ)-D
      YMIS=Y(NJ)
      ERROR=SQRT(XMIS*XMIS+YMIS*YMIS)
C
  301 WRITE(6,310) TG,AG,ERROR
  310 FORMAT(//10H  TENSION=,F9.2,9H  ANGLE=,F6.2,12H  MISCLOSE=,F9.3)
      WRITE(6,1402)YMIS,XMIS
 1402 FORMAT(12H Y-MISCLOSE=,F6.2,12H X-NISCLOSE=,F6.2)
      LOADAM=ERROR
      RETURN
      END
```

4. PRINTD SUBROUTINE. (PRINTS PROGRESSIVE VAL. OF TENS.& X-YCO-ORD)

```
      SUBROUTINE PRINTD
      REAL AG,TG,T(202),XY(2),X(202),Y(202),H(202),V(202)
      INTEGER S
      COMMON /BLOK7/X,Y,NS,NJ,T,AG,TG/ BLOK8/XY/BLOK10/H,V
      TG=XY(1)
      AG=XY(2)
  600 SASS=AG
      GO TO 901
  901 THETA=(Y(NJ-1)-Y(NJ))/(X(NJ-1)-X(NJ))
      DSANG=ATAN(THETA)*180.0/3.14159265
      WRITE(6,902)T(1),SASS
  902 FORMAT(/20H UPSTREAM TENSION =,F11.4,6H LB/FT,9H  ANGLE =,F6.2,9H
     2 DEGREES)
      WRITE(6,903)T(NJ-1),DSANG
  903 FORMAT(/20H DOWNSTREAM TENSION=,F11.4,6H LB/FT,8H  ANGLE=,F6.2,9H
     2 DEGREES)
      WRITE(6,904)ERROR
  904 FORMAT(/10H MISCLOSE=,F5.2,4H FT.)
      AREA=0.0
      DO 666 I=2,NJ
      AREA=AREA+(Y(I)+Y(I- 1))*(X(I)-X(I-1))/2.0
  666 CONTINUE
      WRITE(6,667)AREA
  667 FORMAT(/6H AREA=,F8.3,7H SQ.FT.)
      HMAX=0.0
      DO 3 I=2,NJ
      IF(HMAX-Y(I))777,778,778
  777 HMAX=Y(I)
    3 CONTINUE
  778 S=FLOAT(I)-1.0
      WRITE(6,779)Y(S),S
  779 FORMAT(/12H MAX.HEIGHT=,F6.3,17H FT. AT JOINT NO.,I4)
      WRITE(6,909)
  909 FORMAT(//50H JOINT  X-COORD(FEET) Y-COORD(FEET) TENSION(LB/FT))
      DO 711 I=2,NJ,3
      WRITE(6,712)I,X(I),Y(I),T(I-1),H(I-1),V(I-1)
  712 FORMAT(I5,1X,2F10.4,4X,3F12.3)
  711 CONTINUE
      WRITE  (6,18)
   18 FORMAT(1H1)
      RETURN
      END
```

5. GRADAM SUBROUTINE. (GRAPHS X-Y CO-ORD OF DAM PROFILE).

```
      SUBROUTINE GRADAM
      REAL X(202),Y(202)
      INTEGER TT,Q
      REAL SYMBOL
      DIMENSION M1(202),N1(202),U(101)
      REAL  XBOUND, YBOUND
      REAL  XX,YY
      COMMON /BLOK7/X,Y,NS,NJ,T,AG,TG/ BLOK8/XY
      DATA SYMBOL,BLANK/1H*,1H /
      XBOUND=5.0
      YBOUND=5.0
      DO  32  M=1,NS
      Q=1+M
      DO  32  TT=Q,NJ
      IF(Y(M).GT.Y(TT)) GOTO 32
      ORDCOY= Y(M)
      Y(M) = Y(TT)
      Y(TT) = ORDCOY
      ORDCOY = X(M)
      X(M) = X(TT)
      X(TT) = ORDCOY
   32 CONTINUE
      DO   5  M=1,NJ
             YY=Y(M)  +1.0
C
             XX=X(M) +1.0
C
      M1(M)     =100.00*XX/XBOUND  +  1.00
      N1(M)     = 60.00*YY/YBOUND  +  1.00
    5 CONTINUE
      DO  4  J=1,61
      K=62-J
      DO  6  I=1,101
      U(I)=BLANK
      DO  7  M=1,NJ
      IF(I.EQ.M1(M).AND.K.EQ.N1(M))GOTO  25
    7 CONTINUE
      GOTO 6
   25 U(I)=SYMBOL
    6 CONTINUE
      WRITE (6,24)( U(I),I=1,101)
   24 FORMAT  (1H ,101A1)
    4 CONTINUE
C
C
      RETURN
      END
```

6. DATA.

```
00000000000000000000
  2.40   1.80   0.00   0.00   0.35     50.00     10.
  2.7    1.40   0.00   0.00   0.30     30.00      0.
  2.3    2.10   0.00   0.00   0.46     70.00     10.00
  2.00   2.30   0.00   0.00   0.62    100.00     60.00
00000000000000000000  END OF FILE
```

APPENDIX II

Correct Load Positions for Analogue Method. (Error due to taking load through centre).

Consider a straight segment AB of

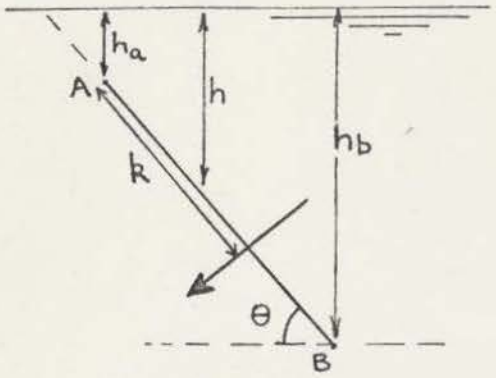

$$h = \frac{h_a + h_b}{2}$$

$$\delta l = \frac{h_b - h_a}{\sin \theta}$$

length δl. Let k be the distance along AB through which the force acts.

$$\text{Water Force on AB} = \frac{h_b - h_a}{2} \cdot \gamma_w \cdot \delta l$$

By taking moments about A,

$$k = \frac{1}{6} (h_a + 2h_b) \frac{\delta l}{h}$$

The difference between centre and point through which load passes is given by

$$k - \frac{\delta l}{2} = \frac{\delta l^2}{12} \frac{\sin \theta}{h}$$

Maximum % Error Δ , for $\theta = 90°$,

$$\Delta = {}^1/_{12} \frac{\delta l}{h} \times 100\%$$

The order of magnitude for a case where $\delta l = .5$ ft and $h = 1.0$ ft.

$$\Delta \doteqdot 4\%$$

As this represents approximately $\frac{1}{4}$ inch and as this was the approximate error in physically positioning the load, this effect of 4% was not regarded as significant.